Investigation of Biomarker Determinants of Treatment Response of Fulvestrant and Capivasertib in Oestrogen Receptor Positive Breast Cancer

Magdalena Meissner

MD, MRCP, MSc Oncology

Submitted in accordance with the requirements for the degree of Doctor of Philosophy (PhD)

Cardiff University

School of Medicine

2021

Summary:

Endocrine therapy is the standard treatment for patients with oestrogen-receptor positive advanced breast cancer. Half of such cancers progress through first-line therapy and half progress after an initial period of disease control. Endocrine resistance remains an ongoing issue. Many clinical trials have added targeted therapy to endocrine treatment to overcome endocrine resistance by inhibiting pathways involved in endocrine resistance, such as the PI3K/AKT pathway. FAKTION trial investigated the efficacy of capivasertib in combination with fulvestrant. Patients who received combination therapy have had improved progression-free survival (PFS) from 4.8 months to 10.6 months, p=0.0044 (Jones et al. 2020). A significant challenge remains to identify biomarkers which can guide the success of endocrine therapy in combination with capivasertib.

As part of the trial formalin-fixed paraffin-embedded (FFPE) tumour tissue, were collected and translational blood samples were taken at baseline, eight weeks of treatment, and on progression.

This thesis investigated the detection of biomarkers of resistance in the tissue DNA and circulating tumour DNA (ctDNA) in baseline samples and serial plasma samples from breast cancer patients undergoing trial treatment.

Potential biomarkers indicative of resistance to endocrine therapy were successfully detected in FFPE DNA and ctDNA, using a commercially available, targeted 44 gene Next Generation Sequencing (NGS) panel and digital droplet PCR (ddPCR).

In the first instance, the concordance of detected mutations in *PIK3CA, AKT1, PTEN, ESR1* and *TP53* genes between 34 baseline tissue and 34 baseline ctDNA samples, was assessed and potential reasons for discordance were identified.

Mutations detected in baseline samples were trackable in longitudinal ctDNA samples of 15 patients. The allele frequency (AF) of detected mutations changed over time. In 40% of patients, the pattern of molecular response followed clinical response. However, in 60% of patients, did not follow the expected pattern, suggesting issues with sample handling or methods errors.

Other biomarkers of endocrine resistance such as *MYC, FGFR1, HER2* amplification detection were explored in the 55 'end of treatment' ctDNA samples, using ddPCR. The study showed that the amplification could be detected in ctDNA but clinical threshold yet to be identified.

This study showed that co-existence of other resistance biomarkers or bad prognostic factors like *TP53* mutations can influence response to new trial treatment and should be considered in stratification in future trials.

Declarations:

STATEMENT 1

This thesis is being submitted in partial fulfilment of the requirements for the degree of PhD.

Signed (candidate)

Date

STATEMENT 2

This work has not been submitted in substance for any other degree or award at this or any other university or place of learning, nor is it being submitted concurrently for any other degree or award (outside of any formal collaboration agreement between the University and a partner organisation).

Signed (candidate)

Date

STATEMENT 3

I hereby give consent for my thesis, if accepted, to be available on the University's Open Access Repository (or, where approved, to be available in the University's library and for inter- library loan), and for the title and summary to be made available to outside organisations, subject to the expiry of a University-approved bar on access if applicable.

Signed (candidate)

Date

Declaration

This thesis is the result of my own independent work, except where otherwise states, and the views expressed are my own. Other sources are acknowledged by explicit references. The thesis has not been edited by a third party beyond what is permitted by Cardiff University's Use of Third Party Editors by Research Degree Students Procedure

Signed

Date

Word Count 46727
(Excluding summary, acknowledgements, declarations, contents page, appendices, bibliography).

Acknowledgments

Related Posters:

- **Meissner M,** Butler R, Casbard A, Madden TA, Carucci M, Howell SJ, Jones RH 'Tracking Endocrine Resistance in Estrogen-receptor Positive Breast Cancer in ctDNA. Abstract published online in Journal of Clinical Oncology, May 2019. DOI: 10.1200/JCO.2019.37.15_suppl.e14550

- **Meissner M,** Butler R, Casbard A, Madden TA, Carucci M, Howell SJ, Jones RH '**Multiple Mutation Detection from Circulating Tumour DNA Can Be a Valid Tool in Endocrine Resistance of Estrogen-receptor Positive Breast Cancer Patients: Experience from the FAKTION Trial.' Presented at NCRI conference, Glasgow, Nov 2018.

- **Meissner, M**. Jones, R. Butler, R. 'Correlation Between PIK3CA Mutations and Clinicopathological Features in Metastatic Hormonal Resistant Breast Cancer.' Presented at 'Circulating Biomarkers' Conference, Dandee, Oct 2016.

Table of Contents

List of Figures

List of Tables

Commonly used Abbreviations:

Abbreviation   **Definition**

AI	Aromatase inhibitor
AWMGS	All Wales Medical Genetics Service
bp	Base pair
BWA	Barrow-Wheeler aligner
cfDNA	Cell free DNA
CI	Confidence Interval
CR	Complete Response
BAM	Binary alignment map (BAM)
CDKN2A	Cyclin Dependent Kinase Inhibitor 2A
CDK4/6	Cyclin-dependent kinase 4 and 6
COSMIC	Catalogue of Somatic Mutations in Cancer
CT	Computed tomography
CTCs	Circulating tumour cells
ctDNA	Circulating tumour DNA
ddPCR	Droplet digital PCR
EGFR	Epidermal Growth Factor Receptor
ER	Oestrogen receptor
ERBB2	Erb-B2 Receptor Tyrosine Kinase 2
ESR1	Oestrogen receptor 1
FFPE	Formalin fixed paraffin embedded
FGFR1	Fibroblast growth factor receptor 1
FISH	Fluorescent in situ hybridisation
HER2	Human epidermal growth factor receptor 2
HR	Hazard Ratio
IGV	Integrative Genomics Viewer
MAF	Mutant Allele Frequency
MRI	Magnetic resonance imaging
MYC	MYC Proto-Oncogene
MREC	Multi-Centre Research Ethics Committee
ncRNA	Non – coding RNAs
ng	Nanogram
NGS	Next generation sequencing
OS	Overall survival
PCR	Polymerase chain reaction
PD	Progressive disease
PFS	Progression free survival
PIK3CA	Phosphatidylinositol-4,5-Bisphosphate 3-Kinase Catalytic Subunit Alpha
PR	Partial Response
PTEN	Phosphatase and Tensin Homolog
qPCR	Quantitative PCR
SAM	Sequence alignment map (file)
CNV	Copy number variant
SD	Stable Disease
SNV	Single-nucleotide variant
VAF	Variant allele fraction
WES	Whole exome sequencing
WGS	Whole genome sequencing
TP53	Tumour Protein P53
µg	microgram

1. Introduction

1.1 Breast Cancer Incidence

Breast cancer is the most common cancer worldwide. In 2017, 54.700 women in the UK were diagnosed with invasive breast cancer. Breast cancer is the 4th most common cause of cancer death in the UK, with around 11.400 death each year. The 5-year survival of women with breast cancer is 85%, and the 10-year survival is approximately 76%. However, when the disease spread to other organs, the 5-year survival falls to 26%. (CRUK 2017)

Breast cancer survival has doubled over the last 40 years. Over the years, significant advances in neo and adjuvant therapies have been made, which increased overall survival and decreased mortality rates (Bosetti et al. 2012). Patients are selected for neo- or adjuvant chemotherapy, radiotherapy, endocrine therapy, targeted therapy based on clinicopathological features such as stage, grade, tumour size, lymph node involvement, and receptor status (Weigelt et al. 2005). When the decision on adjuvant treatment is uncertain, then multi-gene panel analysis of primary tumours such as Oncotype DX can further help in decision making, highlighting the importance of understanding tumour genetics (Sparano et al. 2019). The 21-gene Oncotype DX assay provides prognostic information, whether adjuvant chemotherapy will reduce cancer recurrence for node-negative, oestrogen receptor-positive (ER) and human epidermal growth receptor 2 (*HER2*) negative (Sparano et al. 2019). Other similar tests like Oncotype DX rely on information from primary tissue taken at a single point in time. No further pathological or molecular tests are performed to detect any residual disease or biomarkers to predict response or resistance to adjuvant endocrine therapy.

Approximately 70% of advanced breast cancers express oestrogen receptor (ER), and women with such tumours receive adjuvant endocrine therapy. Endocrine therapy cures approximately 30% of women with undetected micro-metastatic disease but 70% relapse and subsequently die from ER-positive resistant metastatic breast cancer (MBC) (Davies et al. 2011). In ER-positive advanced breast cancer, endocrine therapy is the treatment of choice due to its improved toxicity profile and similar efficacy compared with cytotoxic chemotherapy. However, half of such cancers will progress through the first-line therapy (primary endocrine resistance), and half will progress after an initial period of disease control (secondary or acquired endocrine resistance). Several resistance mutations have been identified, including the oestrogen receptor pathway and other pathways, including alteration of the PI3K/AKT pathway. Multiple clinical trials have been set to understand the endocrine resistance better and evaluate drugs that will overcome endocrine resistance by blocking the identified pathways.

FAKTION trial has focused on the PI3K/AKT pathway and used capivasertib in addition to fulvestrant to overcome endocrine resistance.

1.1.1 ER-Positive Breast Cancer and Endocrine therapy

In clinical settings, the oestrogen receptor is tested with immunohistochemical staining on breast cancer tissue. The Allred score combines the percentage of stained cells and the intensity of their staining (Qureshi and Pervez 2010). The two scores are added together, and the final score gives eight possible values. Scores 0-2 are considered negative, and the scores 3-8 are regarded as ER-positive (Qureshi and Pervez 2010; Murphy and Dickler 2016). Oestrogen receptor became the first molecular target for endocrine therapy and remained the mainstay of treatment of all stages of ER-positive breast cancers for almost four decades (Oesterreich and Davidson 2013; Fribbens et al. 2016).

Endocrine therapy includes drugs such as (Toy et al. 2013):

- Aromatase inhibitors (letrozole, anastrozole, exemestane)
- GnRH agonists (Goserelin) that suppress oestrogen production,
- Selective oestrogen receptor modulators (SERM) - (tamoxifen) that directly inhibits the oestrogen receptor,
- Selective oestrogen receptor degraders (SERD) – (fulvestrant) that degrades oestrogen receptor.

In the premenopausal woman, oestrogen production occurs mainly in the ovary compared to a postmenopausal woman whose primary oestrogen source comes from peripheral aromatisation. Aromatisation occurs in extragonadal tissues and is the aromatase-mediated conversion of androstenedione and testosterone to estrone and oestradiol. As a result, premenopausal women are treated with oestrogen receptor inhibitors like tamoxifen, although recent data show the role of aromatase inhibitors with ovarian suppression in those women (Smyth and Hudis 2015). For postmenopausal women, aromatase inhibitors are the first choice of treatment in adjuvant and metastatic settings.

1.1.2 Oestrogen Receptor and ESR1 Gene

Oestrogen receptor (ER) is a member of the steroid hormone family of the nuclear receptors (NRs). ER acts as a ligand-dependent transcription factor. Its activity is linked to the cell cycle and the regulation

of proliferation. Furthermore, oestrogen is an important sex hormone produced by ovaries in premenopausal women. Oestrogen belongs to the family of steroid hormones that regulate the growth, development, and physiology of humans' reproductive system. The biological functions of oestrogen are transmitted by binding to the oestrogen receptor alpha (ERα) and oestrogen receptor beta (ERβ). ERα is expressed in the breast, uterus, ovarian theca cells and liver in women. ERβ is expressed in ovarian granulosa cells, bone marrow and brain. ERα is present in breast tissue and can be overexpressed in breast cancer cells. (Lee et al. 2012)

ERα is encoded by genes located on chromosome 6. The full-length of ERα protein has 595 amino acids. ERs consist of five domains with different functions, Figure 1. The N-terminal of the A/B domains contains an activation function 1 (AF1), which regulate the transcriptional activity of ERs and is an essential domain for interaction with co-regulators. Stimulation of the AF1 activity can also be achieved by post-transcriptional modifications of specific amino acids contained in the A/B domains. DNA binding domain (DBD) is encoded by the C domain, which is required for sequence-specific binding of ERs to DNA and regulating the expression of target genes. The D domain encodes a hinge region that stimulates nuclear localisation signalling and enables post-translational modification of ERs, which results in the activation of ER signalling in cells. Lastly, the ligand-binding domain (LBD) and ligand-dependent activation function 2 (AF2) are encoded by the E/F domain, located in the C-terminal region. LBD/AF2 interacts with ligands like estrogen and also with co-regulators. (Lee et al. 2012)

Figure 1. Diagram of ER domains with the location of the identified mutations, image adapted from (Toy et al. 2013).
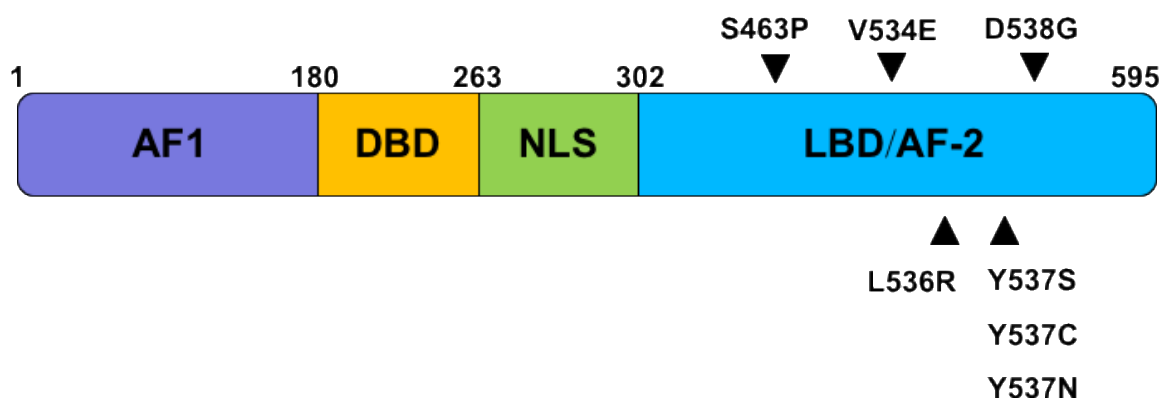
AF-1 - Activation Function-1; DBD - DNA binding domain; NLS - Nuclear localizing signal; LBD - Ligand binding domain; AF-2 - Activation function-2.

Most common mutations reported were from ligand-binding domain *ESR1* gene: p.D538G (36%), p.E380Q (21%), p.Y537S (14%), p.Y537C (6.3%), p.Y537N (5.3%), and p.L536H (4.2%) and 20% of other less frequent mutations (Toy et al. 2017).

ERs remain inactive in the absence of hormones due to their connection with heat shock protein 90 (Hsp90). Hsp90 blocks the degradation of unbound ERs and prevents deactivated ERs from the binding ligand. When ERs binds to the ligand, it gets phosphorylated and transferred to the nucleus. ERs regulate the transcription of target genes by binding to estrogen response elements (EREs) in the DNA sequence (Lee et al. 2012).

1.2. Resistance to Endocrine Therapy

In ER-positive metastatic breast cancer, endocrine therapy is the treatment of choice. The emergence of endocrine resistance is inevitable in advanced breast cancer. However, an oncologist will treat with second- and third-line endocrine therapies patients who initially benefited from first-line treatment. The clinical benefit rate declines from about 70% for first-line treatment fulvestrant or aromatase inhibitors to around 30% for the second and other treatment lines (Ellis et al. 2015).

Nevertheless, endocrine therapy is mostly well tolerated with a response duration of many years in some patients. The main challenge is to improve our understanding of endocrine resistance and develop strategies that will overcome the resistance and extend effective therapy duration while minimising toxicity (Murphy and Dickler 2016). Breast cancers that are not responsive to any form of endocrine therapy are called cross-resistant (Geisler and Lønning 2001). Some breast cancers resistant to one type of endocrine therapy but sensitive to other types would be called non-cross-resistant (Johnston 2004; Perey et al. 2007). Some patients will respond to one AI type but would be resistant to others (Lønning 2009; Beresford et al. 2011).

1.2.1 Mechanisms of Endocrine Resistance

Loss of ER expression

Loss of ER expression would be the most reasonable explanation for endocrine resistance. However, recent studies of matched primary and metastatic tumour tissues indicate that this occurs in only 10% of patients (Sighoko et al. 2014). Ellis et al. found loss of ER expression after neoadjuvant endocrine treatment in less than 10% of cases and fewer than 20% of non-responders who would represent an endocrine-resistant phenotype (Ellis et al. 2008). The ER, progesterone receptor(PR) and HER status can be discordant with primary tumours (Curtit et al. 2013) therefore, it has been recommended that all patients with relapsed metastatic disease have a repeat biopsy where the metastatic lesion is accessible (Cardoso et al. 2014).

Aromatase-independent oestrogen-producing pathway

Steroid hormones like oestrogen and androgen are produced in endocrine organs such as the ovary in premenopausal women. Oestrogen production in the ovaries ceases following menopause. In postmenopausal women, oestrogen is produced mainly by the conversion of androgens which occurs in various tissues such as skin, muscle, fat, bone, aorta, brain. Several steroid-metabolising enzymes catalyse the peripheral conversion from androgen to oestrogen. Several studies proved that this conversion could occur in breast cancer tissue. The initial step in intra-tumour oestrogen production is aromatisation, catalysed by enzyme aromatase (Sasano et al. 2009). This enzyme is a target for Aromatase Inhibitors (AI), which have been established as the gold standard in the treatment of ER-positive breast cancers. However, other enzymes such as the 17β-hydroxysteroid dehydrogenase type 1 (17β-HSD type 1), steroid sulfatase (STS), oestrogen sulfotransferase (EST), 5α-reductase type 1, 3β-hydroxysteroid dehydrogenase type (3β-HSD type 1), play a significant role in intra-tumour production of oestrogen (Sasano et al. 2009). These enzymes can produce multiple androgen metabolites: 5α-androstane-3β, 17β-diol (3β-diol) and androst-5-ene-3β, 17β-diol (A-diol), which can bind to ER and stimulate proliferation in breast cancer cells (Aspinall et al. 2004; Wang et al. 2009), Figure 2. In addition, the oestradiol (E2) can be produced from the biologically inactive oestrogen called estrone sulphate (Honma et al. 2011), Figure 2. This production of estrogenic steroids and E2 by non-aromatase pathways has been suggested to mediate AI resistance (Hanamura and Hayashi 2017).

Figure 2. Production of estrogenic androgens and E2 in stromal cancer cells, image adapted from (Hanamura and Hayashi 2017).
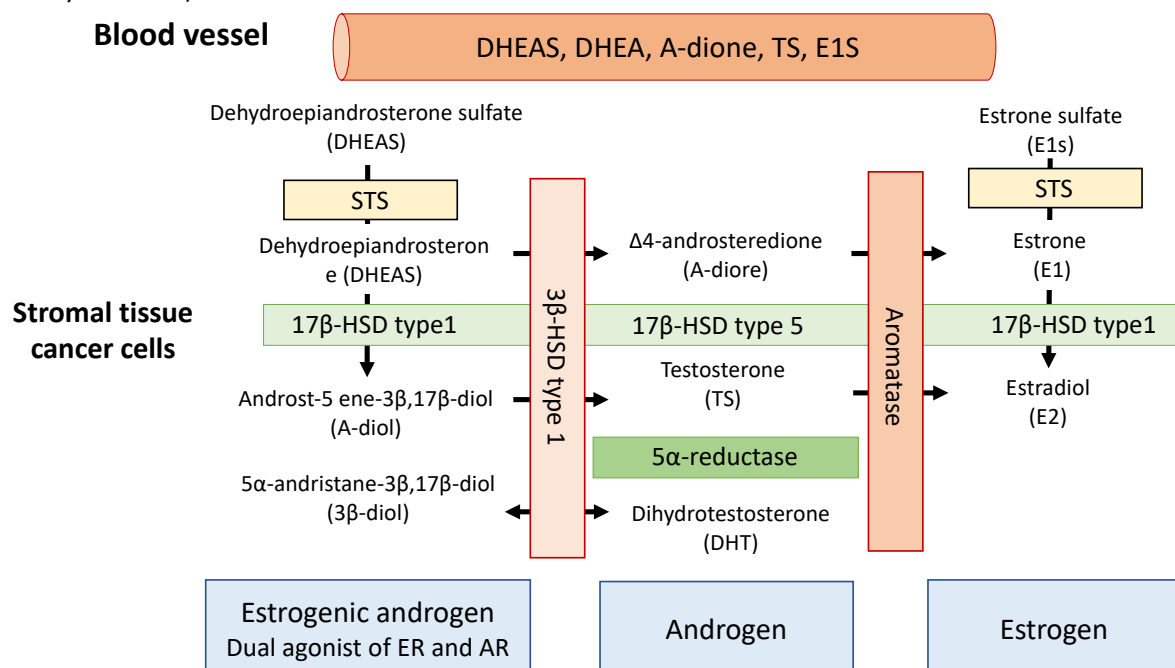
Endocrine resistance through cell cycle checkpoint alterations

Endocrine resistance can be caused by dysregulation of cell cycle progression through modifications of key cell cycle checkpoints (Murphy and Dickler 2015). Cancer cells, as well as normal cells, receive many proliferative and antiproliferative signals. The balance of these signals determines whether the cell will progress from the G1 phase into the S phase (DNA synthesis) and commit to further cell cycle division or quiescent phase (G0) (Pardee 1989).

The retinoblastoma tumour suppressor protein (pRb), p130 and p107 are the primary receivers of antiproliferative signals. RB is regulated by complexes of cyclin and cyclin-dependent kinases (CDK), a family of serine-threonine protein kinases (Morgan 1997). Phosphorylation of Rb by the cyclin-dependent kinase CDK4 or CDK6 in complex with cyclin D1, D2, D3 results in progression through the G1-S phase (Sherr 1995). Hyperphosphorylation of Rb lowers its ability to inhibit the activity of the E2F family of transcription factors, causing the increased synthesis of proteins which are essential for DNA replication and subsequent progression of the S phase and mitotic progression (Weinberg 1995). Many cancers escape senescence by increasing cyclin D-dependent activity via multiple mechanisms such as CDK4 mutation with loss of INK4 binding, CDK4 amplification, cyclin D1 amplification, translocation or overexpression (Shapiro 2006).

Pre-clinical studies indicated a role for CDK4/6 inhibition in ER-positive breast cancer cells, including oestrogen-resistant and sensitive models. CyclinD1 amplification is common in ER-positive breast cancer, found in 29% of luminal A cancers and 58% of luminal B cancers (Network 2012). Antioestrogen therapy results in the arrest of ER-positive breast cancer cells. It is associated with reduced cyclin D1 expression, while the emergence of endocrine resistance is linked to the persistence of cyclinD1 expression and Rb phosphorylation (Watts et al. 1995; Thangavel et al. 2011).

The role of CDK4/6 inhibition in endocrine-resistant ER-positive breast cancers cells emerged during the evaluation of the CDK4/6 inhibitor - palbociclib in vitro. It demonstrated most activity in luminal cancers, including those with oestrogen resistance (Finn et al. 2009). Thus, palbociclib is now indicated in combination with any AI as first-line endocrine treatment of advanced or metastatic ER-positive, *HER2*-negative breast cancer and in combination with fulvestrant in second-line treatment (Brufsky and Dickler 2018).

Oestrogen-independent ER functions:

Constitutive activation of ER by *ESR1* gene mutations

It has been established in other cancers like lung cancer that resistance to targeted therapies such as *EGFR* inhibitors can be related to the appearance of new mutations in the target oncogene (Pao et al. 2005). Therefore, the attention has focused on the mutations in the oestrogen receptor 1 (*ESR1*) gene, which encodes ERα in breast cancer. It has been established that *ESR1* mutations are sporadic in ER-positive primary tumours or treatment naïve tumours but are more frequent in metastatic and pre-treated ER-positive breast cancers (TCGA 2012). There have been several studies that have reported multiple *ESR1* mutations at different frequencies. Toy et al. (2013) found *ESR1* mutations in 11% in ER-positive metastatic cancers previously treated with AIs, and only 3% in pre-treatment tumour biopsies from the BOLERO-2 trial (Baselga et al. 2012). Jeselsohn et al.(2014), in their study, found an *ESR1* mutation rate of 12% in ER-positive breast cancers and 20% in a subset of heavily pre-treated patients. Fribbens et al. (2016) analysed archival plasma samples of ER-positive metastatic breast cancer patients. They found *ESR1* mutations rates of 25% in patients with progression on endocrine treatment in the PALOMA3 study (29% in prior AI therapy) and 39% of patients with prior AIs in the SOPHEA trial.

The most frequent mutations are located at two residues in the ligand-binding domain (LBD): replacement of tyrosine with serine, cytosine and asparagine at residue 537 (p.Y537S/C/N) and replacement of aspartic acid with glycine at residue 538 (p.D538G), Figure 1. These mutations cause ligand-independent oestrogen receptor transcriptional activity, resulting in resistance to tamoxifen and AIs (Jeselsohn et al. 2014). The two most common *ESR1* p.D538G and p.Y537S mutations have been associated with activation of the Insulin-like growth factor (IGF) pathway resulting in increased growth stimulation in cell line assays (Li et al. 2018d). *ESR1* mutations have therapeutic application as Toy and Jeselsohn studies revealed partial resistance to tamoxifen and fulvestrant, which potentially can be revoked by increasing the dose (Murphy and Dickler 2016). Furthermore, in a study by Toy et al. (2017) the degree of ER-independent activities and reduced sensitivity to ER antagonists were assessed for each *ESR1* mutation. It was found that p.Y537S caused a significant change in ER activity associated with fulvestrant resistance *in vivo.* Using xenografts models group identified that fulvestrant could inhibit wild-type, p.E380Q, p.S463P fully and nearly inhibit p.D538G ER driven cancers, but p.Y537S was only partially inhibited despite higher dosing of fulvestrant (Toy et al. 2017). However, this effect has not been confirmed in clinical settings in the plasmaMATCH trial. Fulvestrant activity was similar in patients with and without ESR1 mutations (Turner et al. 2020). Moreover, the researchers found that patients with p.Y537S mutations were no less sensitive to fulvestrant than those with other ESR1 mutations (Turner et al. 2020).

There are currently novel selective oestrogen receptor degraders (SERDS) in the development that have improved drug properties with the potent antagonist and degradation activities against wild-type and Y537S mutated breast cancers (Shomali et al. 2021). Although the pre-clinical studies are promising, the clinical efficacy is yet to be tested in large, randomised clinical trials.

Robinson et al. (2013) and Toy et al. (2013) proved that LBD mutations result in constitutive, ER-independent receptor activity. It has also been reported that mutant ER causes the expression of novel target genes (Toy et al. 2013). Some studies suggested that LBD mutations induce increased interaction with coactivator AIB1 and increased phosphorylation of S118, which is essential for the ligand-dependent and independent ER activity (Ali et al. 1993; Lannigan 2003). All these studies highly suggest that *ESR1* LBD mutations cause highly active ER receptors in the absence of oestrogen and result in resistance to AI therapy (Oesterreich and Davidson 2013).

Toy et al. reported that 67.4% of all patients with *ESR1* mutation were treated with AIs but 32.6% not received AIs (Toy et al. 2017), suggesting that *ESR1* mutations could appear due to other treatments. Also, 18.8% of *ESR1* wild type patients were treated with AIs. However, they have not developed somatic mutations; this group was not characterised by the duration of AIs exposure or metastatic sites. Toy et al. reported that *ESR1* mutations were most frequent in patients with liver and bone metastases, and no *ESR1* mutations were found in brain metastases (Toy et al. 2017). However, the relation of the metastatic site with prior treatment and treatment duration was not assessed. Therefore, it is unknown what duration of AIs is needed to develop *ESR1* mutation, or maybe patients with other than the liver or metastatic bone site will less likely develop those mutations. Potentially, most of the patients with wild type *ESR1* could have brain metastasises, which will not develop *ESR1* mutations despite being on AI treatment.

Cross-talk between growth factor signalling pathways and ER

While data for *ESR1* alterations are consistent with the reduction of tumour dependence on oestrogen, it does not indicate that tumours are entirely dependent on ER signalling for tumour growth (Toy et al. 2017). Many studies have reported that amplification and overexpression of growth factors such as type I growth factor receptors, epidermal growth factor receptor (EGFR), human epidermal growth factor receptor HER2 and HER3, fibroblast growth factor receptor 1 (FGFR1) and Insulin-like growth factor 1 receptor (IGF1R) are associated with the development of endocrine resistance (Ellis et al. 2006; Frogne et al. 2009; Turner et al. 2010; Fox et al. 2011). The pathways of these receptors join at the RAF/MEK/ERK and PI3K/AKT/mTOR pathway (Murphy and Dickler 2016), Figure 3.

Figure 3. Cross-talk between ER signalling and growth factor signalling pathways, image adapted from (Skandalis et al. 2014)
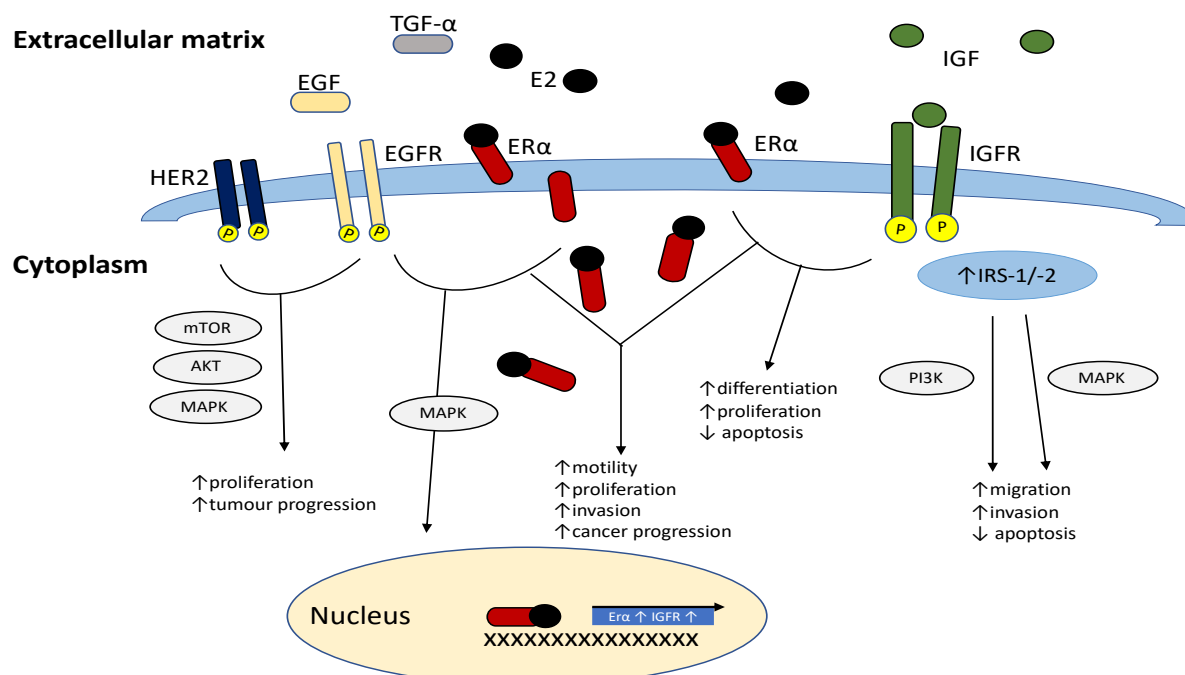
MAPK - mitogen-activated protein kinase; ER - oestrogen receptor; HER2 - Human epidermal growth factor receptor 2. FGF - Epidermal growth factor; FGFR - Epidermal growth factor receptor; IGF -Insulin-like growth factor; IGFR - Insulin-like growth factor receptor.

Overview of the PI3K/AKT pathway and role in endocrine resistance

The PI3K/AKT pathway has been intensively investigated in cancer because of its significant role in cell survival and anti-apoptotic functions (Nitulescu et al. 2018). Various pathogenic mechanisms, including mutations that activate the catalytic subunit of PI3K, mutations in AKT1, AKT2, PDK1 and loss of inhibitory function of PTEN and INPP4B, growth factors receptors, and the amplification of the genes encoding PI3K or AKT can lead to activation of PI3K/AKT pathway in cancer cells (Fu et al. 2013; Wang et al. 2017a). Furthermore, Miller et al. (2011a) suggested that the hyperactivated PI3K/AKT pathway promotes oestrogen-independent ER function. Conversely, the inhibition of this pathway increases oestrogen-dependent ER function; therefore, it has been suggested that combination therapy of PI3K inhibition and endocrine therapy could be used in resistant breast cancer (Murphy and Dickler 2016).

PI3K is an enzyme that belongs to the phosphatidylinositide 3-kinase family (Raynaud et al. 2009). It has been divided into three classes (I, II, III) based on different structures and specific substrates (Katso et al. 2001; Engelman et al. 2006). Class I PI3K is comprised of classes IA and IB. Class IA PI3K is mostly implicated in human cancer. It consists of two subunits: p85 regulatory unit and p110 catalytic subunit (Donahue et al. 2012). The catalytic subunit (p110) occurs in 4 isoforms: p110α, β, γ, and δ. The p110α

isoform is encoded by *PIK3CA* gene, which can be mutated up to 40% in breast cancers (Campbell et al. 2004; Levine et al. 2005; Saal et al. 2005; Arthur et al. 2014).

The p85 regulatory unit integrates and binds signals from various transmembrane and intracellular proteins such as tyrosine kinase-associated receptors, protein C (PKC), Src homology 2 domain-containing protein tyrosine phosphatase 1 (SHP1), Rac, Pho, hormonal receptors, Src and mutated Ras (Hennessy et al. 2005). This causes the integration point for activation for p110 and molecular downstream. The overview of the PI3K/AKT pathway is presented in Figure 4 (Yang et al. 2019). The PI3K/AKT pathway's main key downstream effector is the mammalian target of rapamycin (mTOR) protein kinase complex and occurs in two distinct multiprotein complexes mTORC1 and mTORC2 (Lauring et al. 2013). AKT1 phosphorylation increases mTORC1 activity with subsequent effects on cellular metabolism and protein synthesis (Murphy and Dickler 2016).

Figure 4. Overview of the PI3K/AKT/mTOR pathway, image adapted from (Yang et al. 2019).
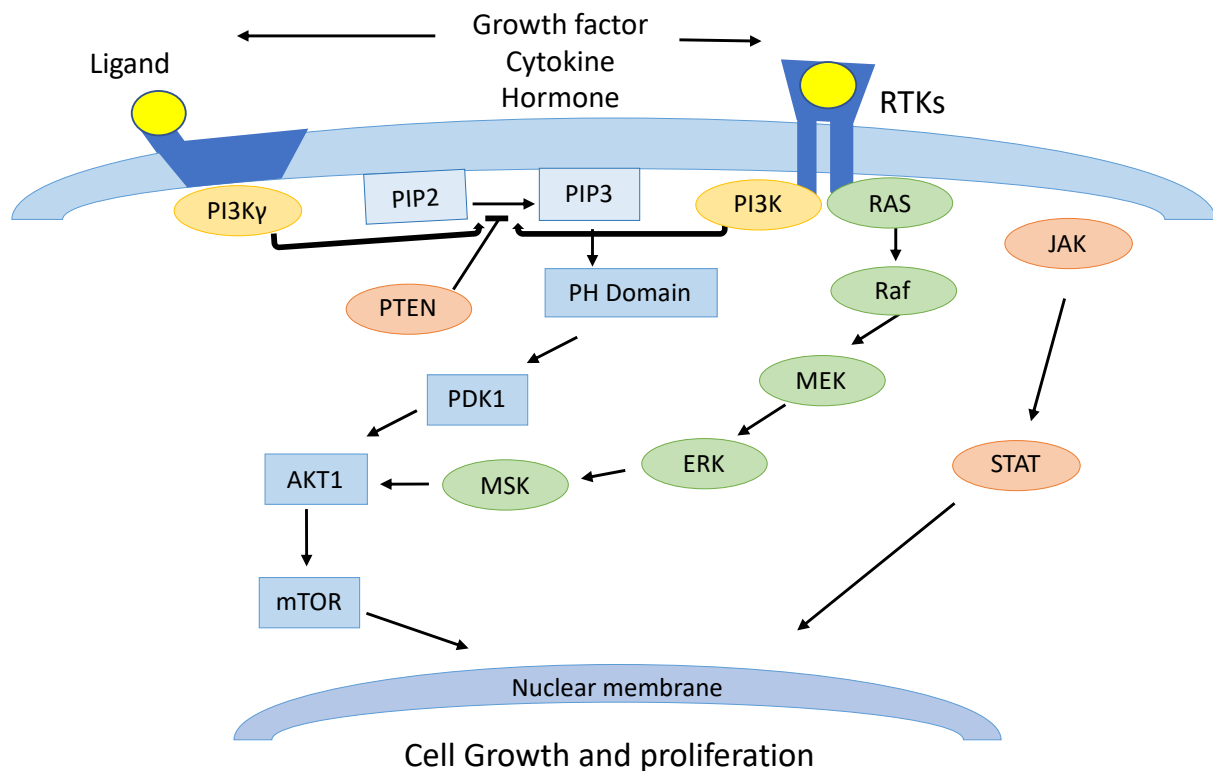
PI3K - Phosphatidylinositol; PIP2 - Phosphatidylinositol 4,5-biphosphate; PIP3 - Phosphatidylinositol 3,4,5-trisphosphate; PTEN - Phosphatase and Tensin Homolog; mTOR - mammalian target of rapamycin; PDK1 - 3-phosphoinositide-dependent kinase 1; ERK - Extracellular signal-regulated kinase; MEK - Mitogen-activated protein kinase.

Activation of PI3K signalling

In physiological conditions, the p110 catalytic subunit is stabilised in the dimer with the regulatory p85 subunit (Manning and Cantley 2007). Normally, PI3K is activated by various extracellular factors like

growth factors, hormones and cytokines (Guo et al. 2015). Activated PI3K converts by phosphorylation phosphatidylinositol 4,5-bisphosphate (PIP2) to phosphatidylinositol (3,4,5)-trisphosphate (PIP3). The PIP3 binds to lipid-binding domains of downstream targets such as a subset of pleckstrin-homology (PH), FYVE, Phox , C1, C2. Kinases like PDK1 and AKT binds to lipid products of PI3K and are thus confined to the cell membrane to activate cell growth and cell survival pathways (Manning and Cantley 2007). Phosphatase and tensin homologue encoded by the *PTEN* gene regulates the pathway by dephosphorylation of PIP3 to PIP2 and prevents activation of the AKT signalling pathway (Hennessy et al. 2005). The PI3K/AKT pathway has been dysregulated in human cancers. Mutations in genes encoding kinases or/and decreased expression of *PTEN* can lead to cancerogenic transformation (Hennessy et al. 2005). Also, pathological stimulation of the PI3K/AKT pathway can occur through other ways such as tyrosine kinase growth factors (epidermal growth factor receptor 2 - *EGFR*2 or insulin-like growth receptor 1 - IGR1), cell adhesion molecules (integrins, GPCR), and oncogenes like RAS (Bauer et al. 2015).

In addition, non – coding RNAs (ncRNAs) have been described as an important regulator of the PI3K/AKT pathway (Dong et al. 2014; Benetatos et al. 2017). The ncRNAs can directly or indirectly target multiple components of the pathway (PI3K, AKT, PTEN, mTOR), regulating the signalling activity. However, the mechanism of action has not been fully understood.

PIK3CA mutations

The subunit p110α isoform is encoded by *PIK3CA* gene, located on chromosome 3 (Arthur et al. 2014). The frequency of *PIK3CA* mutations is similar in primary and metastatic breast cancers, with usually high concordance between matched samples for *PIK3CA* status (Meric-Bernstam et al. 2014). However, Jensen et al. (2011) reported instances where metastases were wild type in patients with *PIK3CA* mutant primary tumours and highlighted that *PIK3CA* status could change between primary and metastatic disease. This is an important aspect for trials when selecting the type of tissue for *PIK3CA* testing prior to *PIK3CA* inhibitor therapy.

The most common *PIK3CA* mutations are reported around two specific coding sequences (exons 9 and 20). Two of the most frequent mutations, E542 and E545, are located within the helical domain (exon 9), often substituted with lysine (Bachman et al. 2004). Another residue, H1047, placed in the kinase domain (exon 20), is frequently substituted with arginine (Bachman et al. 2004). Functional studies suggested that these *PIK3CA* mutations lead to increased PI3K activity (Ikenoue et al. 2005; Jiang et al. 2018). In colorectal cancer, exon 9 play a more important role than exon 20, but in endometrial, the

opposite was described (Zhao and Vogt 2008). This is controversial in breast cancer, as some studies described that patients with exon 20 mutations have better survival than wild-type, but exon 9 mutations have worse survival than wild-type (Wu et al. 2019). Other studies reported that patients with exon 20 have a worse prognosis (Mosele et al. 2020). The coexistence of mutations in both helical and kinase domains leads to synergistic enhancement of p110 activity and cancerogenic enhancement (Zhao and Vogt 2008). Mutations found in the C2 domain are also essential and can play a role in the dysregulation of the pathway (Croessmann et al. 2018). Dysregulation of the PI3K pathway stimulates cell proliferation, migration and angiogenesis, promoting cancer initiation, progression and maintenance (Levine et al. 2005).

In addition, mutations in other catalytic subunits p110β, p110γ and p110δ are rare, but overexpression of these subunits can induce an oncogenic phenotype in cultured cells (Yang et al. 2019). Subunit p110β plays a vital role in promoting cell proliferation, invasiveness, and tumorigenesis in breast cancer (Dbouk et al. 2013). PI3Kδ is important in T and B cells development and is activated by cytokine receptors, antigen receptors, growth factor receptors and costimulatory receptors (Fung-Leung 2011). Furthermore, p110δ protein has been detected in breast cells, and it has been reported to regulate cell migration in breast cancer lines and tumour progression (Sawyer et al. 2003). PI3Kγ is mainly expressed in immune cells but not cancer cells, regulating innate immunity in cancer and inflammation (Kaneda et al. 2016).

The frequency of *PIK3CA* mutations in breast cancer ranges from 16.4 to 45% (Samuels and Waldman 2010). However, the association between *PIK3CA* mutations and specific clinicopathological features of breast cancer is still debated. Furthermore, the relationship between *PIK3CA* mutations in breast cancer patients and overall survival (OS) and disease-free survival (DFS) remains controversial. Some studies have found that breast cancer patients with *PIK3CA* gene mutations have improved OS and DFS rates compared with breast cancer patients lacking such mutations (Dupont Jensen et al. 2011). Conversely, other studies have found that *PIK3CA* mutations are correlated with poor outcomes (Li et al. 2006; Lai et al. 2008).

Loss or inactivation of *PTEN*

PTEN is a negative regulator of the PI3K/AKT pathway. It inhibits PI3K activity through dephosphorylation of PIP3 to PIP2 (Yang et al. 2019). *PTEN* is a well-described tumour suppressor gene and plays an important role in growth, survival and metabolic regulatory functions. Loss or inactivation of *PTEN* leads to increased PI3K signalling and tumorigenesis (Papa et al. 2014). Furthermore, it has

been reported that the main tumorigenic driver in *PTEN*-deficient cancers is the overactivation of AKT, caused by the loss of *PTEN* lipid phosphatase function (Papa et al. 2014; Haddadi et al. 2018). In mice, *PTEN* mutations such as *PTEN* C124S and *PTEN* G129E can inhibit the *PTEN* activity leading to increased PI3K signalling pathway and tumorigenesis (Papa et al. 2014). *PTEN* mutations can have a similar effect in humans.

AKT mutations

The next crucial downstream target of PI3K is the serine/threonine kinase AKT, consisting of three isoforms (AKT1, AKT2, AKT3) (Scheid and Woodgett 2001; Vivanco and Sawyers 2002). It has a vital role in many cellular functions, including cell cycle progression, neovascularisation, glucose metabolism regulation, genome stability, transcription, and protein synthesis. AKT stimulates cell survival by mediating cellular growth factors and inhibiting apoptosis by inactivation of pro-apoptotic proteins (Bellacosa et al. 2005; Nitulescu et al. 2018). Activated AKT phosphorylates multiple proteins located either in the plasma membrane, in the cytosol or nucleus, promoting cell growth and survival. AKT phosphorylates target such as PRAS40, a component and regulator of mTOR complexes, the cell cycle inhibitors p21, p27, the actin-associated protein palladin, and vimentin. All play a role in enhancing tumour invasion, motility and metastatic growth (Hers et al. 2011).

AKT contains three domains: An amino-terminal – N terminal, a central and a carboxyl-terminal fragment - C terminal, Figure 5. The N-terminal domain, a pleckstrin homology (PH) domain, interact with membrane lipid products such as PIP3 and PIP2 (Nitulescu et al. 2018).

Figure 5. AKT protein domains, image from (Cerami et al. 2012; Gao et al. 2013).
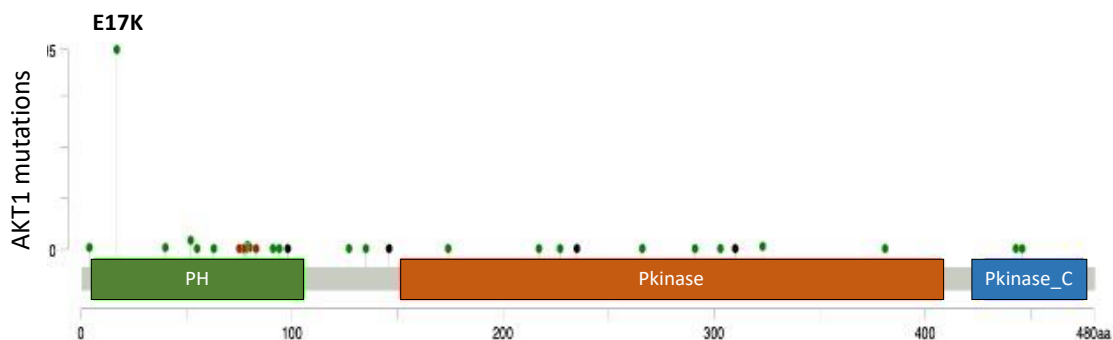
PH - pleckstrin homology

The AKT signalling is activated by various signals, including receptor tyrosine kinases (RTKs), integrins, T and B cell receptors, cytokine receptors and GPCRs (Jhaveri and Modi 2015). AKT is triggered by recruitment to the plasma membrane through direct contact of its PH domain with PIP3 and

phosphorylation at Thr308 and Ser473 by two kinases: 3-phosphoinositide-dependent protein kinase (PDK1) (Williams et al. 2000) and DNA-dependent protein kinase (previously called PDK2) (Feng et al. 2004).

Most common *AKT* mutation is p.E17K, a driving mutation with a high frequency of about 15% of all *AKT1*-3 mutations in cBioportal data. It activates AKT signalling and can transform cells (Yi and Lauring 2016). However, Yi et al. (2016) also shown that non-p.E17K *AKT* variants are mainly passenger mutations with no effect on drug sensitivity. Several studies reported a connection of AKT with breast cancer origination (Renner et al. 2008), poor prognosis (Schmitz et al. 2004), metastasis (Li et al. 2014), resistance to chemotherapy (Clark et al. 2002) and hormonal therapy (Pérez-Tenorio and Stål 2002; Kirkegaard et al. 2005). The importance of AKT in cancer has become a target for anticancer therapy, and many companies have been working on finding selective and potent inhibitors. This also gave the basis to use AKT inhibitor in the FAKTION trial.

1.3 Role of Copy Number Variations in Endocrine Resistance

The most common amplified and best described gene in breast cancer is the ERBB2 Receptor Tyrosine Kinase 2 (*ERBB2)* gene located in the 17q21-24 chromosome that encodes the HER2 protein, which is overexpressed in 25-30% of breast cancers (Hudis 2007). Other frequently amplified genes in breast cancer are *MYC* and *FGFR1*. *MYC* gene encodes a transcription factor, a key regulator of cell growth, metabolism, proliferation, differentiation and apoptosis. *MYC* is amplified in about 15% of breast cancers and is associated with a high risk of relapse and death (Green et al. 2016). *FGFR1* encodes tyrosine kinase receptor, which belongs to the fibroblast growth factor receptor family and is amplified in 9 - 15% of breast cancers (Turner et al. 2010). *FGFR1* amplification has been linked with poor prognosis in breast cancer (Turner et al. 2010; Jang et al. 2012). In addition, all three amplifications have been associated with endocrine resistance. In addition, *MYC* amplification is related to resistance to the PI3K/AKT1 pathway inhibitors (Dey et al. 2015).

1.3.1 HER2 Amplification Role in Endocrine Resistance

HER2 amplification is associated with a high risk of relapse and worse clinical outcome but can be effectively treated with anti-HER2 therapy (Arteaga et al. 2011; Heredia et al. 2013; Ha et al. 2014). The *HER2* status of metastatic lesions is not always concordant with the primary tumour. It was reported that the *HER2* status of the primary and metastatic lesions was concordant in only 66% of patients. The rate of molecular conversion from a primary HER2-negative tumour to HER2-positive

metastatic breast cancer was about 10% (Regitnig et al. 2004; Lower et al. 2009). This suggested that the molecular conversion of the primary breast cancer occurred during disease progression. Agents that target the HER2 family of growth factor receptors are anti-HER2 antibodies (trastuzumab, pertuzumab) and small molecule tyrosine kinase inhibitors (lapatinib).

In addition, pre-clinical and clinical evidence suggests that HER2 overexpression plays a role in the development of endocrine resistance, especially after tamoxifen (Shou et al. 2004). The data from various studies indicate that cancers switch from ER to HER2 and vice versa as the favoured signalling pathway, with anti-HER2 therapy leading to an activation of the ER or HER2 pathway (Gutierrez et al. 2005; Creighton et al. 2008). The dependence of both pathways has been highlighted in metastatic breast cancer (MBC) patients who have been treated with an AIs or fulvestrant and had progressed with trastuzumab or lapatinib (Rani et al. 2019). Based on evidence suggesting that cross-talk between the ER and HER2 pathways stimulates endocrine therapy resistance, Figure 6 (Schettini et al. 2016), several clinical trials examined inhibition of HER2 and ER pathway (Bender and Nahta 2008). A TAnDEM phase III study confirmed that combination therapy of the ER and HER2 inhibition benefited dual ER and HER2 positive patients (Kaufman et al. 2009). Patients were treated with trastuzumab plus anastrozole, and this study showed an improved PFS compared with the women on anastrozole alone (Kaufman et al. 2009). In similar a phase II trial, the combination of letrozole and trastuzumab was tested in patients with ER and HER2-positive advanced breast cancer (Marcom et al. 2007). The overall response rate was 26% with a clinical benefit rate of 52%, implying a possible benefit from combination letrozole and trastuzumab in patients with ER and HER2-positive breast cancer. Interestingly, in another phase III study, a combined treatment with AI and lapatinib (anti-HER2 therapy) or AI alone, showed a benefit in the combination arm with a significantly higher PFS in MBC with ER/HER2-positive tumours (Johnston et al. 2009). Breast cancers driven by a HER2 amplified mechanism are recognised to be resistant to endocrine therapy (Johnston et al. 2009; Kaufman et al. 2009; Schwartzberg et al. 2010).

Furthermore, acquired HER2 mutations can cause endocrine resistance in a proportion of patients with ER-positive MBC (Rani et al. 2019). Hotspot mutations in the *HER2* gene (p.D769Y, p.L755S, and p.S310Y) were identified by a whole-genome study (Razavi et al. 2018). These mutations are common in ER-positive MBC patients (Croessmann et al. 2019). They lead to ER independence and resistance to the first-line endocrine therapy, including tamoxifen, fulvestrant, and CDK4/6 inhibitor – palbociclib (Fox et al. 2011; Rani et al. 2019). A combination of endocrine therapy with neratinib (a pan-HER2 inhibitor) can be effective therapy (Nayar et al. 2019). In the ExteNET phase III trial, the greater efficacy of neratinib was attributed to the successful inhibition of cross-talk between ER and HER2 (Johnston 2010). Patients with these cancers benefited from neratinib in the extended adjuvant therapy post-

trastuzumab. This trial showed improved disease-free survival (DFS) for the neratinib group compared with the placebo arm (Chan et al. 2020). Based on that trial FDA has approved neratinib in the adjuvant setting in patients with early HER2 amplified disease (Deeks 2017; Singh et al. 2018; Delaloge et al. 2019).

The accurate HER2 status assessment is critical as it allows patients to receive HER2-targeted therapy, which could lead to better survival outcomes (Tchou et al. 2015; Kim et al. 2018). There is a possibility that the additional benefit of targeted therapy is separate from the endocrine pathway. However, pre-clinical studies suggest cross-talk between signalling pathways. Therefore, the acquired resistance to AIs in ER-positive/HER2-negative cancers may be caused by HER2 upregulation or adaptive epidermal growth factor receptor (Miller and Larionov 2012). This could potentially be delayed or prevented by drugs directed against these targets if only patients were tested at progression to hormonal therapy.

Figure 6. Cross-talk between ER and HER2 pathways, image adapted from (Schettini et al. 2016).
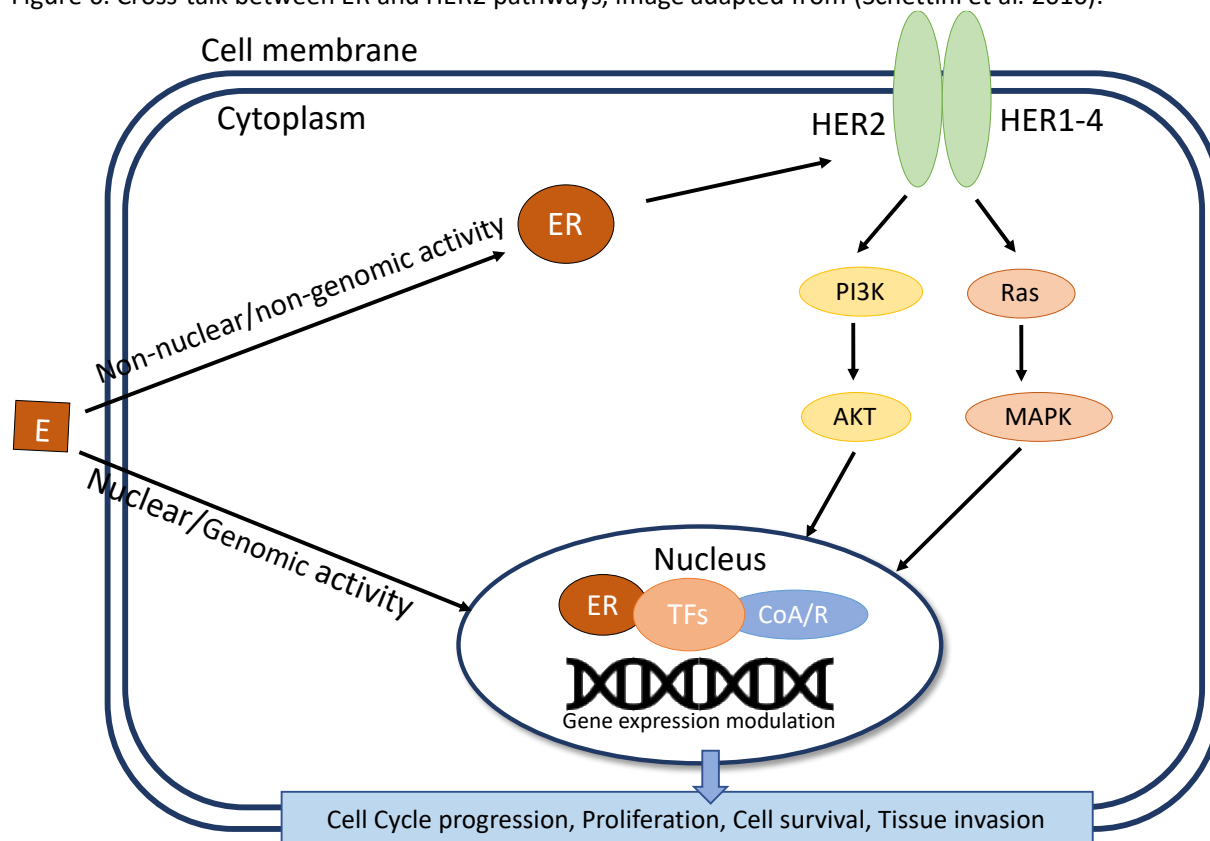
E – Estrogens; Non-nuclear oestrogen receptor (ER) interacts directly or indirectly (via G proteins) with human epidermal growth factor receptor HER2/HER1-4 dimers activating their downstream kinase (Ras/MAPK and PI3K/AKT) pathways, which phosphorylate ER and other transcription factors (TFs) and coactivators/corepressors (CoA/R), modulating gene expression. HER2 signalling pathways also reduce ER expression at both mRNA and protein levels. (Schettini et al. 2016)

1.3.2 MYC Amplification Role in Endocrine Resistance

The oncogenic transcription factor MYC, which encodes a c-MYC protein, is a well-known oestrogen receptor-regulated gene (Shang et al. 2000; Wang et al. 2011). MYC plays an essential role in cell proliferation, growth, differentiation, survival and apoptosis (Grandori et al. 2000). MYC regulates glutamine metabolism in cancer cells and has been linked to endocrine resistance (Miller et al. 2011b; Shajahan-Haq et al. 2014; Chen et al. 2015; Green et al. 2016). Chen, Z. et al.(2015) have shown in pre-clinical studies that glutamine metabolism was independent of oestrogen but still required oestrogen receptor (ER) in AI resistant breast cancer cells. The expression of MYC oncogene was upregulated through the cross-talk between ER and HER2 in AI resistant breast cancer cells. ER down-regulator, fulvestrant blocked MYC expression in AI resistant breast cancer cells. This suggested that MYC is upregulated by constitutively activated ER in AI resistant breast cancer cells. Inhibition of MYC decreased AI resistant breast cancer cell proliferation. They have shown that HER2 regulates MYC expression via the MAPK pathway and activation of ER, Figure 7. However, the AKT inhibitor did not reduce, MYC expression despite decreased phosphorylation of AKT and ERα in AI resistant breast cancer cells (Chen et al. 2015).

Figure 7. Cross-talk between ER and HER2 in AI resistant breast cancer cells, image adapted from (Chen et al. 2015).
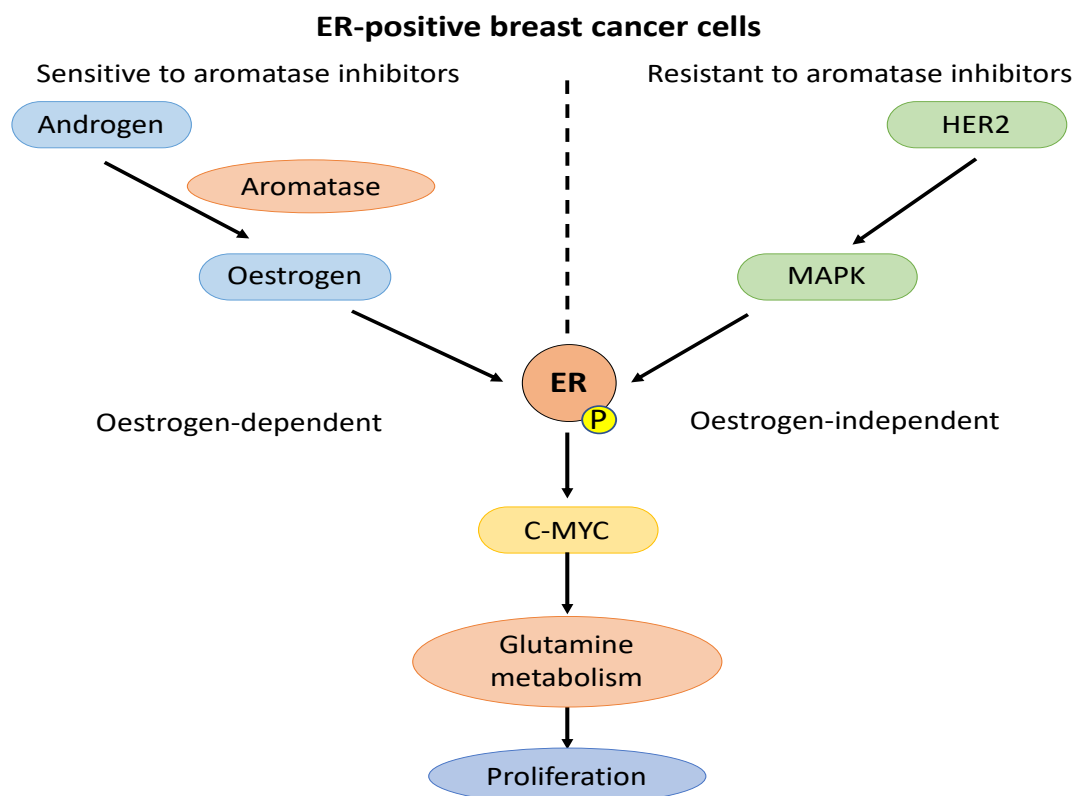
MAPK - mitogen-activated protein kinase; ER - oestrogen receptor; HER2 - Human epidermal growth factor receptor 2.

In mouse models of breast cancer, *PIK3CA* activating mutations led to mammary tumours in mice and sustained PI3K signalling was essential to maintain malignant mammary tumours (Liu et al. 2011). However, after the withdrawal of inducible *PIK3CA* p.H1047R, a significant proportion of mammary tumours restarted growth in PIK3CA-independent manner, and genomic analysis revealed amplification of *MYC* and *MDM2* in these tumours (Liu et al. 2011). Equally, forced *MYC* expression causes resistance to otherwise sensitive *PIK3CA* p.H1047R mutant mammary tumours (Liu et al. 2011). Several human breast cancer databases confirm increased *MYC* amplification in *PIK3CA* mutant breast cancers ranging from 27-47% (Dey et al. 2015). Together, this data highlighted that *MYC* is a vital regulator and plays a role in resistance to PI3K/AKT/mTOR targeted therapies (Liu et al. 2011). It has been suggested that to achieve better responses to PI3K/AKT pathway inhibitors, better patient selection based on tumour testing will be required (Dey et al. 2015).

Figure 8 shows the mechanisms of resistance to PI3K-mTOR targeted therapy described by Tan et al. (2013). This therapy can induce PI3K-dependent and MYC-dependent resistance mechanisms. Inhibition of the PI3K/AKT pathway activates MYC signalling through PDK1-dependent MYC phosphorylation and *MYC* amplification, parallel to PIK3CA-dependent AKT and MAPK activation, decreasing the therapeutic effect of PI3K-mTOR targeted therapy (Tan and Yu 2013).

Figure 8. Potential mechanisms of resistance to PI3K-mTOR inhibitors in human cancers, image adapted from (Tan and Yu 2013).
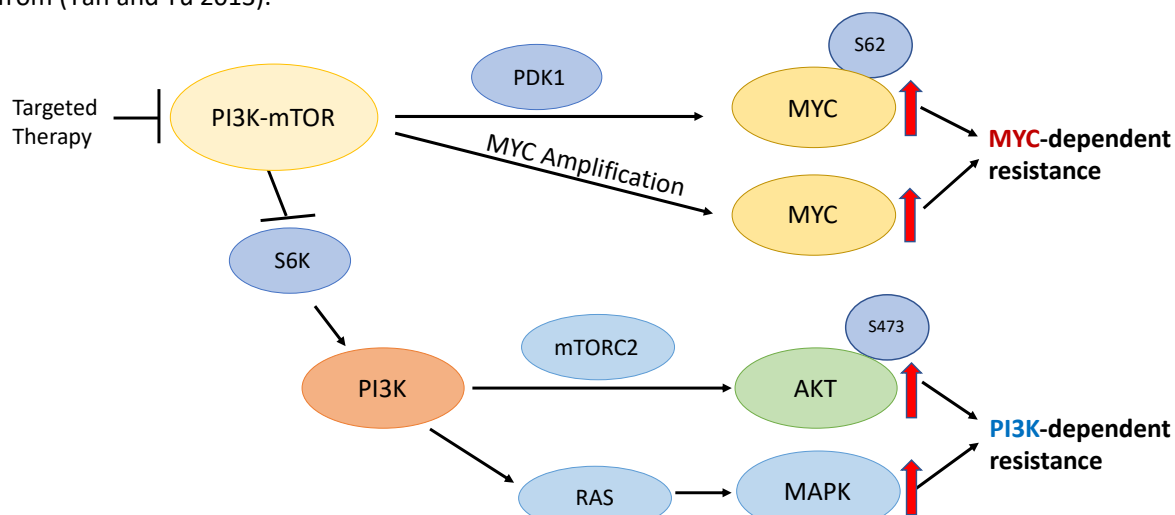
PI3K - phosphatidylinositide 3-kinase; mTOR - mammalian target of rapamycin; PDK1 - 3-phosphoinositide-dependent kinase 1; PIK3CA - phosphatidylinositol-4,5-bisphosphate 3-kinase, catalytic subunit alpha; MAPK - mitogen-activated protein kinase.

1.3.3 FGFR1 Amplification Role in Endocrine Resistance

The fibroblast growth factor receptor (FGFR) family includes five transmembrane receptors (Perez-Garcia et al. 2018). Over the past few years, extensive research has confirmed the vital role of FGFR signalling in cancer cell proliferation, angiogenesis, and survival (Turner and Grose 2010; Babina and Turner 2017), Figure 9. *FGFR1* amplification occurs in approximately 14% of breast cancers, predominantly in the ER-positive/HER2-negative subtype (Elbauomy Elsheikh et al. 2007; Turner et al. 2010; Helsten et al. 2016; Drago 2017). It has been associated with poor prognosis (Turner et al. 2010). Also, studies have shown that FGFR1 overexpression is robustly associated with *FGFR1* amplification (Turner et al. 2010). In vitro studies demonstrated that *FGFR1* amplified breast cancer cell lines express enhanced ligand-dependent signalling with increased activation of the PI3K/AKT and MAPK signalling pathways in response to fibroblast growth factor (FGF) (Turner et al. 2010). Also, the cells express basal independent signalling and are dependent on FGFR signalling to encourage independent growth. This suggests that FGFR1 expression is essential for the survival of *FGFR1*-amplified breast cancer cell lines and supports the oncogenic potential of *FGFR1* amplification (Reis-Filho et al. 2006; Elbauomy Elsheikh et al. 2007).

Figure 9. The FGFR Signalling pathway, image adapted form (Perez-Garcia et al. 2018).
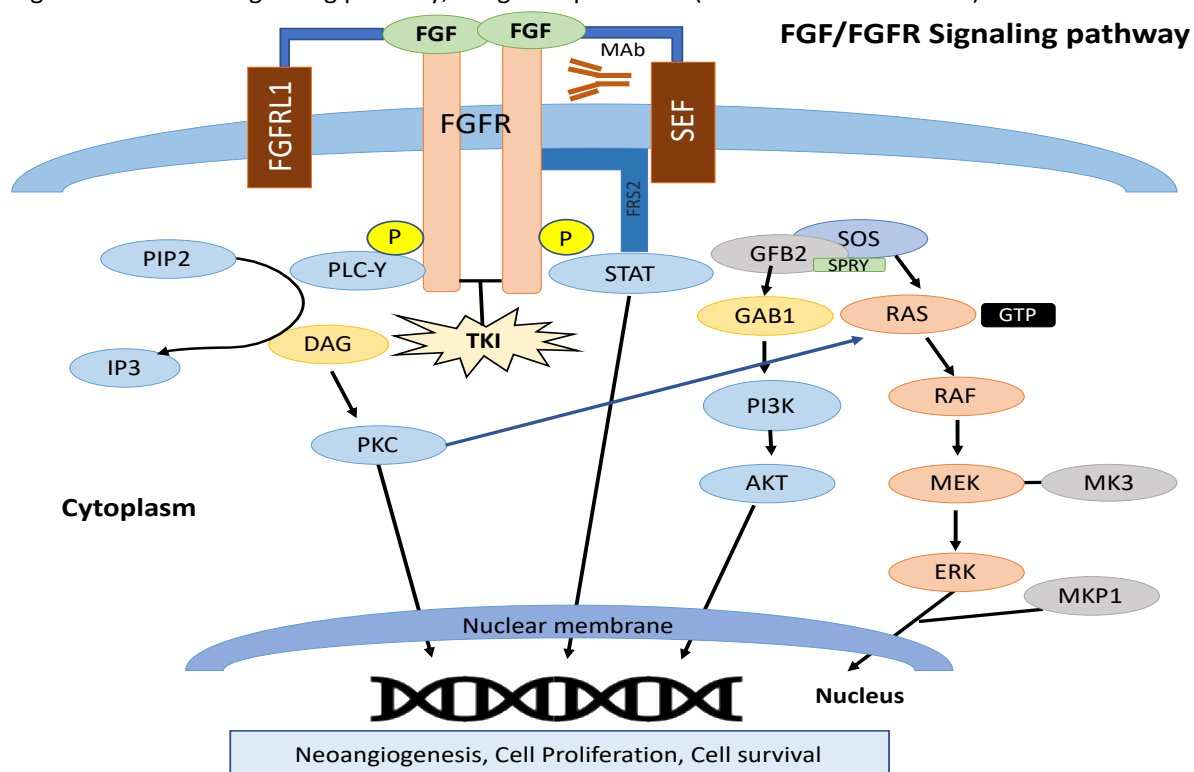
FGF - Fibroblast growth factor; FGFR - Fibroblast growth factor receptor; FGFRL1 - Fibroblast growth factor receptor ligand 1; FRS2 -Fibroblast growth factor receptor substrate 2; ERK - Extracellular signal-regulated kinase; IP3 - Phosphatidylinositol 3,4,5-triphosphate; Mab - Monoclonal antibody; MEK - Mitogen-activated protein kinase; PI3K - Phosphatidylinositol 3-kinase; PIP2 - Phosphatidylinositol 4,5-biphosphate; PKC - Protein kinase.

Several studies have confirmed the clinical and biological importance of *FGFR1* amplification. First, *FGFR1* gene amplification was primarily reported as significantly correlated with shorter overall survival, mainly in ER-positive breast cancer (Reis-Filho et al. 2006). Subsequently, Turner et al. (2010), established an association between *FGFR1* amplification and resistance to endocrine therapy. They demonstrated that *FGFR1*-amplified cell lines showed resistance to an active metabolite of tamoxifen (4-hydroxytamoxifen). These findings confirmed that *FGFR1* amplification had been related to a shorter time to progression on first-line endocrine therapy in patients with ER-positive metastatic breast cancer (Racca et al. 2016; Drago 2017).

FGFR1 amplification has also been treated as a predictive marker for lack of efficacy CDK4/6 inhibitors (Formisano et al. 2017). Experiments in vitro have shown that *FGFR1*-amplified cell lines and xenografts are resistant to oestrogen deprivation, fulvestrant, and palbociclib compared to *FGFR1*-nonamplified models. Also, the group has shown that this resistance to fulvestrant can be overcome by TORC1 inhibition but not by PI3K or CDK4/6 inhibition (Drago et al. 2019). These results suggested that *FGFR1* amplification is responsible for broad resistance to ER, PI3K, and CDK4/6 inhibitors (Drago et al. 2019). However, resistance to AKT1 inhibitors was not explored.

Despite a clear rationale to target the FGFR signalling pathway in breast cancer, the results from various clinical trials testing FGFR inhibitors have shown no sufficient clinical efficacy, even in patients specifically selected (Perez-Garcia et al. 2018). The reason for this has not been identified. There have been some suggestions that *FGFR1* amplification might not be the sign to allow for the identification of sensitive patients. Furthermore, FGFR amplification might not be sufficiently significant to promote breast cancer growth or might not be a driver in breast carcinogenesis, or patients with *FGFR1* amplification are not reliably identified with methods used (Perez-Garcia et al. 2018). However, most of these studies and trials have been focusing on one FGFR1 target. Drago et al. (2019) has pointed out that patients with *FGFR1* amplification were more likely to have co-existent *TP53* mutation and PR-negative disease. Patients with co-existent *TP53* had shorter PFS in response to endocrine therapy and CDK4/6 inhibitor. No studies looked at other co-existence amplifications such as *MYC* and *HER2* amplification combined with other SNVs like *TP53,* which could answer why previous trials with targeted anti-FGFR therapy failed or have not shown the full benefit of targeted therapy.

The pre-clinical studies also revealed that *FGFR1* amplification enhanced PI3K and MAPK signalling pathways, leading to resistance to endocrine therapy (Rugo et al. 2016). Dysregulated PI3K/AKT pathway is frequently seen in cells with *FGFR1* amplification and overexpression (Turner et al. 2010). It has been reported that the response to the PI3K inhibitors is decreased in ER-positive, *PIK3CA* mutant

breast cancer cells that have *FGFR1* amplification (Mayer et al. 2017). This raises the question, whether AKT inhibitors would also have a reduced effect in FGFR1 amplified breast tumours?

1.4 Targeting the PI3K/AKT Pathway and Clinical Trials

Multiple studies reported an association of the PI3K/AKT pathway with resistance to endocrine therapy. Therefore, many laboratories started working on therapeutics that target the PI3K/AKT pathway, such as mTOR inhibitors, PI3K inhibitors and AKT inhibitors, Figure 10. There have been multiple trials with novel drugs inhibiting multiple PI3K/AKT1 pathway targets, Table 1.

Figure 10. Targeting the PI3K pathway in cancer, image adapted from (LoRusso 2016).
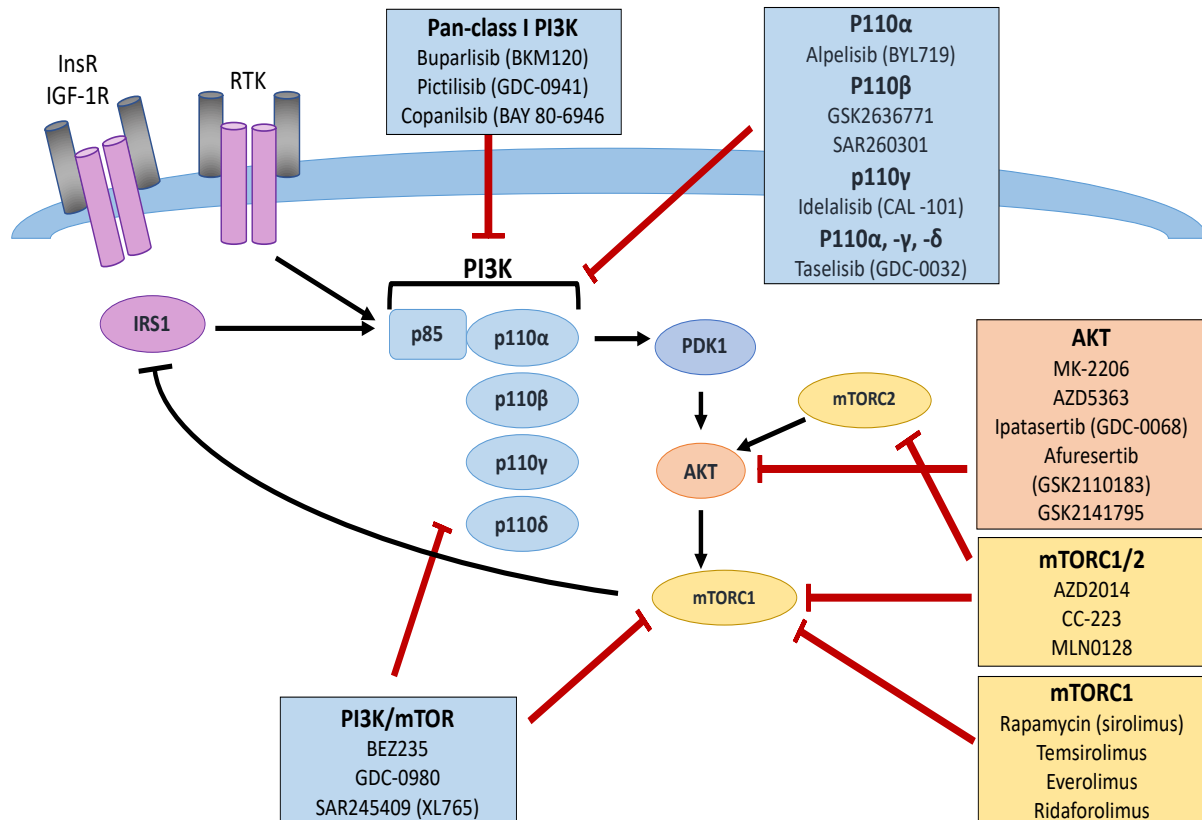
Table 1. Clinical trials that include targeted therapy to overcome endocrine resistance.

Target	Drug name	Trial name ID	Phase	Prior therapy	Control arm	Investigational arm	Primary endpoint	PFS (months)	OS (months)	ORR (%)	Clinicltrials.gov identifier	Status
mTOR inhibitor	Evelorimus	-	II	NO	LET	LET + everolimus	clinical response	NA	NA	59.1 vs 68.1	NCT00107016	completed
		BOLERO-2	III	NSAI	EXE	EXE + evelorimus	TTP	7.8 vs 3.2	26.6 vs 31		NCT00863655	completed
		BOLERO-4	II	NO	single arm	LET + everolimus then EXE + evelorimus	PFS	22 then 3.7	NA	NA	NCT01698918	active
		BOLERO-6	II	AI	1. Evelorimus 2. Capecitabine	3. EXE + evelorimus	PFS	1- 6.8 2- 9.6 3- 8.4	1- 29.3 2- 25.6 3- 23.1	NA	NCT01783444	completed
		TAMRAD	II	AI	TAM	TAM + evelorimus	CB at 24 weeks	8.5 vs. 4.5	Not reached vs. 32.9mo	CBR at 6 mo 61 vs. 42	NCT01298713	completed
	Tensirolimus	HORIZON	III	NO	LET	LET + tensirolimus	PFS	NA	NA	NA		terminated
dual TORC1/2 inhibitor	MLN0128 Sapanisertib	-	I/II	Everolimus + EXE or Fulvestrant	MLN0128 + EXE	MLN0128 + FUL	CBR at 16 weeks	4.1 vs 3.4	15.9 vs 14	45 vs 23	NCT02049957	ongoing
	AZD2014 Vistusertib	MANTA	II	AI	1. FUL	2. Vist + FUL (cont) 3. Vist + FUL (inter) 4. Everolimus + FUL	PFS	1- 5.4 2- 7.6 3- 8.0 4.12.3	NA	NA	NCT02216786	completed
Pan-PI3K inhibitor	BKM120 Buparlisib	BELLE-2	III	AI	FUL	FUL + BKM120	PFS	6.9 vs 5.0 PIK3CA mut 6.8 vs 4.0	33.2 vs 30.4	33.2 vs 30.4 PK3CA mut 26.0 vs 24.8	NCT01610284	completed
		BELLE-3	III	AI and mTORi	FUL	FUL + BKM120	PFS	3.9 vs 1.8	21.2 vs 22.1	NA	NCT01633060	terminated
		BELLE-4	III	NO	PTX +placebo	BKM120 + PTX	PFS	8 vs 9.2	NA	NA	NCT01572727	completed
	BYL719 alpelisib	SOLAR-1	III	AI	FUL	FUL + alpelisib	PFS	5.7 vs 11	NR	12.8 vs 26.6	NCT02437318	active
	Taselisib	Sandpiper	III	AI	FUL	FUL + taselisib	PFS	5.4 vs 7.4	23.6 vs 26.8	12 vs 28	NCT02340221	active, not Recruiting
dual PI3K/mTOR inhibitor	XL147 pilaralisib XL765 voxtalisib	-	I/II	AI	pilaralisib + LET	voxtalisib + LET	MTD/ORR/PFS at 6 mo	PFS at 6 mo 17% vs 8% PFS 2 vs 2	NA	4 vs 0	NCT01082068	completed, terminated
dual PI3K/mTOR inhibitor	GDC0941 pictilisib GDC0980	FERGI	II	AI	FUL	FUL + pictilisib vs.FUL + GDC0980	PFS	6.6 vs 5.1, PIK3CA mut 6.5 vs 5.1	NA	7.9 vs. UN vs. 6.3	NCT01437566	completed
Akt inhibitor	AZD5363 capivasertib	BEECH	I/II	YES	capivasertib + wPTX vs. wPTX	capivasertib + wPTX	PFS	8.4 vs 10.9	n.s	NA	NCT01625286	completed
	AZD5363 capivasertib	STAKT	II WOO	NO	placebo	capivasertib 480, 360, 240mg dose	Biomarker analysis	NA	NA	NA	NCT02077569	completed
	AZD5363	FAKTION	I/II	AI	FUL	FUL+ capivasertib	PFS	4.8 vs 10.6	NR	NA	NCT01992952	completed
	MK2206	-	II	YES	Monotherapy	MK2206	ORR and PFS at 6 mo	NA	NA	4.7	NCT01277757	terminated - fultility
CDK4/6 inhibitor	palbociclib	PEARL	III	NSAI	Capecitabine	EXE + palbociclib	PFS	11 vs 8	NR	NA	NCT02028507	active
	ribociclib	MONALEESA-2	III	NO	LET	LET + ribociclib	PFS	16 vs 25.3	NR	NA	NCT01958021	completed accrual
	abemaciclib	MONARCH 2	III	YES	FUL	FUL + abemaciclib	PFS	9.3 vs 16.4	37.3 vs 46.7	NA	NCT02107703	completed accrual
	abemaciclib	MONARCH 3	III	NO	AI	AI + abemaciclib	PFS	28.18 vs 14.76	NA	NA	NCT02763566	active, not trecruting
	palbociclib	PALOMA-2	III	NO	LET	LET + Palbociclib	PFS	14.5 vs 24.8	NA	38 vs 46	NCT01740427	completed
	palbociclib	PALOMA-3	III	YES	FUL	FUL + Palbociclib	PFS	4.6 vs 11.2	28 vs 35	NA	NCT01942135	completed

FUL – fulvestrant, LET- Letrozole, EXE – Exemestane, AI – Aromatase inhibitors, NSAI – non-steroid aromatase inhibitors, PFS – Progression-Free survival, TTP – Time to Progression, OS – Overall survival, NR – Not reported, NA – Not Available, CB Clinical benefit, CBR – Clinical benefit rate, WOO – Window of opportunity.

1.4.1 CDK4/6 Inhibition and Clinical Trials

Trials with CDK4/6 inhibitors, reported a significant PFS and OS improvement in combination with endocrine therapy in patients with advanced ER-positive breast cancer.

PALOMA-1 phase II trial compared palbociclib and letrozole with letrozole alone in patients with ER-positive breast cancer (Finn et al. 2015). The combination therapy was associated with significantly longer PFS (20.2 vs 10.2 months; p = 0.0004) (Finn et al. 2015). Overall survival was not as significant (37.5 vs 34.5 months, p=0.28) (Finn et al. 2017). This landmark study led to accelerated approval by the FDA for the combination treatment for advanced ER-positive and HER2-negative breast cancers.

Subsequently, PALOMA-2 phase III trial was developed to confirm the benefit of palbociclib plus letrozole over letrozole alone in patients with untreated ER-positive breast cancer. The combination therapy of letrozole and palbociclib had longer median PFS (24.8 vs 14.5 months, p<0.001) (RS et al. 2016). PALOMA-3 phase III trial compared palbociclib plus fulvestrant to fulvestrant alone in patients who progressed on endocrine therapy. This trial met its primary endpoint of improved median PFS by 6.6 months (11.2 vs 4.6 months, p<0.0001). The combination improved OS by 6.9 months, although this did not reach statistical significance (34.9 vs 28.8 months, P=0.09) (Turner et al. 2018).

The second CDK4/6 inhibitor - ribociclib, was approved by the FDA for the first-line treatment with any AI in women with advanced ER-positive and HER2-negative breast cancers. The approval was based on the outcome of MONALEESA-2 phase III trial, favouring a combination of ribociclib and letrozole over letrozole only. Updated results showed that median PFS was better for combination therapy (25.3 vs 16 months, $p = 9.63 \times 10^{-8}$) however, OS data remains immature (Hortobagyi et al. 2019). Also, ribociclib is investigated in MONALEESA-7 trial. The interim analysis reported a statistically significant OS improvement in combination with endocrine therapy in premenopausal or perimenopausal patients with ER-positive breast cancer (Im et al. 2019).

Another two phase III trials (MONARCH-2 and MONARCH-3) assessed third CDK4/6 inhibitor abemaciclib with fulvestrant (MONARCH-2) in advanced endocrine resistant ER-positive breast cancer and with AI (MONARCH-3) in the first line setting for advanced ER-positive breast cancer. Both studies reported improved PFS for combination therapy as initial treatment for patients with advanced ER-positive breast cancer (28.18 vs 14.76 months, p = 0.000002) in MONARCH-3 trial (Goetz et al. 2017), and as well as a sequential treatment after progression on endocrine therapy (16.4 vs 9.3 months, p < 0.001) in MONARCH-2 trial (Sledge et al. 2019). MONARCH-2 trial also reported OS benefit of 9.4

months (46.7 vs 37.3 months, p = 0.01) regardless of menopausal status. These trials have reported significant PFS and OS improvements compared to trials with the PI3K/AKT pathway inhibitors. It would be hard for PI3K/AKT inhibitors to compete in first-line treatment. However, possibly it could be a place for these inhibitors in selected patients or in the next treatment line after progression on CDK4/6 inhibitors.

1.4.2 MTOR Inhibition and Clinical Trials

Several clinical studies reported improved progression-free survival (PFS) with inhibitors of the PI3K/AKT pathway combined with endocrine therapies, Table 1. The mTOR inhibitors have been developed, including everolimus (Novartis) (Tabernero et al. 2008) and temsirolimus (Wyeth) (Chan et al. 2005) as rapamycin derivatives that inhibit mTOR through binding to mTORC1. Pre-clinical studies showed synergistic inhibition of proliferation and induction of apoptosis when everolimus is combined with AIs. Several phase II and III trials with mTOR inhibitor were completed in patients with ER-positive breast cancers, and three main randomised trials reported efficacy data (Bachelot et al. 2012; Baselga et al. 2012; Wolff et al. 2013), Table 1.

In BOLERO-2 phase III study, the mTOR inhibitor everolimus improved PFS in combination with the aromatase inhibitor exemestane (3.2 months versus 7.8 months, p < 0.0001) irrespective of the status of the PI3K pathway, although at the cost of additional toxicity (Yardley et al. 2013; Hortobagyi et al. 2016). This has led to FDA and EMA approval of everolimus to be used in combination with exemestane in patients who previously failed treatments with AIs. However, the updated results did not find a significant overall survival (OS) benefit for combination therapy, with a median OS of 31 months for the everolimus arm versus 27 months for the placebo arm (HR = 0.89; p = 0.14) (Piccart et al. 2014).

Similarly, TAMRAD phase II study randomised tamoxifen with everolimus versus tamoxifen alone in patients with metastatic ER-positive breast cancer previously treated with endocrine therapy (Bachelot et al. 2012). In this study, clinical benefit at six months was better for combination therapy than tamoxifen alone (61 % versus 42 %, respectively, p = 0.045). Also, time to progression (TTP) was superior in the combination arm (8.6 versus 4.5 months; HR 0.54, p = 0.0021), and also OS was favourable for the combination arm (Bachelot et al. 2012). Interestingly, HORIZON phase III trial that randomised another combination of mTOR inhibitor - temsirolimus with letrozole versus letrozole plus placebo as first-line endocrine treatment was terminated prematurely due to futility (Wolff et al. 2013). This trial's analysis showed no difference in PFS between the two arms (median PFS of 9 months, p = 0.25) (Wolff et al. 2013).

BOLERO-4 phase II trial will determine the benefits from everolimus with letrozole in the first-line settings and evaluate whether the lack of benefit seen with temsirolimus in the HORIZON trial was related to the patient population. Although some preclinical studies have observed that the PI3K/AKT pathway is activated after previous exposure to endocrine therapy, this will need to be confirmed in clinical trials (Yamamoto-Ibusuki et al. 2015).

BOLERO-6 phase II trial randomised patients to three arms: everolimus plus exemestane, exemestane alone, and capecitabine in patients who were exposed previously to endocrine therapy (Jerusalem et al. 2018). This was the first trial that allowed direct comparison of endocrine therapy with mTOR inhibitors with chemotherapy. In this study, the median PFS with everolimus plus exemestane was 8.4 months, consistent with reported in the BOLERO-2 study (7.8 months), and the PFS was longer than arm with everolimus alone (6.8 months). There was a favourable PFS difference of capecitabine (9.6 months) versus everolimus plus exemestane (8.4 months). However, the authors pointed out that the results needed to be interpreted cautiously because the capecitabine outcome was inconsistent with previous capecitabine studies (PFS range, 4.1-7.9 months) (Jerusalem et al. 2018). It was reported that the PFS difference between the two arms was possibly due to informative censoring in the setting of an open-label study and possible imbalances in prognostic factors and baseline characteristics (Jerusalem et al. 2018).

Unfortunately, the median OS for the combination of everolimus with exemestane in BOLERO-6 (23.1 months) was inconsistent with the BOLERO-2 study (31.0 months) (Piccart et al. 2014), with the same median follow-up time (approximately four years). This could be due to smaller sample size of the study (n = 104 in BOLERO-6 versus n = 485 in BOLERO-2) or due to different patterns of anticancer therapies commenced between the two studies after treatment discontinuation. In addition, in BOLERO-2, more patients were fitter with an ECOG performance status of 0, and fewer patients had three or more metastatic sites than in the BOLERO-6 study. This highlights the fact of how basic characteristics can be important and influence trials results. Interestingly, the median OS with everolimus plus exemestane (23.1 months) was also shorter compared to everolimus alone (29.3 months) and capecitabine (25.6 months) in this study. However, the median OS for the capecitabine arm was consistent with previous capecitabine studies (18.6-29.4 months) (Jerusalem et al. 2018). Unfortunately, the patient stratification was not based on biomarkers analysis which could potentially help explain the results.

Many efforts have been put to identify potential biomarkers of benefit from mTOR inhibition in breast cancer patients. TAMRAD trial examined 55 formalin-fixed paraffin-embedded (FFPE) primary samples, using Immunohistochemistry (IHC) and suggested that everolimus is more effective in patients with

high levels of p4EBP1 (a downstream effector of the mTOR pathway), implying that baseline mTOR activation might be associated with sensitivity to mTOR inhibition (Treilleux et al. 2013). In BOLERO-2, 309 samples were tested with next generation sequencing and found that PFS for everolimus was maintained regardless of the genetic alteration *in PIK3CA, FGFR1 CCND1* (Hortobagyi et al. 2016). Interestingly, the presence of *PIK3CA* mutations was not predictive of benefit from everolimus treatment. This suggested that mTOR inhibitors' primary resistance might depend on the coexistence of mutations or amplifications in other pathways. Therefore, combination therapy with other target agents should be considered for these patients. However, this is not always possible as 1. Lack of or in development of other target inhibitors; 2. Adding another target can add more toxicity to already toxic treatment; 3. The new combination would require further trials in a selected and smaller group of patients, which can be challenging to perform and take a long time. Another solution could be to identify other co-existing targets prospectively and run future trials, excluding these patients or randomised against standard treatment chemotherapy until a target is developed.

1.4.3 PI3K Inhibition and Clinical Trials

Other approaches have been developed to inhibit the PI3K/AKT pathway. The development of drugs that inhibit the pathway at a proximal level of PI3K. There are two types of PI3K inhibitors in development: Pan-PI3K inhibitors that target all isoforms of PI3K and the isoform-specific PI3K inhibitors such as PI3K subunit α (Rodon et al. 2014). The isoform-specific PI3K inhibitors can better block the target whilst minimising off-target side effects from inhibition of other isoforms (Rodon et al. 2014). Several studies with pan-PI3K inhibitors include XL147 (pilaralisib) (Shapiro et al. 2014), GDC-0941 (pictilisib) (Sarker et al. 2015), and BKM120 (buparlisib) (Rodon et al. 2014), Table 1.

Pan-PI3K Inhibitors

Buparlisib, as a single agent, showed a modest effect (Rodon et al. 2014). Subsequently, buparlisib was studied in three phase III trials, in combination with fulvestrant in patients previously treated with an AIs (BELLE-2), after the resistance of mTOR inhibitor (BELLE-3) and also in combination with chemotherapeutic drug – paclitaxel (BELLE-4), Table 1**.** Buparlisib showed minimal clinical activity in BELLE-2 with a median PFS of 6.9 months versus 5 months (p=0.00021) for a combination of fulvestrant and buparlisib (Campone et al. 2018). For patients with *PIK3CA* mutation, the benefit was only slightly better but not significant (6.8 vs 4.0 months, p=0.014) (Campone et al. 2018). OS benefit (33.2 vs 30.4 months, p = 0.045, for *PIK3CA*-mutant 26.0 vs 24.8 months) was in favour of combination therapy but again not significant and had an unfavourable toxicity profile.

Another FERGI phase II trial of GDC-0941 (pictilisib) in combination with fulvestrant did not show a significant improvement in PFS in the combination group compared with placebo (6.6 vs 5.1 months, respectively, p=0.096) (Krop et al. 2016). The combination arm showed no correlation in the subgroup with *PIK3CA* mutation (6.5 vs 5.1, p=0.268) (Krop et al. 2016). However, patients with *PIK3CA* mutation had a higher objective response rate (16 % vs 3.0 %, p=0.73) (Krop et al. 2016). Due to modest activity and adverse toxicity profile, Pan-PI3K inhibitors are no longer in development for this indication. BELLE-4 trial was terminated due to futility. BELLE-3 trial was closed early, and drug development was stopped.

PI3K-α subunit inhibitors

However, Alpelisib, a PI3K-α subunit inhibitor, showed promising activity in early-phase trials with pre-treated *PIK3CA* mutant breast cancers (Gonzalez-Angulo et al. 2013). Recently, phase III SOLAR-1 trial reported the significantly improved efficacy of fulvestrant by 5.3 months (5.7 vs 11 months, p=0.00065), but only in tumours with *PIK3CA* hotspot mutations (André et al. 2019), Table 1. This result led to selected approval for alpelisib combined with fulvestrant in patients with ER-positive, *PIK3CA* mutated advanced breast cancer. However, the side effects continue to be problematic. Furthermore, a similar study with another PI3Kα inhibitor (taselisib) showed only two months advantage in PFS (5.4 vs 7.4 months, p=0.0037) in patients in *PIK3CA* mutant tumours. Thus, the unmet need remains for patients with no *PIK3CA* mutation but have the PI3K/AKT pathway activated.

1.4.4 Dual Inhibition of PI3K and mTOR in Clinical Trials

The presence of a negative feedback loop in the PI3K/AKT pathway has been identified, in which activation of mTORC1/S6K1 inhibits growth factor signalling to PI3K, using negative feedback to IGF-1 signalling (Yamamoto-Ibusuki et al. 2015). Loss of this negative feedback mechanism occurs in tumours exposed to mTOR inhibitors, especially those that block mTORC1, which leads to mTORC2 assembly and an increase in phosphorylation of AKT Ser473 (Shah et al. 2004). Also, mTOR inhibition can lead to an escape pathway to MAPK signalling (Shah et al. 2004; Gupta et al. 2007) and an up-regulation of platelet-derived growth factor receptor (PDGFR) signalling (Gupta et al. 2007). Therefore, inhibition from upstream to mTOR in the PI3K/AKT pathway might enhance the mTOR inhibition and maximise an anti-tumour effect (Yamamoto-Ibusuki et al. 2015).

In order to overcome this AKT activation by the escape loop caused by mTORC1 inactivation, several different approaches have been studied. The first one included PI3K and mTOR's dual blockade by

combining a PI3K inhibitor with an mTOR inhibitor. The combination of alpelisib (PI3K-α subunit inhibitor) in combination with everolimus (mTOR inhibitor) and exemestane was tested in the phase IB study (Novartis 2020) but results have been not published yet.

Another approach includes mTORC1/mTORC2 complex inhibitors. These were studied in the four-arm phase II, MANTA trial with vistusertib in two different schedules (continuous or intermittent) combined with fulvestrant versus fulvestrant and everolimus versus fulvestrant alone - control arm (Schmid et al. 2019). Unfortunately, there was no significant difference in PFS between those receiving a fulvestrant with continuous or intermittent vistusertib and fulvestrant alone (5.4 vs 7.6 vs 8.0 months respectively, p = 0.46). Thus, the trial failed to demonstrate the benefit of adding the dual mTORC1/2 inhibitor to fulvestrant. However, median PFS of fulvestrant and everolimus (PFS = 12.3 months) was significantly longer compared with fulvestrant plus continues vistusertib (7.6 months, p = 0.01) and to fulvestrant alone (5.4 months, P = .01), Table 1.

1.4.5 AKT Inhibition and Clinical Trials

Several AKT inhibitors are currently being studied in clinical trials to establish their benefit, Table 1. Most AKT inhibitors like MK2206, GSK2141795 and AZD5363 (capivasertib) are pan-AKT inhibitors that block all three AKT isoforms (AKT1, AKT2, AKT3) (Hinz and Jücker 2019). AKT1/2 inhibitor had good results in preclinical studies but failed in clinical trials due to toxicity (Pérez-Tenorio et al. 2014). Therefore, no isoform-specific inhibitors are under clinical investigation. This is the opposite effect of PIK3CA inhibitors, where specific isoform inhibitors are being developed, such as alpelisib and teselisib, but pan-PIK3 inhibitors development was discontinued due to high toxicity and minimal clinical effect.

In addition, treatment with pan-AKT inhibitors with a low dose can increase metastasis development as it predominately inhibits AKT1. Therefore, creating AKT isoform-specific drugs could be questionable and require further investigations (Li et al. 2018c). However, they can have a more powerful effect than treatment with mTOR inhibitor in vitro (DeFeo-Jones et al. 2005) as AKT1 is responsible for proliferation and survival of breast cancer cells whilst having an anti-metastatic effect. AKT2 is involved in the metastatic process. The AKT3 effect is not fully known, but it seems to have an anti-migratory effect (Hinz and Jücker 2019).

Capivasertib (developed by AstraZeneca) is a potent ATP-competitive inhibitor of all three isoforms of the serine/threonine kinase AKT (AKT1, AKT2, AKT3). Capivasertib inhibits phosphorylation of PRAS40, GSK3β (AKT substrates), S6 and 4E-BP1, but it increases the phosphorylation of AKT at Thr308 and

Ser473 (Davies et al. 2012). In preclinical studies, breast cancer cells lines were the most sensitive cells (Addie et al. 2013). In addition, activating mutations in PIK3CA and AKT1 or loss of PTEN significantly increased capivasertib sensitivity (Shariati and Meric-Bernstam 2019). The combination of capivasertib with fulvestrant demonstrated the synergistic efficacy in ER-positive, endocrine-sensitive and endocrine-resistant breast cancer cell lines, particularly those with *PIK3CA* mutation or loss of *PTEN* function (Ribas et al. 2015). In contrast, wild type cell lines were resistant to capivasertib (Ribas et al. 2015).

In addition, capivasertib had minimal clinical activity as a single agent in ER-positive breast cancer patients with *AKT1* and *PIK3CA* mutation. In the BEECH study, capivasertib did not increase the effect of paclitaxel in ER-positive breast cancers (Turner et al. 2019). However, in the PAKT study, the combination of capivasertib and paclitaxel increased the median PFS from 3.7 to 9.3 (p=0.1) for patients with PIK3CA/AKT1/PTEN-altered triple-negative breast cancers (Schmid et al. 2020). Furthermore, capivasertib improved the efficacy of fulvestrant in the FAKTION trial by improving PFS from 4.8 months to 10.6 months, p=0.0044 (Jones et al. 2020).

1.4.6 FAKTION Trial Overview and Rationale

FAKTION was a randomised, double-blind, placebo-controlled, phase 2 trial for postmenopausal women with ER-positive, HER2-negative metastatic or locally advanced inoperable breast cancers who had progressed or relapsed on aromatase inhibitors. The trial aimed to evaluate whether the addition of capivasertib to fulvestrant can improve progression-free survival in patients with endocrine-resistant advanced breast cancer. Patients were recruited from 19 UK hospitals and randomly assigned (1:1) to receive intramuscular fulvestrant 500mg every 28 days (plus loading dose on day 15 of cycle 1) with either capivasertib 400mg or placebo, orally twice a day on an intermittent weekly schedule of 4 days on and 3 days off (starting on cycle 1 Day 15) until disease progression, unacceptable toxicity, loss of follow-up, or withdrawal from the trial. Randomisation was performed using an interactive web-response system using a minimisation method and the minimisation factors (measurable or non-measurable disease, primary and secondary AI resistance, PIK3CA and PTEN status). The primary endpoint was PFS, Figure 11. (Jones et al. 2020).

140 patients were recruited to the trial over three years (2015-2018), of which 69 received fulvestrant with capivasertib and 71 received fulvestrant and placebo. Median PFS was significantly longer in the capivasertib group with 10.3 months versus 4.8 months in the placebo group (HR - 0.58, p = 0.0044), Figure 12. The objective response rate was 29% in the capivasertib group compared with 8% in the

placebo group (odds ratio - 4.42, p = 0.0031). Overall survival data were immature at the time of reporting PFS data. However, the median overall survival (OS) was 26.0 months in the capivasertib group and 20.0 months in the placebo group (HR - 0.59, p = 0.071). (Jones et al. 2020)

Figure 11. FAKTION trial design.

FAKTION trial

Randomized, double-blind, placebo-controlled, phase 2 trial

Patient Stratification

- **PIK3CA/PTEN** status
- Measurable vs non-measurable disease
- Primary vs secondary endocrine resistance

RANDOMISATION

Experimental Arm (n=69)
Fulvestrant 500mg + Capivasertib 400mg

Control Arm (n=71)
Fulvestrant 500mg + placebo

Primary endpoint:
- PFS

Secondary Endpoints:
- OS
- Safety
- Tolerability
- Clinical benefit rate
- Efficacy relative to baseline PIK3CA pathway activity

Treatment was continued until progression, excess toxicity or withdrawal

n = number of patients

Figure 12. Progression-free survival data of FAKTION trial, image from (Jones et al. 2020)

HR - hazard ratio, CI – Confidence Interval
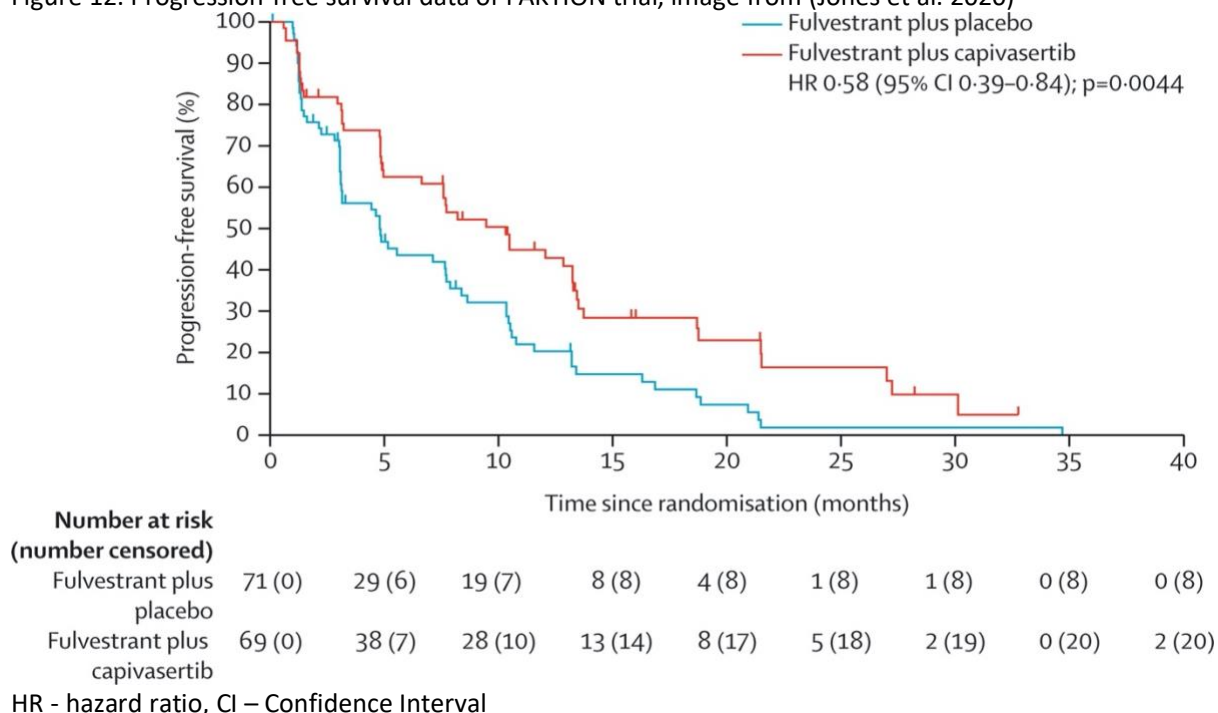
Assessment of the efficacy of capivasertib with fulvestrant in patients with PI3K/PTEN pathway altered versus non-altered tumours was a prespecified objective of the trial. The PI3K/PTEN pathway altered breast cancer was defined by detection of mutations in exon 9 and 20 of PIK3CA in FFPE DNA or circulating tumour DNA (ctDNA) or PTEN loss in FFPE (tumours that scored "0" in immunohistochemistry). (Jones et al. 2020)

59 (42%) of 140 tumours had PI3K/PTEN pathway altered with 31 (45%) of 69 in the capivasertib group and 28 (39%) of 71 in the placebo group. 81 (58%) of 140 tumours were non-altered, with 38 (55%) of 69 in the capivasertib group and 43 (61%) of 71 in the placebo group. (Jones et al. 2020)

In the altered group, median PFS was 9.5 months in the capivasertib group and 5.2 months in the placebo group (HR 0.59, p = 0.064). In the non-altered group, median PFS was 10.3 months in the capivasertib group and 4.8 months in the placebo group (HR 0.56, p = 0.035), Figure 13. This showed that the significant improvement in PFS seen with combination therapy was preserved in the non-altered group but not in the altered group. (Jones et al. 2020)

Provisional overall survival data showed that in the altered group, median OS was longer in the capivasertib group with 30.5 months versus 18.7 months in the placebo group (HR 0.53, p = 0.17). However, in the non-altered group, median OS was not significantly longer between the capivasertib group and the placebo group, 23.7 versus 20.3 months, respectively (HR 0.62, p = 0.20) (Jones et al. 2020). Although these results were not statistically significant, the trends might be preserved once mature overall survival data will be reported.

Figure 13. Progression-free survival in subgroups by PI3K pathway alteration status, image form (Jones et al. 2020)
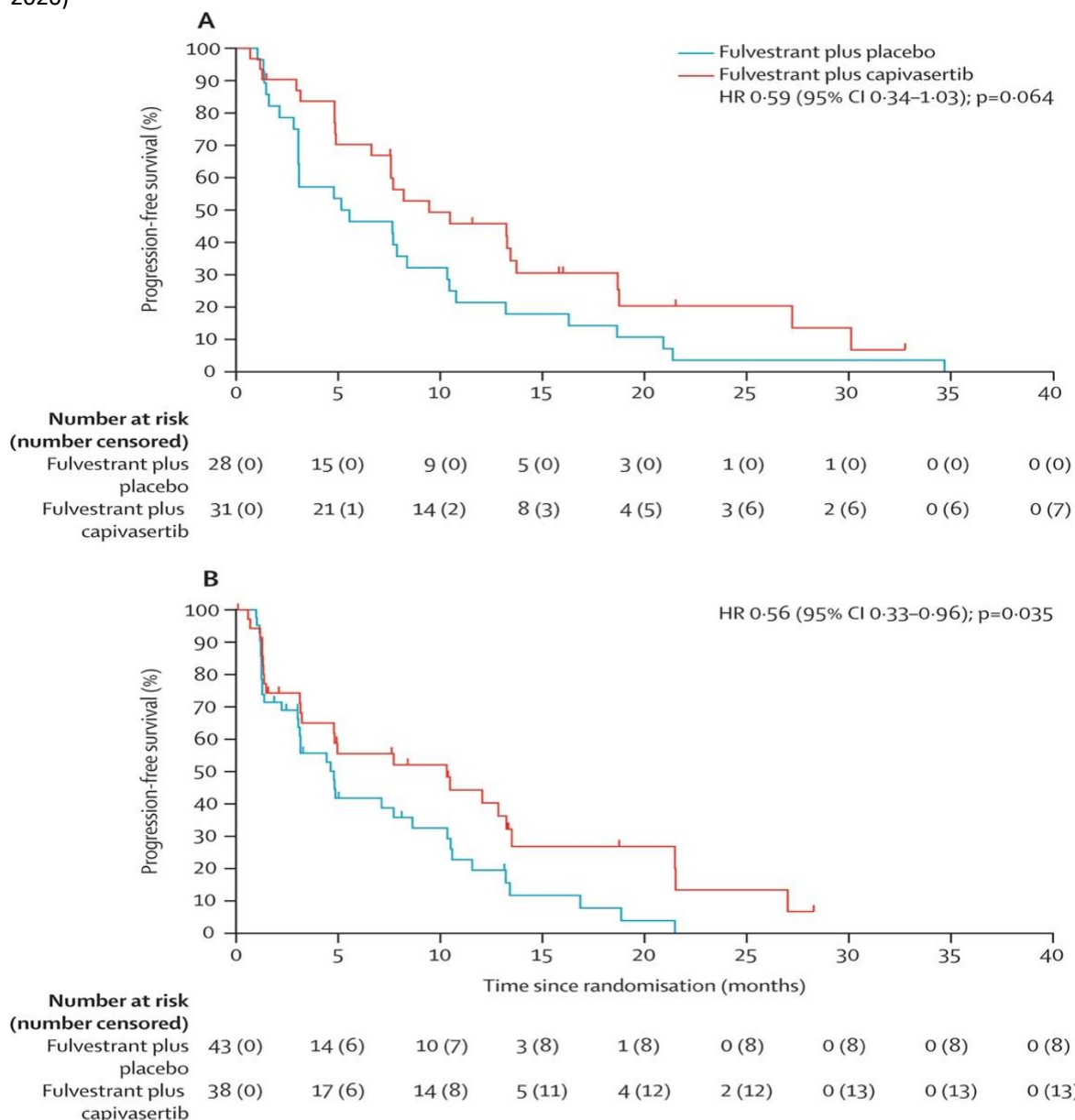
(A) The pathway-altered subgroup. (B) The pathway non-altered subgroup. HR - hazard ratio, CI - Confidence Interval.

In the FAKTION trial, archival tumour tissue and translational blood samples were collected before treatment, following two treatment cycles and at progression to trial therapy, Figure 14. These samples, as well as the clinical outcome data, formed the basis of this research project. Longitudinal analysis of the genetic markers during therapy is recognised as an essential step in informing rational treatment choices, and ctDNA provides material representative of the overall genetic profile of cancer at a particular time point. In addition, interrogation of exploratory biomarkers within the context of a clinical trial provides an opportunity for a controlled analysis concerning clinical outcomes.

Figure 14. Sample collection in the patient journey before and during the FAKTION trial.
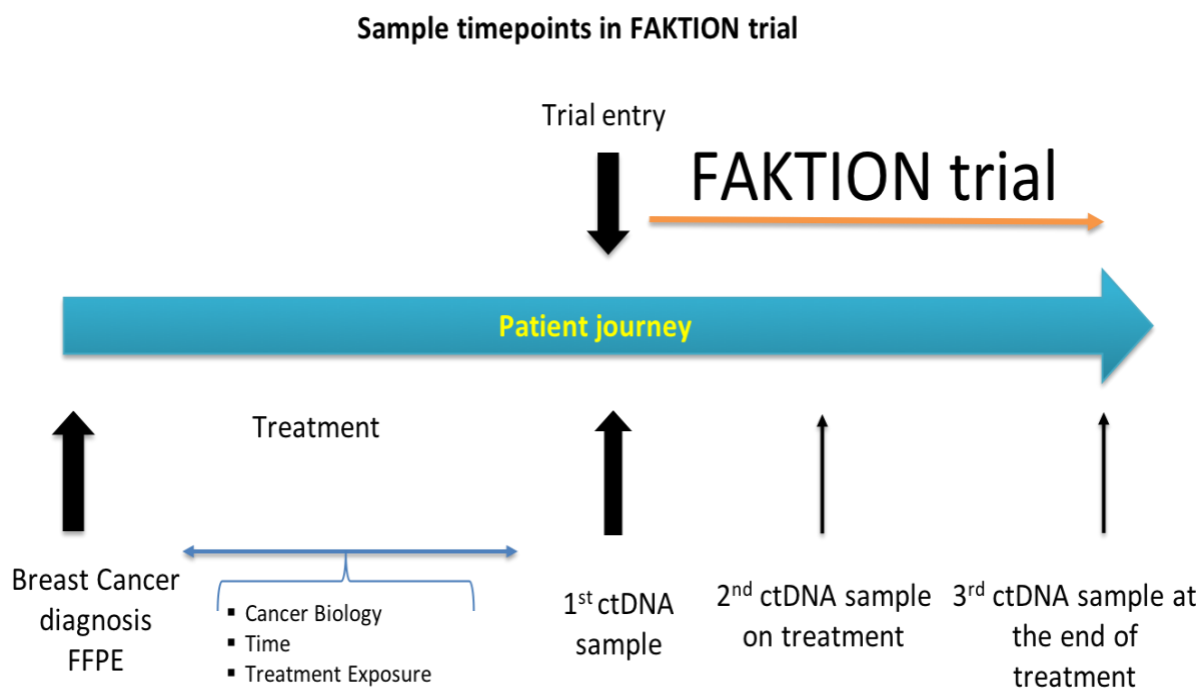
FFPE – Formalin Fixed Paraffin Embedded tissue, ctDNA – Circulating Tumour DNA.

1.5 Circulating Tumour DNA as a Biomarker

1.5.1 Background

Circulating tumour DNA (ctDNA) is a tumour-derived DNA shed to circulation and is part of circulating free DNA (cfDNA). CtDNA was first described in plasma by Mandel and Metais in 1948 (Mandel and Metais 1948). It has been detected in patients with various solid cancers, including breast cancers. Previous studies have demonstrated that ctDNA is released through cell death via necrosis, apoptosis (Jahr et al. 2001; Diehl et al. 2008), and active secretion (Stroun et al. 2001; Assou et al. 2014). In a recent study, Weng et al. (2017b) showed that active release could occur via extracellular vesicles, such as exosomes. Also, it is essential to note that most ctDNA is not derived from circulating tumour cells (CTCs), as CTSs are rare in circulation and ctDNA levels are 100 to 1000 times the concentration generated from apoptosis of CTCs (Thierry et al. 2016).

The necrotic or apoptotic release of ctDNA causes the fragmentation of DNA. The ctDNA released by necrosis is generally less fragmented DNA (fragments >10,000bp) than that generated via apoptosis, which produces fragments of 160–180 bp (Jiang et al. 2015; Barbany et al. 2019). This difference is anticipated to occur due to the higher DNAase activity during apoptotic cell death (Nagata 2000). DNA

can be released into the circulation by either tumour, and this would be called circulating tumour DNA (ctDNA) or non-tumour tissue, which will be called cell-free DNA (cfDNA) (Thierry et al. 2010).

In general, the ctDNA proportion of total cfDNA varies, ranging from <0.01% to 90% (Jahr et al. 2001) but a very high proportion is very uncommon. The range between 0-65% is more frequent in metastatic patients, and lower levels are more common in patients with localised disease (Jung et al. 2010). The fraction of ctDNA compared to background wild-type DNA is known as the variant allele frequency (VAF) or mutant allele frequency (MAF). The rate of ctDNA shedding into the circulation depends on the size, grade, location and vascularity of the tumour, which leads to a difference in ctDNA levels among patients (Fernandez-Cuesta et al. 2016). Bettegowda et al. (2014) investigated the quantification of ctDNA fragments in multiple cancers, including breast cancer, Figure 15. They were able to detect ctDNA in most patients with metastatic cancers; however, the concentration varied among tumour types and patients within the same tumour type (Bettegowda et al. 2014). In breast cancer, the median cfDNA concertation can differ between subtypes. Salimi and Sedaghati Burkhani (2019) reported a median cfDNA concertation of 23 ng/ml of plasma (range 11-100) for triple-negative cancer (TNBC); however, for ER, PR positive or HER2 positive breast cancers (non-TNBC), a median cfDNA concentration was 13ng/ml (range 5.1-78). In addition, the lymph node-positive and stage IV breast cancers in both TNBC and non-TNBC showed significantly higher cfDNA concentrations (Salimi and Sedaghati Burkhani 2019).

Despite the low cfDNA concentrations, it is possible to detect genetic mutations with polymerase chain reaction (PCR) based technologies (Diaz and Bardelli 2014), such as next-generation sequencing (NGS) and digital droplet PCR (ddPCR).

Figure 15. Quantification of mutant DNA fragments in advanced malignancies, figure adopted from (Bettegowda et al. 2014)
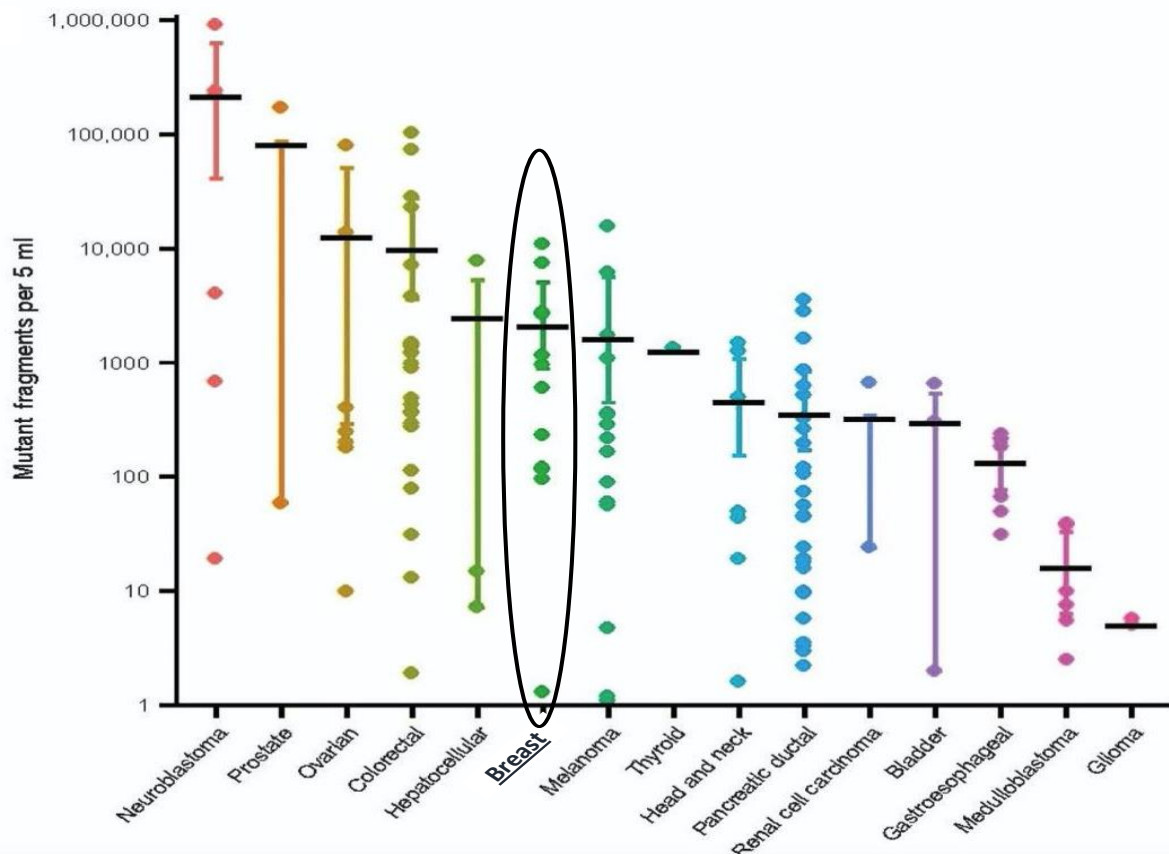
Error bars represent the 95% bootstrapped confidence interval of the mean

1.5.2 Clinical Utility of ctDNA

The collection of ctDNA samples is minimally invasive as it requires only a few millilitres of blood from the peripheral blood draw. A blood sample can be collected at diagnosis with a tissue or obtained sequentially in 'real-time' as a patient undergoes anticancer treatment. The ability of ctDNA to provide the genetic profile of a tumour that was previously only available through a biopsy has led to the term "liquid biopsy" to describe ctDNA. However, whether 'liquid biopsy' can act as a valid surrogate for tissue biopsy depends on its presence and detectability in patients with cancer and the reflection of genetic changes in the tumour over time and response to treatments. In addition, the sequential 'liquid biopsies' are more acceptable to repeat than invasive tissue biopsies.

The applications of ctDNA can be divided into the following categories: target identification and treatment selection, prognosis determination, monitoring of treatment response, detection of resistance mutations at relapse, minimal residual disease identification and early cancer detection.

Target Identification and therapeutic management

CtDNA has become commonly used for target identification in patients with advanced cancer, where biopsy is not obtainable, or insufficient genetic material left from tissue biopsy, or for patients with unknown primary cancer. In addition, studies have shown that ctDNA can be a surrogate for tumour biopsy in assessing driver mutations such as *EGFR* mutations in lung cancer (Douillard et al. 2014). However, there is an ongoing clinical need to discover biomarkers to identify patients with long-term benefits from new therapies. For example, a recent phase III trial (SOLAR-1 described in the previous section) was able to identify predictive biomarkers (*PIK3CA* mutations) in tissue and ctDNA for selected patients that will benefit from PI3K inhibitor (alpelisib).

Prognosis Determination

ctDNA has also been investigated as a prognosis biomarker in multiple cancers. In metastatic melanoma, detection of ctDNA was associated with shorter PFS (Marczynski et al. 2020). Howell and Sharma (2016) found that higher ctDNA levels in patients with hepatocellular carcinoma were associated with shorter survival. In another study of ovarian cancer treated with bevacizumab, PFS and OS were significantly shorter in patients with high levels of cfDNA, indicating that cfDNA could be an independent prognostic factor in patients treated with bevacizumab (Steffensen et al. 2014).

Monitoring of treatment response

Multiple studies reported that dynamic changes in the level of ctDNA on treatment could become a surrogate for treatment response across multiple tumour sites (Dawson et al. 2013). It has been thought that the level of ctDNA is a function of two factors: tumour burden and tumour cell turnover (Parkinson et al. 2016), volume (Abbosh et al. 2017), therefore ctDNA level can fall in cancers that are responding to treatment (Hrebien et al. 2019). Dawson et al. (2013) compared ctDNA with Ca15-3, a commonly used biomarker in breast cancer and concluded that monitoring somatic mutations in ctDNA can be an informative, specific and sensitive biomarker. In addition, previous research has also suggested that early changes in ctDNA levels may predict response to treatment and progression-free survival (Hyman et al. 2017).

Investigating ctDNA offers significant dynamic change and sensitivity in assessing patients response to therapy by comparing on-treatment ctDNA levels with baseline ctDNA levels (Dawson et al. 2013). This approach was used in phase II, BEECH study, where ctDNA dynamic change was assessed in response to first-line paclitaxel chemotherapy combined with capivasertib versus placebo. The study

demonstrated that early ctDNA change was a strong surrogate for PFS and the early ctDNA dynamics predicted no difference between the treatment arms (Turner et al. 2019).

Parkinson et al. (2016) detected *TP53* mutations in tissue samples in ovarian cancer, and they were able to track these mutations in longitudinal samples using ddPCR. The findings were compared with Ca-125 levels, a commonly used biomarker in ovarian cancer. *TP53* mutations detected in ctDNA correlated with Ca-125 and volume of disease. However, ctDNA was detected sooner than Ca-125. This suggested that ctDNA had the potential to be a highly specific early molecular response marker in high grade serous ovarian cancer (Parkinson et al. 2016).

Detection of Resistant Mutations at Relapse

The early change in ctDNA can identify response and resistance to treatment before radiological disease progression in tumour size, which would allow early switch ineffective therapy to effective therapy before further cancer progression (Garcia-Murillas et al. 2015; O'Leary et al. 2018). Furthermore, detection and changes of level of ctDNA during treatment could expedite drug development by identifying new biomarkers of resistance and providing an assessment of drug efficacy (Frenel et al. 2015). A successful example of the identification of resistant mutations with the development of effective treatment was the detection of resistant EGFR T790M mutation in patients with lung cancer who benefit from a new generation of anti-EGFR therapy – osimertinib.

However, this has not been successful with resistant *ESR1* mutations in breast cancer (described in the previous section). These mutations are examples of mutations occurring due to constant activation of the oestrogen receptor (ER) (Toy et al. 2013; Fanning et al. 2016) and develop in response to AIs in about 30% of patients with breast cancer (Toy et al. 2013; Schiavon et al. 2015). Brufsky and Dickler (2018) showed that *ESR1* mutations are commonly subclonal and weak predictors of outcome. Recent PlasmaMATCH trial reported no benefit of increased dose of fulvestrant in ESR1 mutated breast cancers (Turner et al. 2020), despite preclinical data suggesting that increased fulvestrant dose would be beneficial.

Minimal Residual Disease Identification

In clinical practice, it can be difficult to determine which patients have achieved complete remission and who have a minimal residual disease (MRD). Studies have shown that the presence of ctDNA after surgery is highly associated with the risk of relapse. CtDNA can be detected months before the

recurrent tumour is visible on imaging (Fiala and Diamandis 2018). Furthermore, ctDNA can be a reliable residual disease biomarker after neoadjuvant chemotherapy in localised breast cancer. After neoadjuvant therapy, ctDNA concentrations were lower in patients who achieved complete pathological response than those with MRD (McDonald et al. 2019).

CtDNA in Early Cancer Detection

Early detection in cancer is a very important aspect and is proven to improve the outcomes of many cancer patients. CtDNA has been currently being evaluated in multiple early detection trials. Cohen et al. (2018) developed an early detection test - "CancerSEEK" to target difficult-to screen cancers using a 61-amplicon panel to analyse ctDNA samples, in addition to a set of eight common proteins (CA-125, CEA, CA19-9, etc.). The test showed 99% specificity and sensitivies ranging from 33% for breast cancers to 98% for ovarian cancers. Overall, the researchers discovered cancer-specific profiles that could be used for the early detection in over 82% of the cancers (Cohen et al. 2018). Another biotechnology company, GRAIL (https://grail.com), developed a ctDNA-based multicancer screening test using the NGS method and machine learning. In addition, there are ongoing studies evaluating data from hundreds of thousands of patients to generate a reference library for mutations detected in the ctDNA of patients with the most common cancers (Aravanis et al. 2017).

1.5.3 Tumour Heterogeneity and ctDNA

It is well known that cancers show a significant degree of intratumoral heterogeneity (Allott et al. 2016). It is also believed that resistance to treatment can occur through clonal selection and evolution of resistant cells (Aparicio and Caldas 2013), which can depend on inherent heterogeneity. CtDNA can be detected in most patients with advanced and metastatic cancers (Bettegowda et al. 2014). Chan et al. suggested that ctDNA might be more representative of tumour heterogeneity in a patient than a single biopsy that can only represent a single cancer region in tissue (Chan et al. 2013) because all metastatic lesions contribute to one ctDNA pool (Thierry et al. 2016). Thus, CtDNA as a biomarker allows assessment of tumour heterogeneity more frequently and with reduced risks compared to tissue biopsies. The advantages and disadvantages of the two types of biopsies are shown in Table 2.

Table 2. Advantages and disadvantages of tissue and liquid biopsies.

Standard tissue biopsy	Liquid biopsy
Time-consuming	Quick
Localised region of tissue	Comprehensive tissue profile
Not easily obtained, requires specialist skills	Easily collected through a blood draw
Some pain and carries risks	Minimal pain and risk
Invasive	Minimally invasive
Collected at one time-point, limited material	Can be repeated at multiple time points
Issues with formalin fixation	Issues with sample handling
Ability to detect most mutations types	Inability to detect certain mutation types, Risks of false negatives
Full histology and cell characterisation	No histology

1.5.4 Methods of ctDNA Detection

Somatic mutations are acquired in the cancer cells' DNA in response to genotoxic DNA damage and replicative errors (Hanahan and Weinberg 2011). The somatic genetic alteration can include single-nucleotide variants (SNVs), somatic copy number variants (CNVs), chromosomal rearrangements and translocations (Nik-Zainal et al. 2012). As these somatic changes are not present in normal cells, identifying these genetic variants helps ctDNA be distinguished from cfDNA. In order to detect multiple somatic changes in cancer, several methods have been developed with different advantages and disadvantages.

1.5.4.1 Next Generation Sequencing (NGS)

The NGS development allowed significant progress in the analysis of tumour and cell-free DNA. NGS is used to detect the simultaneous sequencing of many millions of DNA sequences 50-500 bp in length. In comparison to Sanger sequencing that uses chain termination PCR followed by capillary-based fragment separation, NGS allows the determination of DNA sequence by synthesis, where nucleotides are added using various techniques such as bead and flow cell method (Bahassi and Stambrook 2014). The main difference between the Sanger method and NGS is sequencing volume. Whilst the Sanger method sequences a single DNA fragment at a time, NGS sequences millions of fragments simultaneously per run (Illumina 2020). Thus, the NGS method enables the sequence of hundreds to thousands of genes at one time and offers a greater ability to detect rare and novel variants with deep sequencing (Illumina 2020).

Whole exome sequencing (WES) is a technique that involves sequencing the whole coding regions of genes in the genome (>30.000 genes). The coding region makes up 1% of the genome, and mutations in coding regions are often associated with the disease. WES's costs have decreased over time, and therefore it has been used more frequently in genetic tumour analysis (Ross and Cronin 2011) and sometimes can be used to analyse cell-free DNA (Butler et al. 2015). However, since WES covers all coding genes, it has broad coverage, and therefore it has reduced read depth which increases the limit of detection for mutation detection. These can be the limiting factors of WES usage for ctDNA mutation detection.

Targeted NGS panels allow the sequencing of a limited number of specific genes. Some panels will cover only specific hotspot mutations in the specific genes and panels that cover entire genes. The sequencing DNA pool for specific genes or regions needs to be enriched before sequencing using various methods, including PCR or hybrid-capture methods (Parla et al. 2011), Figure 16. The amplicon-based target enrichment relies on the PCR amplification of the interest region using probes and primers (Parla et al. 2011). The hybrid capture-based target enrichment employs biotinylated oligonucleotide probes targeting regions of interest pulled down using magnetic beads (Parla et al. 2011). The difference between hybrid-capture and PCR based methods have been shown in Figure 16, and the advantages and disadvantages in Table 3.

PCR method is particularly advantageous when there is limited DNA from small tumour tissue samples or cfDNA. Consequently, commercial targeted hotspots or multiple gene panels are often available and often tailored to specific genetic alterations to specific cancers. The limit of detection of amplicon-based targeted NGS panels has improved over the years. The introduction of high average read depth (defined as many times each base in a gene is read) and the unique molecular barcodes (Kivioja et al. 2011) have increased the limit of detection from VAF of >1% to ~0.1% (Lanman et al. 2015; Gale et al. 2018). However, each panel's detection limit depends on the number of mutations covered, panel complexity, and the amount of total input DNA.

Figure 16. Comparison of two sequence enrichment methods – PCR vs Hybrid-capture, image addapted from (Wiley et al. 2014).
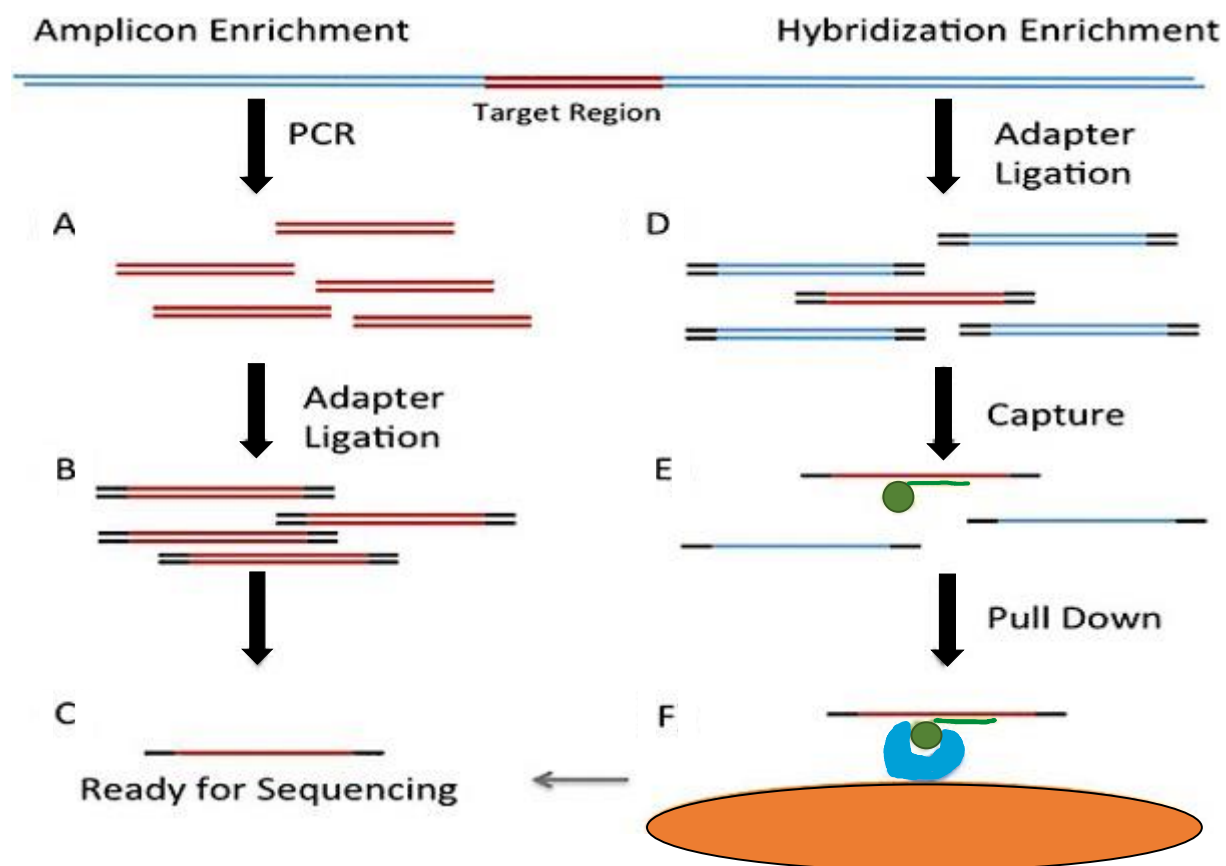
(A) PCR primers specific to the target region for amplification. (B) PCR products for ligation with sequencer-specific DNA molecules (adapters). (C) DNA molecules ready for sequencing. (D) Genome sheared into small fragments and ligated to sequencer-specific adapter DNA molecules. (E) Biotinylated oligomers complementary to the region of interest incubated with the previously generated library. (F) Captured molecules from the target regions pulled down with streptavidin-coated magnetic beads. (Wiley et al. 2014)

Table 3. Advantages and disadvantages of both enrichments' methods - PCR vs Hybridisation, table adapted from (Samorodnitsky et al. 2015).

	Advantages	Disadvantages
PCR -based enrichment	• Permits low DNA inputs • Simple and fast workflow – 1 day • Low start-up costs	• Cannot remove PCR duplicates/bias – obscures true complexity • Allelic drop-out due to variants in primer sites • Poor uniformity of coverage
Hybridisation based enrichment	• Highly uniform coverage • Tolerant of variants throughout target region • High sensitivity	• Requires greater DNA input • Multistep workflow – 1-3 days

1.5.4.2 Droplet Digital PCR

Droplet digital PCR(ddPCR) is an oil-based technology where thousands of separate PCR reactions occurs concurrently within one tiny oil droplet. The DNA alterations are detected with fluorescently labelled TaqMan® probes, which are mutation-specific and makes each droplet containing mutant DNA fluoresce differently to droplets with wild-type DNA. The droplets are counted by an automated droplet flow-cytometer (Hindson et al. 2011). DdPCR has greater sensitivity than NGS in mutation detection, about 0.01% VAF with 10ng of total input DNA. However, this method can only detect known specific mutations or a few mutations in a single assay, for example, *EGFR* p.T790M mutation testing in lung cancer or BRAF V600E in malignant melanoma. In contrast, NGS can detect any mutation in an amplicon included in the panel and detect multiple different mutations in one run. DdPCR is a highly sensitive method that can detect point mutations and gene amplifications in the tissue biopsy and blood samples of breast cancer patients (Heredia et al. 2013; K et al. 2016; Angus et al. 2017).

Copy Number Variation (CNV) detection

NGS technique can be very good at detecting multiple somatic mutations simultaneously, mostly single nucleotide variations (SNVs) but is less frequently used for copy number variations (CNV) (Hehir-Kwa et al. 2015). Traditional methods for detecting copy number variations in tumour tissue used in clinical practice for *HER2* amplification are immunohistochemistry (IHC) and FISH. These methods cannot be used to detect CNVs in ctDNA. However, ddPCR can be used for CNV detection in the tissue and ctDNA (Shoda et al. 2017) This technique has been used with high concordance in gene amplification detection in ctDNA in several cancers such as gastric cancer, colorectal cancer and breast cancer (Kinugasa et al. 2015; Shoda et al. 2015; Shoda et al. 2017; Sakai et al. 2018). Serial Blood sample gives the opportunity with detection and monitoring of detected CNVs. This could be very beneficial to patients as the clinically significant CNV could be detected in a blood sample instead of invasive and risky biopsy procedures.

DdPCR can detect CNVs using small amounts of DNA (<10ng), which allows cfDNA analysis. This method generates gene ratios, the gene of interest to the standard non-amplified reference gene, to detect gene amplification. Also, it relies on the same PCR (TaqMan®) technology where primers for the gene of interest are designed with TaqMan® fluorescent probe, enabling gene amplification detection.

1.6 Thesis Overview, Hypothesis and Aims

The interest in the utility of ctDNA has increased over the years, especially with the development of new technologies and better understanding the association between genetic mutations in tumours and ctDNA. Multiple somatic mutations occur in cancer tissue and can also be detected in ctDNA. This gives the opportunity of ctDNA to play a role in disease detection, disease monitoring, prediction of relapse or resistance to treatment. CtDNA analysis might transform the management of a wide range of cancers cancer in the future (Shaw and Stebbing 2014). However, the use of ctDNA in the clinic is still at its early stages and for some still controversial (Thoma 2018; Torga and Pienta 2018). The reasons for this could be a poor understanding of the technology and inadequate interpretation of results. For the ctDNA to become widely used in clinical practice, it must be well understood by pathologist and oncologist, and the benefits need to be proven in large phase III trials.

This thesis will focus on the use of ctDNA as a biomarker in advanced endocrine-resistant breast cancer. I hypothesised that ctDNA can be detectable in patients with endocrine-resistant breast cancer, and it can provide prognostic and predictive information about the response to fulvestrant and capivasertib in patients in FAKTION trial. More specifically, I would use pre-existing methods to monitor response to therapy and predict therapeutic resistance. The aim is to contribute to the improvement of the patient selection in clinical trials that will identify patients with breast cancer that most likely will respond to the experimental treatment and improve the management of patients treated with new targeted therapies.

The aims of the thesis:

- To determine whether selected NGS platform and gene panel can detect somatic mutations in FFPE (formalin-fixed paraffin-embedded) tissue and ctDNA samples of patients with an advanced or metastatic breast cancer patients.
- To determine whether NGS and ddPCR are sufficiently sensitive to detect mutations in ctDNA samples at low mutant allele frequency (MAF).
- To investigate concordance *PIK3CA*, AKT, *PTEN*, *ESR1*, *TP53* between FFPE tissue and ctDNA samples.
- To assess the potential utility of longitudinal ctDNA sampling as a surrogate biomarker of treatment response to fulvestrant and capivasertib.

- To investigate the potential utility of ctDNA to detect copy number variation *HER2*, *MYC* and *FGFR1* which play a role in endocrine resistance, and whether CNVs can help predict resistance to fulvestrant +/- capivasertib.

- To assess whether a combination of multiple molecular biomarkers (SNVs and CNVs) can be more predictive of treatment response than a single biomarker

2. Materials and Methods

2.1 Project Governance, Patients and Samples Collection in FAKTION trial

Velindre Cancer Centre sponsored a FAKTION trial. FAKTION trial protocol was approved by a Multi-centre Research Ethics Committee recognised by the United Kingdom Ethics Committee Authority (REC reference 13/NW/0842). Patients recruited to the trial consented to donation of tumour samples (FFPE - formalin-fixed paraffin-embedded tissue), blood samples and genetic testing using the approved Participant Information Sheet and Consent Form. Samples collection was mandatory for trial enrolment. According to the Clinical Trial Laboratory Manual, blood samples were collected in hospital out-patients departments from 140 patients.

2.2 Pre-Analytical Sample Handling

Designated staff at participating sites were responsible for ensuring that all samples were collected and handled at their site following the Clinical Trial Laboratory Manual. The staff were fully trained and listed on the FAKTION Delegation Log as authorised by the Principal Investigator to carry out these tasks before any sampling took place. Tumour blocks and blood samples were tracked from the time of consent to randomisation to enter the trial.

2.2.1 FFPE Tissue Samples Collection

FFPE tumour blocks were obtained from archival primary breast cancer tissue or metastatic biopsy from 19 UK centres. The archival tumour tissue FFPE blocks were sent to the central Cell Pathology Laboratory, University Hospital Wales in Cardiff. The FFPE samples were tested there for PTEN status by immunohistochemistry. In addition, the slides were sent to All Wales Medical Genetics Service (AWMGS) for DNA extraction and *PIK3CA* mutation testing. The study required prospective PTEN and PIK3CA status before participants could be randomised for treatment within the trial.

2.2.2 FFPE Tumour DNA Extraction

The tumour slides were prepared at the histopathology department at the University Hospital of Wales in Cardiff. The slides were sent with a matched H&E slide and the tumour area ringed, and the percentage of nucleated tumour cells indicated on the slide to All Wales Genetic Laboratory. DNA extraction from FFPE tissue was managed by trained NHS staff.

According to the manufacturer's instructions, DNA was extracted from FFPE tumour tissue using the Promega Maxwell 16 FFPE Plus Low Elution Volume Purification Kit (AS1130). The FFPE tissue was assessed and macro-dissected to confirm tumour content was >20%. FFPE tissue was scraped from slides with a scalpel blade to Proteinase K and Promega Incubation Buffer for deparaffinisation and protein degradation. Samples were incubated for approximately 16-18 hours at 70°C and shaken at 1300rpm in an Eppendorf Mixer C (15158953). Samples with added Lysis Buffer were transferred to Promega Maxwell Cartridges for the automated FFPE DNA protocol on the Maxwell 16 Instrument. The process involved binding DNA to silica clad paramagnetic particles, which underwent sequential washes with ethanol before elution. Samples were eluted in nuclease-free water and quantified with the Invitrogen High Sensitivity Qubit Fluorometer (see section 2.3.4.1). Extracted FFPE DNA was stored at 4°C. FFPE DNA extraction results are presented in Table 52 (Appendices, Section 8.3)

2.2.4 Blood Samples Collection

2 x 10 mls of whole blood by venipuncture or from the venous port was taken into the supplied Streck preservative tubes at selected time-points – baseline, at eight weeks of treatment and at the time of disease progression. The tubes were filled until the flow stopped to ensure the correct ratio of sample to anticoagulant and preservative. The tube was required to be gently inverted eight times to mix; to prevent clotting. The sample must have arrived within 96 hours to AWMGS.

2.2.4.1 Plasma Separation

Plasma was separated using the double spin protocol to minimise cell lysis and reduce any extra genomic DNA entering the plasma compartment. First, the blood in Streck tubes was centrifuged at 1000g for 10 minutes at 4°C. This centrifugation separated the blood into red cells, buffy coat (white cells) and plasma. Next, the plasma was transferred into 2 ml Eppendorf tubes and centrifuged at 2000g for a further 10 mins at 4°C to remove the remaining cellular debris (Page et al. 2006). The plasma was stored at -80°C in 1 ml aliquots for future cfDNA analysis.

2.2.5 Cell-Free DNA Extraction

1ml or 2ml of frozen plasma were thawed at room temperature before DNA extraction. According to manufacturers' instructions, the extraction of ctDNA was performed using the QiaAmp circulating nucleic acid extraction kit (55114). This method had previously been shown to be the most optimal for cfDNA extraction (Page et al. 2013).

The first step involved proteinase-K digestion at 60°C for 60 minutes to release any plasma protein-bound nucleic acids. Next, the plasma was mixed with the ACL Buffer (Qiagen buffer containing trometamol and guanidine thiocyanate) to optimise DNA binding to a silica membrane. The membrane was contained within the QIAamp® Mini column attached to a vacuum manifold. The cfDNA was bound to the membrane whilst contaminates passed through. Three wash steps removed the contaminates such as cations and proteins, which could interfere with subsequent PCR reactions or cause DNA degradation. The bound cfDNA was eluted into a final volume of 40μl of elution buffer AVE (Qiagen buffer of 0.04% sodium azide in RNase free water). Eluted cfDNA samples were placed on ice and quantified using the fluorometric method with the Qubit system described below and stored in -80°C. CtDNA extraction results are presented in Table 52 (Appendix, 8.3)

2.2.6 DNA Quantification

2.2.6.1 DNA Quantification by Qubit 2.0 fluorometer

The Qubit® dsDNA HS (High Sensitivity) Assay Kit (ThermoFisher Scientific, UK) was used to determine the final concentration of extracted cfDNA using fluorometric quantitation. First, 2μl of extracted DNA solution was mixed with a fluorescent dye and buffer mix. The dye increases the fluorescence once bonded to double-stranded DNA molecules. Thus, the DNA concentration is directly proportional to the amount of fluorescence signal from the dye in the solution. The fluorescence of each sample was measured using Qubit® Fluorometer 2.0. Each kit contains two pre-diluted standards; 10 μl of each standard was used to calibrate the Qubit fluorometer 2.0 before quantification of each DNA sample in the fluorometer. This assay has a concentration detection range of 0.2 – 100ng of double-stranded DNA.

2.2.6.2 DNA Quantification by Agilent 2100 Bioanalyzer

The Agilent Bioanalyzer allowed to assess the range of fragment sizes and to quantify DNA libraries. The Agilent high sensitivity kit was used to separate and size total cfDNA and DNA libraries of 50-7000bp at concentrations down to 100pg/μl. It involved a 12 well chip with engraved microchannels. The microchannels were filled with a gel polymer and fluorescent dye during chip preparation according to the manufacturer's instructions. 1μl of DNA was loaded into each well. Every sample was also loaded with a lower (35bp) and upper (10380bp) DNA marker. One of the 12 wells in each chip was loaded with a DNA ladder. The DNA was dragged through the gel by a voltage gradient during electrophoresis, which allowed the separation of fragments dependent on size, as DNA is positively charged. Each sample was analysed sequentially across a single detector to determine DNA fragment

concentration. The results were used to assess DNA quality by evaluating the relative number of different-sized fragments and overall DNA quantification.

2.3 Methods of ctDNA Detection

A variety of methods have been developed to detect the cancer genetic alterations in FFPE DNA and ctDNA. Each of the methods has different advantages and disadvantages. Two methods were used in this project: Next Generation Sequencing (NGS) and droplet digital PCR (ddPCR).

2.3.1 Next Generation Sequencing (NGS)

The targeted NGS panel chosen for this project included those previously identified genes as important in the oestrogen receptor signalling pathway and PI3K/AKT pathway. The gene panel was selected based upon previous publications (e.g. have identified 18 candidate genes for ER-positive breast cancer (Ellis et al. 2012), peer review, involved in PI3K/AKT pathway, and the practical limitations of the technology (i.e. the literal size of the panel and the required depth of analysis).

The 44-gene GeneRead™ DNAseq Targeted Panels V2 (Qiagen, 181900, NGHS-001X), amplicon-based, off-the-shelf, was chosen for validation with cfDNA, which include most of the essential genes of the PI3K/AKT, ER signalling pathway and other potential indirect resistance mutations, Table 4. This panel specifically covered 44 cancer genes regions, known oncogenes and tumour suppressor genes in breast cancer. It required four primer pools per DNA sample (10ng of DNA per pool, a total of 40ng of total input DNA).

44-gene panel was validated for FFPE DNA which usually contains fragmented but longer DNA fragments (~180-3000) (McDonough et al. 2019) than cfDNA (160-180). Normally, the FFPE NGS panel would create longer PCR amplicons, and therefore this panel would not generate PCR amplicons for shorter cfDNA fragments. This could influence the sensitivity of the panel for ctDNA and limits its use for ctDNA. Optimisation and validation of this panel for cfDNA will be presented in the next chapter.

GeneRead DNAseq Targeted Panel V2 was part of a total workflow for targeted next-generation sequencing. This panel was used in combination with GeneRead DNAseq Panel PCR Kit V2 to perform targeted enrichment using multiplex PCR. Once targets have been enriched, the NGS library was constructed. This process involves library preparation, template preparation, DNA sequencing, and data analysis, Figure 17. NGS was performed using Illumina platform.

Table 4. Genes covered by 44-Gene Breast Panel.

ACVR1B	EP300	IRAK4	PBRM1	TP53
AKT1	ERBB2	ITCH	PCGF2	TRAF5
ATM	**ERBB3**	KMT2C	**PIK3CA**	WEE1
BAP1	**ESR1**	**MAP2K4**	**PIK3R1**	ZBED4
BRCA1	EXOC2	**MAP3K1**	PPM1L	
BRCA2	EXT2	MDM2	**PTEN**	
CBFB	FBXO32	MUC16	PTGFR	
CDH1	FGFR1	**MYC**	**RB1**	
CDKN2A	FGFR2	NCOR1	**RET**	
EGFR	**GATA3**	NEK2	SEPT9	

Genes involved directly in the PI3K/AKT and ER pathway in yellow, indirectly in green. The rest of the genes associated with breast cancer but not directly involved in endocrine resistance or PI3K/AKT pathway.

Figure 17. GeneRead DNAseq Targeted Panels workflow, image adapted from (Qiagen 2015).
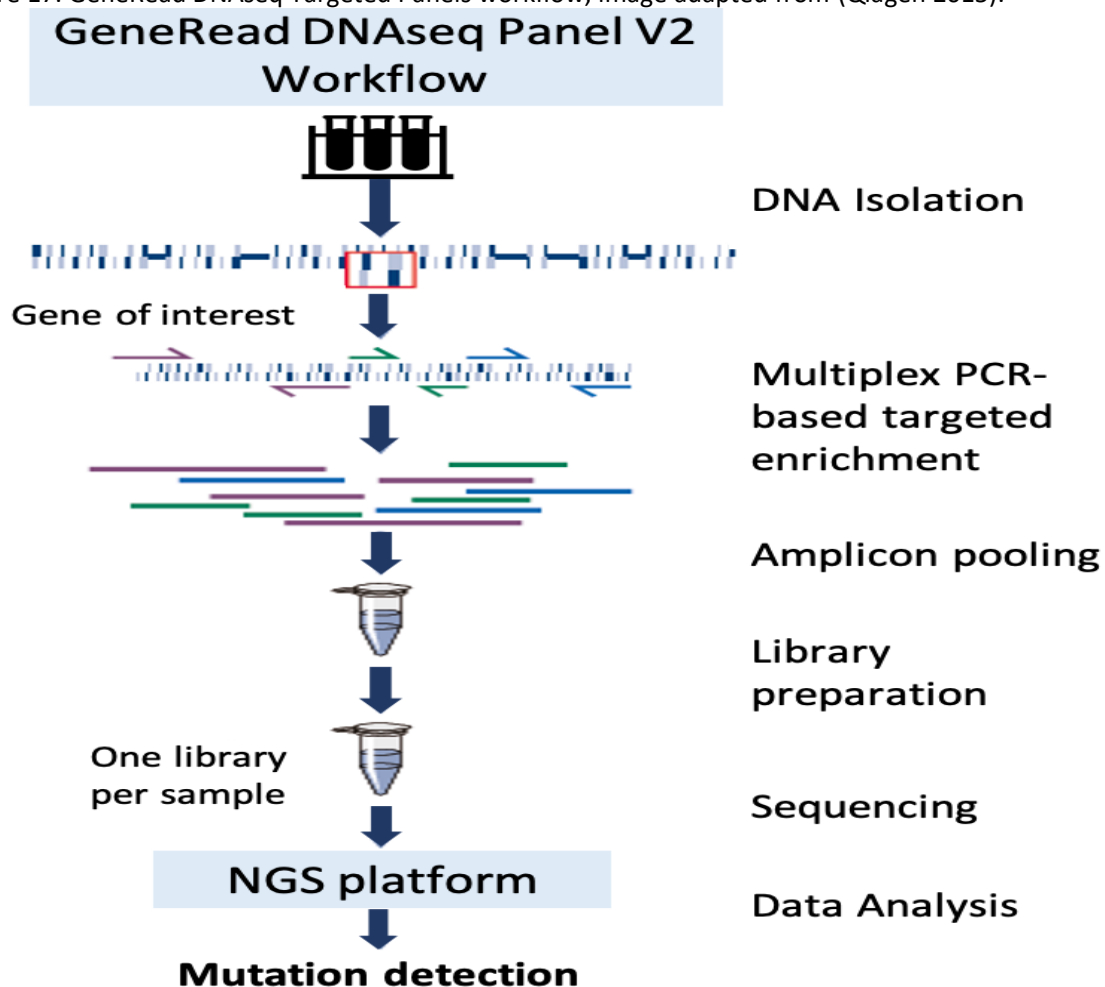
Overview of the sample-to-insight NGS workflow with GeneRead DNAseq Targeted Panels V2. The complete sample-to-insight procedure begins with DNA extraction, followed by targeted enrichment with GeneRead DNAseq Targeted Panels V2, NGS library construction, sequencing and data analysis.

2.3.1.1 Library Preparation

Following DNA extraction and quantification, 5-10ng of DNA was used to generate libraries using the GeneRead™ Library Kit (Qiagen). In this process, the extracted DNA was mixed with short single-stranded DNA primers and DNA polymerase in a polymerase chain reaction - PCR, to enrich the DNA sequence of interest. The PCR was multiplexed so that one DNA sample was mixed with four 'pools' of primers to amplify several 'target' genetic regions simultaneously. After PCR, the four 'pools' mixed with one DNA sample were combined, Table 5.

Table 5. Multiplex PCR: Reagents and PCR conditions for GeneRead™ library preparation.

Reagent	Volume (µl)	PCR Conditions	
GeneRead DNAseq Panel PCR Buffer (5x)	4.4	95°C 15 minutes	1
Primer mix pool (2x)**	11	95°C 15 seconds	21 cycles - cfDNA samples 26 cycle - FFPE DNA samples***
GeneRead HotStarTaq DNA Polymerase (6 U/µl)	1.5	60°C 4 minutes *	
Extracted DNA	4		
DNase-free water	0.7	72°C 10 minutes	1
Total volume	21.6	4°C ∞	1

*For pools with primer pairs <1200 - 4 min; for Pools with primer pairs 1201– 2500 - 8 min. **This panel had a total number of primer pairs of 2915 in four pools, 729 primers per pool. *** The number of PCR cycles depended on the type of DNA, FFPE DNA or ctDNA. 21 cycles were used for PCR with cfDNA, 26 PCR cycles were used FFPE DNA.

The amplicon libraries were prepared for sequencing following several steps, as shown below:

1. <u>Sample Pooling and Purification</u> - After PCR, four pools for each sample were combined into one pool. Library purification was performed with Agencourt AMPure XP™ beads (Beckman Coulter) using two 80% ethanol washes to remove the reagents and buffers from the PCR step. The concentrations of each pool were determined using the Qubit High Sensitivity kit (Agilent Technologies).

2. <u>End repair of DNA</u> - Only 10-200ng PCR-enriched DNA was used, ensuring optimum efficiency of library construction. During 'End repair of DNA', PCR-enriched DNA was mixed with End-Repair Buffer and Enzyme, and incubated in a thermocycler for 30 min at 25°C followed by 20 min at 75°C (Qiagen 2015). This reaction aimed to convert fragmented DNA into blunt-end DNA containing 5' phosphate and 3'-hydroxyl groups. The 5'→3' polymerase activity filled in 5' protruded DNA ends while 3'→5' exonuclease activity removed 3'-overhangs.

3. <u>A-addition</u> - During an A-addition reaction, the end-repaired DNA was mixed with A-addition buffer and Klenow Fragment (3' ®5' exo-). The mix was incubated on the thermocycler for 30 min at 37°C, followed by 10min at 75°C (Qiagen 2015). This step's purpose was to add "A" base to the 3' end of a blunt phosphorylated DNA fragment and enable DNA fragments to be ligated to adaptors with complementary dT-overhangs.

4. <u>Adapter ligation</u> – This step aimed to ligate unique adapters to each patient's DNA sample. After A-addition, amplicons were ready to add barcode adapters which are unique DNA sequences for each DNA library, to assign each DNA molecule to the correct library during sequencing analysis. Each Library was mixed with Ligation Buffer, T4 DNA Ligase and a unique barcode adapter. The mix was incubated on thermocycler for 10 min at 25°C (Qiagen 2015).

5. <u>Clean-up of adapter-ligated DNA with AMPure XP beads</u> (Beckman Coulter) - A purification step with two 80% ethanol washes to remove the buffers and reagents from the previous step.

6. <u>PCR amplification of purified library -</u> Purified library required last PCR amplification with HiFi PCR Master, Primer Mix, with 5-10 cycles of the final PCR, seven cycles were commonly used, Table 6 (Qiagen 2015). HiFi amplification enables high yields of DNA libraries with low error rates from extremes of GC content and minimal sequence bias (Head et al. 2014).

Table 6. Reagent and PCR for Library amplification step.

Reagent	Volume (µl)	PCR conditions	
HiFi PCR Master Mix, 2x	25	98°C 2 minutes	1 cycle
Primer Mix (10 µM each)	1.5	98°C 20 seconds	5-10 cycle
Library DNA	17	60°C 30 seconds	(7 cycles was used)
		72°C 30 seconds	
RNase-free water	1.5	72°C 1 minute	1 cycle
Total volume	50	4°C ∞	hold

7. <u>Clean-up of the amplified library with AMPure XP beads</u> - A second purification step with two 80% ethanol washes.

8. <u>Library Elution</u> in 28µl of nuclease-free water. The final concertation was assessed using Qubit (High Sensitivity kit, Agilent Technologies) and the Agilent 2100 Bioanalyzer (Agilent Technologies). The bioanalyser was also used to assess the length of amplicons. For Illumina libraries, a peak around 280bp was required and with no significant peak observed around 120bp, representing adapter dimers (Qiagen 2015). However, the Bioanalyzer results revealed an additional peak at

150-180bp, suggesting an excess of adapters; therefore, an additional clean-up with magnetic beads at a ratio of 0.8X was performed, Figure 18. These libraries were then appropriately diluted with nuclease-free water to obtain 4nM libraries.

Figure 18. Sample Agilent Bioanalyzer image of Illumina Sequencer library.
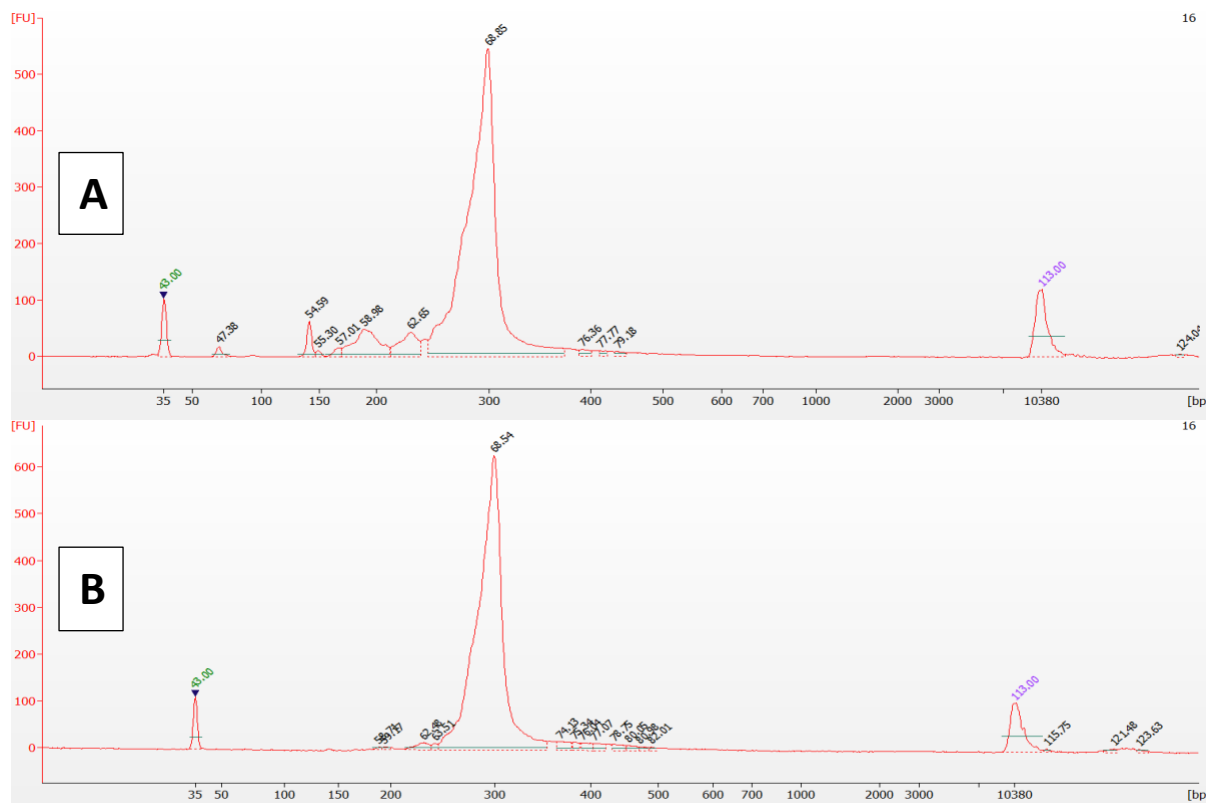
A: peaks at 140-180bp - an excess of adapters. B: Additional peaks removed with additional cleaning with the preserved peak at about 280 bp.

2.3.1.2 Illumina sequencing of DNA templates using Hiseq2500 platform

'Sequencing by synthesis' (SBS) technology has been used by Illumina. It uses four fluorescently labelled nucleotides to sequence the millions of clusters on the flow cell surface in parallel. A single labelled deoxynucleoside triphosphate (dNTP) is added to the nucleic acid chain during each sequencing cycle. The nucleotide label works as a terminator for polymerisation. After each dNTP incorporation, the fluorescent dye is imaged to recognise the base and then enzymatically cleaved to incorporate the next nucleotide. (Illumina 2010)

Final libraries were diluted to 4nM concentration and combined into one library, further diluted to final concentration 7pM. The final library at 7pM was loaded to the HiSeq2500 platform. For sequencing, as per Illumina recommendation, a PhiX Control library v2 (Illumina) was spiked into the final pool of libraries at a proportion of about 1% to provide quality and calibration control.

Before sequencing can occur, cluster generation needs to take place. First, the library is loaded into a flow cell where DNA fragments are caught on a lawn of surface-bound sequencing templates complementary to the library adapters. Each fragment is then amplified into individual, clonal clusters through bridge amplification (Illumina 2010). This creates up to 1000 identical copies of each single template molecule (Illumina 2010). Once cluster generation is complete, the templates are ready for sequencing. Cluster generation was performed on board of HiSeq 2500 (Illumina) using an Illumina HiSeq Rapid Paired-End (PE) Cluster kit v2 (PE 402-4002) chemistry.

The sequencing was completed using HiSeq Rapid SBS Kit v2 (FC-402-4021) over 330 cycles. Illumina Real-Time Analysis software was used for Base-calling. Sequencing runs were performed over 27 hours on the Illumina Hiseq 2500 Machine, as per the manufacturer's recommendations. The sequencing data was downloaded onto the NHS server.

Complete NGS Product Configurator (Qiagen) was used to determining the number of DNA samples that can be sequenced per Hiseq Rapid run and the desired average sequence depth (per amplicon). The Illumina HiSeq 2500 platform allowed sequence 20-26 ctDNA samples with an average 8-10000 read depth and 34 FFPE samples with 6000 read depth.

2.3.1.3 Data Pre-processing

The somatic amplicon pipeline was designed to detect low-level variation from amplicon next-generation sequencing library preparations. The pipeline accepted paired-end FASTQs files and required a minimum of 10bp overlap between the first and second read.

Once the sequencing data was downloaded, the paired-end FASTQ files were cleaned for technical biases caused by the sequencing process. Then, file processing and variant calling was carried out by Matthew Lyon, Lead Bioinformatician at All Wales Medical Genetics Service, NHS. The specific steps of the pipeline are presented in Figure 19.

Figure 19. Steps of data analysis.
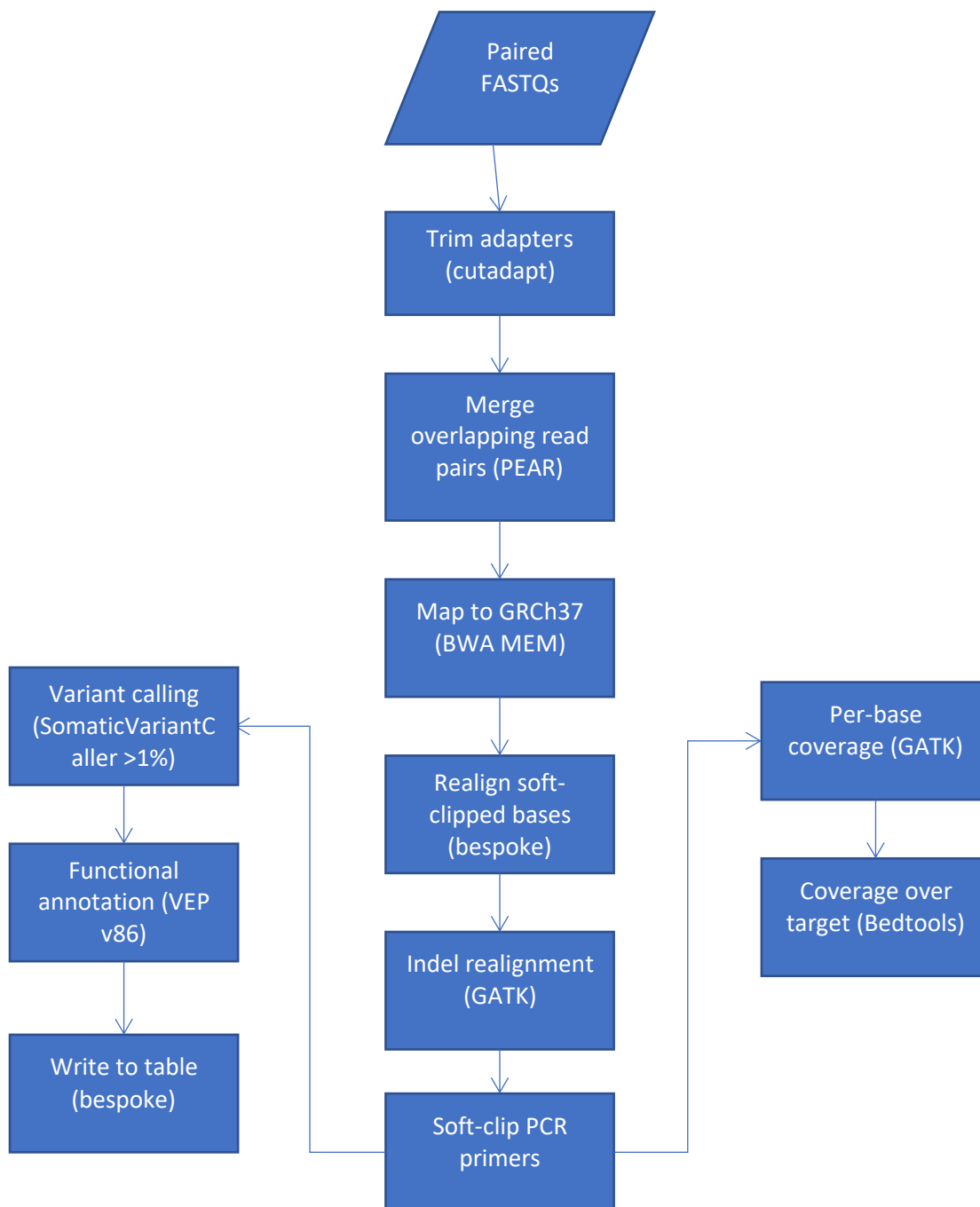
0. **FASTQs analysis** - The sequences were initially evaluated using the FASTQC programme (version 0.11.6, Babraham Bioinformatics - a quality control tool for high throughput sequence data) to look for evidence of residual adapter sequences and duplicated reads caused by the PCR steps.

1. **Trimming adapters** - Cutadapt software was used for trimming the adapters from the reads. The adapters were added to each sample during library preparation so that DNA from each sample carried a unique barcode. This allowed each sequenced DNA sample to be assigned to the sample

from which it came following sequencing. The software from Illumina sequencing removed most of the barcode sequences. However, some adapter sequences remained, which must have been removed before analysis.

2. **Merging overlapping read pairs -** Overlapping read pairs were merged into one contiguous sequence to increase the overall read length and resolve sequencing errors present in one read direction using PEAR. Non-overlapping reads were discarded. PEAR software merged Illumina paired-end reads from fragments that vary in length and therefore did not require fragment size as input. Also, PEAR implemented a statistical test for minimising false-positive results (Zhang et al. 2014).

   a. Most amplicons in the GeneRead kit were short enough to be covered in both directions using 2 x 151bp sequencing. This information was used to eliminate sequencing errors seen in one direction.

   b. Once merged, the reads must have started and ended with PCR primer, which was useful for downstream processes (i.e. steps 5 and 6)

3. **Whole-genome alignment -** BWA-MEM alignment algorithm from a BWA software package was used for aligning sequence reads against a human reference genome. This produced an aligned BAM file for each sequenced sample

4. **Realignment of soft-clipped bases -** In general, aligners reaching high effectiveness often perform "soft-clipping" of reads. This means that the proportion of the reads that do not match well to the reference genome on either side of the read are ignored for the alignment (Bioinformatics 2016). However, this is an amplicon assay with carefully chosen PCR primer sequences. Therefore, read soft-clipping may indicate the presence of a large insertion-deletion that was not correctly aligned. Realignment of soft-clipped bases against the expected amplicon sequence may resolve these variants.

   a. Following paired-end read merge (step 2), all sequences must have started and ended with PCR primer and should align correctly to the reference genome. Evidence of soft clipping can suggest the presence of a large indel.

   b. Reads overlapping the region of interest (ROI) showing soft-clipping were realigned to the expected amplicon sequence using global alignment (Needleman–Wunsch).

5. **Indel realignment using GATK -** Local realignment around indels allows correcting mapping errors made by genome aligners and making read alignments more consistent in regions containing indels (Practices 2016).

6. **Soft-clipping PCR primers -** The aim of this process is masking (but not removing) aligned sequences in the BAM file to avoid making variant calls in the primer sequence that are not from the patient.

   a. PCR primers contain errors in a synthesis which can appear as a false-positive variation.

   b. A true variant under the primer binding site will have skewed allele frequency if the primer sequences are included during analysis.

7. **Per-base coverage (GATK) -** The number of reads overlapping each target base (vertical coverage) was calculated using GATK DepthOfCoverage function excluding reads with a low mapping quality (Q < 20) and bases with poor sequence quality (Q < 20).

8. **Coverage over the target -** Taking the per-base coverage, Bedtools was used to estimate the mean coverage of each amplicon.

2.3.1.4 Data Analysis

Variants were called with the Somatic Variant Caller (Illumina) to detect mutations in each barcoded sample. All called variants were individually analysed using the Integrative Genomics Viewer (IGV) software (version 2.3.86), ensuring they were not due to an artefact of the sequencing process. Especially, called variants that were present in the last three bases of reads were excluded. Variants called in tumour samples but not present in matched cfDNA samples were also analysed to look for low-frequency mutations. The significance of each mutation was confirmed using the Catalogue of Somatic Mutations in Cancer (COSMIC), the Database of Single Nucleotide Polymorphisms (dbSNP) and The Human Gene Mutation Database (HGMD).

For the 44-gene GeneRead™ DNAseq Targeted Panels V2, variants were reviewed and accepted as a true variant if they had:

- Mutant reads(10 in each direction) >20
- Reference reads >30
- Quality score > 30
- Reviewed on IGV and not in the last three bases of the read

Mutations that have not fitted the above criteria were only accepted as true variants confirmation with a mutation-specific ddPCR assay.

2.3.1.5 Sequencing Coverage and Depth

The sequencing coverage is known as the degree of target DNA sequencing, ranging from a single gene to the whole genome. The sequencing depth is determined by the number of amplicons that cover a specific DNA region. In general, there are limitations to the capacity of DNA sequencing, per DNA sample, per primer pool, per flowcell, per microchip. This means that the NGS panel that covers the whole genome have reduced sequence depth potential. Equally, a smaller NGS panel covering a targeted genetic region - a panel of 5-50 genes, will provide better sequencing depth and reduce the chance of missing low-frequency mutations of the genes included (Stasik et al. 2018). In summary, the lower the degree of coverage of the genome, the greater the sequencing depth, therefore the higher the sensitivity is for detecting rare mutations, such as those present in cfDNA (Abel and Duncavage 2013).

DNA samples from cancer patients contain a mixture of tumour and germline DNA. Hence, the NGS sequence depth must be adequate so that amplicons created in the library preparation represent both germline and tumour DNA within the sample.

For FFPE samples, histopathologists can estimate the ratio of the number of cancer cells to germlines during a histopathological examination. This can influence the requirement of sequencing depth. For example, samples containing 100% of tumour cells can require at least 100X sequence depth as all amplicons will be generated from cancer DNA. However, samples containing 10% tumour cells may require 1000X sequencing depth, so at least 100 amplicons can be generated from tumour DNA. Unfortunately, this information was not available for all FFPE samples; consequently, 34 FFPE samples in this project were sequenced with an average high sequencing depth of 5-6000X read depth.

The ratio of cancer to the normal cell cannot visually be estimated for cfDNA samples. Circulating tumour DNA (ctDNA) may be at only 0.1% of cfDNA. Therefore, NGS sequencing depth needs to be significantly deeper than with FFPE DNA to increase the chances of amplicons being generated and detected from the cfDNA. Hence, the aim was to sequence the cfDNA samples with a high sequence depth of 8-10000X.

2.3.2 Droplet Digital Polymerase Chain Reaction (ddPCR)

Droplet Digital PCR was used in this project to detect known changes in single nucleotide variation (SNVs) in *PIK3CA*, *AKT1* and *ESR1* genes and quantify their MAF; and to detect copy number variation (CNV) of *HER2*, *MYC* and *FGFR1* genes in FFPE DNA and cfDNA samples from patients with endocrine resistance breast cancer in FAKTION trial. DdPCR was selected due to greater sensitivity, precision and reproducibility over similar methods such as qPCR (Huggett and Whale 2013). In addition, ddPCR was used to validate NGS results for ctDNA and FFPE DNA and track variants of interest in longitudinal samples and detect CNV of interest in ctDNA and FFPE DNA.

2.3.2.1 Principles of Droplet Digital PCR

This method was developed around the same principles as qPCR, allowing real-time quantification of amplified DNA using oligonucleotide probes with a tagged fluorescent reporter and a quencher (Gut et al. 1999). The oligonucleotide probe is complementary to a specific DNA sequence of interest and can be about 20bp long. These probes include fluorophore reporters, which naturally emit light at a specific wavelength that varies between fluorophores. In this study, three molecular reporters were used: 6-carboxyfluorescein(FAM), hexachlorofluorescein(HEX) and 2'-chloro-7'phenyl-1,4-dichloro-6-carboxyfluorescein(VIC), which emit light at a wavelength up to 525nm, 556nm and 554 nm, respectively. The difference in light emission at a different wavelength and consequent absorption from each fluorophore is used to distinguish between two reporters. Therefore, FAM and HEX/VIC probes are associated with separate gene sequences. In this project, they were used to represent mutant and wild-type DNA, respectively. The reporters are joined with a quencher on their respective oligonucleotide, Figure 20.

A black hole quencher (BHQ) is a dye that can absorb fluorescence. When close to FAM or HEX/VIC, the BHQ absorbs the released fluorescent light. The quenchers are located at the 3' end and the fluorescent reporters at the 5' end of oligonucleotide probes. When a probe binds to complementary DNA during PCR, reporters and quenchers are detached from each other by Taq polymerase. This separation of the fluorophore from the quencher results in a fluorescence signal proportional to the amount of amplified DNA. This allows for the reliable detection of fluorescence from the reader. Therefore, when a mutant (FAM) or wild-type probe (HEX or VIC) binds to DNA, the probe is fragmented by the enzyme and the reporter is separated from the quencher, allowing the detection of FAM or HEX/VIC, which means detection of mutant or wild-type DNA, Figure 20.

Figure 20. DNA quantification mechanism using fluorescent reporter labelled probes, and black hole quenchers during ddPCR, image modified from (Biosearch 2016).
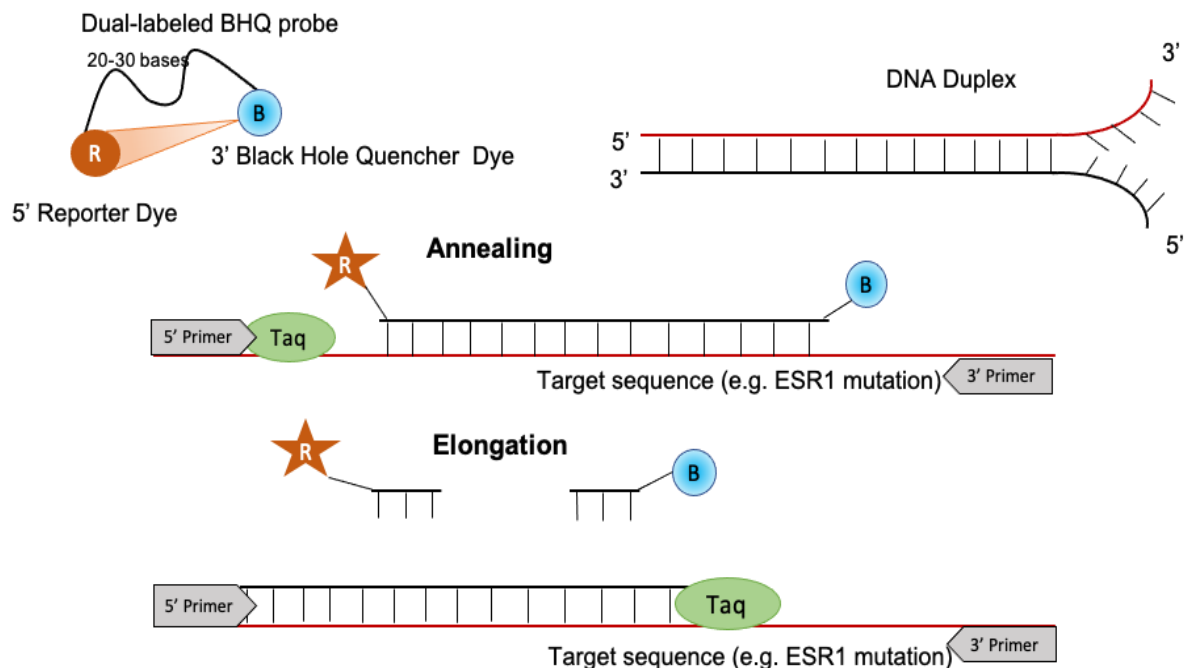
B - BHQ - Black Hole Quencher, R - 5' Reporter Dye, Taq – Taq polymerase enzyme.

The Bio-Rad ddPCR system partitions a single qPCR reaction into ~15.000 – 20.000 droplets using water-oil emulsion chemistry, and qPCR reaction occurs in each droplet. Partitioning delivers remarkable sensitivity and absolute quantification of DNA. Also, emulsion-based technology can provide a higher number of partitions at a lower cost. Other forms of ddPCR that compartmentation of reaction use solid partitions on chips (Hindson et al. 2011; Kreutz et al. 2011). In general, ddPCR has greater sensitivity due to the increased number of partitions and is less prone to PCR inhibitors (Huggett and Whale 2013).

However, ddPCR has limitations which include the concentration of DNA input. A lower DNA concentration results in a smaller number of DNA-positive droplets and decreases the reliability of detecting or quantifying DNA. Overloading a ddPCR can have a similar effect. Each reaction is designed to contain one single DNA droplet, and when the ddPCR is overloaded, more than one DNA molecule can be present in one droplet. Thus, the quantification of DNA becomes less reliable.

2.3.2.2 DdPCR Protocol

The total volume of the ddPCR reaction mix was set for 25 μL. Each set of probes was diluted to 5mM whilst primers were diluted to 18mM per individual ddPCR reaction. The mutant primer mix contained a FAM labelled probe complementary to the mutant allele, whilst the wild-type primer mix contained

a HEX labelled probe complementary to the wild-type sequence. A total of 20ng of DNA was tested using a 'mutation rare detection' assay, with the remaining volume made up of nuclease-free water. The ddPCR reagents and conditions are presented in Table 7.

Table 7. ddPCR reagent mix and PCR conditions, table from Bio-Rad manual (Bio-Rad).

Reagent	Volume µl	Cycling Step	Temperature	Time	No. of cycles
2 x ddPCR Super Mix for probes (no dUTP)	12.5	Enzyme Activation	95°C	10 min	1
20 x Variant primers and probe (FAM)	1.25	Denaturation	94°C	30 sec	40
20 x Wild-type primers and probe (HEX/VIC)	1.25	Annealing/Extension	55-65°C	1 min	
DNA template	x	Enzyme Deactivation	98°C	10 min	1
Nuclease free water	10 - x	Hold	4°C	infinite	1
Final Volume	25				

X = 50fg to 100 ng; Lid heated at 105°C and sample volume set to 45µl.

DdPCR mix was transferred to a Bio-Rad DG8 Cartridge (1864008) with 70µL of Bio-Rad Droplet Generation Oil for Probes (1863005), covered with a Bio-Rad DG8 Gasket (1863009) and placed into the Bio-Rad QX200 Droplet Generator. The Droplet Generator produces approximately 20.000 droplets per sample. On average, a single DNA molecule is incorporated into each droplet, depending on DNA concentration. The generated droplets suspensions (45µL) were carefully transferred to a new PCR plate and sealed using the Bio-Rad DX1 Plate Sealer. The sealed plate was placed in the Bio-Rad T100 Thermocycler, and the reaction was amplified using the program detailed in Table 7. The amplification has occurred in each droplet. Next, the droplets were read with a Bio-Rad QX200™ Droplet Reader, and final analyses were performed using the Bio-Rad QuantaSoft™ software.

Positive, wild-type and no template controls (NTC) were used for each ddPCR run to ensure the assays correctly called positive and wild-type samples whilst excluding contamination.

2.3.2.3 DdPCR analysis using QuantaSoft software

The QuantaSoft software was provided by Bio-Rad and was used to detect single nucleotide and copy number variation. The Droplet Reader was used to determine which droplet contained mutant DNA template or gene of interest, which contained wild-type DNA or reference gene by quantifying the fluorescence levels of FAM or HEX/VIC within each droplet, respectively.

QuantaSoft software provides tools for reading the positive and negative droplets in each sample and plots fluorescence droplets by droplet. Amplified targets within droplets are analysed using 1D and 2D amplitude plots to define droplet positivity with the threshold obtained from positive control samples, Figure 21. Once the thresholds had been established, the ratio of FAM and HEX/VIC positive droplets were used to calculate MAF or Copy number (CN) for ctDNA. Finally, MAF, CN and respective standard deviations were calculated using Poisson distribution.

The total number of droplets generated during ddPCR was also analysed to ensure the generation droplet process happened efficiently, and the results were not influenced by droplet lysis at any stage. For the ddPCR run to be successful, a minimum total of 10.000 droplets was required.

Figure 21. The 2D plot of *ESR1* D538G assay.
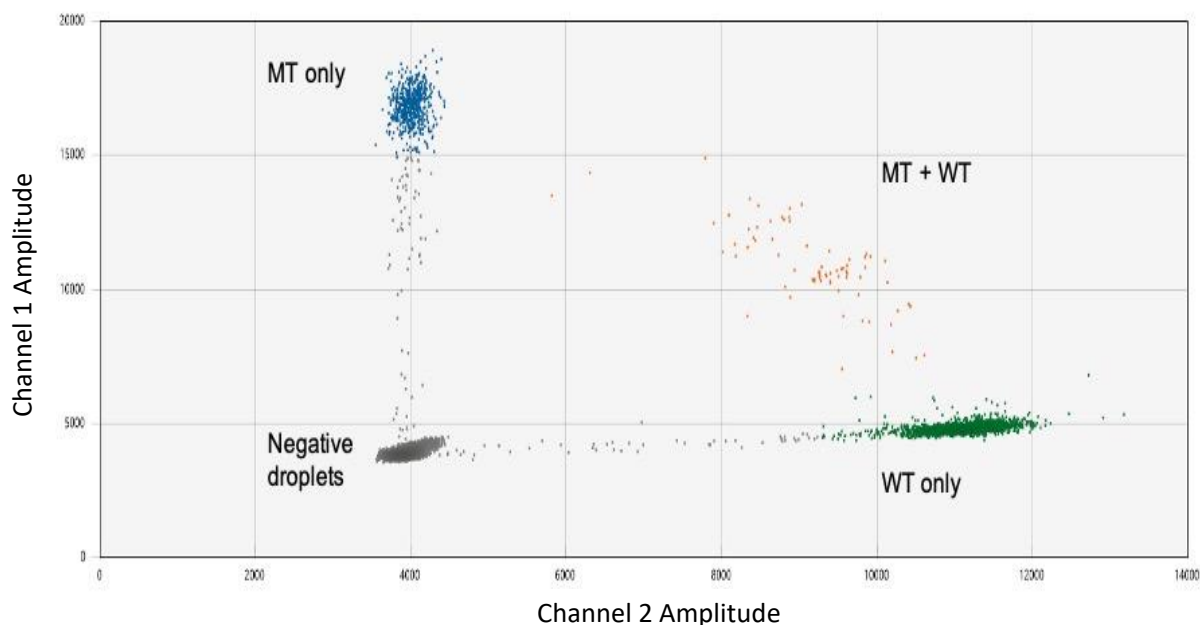
In this figure, blue cluster – FAM-positive droplets with the only mutant template (MT), orange cluster – double-positive droplets with both templates inside (MT+WT), grey cluster - negative droplets with no template, green cluster - HEX-positive droplets with only wild-type template (WT). MAF is calculated as Fractional Abundance (MT/MT+WT).

In this chapter, I described a workflow of 44-gene NGS panel and ddPCR assays used to detect SNV and CNV. In the next chapter, I will present optimisation with limit of detection of these methods for cfDNA.

3. Optimisation and Validation of cfDNA Testing Methods

3.1 Introduction

Over the years, ctDNA has become frequently tested in clinical trials to find clinically relevant biomarkers to select patients for new targeted therapies and monitor response and resistance to the new treatments. The emergence of NGS and ddPCR technologies facilitated testing genomic or FFPE DNA in detail. In addition, NGS development allowed high-throughput sequencing of multiple genes, whilst ddPCR enabled very sensitive and specific gene mutations detection in low-concertation DNA samples. However, the application of these methods to test ctDNA can be challenging.

3.2 Aims and Objectives

3.2.1 Aims

As part of this study, I intended to use the NGS targeted panel and ddPCR to investigate the most relevant genes mutated in endocrine-resistant breast cancer and genes involved in PI3K/AKT pathway in FFPE DNA and ctDNA samples from patients in the FAKTION trial. However, most commercial NGS panels and ddPCR assays have been validated for genomic or FFPE DNA. In this chapter, I aimed to validate 44-gene NGS panel and ddPCR assays for cfDNA testing.

3.2.2 Objectives

The main objectives are:

- To validate the ability of the targeted panel to detect cancer-specific mutations in ctDNA.
- To determine the limit of detection of 44-gene NGS panel for ctDNA by using reference cfDNA standards.
- To determine the limit of detection of ddPCR assays
- To validate ddPCR for the detection of copy number variations in ctDNA.

3.3 Limit of Detection of NGS panel for cfDNA samples

As human cfDNA samples mostly contain very low DNA concertation. This section aimed to evaluate whether the 44-gene NGS panel will detect low-frequency mutations in low input cfDNA. Also, to identify what minimum sequencing depth is required to detect the mutation in cfDNA. The reference standard cfDNA (HorizonDiscovery) samples at low concentrations with known mutations and their

allele frequency were used for the assessment of the limit of detection, as would closely represent human samples. The detection limit was not assessed for FFPE samples as standard NGS protocol was validated by the AWMGS laboratory.

Two Reference Standard cfDNA (HorizonDiscovery) samples contained variants at various allele frequency –16.7%, 5.6%, 5.3%, 2.5%, 1%, 0.5%, wild-type. Each frequency was sequenced in triplicate at two total DNA inputs (5ng and 10ng), which created a total pool of 27 samples, Table 8. Two samples (2.5% - 10ng and 1% - 5ng) failed library preparation; therefore, were excluded from the sequencing final pool, Table 8. Reference standards were sequenced at expected minimum coverage of 5000X. At this depths, 16.7%, 5.6%, 5.3%, 2.5%, 1%, 0.5%, VAFs were sequenced alongside wild-type (0%) controls. The accuracy of detected allele frequency of *EGFR* mutations across different expected AF 0.5%, 1%, 2.5% and 5% are presented in Figure 22.

Table 8. NGS detection results for cfDNA samples with known allele frequency mutations.

Total cfDNA input - 10ng

Gene	Variant	Expected AF (%)	Library DNA yield (ng/ul)	Depth	Observed AF (%)	Library DNA yield (ng/ul)	Depth	Observed AF (%)	Library DNA yield (ng/ul)	Depth	Observed AF (%)
PIK3CA	H1047R	16.7	3.12	4579	22.38	3.45	3651	20.71	3.15	3513	16.60
AKT1	E17K	5.6		4015	2.57		3297	5.34		2853	6.73
BRCA2	L1691fs			6080	6.55		5213	7.17		5462	9.94
EGFR	V769-D770insASV	5.6		3093	1.65		2847	3.13		2426	4.58
EGFR	G719S	5.3		1839	2.83		2081	1.25*		1661	5.90
	E746-A750del15			5155	7.58		4451	5.66		4267	6.07
EGFR	T790M	2.5	5.01	1879	2.34	4.34	2302	2.87	0.58	Failed	
	L858R			2466	2.43		2186	1.56*			
	E746-A750del			3506	6.05		3574	1.90			
	V769-D770insASV			4327	2.13		3501	0			
EGFR	T790M	1	6.78	1648	1.03*	3.28	1484	0	3.59	1731	0
	L858R			2687	2.05		2285	0		1531	0
	E746-A750del			6336	2.86		5894	0		4216	2.35
	V769-D770insASV			4366	0		4640	0		4589	0.92*
EGFR	T790M	0.5	3.68	1306	0	2.11	1727	0	2.60	1579	0
	L858R			1566	0		1924	1.30*		1943	0
	E746-A750del			5195	0.69*		5081	0.87*		5792	0
	V769-D770insASV			4816	0		6094	0		4874	0
EGFR	T790M	WT	4.02	1727	0	2.89	2063	0	NT		
	L858R			2442	0		1765	0			
	E746-A750del			6154	0		3994	0			
	V769-D770insASV			3094	0		2643	0			

Total cfDNA input - 5ng

Gene	Variant	Expected AF (%)	Library DNA yield (ng/ul)	Depth	Observed AF (%)	Library DNA yield (ng/ul)	Depth	Observed AF (%)	Library DNA yield (ng/ul)	Depth	Observed AF (%)
PIK3CA	H1047R	16.7	1.99	2960	13.92	1.97	2658	13.13	1.67	3714	14.65
AKT1	E17K	5.6		2646	2.95		2539	5.00		2059	10.25
BRCA2	L1691fs			4275	10.32		2562	11.24		3969	4.01
EGFR	V769-D770insASV	5.6		2398	1.29*		2213	2.89		2888	1.62*
EGFR	G719S	5.3		1135	0		930	2.69		1478	9.00
	E746-A750del15			3403	7.26		2277	3.47		4015	8.49
EGFR	T790M	2.5	2.90	1067	2.62	3.41	899	2.45	3.33	1332	4.88
	L858R			1746	3.49		1619	2.41		1796	4.62
	E746-A750del			3671	3.60		3689	3.82		3731	11.82
	V769-D770insASV			2907	1.41*		2913	1.47*		3156	3.23
EGFR	T790M	1	1.35	1216	2.96	2.99	2144	0	0.55	Failed	
	L858R			1446	0		1664	0			
	E746-A750del			3739	1.87		3720	3.60			
	V769-D770insASV			5243	0.95*		4674	0			
EGFR	T790M	0.5	1.66	1346	0	1.27	1229	0	2.56	2578	0
	L858R			1985	0		1263	0		2624	0
	E746-A750del			4076	0		2558	0		6268	0
	V769-D770insASV			3187	0		2544	0		3722	0
EGFR	T790M	WT	3.35	2763	0	NT			NT		
	L858R			1981	0						
	E746-A750del			5574	0						
	V769-D770insASV			3882	0						

NT – Not tested –two 10ng WT and one 5ng WT reference ctDNA samples were tested. Samples that failed library preparation were excluded from the final sequencing pool, *detected in IGV but missed by the variant caller.

Figure 22. Expected versus detected Mutant Allele Frequency of EGFR mutations.
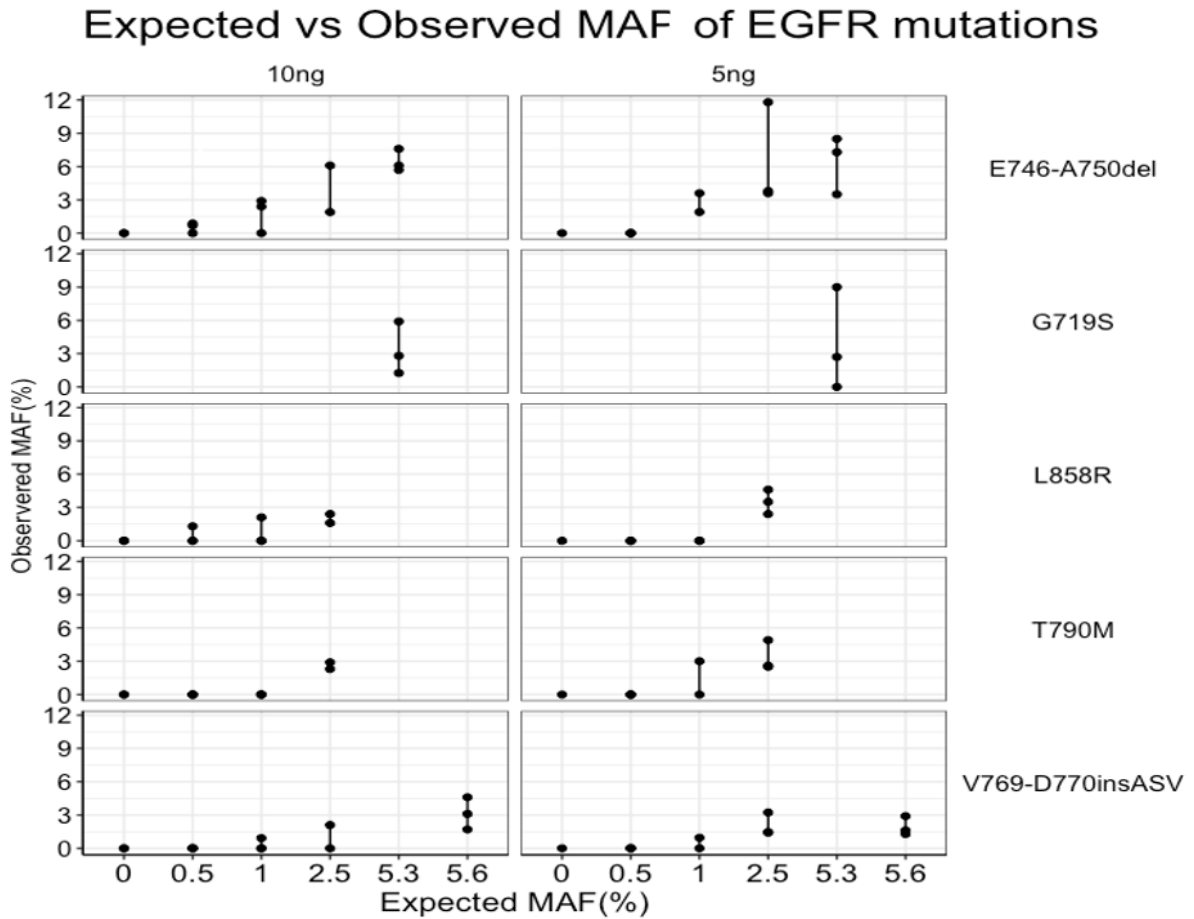
This figure shows the difference in observed MAF compared to expected MAF at two different DNA input concentrations for EGFR mutations.

Figure 23. Expected versus detected Mutant Allele Frequency (MAF).
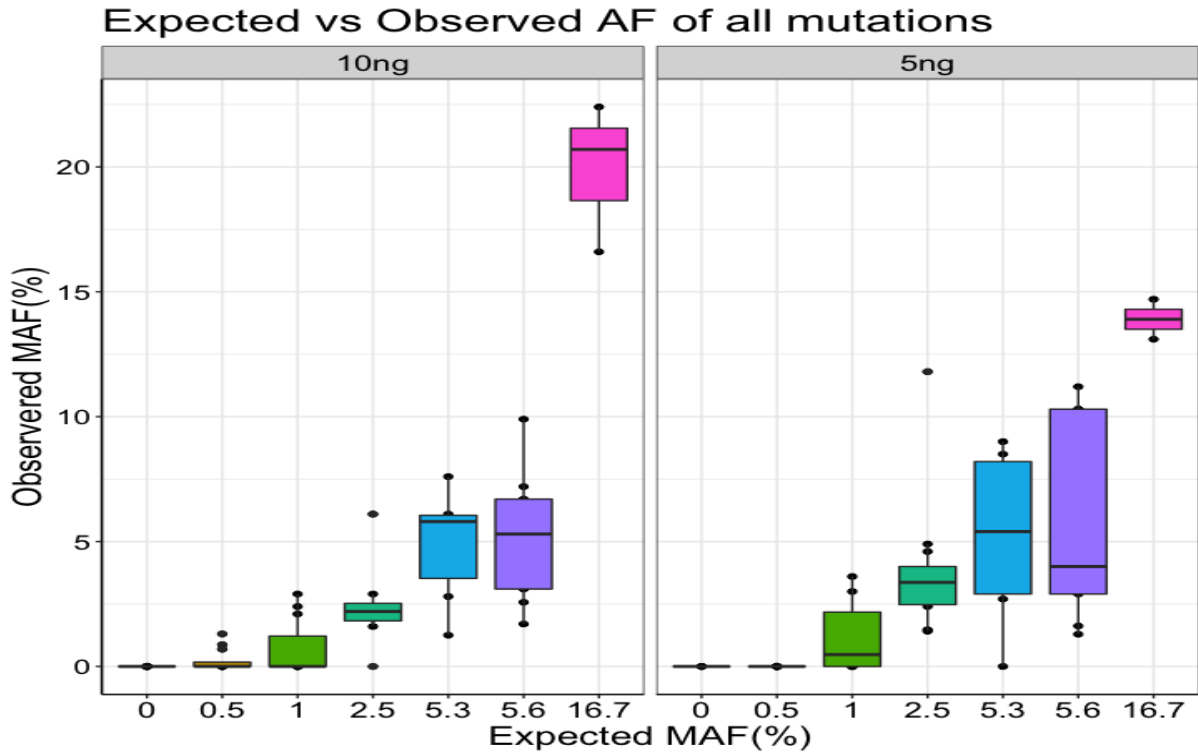
The variants were visually assessed in Integrative Genomic Viewer (IGV) when the variant caller did not detect mutations. If the variant was found in IGV with (equally distributed reads of the above total of 20, it was included in positive results. This indicated that variant reporter could miss some mutations; therefore, an inspection of the variant of specific interest with further validation by another method like ddPCR can be valid and necessary when analysing human samples. Furthermore, the detected allele frequency can differ from the expected frequency, and the difference can be much higher in lower DNA concentrations, Figure 23.

The observed allele frequency was very close to the expected frequency in half of the samples. *AKT1, PIK3CA, BRCA2* (16.7% and 5.6% VAFs) mutations were detected at both DNA concentrations(total 5ng and 10ng input). The variant caller missed EGFR insertions frequently, and visual inspection in IGV was required, Table 8. The wild-type samples were sequenced during the same run, two at 10ng and one at 5ng, to exclude the possibility of generating false-positive results. No mutations were found

The results showed that the variants could be detected at the lowest allele frequency of 2.5% for 5ng and 10ng cfDNA concertation, Table 8. However, in 5ng cfDNA concertation, the AF can be less accurate, Figure 23. The average sequencing depth achieved was 2700X, with a minimum of 900X. **This led to infer that the limit of detection for this panel was around 2.5% at 5ng and 10ng of total DNA input.** Although some of 1.0 % and 0.5% VAF mutations were present on review of the data in IGV, the variant caller program did not call this. Detection at this level would require higher sequencing depth but could create a risk of false positives.

3.3.1 Conclusions and Plan for Further cfDNA analysis

44 gene NGS targeted breast cancer panel detected mutations in various mutations at various allele frequencies. The lowest MAF for SNVs was 2.5% at 5ng of total DNA input. The average sequencing depth required was 2700X. The detected MAF was not as accurate as of the expected frequency and with less accuracy presented at 5ng DNA concentration. In the next chapters, I will present detected mutations by 44-gene NGS panel in human cfDNA samples from patients treated in the FAKTION trial and further evaluate mutation detection with a more sensitive method such as droplet digital PCR.

3.4 Limit of Detection Analysis for Droplet Digital PCR for Somatic Mutations

Droplet digital PCR (ddPCR) allows mutation detection at higher sensitivity, against a background of wild type DNA, compared with NGS. Mutations in ctDNA can be as low as 0.1% alternate allele

frequency. The yield of ctDNA extracted from plasma can vary and can be low, affecting the assay. Therefore, the method must have a low limit of detection to help overcome this. Also, the blood sample must be appropriately handled to limit DNA degradation from white blood cells.

3.4.1 ESR1 ddPCR Assays

ESR1 PCR assays were not commercially available and therefore needed to be designed, validated and optimised. Therefore, the sequences of *ESR1* mutations were put on ddPCR Expert Design Assays – Bio-Rad company website (https://www.bio-rad.com/en-uk/product/ddpcr-expert-design-assays?ID=PG9AOFRT8IG9), where primers and probes were designed and then manufactured. *ESR1* mutations sequences that required ddPCR assay design are presented in Table 9.

Table 9. ESR1 probes sequences.

Gene	Location	Mutation	Sequence
ESR1	chr6:152098791A>G	D538Gc.1613A>G	5'GCCCCTCTATG[G]CCTGCTGCTGG'3 (FAM)
ESR1	chr6:152098788A>C	Y537S c.1610A>C	5'GCCCCTCT[C]TGACCTGCTGCTGG'3 (FAM)
ESR1	chr6:152098788A>G	Y537C c.1610A>G	5'GCCCCTCT[G]TGACCTGCTGCTGG'3 (FAM)
ESR1	Chr6:152098787T>A	Y537N c.1609T>A	5'GCCCCTC[A]ATGACCTGCTGCTGG'3 (FAM)
ESR1	Chr6	Wild-type	5'GCCCCTCTATGACCTGCTGCTGG'3 (HEX)

Base change is highlighted in green.

ddPCR Optimising Conditions

A temperature gradient was performed to determine the optimum annealing temperature for each ddPCR probe/primer set. The reactions were run with an eight-step temperature gradient above and below the primers' melting temperature (usually 50-60°C). The results were analysed using QuantaSoft software as described previously. Primer/probe assays were validated using positive, wild-type ESR1 gblock controls and no template control (NTC) samples to ensure assay sensitivity and specificity.

For *ESR1* mutations primer and probes sets, the optimum annealing temperature was between 52.9 - 55.7°C. Therefore, a temperature of 55°C was used, see example in Figure 24. This temperature was selected as it allowed the most significant separation between positive and negative droplets whilst avoiding false-positive droplets caused by non-specific amplification.

Figure 24. Gradient temperature for *ESR1* Y537C mutation ddPCR assay.
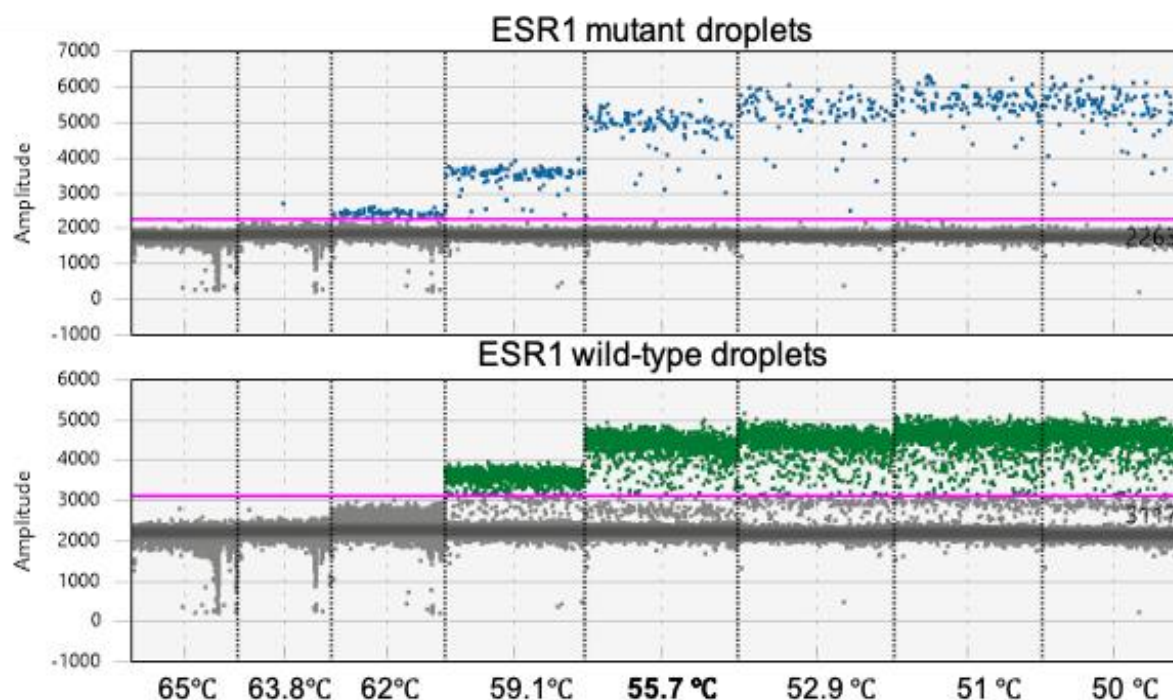
QuantaSoft analysis - 1D amplitude plots with *ESR1* mutant droplets (blue) and *ESR1* wild-type droplets (green).

Limit of Detection of *ESR1* mutations using Gblock mutant

Diluted ESR1 mutated gblock and wild type ESR1 gblock to ~ 5000 copies each to achieve a working range of the Bio-Rad ddPCR system (as described in section 2.2.1.1) was used for the limit of detection assessment. The dilution series of *ESR1* mutated gblock controls with wild-type *ESR1* gblock were performed to achieve VAF of 5%, 2.5%, 1.2%, 0.6%, 0.3% and 0.1%, Table 10. The negative sample was wild-type *ESR1* gblock, NTC – nuclease-free water. The series of dilutions were run with an annealing temperature of 55°C.

Table 10. Limit of Detection of *ESR1* variants.

ESR1 mutations	Number of mutant droplets (FAM positive)					
	5%	2.5%	1.25%	0.6%	0.3%	0.1%
D538G	416	217	100	51	24	19
Y537S	NT	11	3	4	3	0
Y537N	210	59	35	20	16	4
Y537N Repeat	NT	37	15	10	9	4
Y537C	188	21	failed	13	failed	3
Y537C Repeat	12	7	5	4	3	1

NT – not tested, Values in bold are where error bars did not cross 0; thus, this assay confidently detected the variant in question. Five or more mutant droplets were required for confident detection of an individual variant.

Working with diluted gblock can be challenging. Gblocks are synthetically made DNA fragments, and 1ng gblock DNA is not equivalent to 1ng of genomic DNA. In 1ng genomic DNA (3.3^9bp), there are ~300 copies of the target gene in the background of other genes. In contrast, 1ng of gblock DNA has ~2 billion copies of pure synthetic DNA (500bp) of the only target (e.g., ESR1) gene with no background of genomic DNA; therefore, this required serial dilutions to the operating range of the Bio-Rad ddPCR system (~9000 copies per ul). These samples were required to be diluted by more than a factor of 1,000,000 for useable levels for a ddPCR system of ~9000 copies per ul. The formula for determining how many DNA fragments were contained in 1ng of gblock is presented in Appendix 8.1 (Prediger 2013). The dilutions were undetectable by the Qubit fluorescence method; therefore, a desirable number of DNA copies relied on calculations and accurate dilutions. Table 10 shows that the different number of DNA copies occurred for different ddPCR assays, using the same dilution calculation to achieve the same MAF. This shows how difficult it was to achieve the desired DNA copy number for the assay.

The lower limit for positive mutation was challenging to establish due to difficulty in achieving accurate dilutions. There are currently no clinical guidelines to standardise ctDNA detection across patients with cancer. Moreover, the droplet values used in the literature are variable, with some studies only requiring two droplets (Hrebien et al. 2016; Riva et al. 2017) and others five (Huang et al. 2016). This cut-off of five droplets was chosen and applied in clinical practice by the AWMGS (ddPCR Standard Operating Procedure; LP-GEN-ddPCR). I proceeded to analyse our data using a minimum of five mutant droplets needed for confident ctDNA detection providing all controls were free of contamination. Although this may have compromised the sensitivity of ctDNA detection, this provided confidence in the findings.

One or more inappropriate DNA molecules in a control sample would invalidate any results obtained from cfDNA. In all accompanying wild-type and NTC reactions, no mutant droplets were detected, providing this assay with a specificity of 100%.

3.4.2 PIK3CA ddPCR Multiplex Assays

PIK3CA multiplex assays used in this project were designed and validated by AstraZeneca (AZ) and manufactured by Integrated DNA Technologies (IDT). Further optimisation was performed by AWMGS NHS laboratory. These assays were used in the FAKTION trial as part of patient stratification. The trial mainly focused on detecting Exon 9 mutations (p.E542K and p.E545K) and Exon 20 mutations (p.H1047R and p.H1047L). DdPCR assays were used for the detection of *PIK3CA* mutations in cfDNA

and FFPE DNA. Two multiplex assays were used to test for four mutations, but the results from these assays can inform that a *PIK3CA* mutation was found in a specific exon but could not be characterised.

The limit of detection was performed by AWMGS NHS staff and concluded that samples containing ~5 mutant droplets with the generation of >10,000 total droplets were classified as positive. The detection limit of both *PIK3CA* assays was between 0.5-0.7% at 10ng of DNA. When using lower concentration DNA, e.g., 5ng, then the level of detection was reduced.

3.4.3 AKT1 ddPCR assay

AKT1 assay (FAM-10031246, HEX- 10031249) was an 'off the shelf' assay validated by the Bio-Rad company; therefore, no gradient temperature was performed. The recommended temperature of 55°C was used for testing. Bio-Rad reported the sensitivity of 0.1%, using Horizon MCF10a (MUT), Promega female human genomic DNA (WT) in dilution series of mutant DNA in ~40,000 copies of wild-type DNA background.

The limit of detection was also performed with available genomic *AKT1* p.E17K controls, Horizon reference standard gDNA (HD753). The series of dilutions of 5% *AKT1* positive controls with AKT1 wild-type DNA, Horizon reference standard (HD172), were performed to achieve MAF at − 5%, 1%, 0.5%, 0.1%, and 0.05%. WT and NTC were used to exclude false-positive results and contamination, respectively. As a result, *AKT1* p.E17K was detected at the lowest level of 0.2% MAF in 10ng DNA input.

3.4.4 Summary of SNVs detection

Three ddPCR assays validations were performed for this project. Three different limits of detections were found. This depended mainly on the type of sample, was used for validation. The validation of ESR1 ddPCR assay with gblock was not the optimal validation due to reliance on the accuracy of calculations and multistep dilutions, which was challenging to achieve the accurate limit of the detection. Although the ESR1 gblock was probably less suitable for validation than human cfDNA samples, it was available at that time of the experiments. PIK3CA ddPCR assay was validated by AWMGS using FFPE DNA samples. AKT ddPCR assay was validated with genomic standard references.

3.5 Comparison Between NGS and ddPCR Detection of Mutations in FFPE DNA and ctDNA

NGS was used to detect mutations in FFPE and ctDNA in baseline samples and at the end of treatment ctDNA samples. It was cost-effective to track these mutations in ctDNA using ddPCR. This was acceptable as there was a good correlation between the two methods. The correlation was assessed using Bland-Altman plots for both ctDNA and FFPE tumour tissue DNA, Figure 25. Data used here included detection of *PIK3CA*, *ESR1*, *AKT1* mutations by NGS and ddPCR in FFPE DNA and baseline and end of treatment ctDNA samples.

Figure 25. Correlation between NGS and ddPCR.
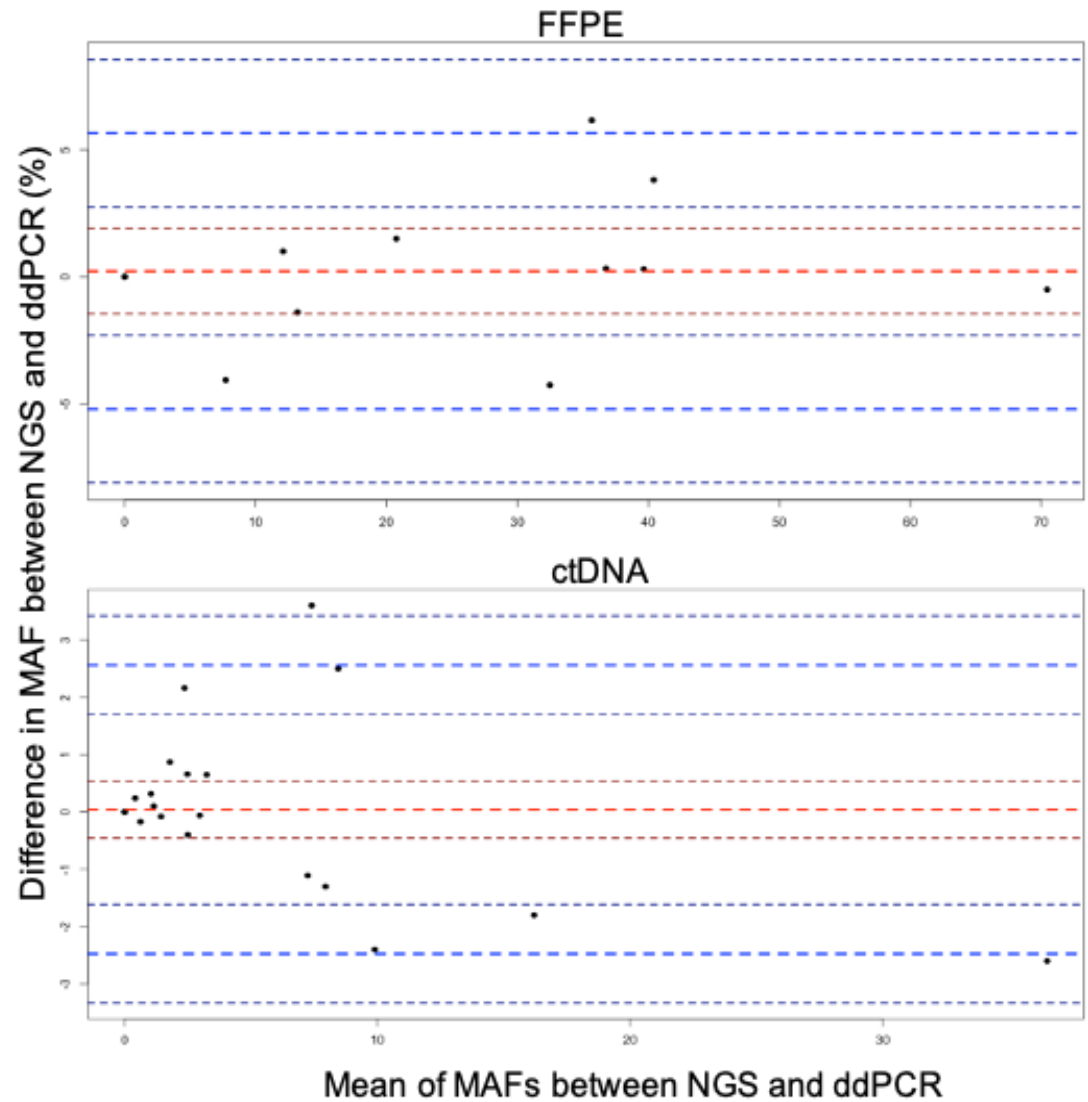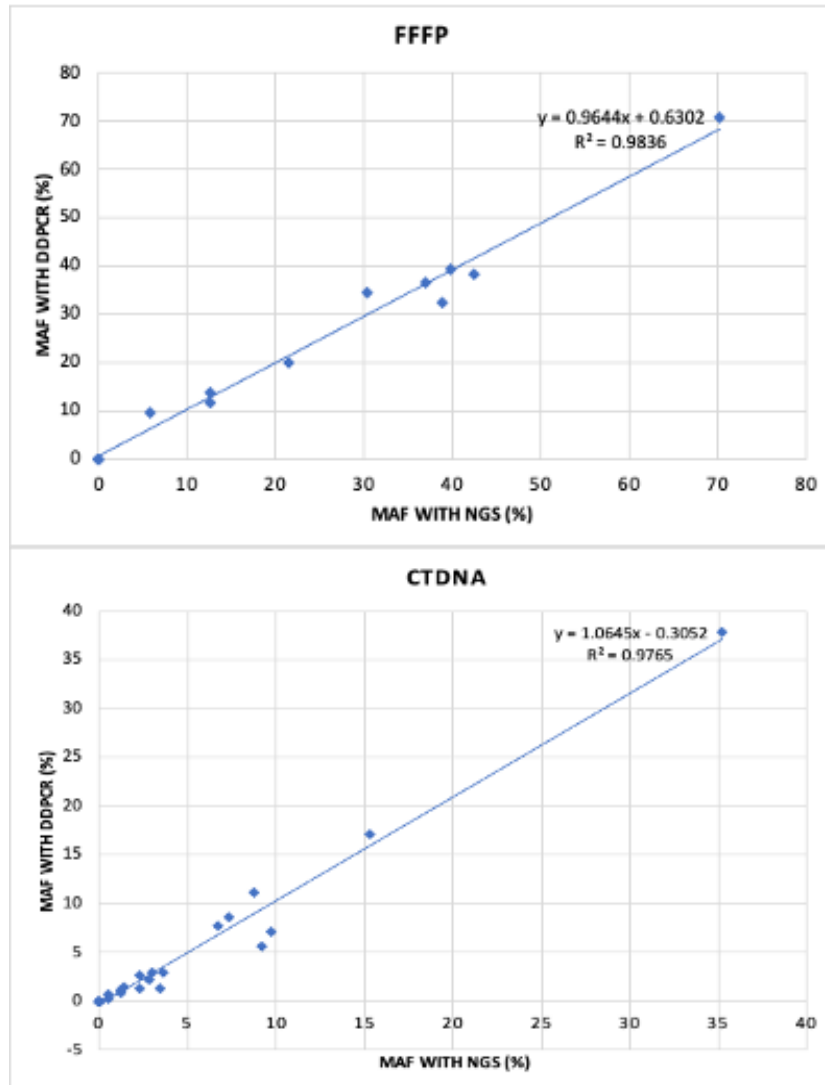
Correlation of mutant allele frequency (MAF %) of mutated DNA in FFPE (A) and ctDNA (B) samples, as detected by both methods ddPCR and NGS. Each data point represents one sample tested. Scatter plot on the left and Bland-Altman plots on the right

3.6 Copy Number Variation (CNV) ddPCR Assay Validation

Detection of *HER2*, *MYC*, and *FGFR1* amplification in ctDNA was assessed in this study, where the wide-type gene can be present in multiple copies. The normal human genome has two copies of each gene. If the gene is amplified, more than two copies can be found. The amplification can be detected in tumour tissue DNA using immunochemistry (IHC) and FISH techniques. However, it can be challenging to identify the increased number of copies of a gene in ctDNA when a sample is contaminated with normal DNA, Figure 26. The immunochemistry and FISH methods cannot be used to detect amplification in ctDNA. However, ddPCR allows the detection of small copy number differences and provides highly accurate measurements.

Figure 26. Illustration of the difference between FFPE DNA and ctDNA in the proportion of tumour CNV containment.
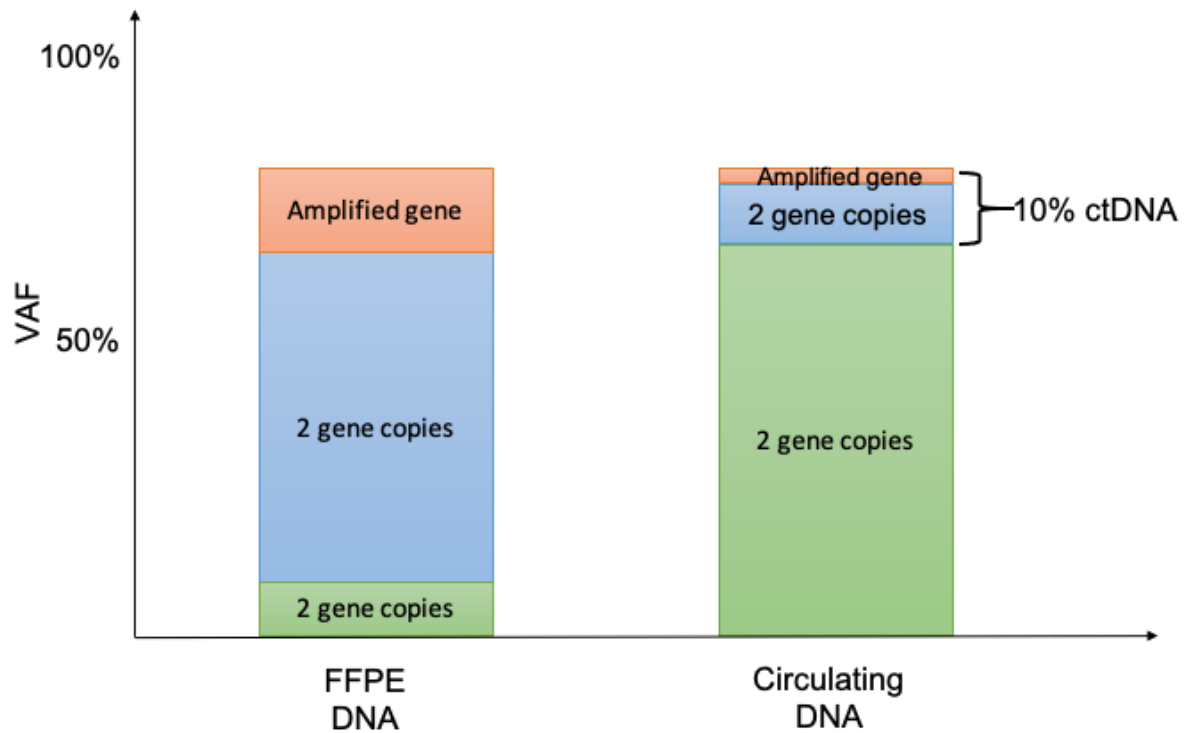
Green colour represents normal DNA with two copies of genes. **Blue** represents cancer DNA with two copies of genes. **Red** represents cancer DNA with an amplified gene.

The CNV ddPCR assays contain primer mixes against two separate genes. The primer mixture which contained the FAM probe was designed against a region in the gene of interest, whilst the mixtures containing the VIC probe was designed against a region in a gene that is a static non-amplifiable gene, therefore used as a reference gene. DNA was partitioned into ~14,000 - 20,000 droplets per reaction.

PCR setup and droplet generation were performed as described in section 2.3.2.2, and cycling conditions were described in Table 7 with an annealing temperature of 60°C. The Copy Number Variation settings were used on the QuantaSoft software at the point of droplet reading. This software-generated ratio between the target droplets and control droplets automatically, producing a copy number value, Figure 27.

To call a gene amplification in the sample, the assay conditions required to be achieved include a minimum of 400 droplets of the reference gene and 400 droplets for the target gene, minimum of total droplets above 10.000. If conditions have not been met, the test can be inconclusive and require further sampling if possible. In this study, we were limited with samples, but more samples could be requested from patients in diagnostic settings.

Figure 27. The 2D plot of CNV *HER2* assay.
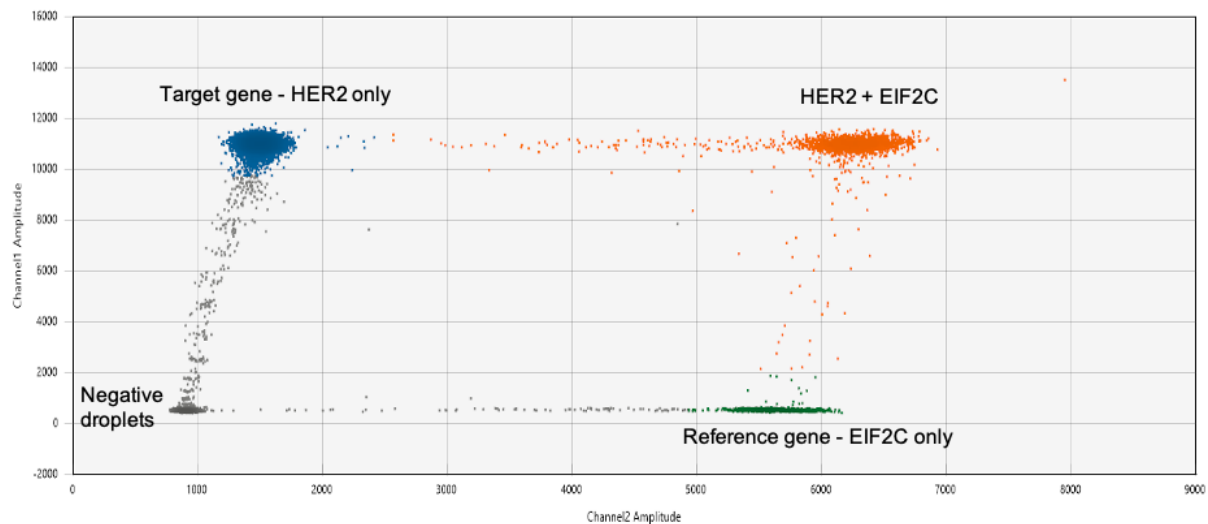
In this figure, blue cluster - FAM-positive droplets with only target gene *HER2*, orange cluster - double-positive droplets with both templates inside(*HER2*+EIF2C), grey cluster - negative droplets with no template, green cluster - VIC-positive droplets with only reference gene EIF2C. Copy Number(CN) calculation: CN = Target gene/Reference gene *Nb(number of copies of reference loci in the genome (usually 2).

3.6.1 *HER2* amplification

HER2 amplification and tumour percentage content in the sample

Two tissue samples with known *HER2* copy number and tumour percentage content were used to assess the minimum of tumour DNA at which amplification can still be detected. First, the pathologist

established the tumour content during the histopathological assessment. Then, these tissue DNA samples were diluted in series dilutions with wild-type cfDNA, reducing tumour DNA content and number of copies, Table 11 and Table 12. The aim was to mimic cfDNA, which contains significantly more wild-type DNA than cancer DNA. The ratio of tumour DNA and wild-type DNA in cell-free DNA can vary, but the most common ratio was 90 - 99% of wild-type DNA to 0.1-10% of tumour DNA. This experiment aimed to establish the percentage of tumour DNA in the sample at which the amplification can be confidently detected.

1. Extracted FFPE DNA sample with confirmed 12.4 copies of *HER2* gene detected previously by FISH was used for dilutions, Table 11. A pathologist estimated tumour cell content at 70% before DNA extraction. AP3B1 reference gene (see Appendix 8.2) was used for the assay. The sample was diluted with wild-type DNA in series dilutions to the level of 0.5% of tumour cell content. The 12.4 copy number of *HER2* was also being diluted whilst being mixed with wild-type DNA. The samples with lower tumour DNA content (2.2-0.5%) were tested in duplicate and triplicate. The amplification was detected at level 3.43 copies at 4.35% of tumour DNA, Table 11. However, the samples with low tumour content of 2.2-0.5% had results close to two copies, and therefore the amplification could not be detected. This shows that the amplification might not be detected by testing cfDNA samples with very low ctDNA content.

Table 11. Series dilutions of *HER2* DNA sample with known 12 *HER2* copies and tumour content of 70%.

Tumour Content %	*HER2* CN	*HER2* CN Repeat 1	*HER2* CN Repeat 2
70	12.40		
35	9.03		
17.5	6.57		
8.7	4.06		
4.3	**3.43**		
2.2	2.54	2.32	
1.1	2.05	2.23	2.39
0.5	1.93	2.1	2.01

X – Not tested, CN – Copy Number. Lower percentages of tumour content < 4.3% were tested in duplicate or triplicate.

2. Breast cancer sample with confirmed 6 *HER2* copies confirmed by FISH and 20% of tumour cell content. This sample's extracted DNA was mixed with wild-type DNA in series dilutions to 1.25% of tumour DNA. The 5% of tumour content was the level where I could confidently detect *HER2* amplification at 3.09 copies. 2.5% tumour content was tested on two occasions: once in triplicate and the second time in duplicate, Table 12.

Table 12. Series dilutions of *HER2* DNA sample with 6 *HER2* copies and tumour content of 20%.

Tumour Content %	*HER2* CN 1st test	*HER2* CN Repeat 1	*HER2* CN Repeat 1	*HER2* CN 2nd test	*HER2* CN Repeat 2	*HER2* CN Repeat 2
20	6.46			6.96		
10	4.41			4.54		
7.5	3.9	4.2		x		
5	<u>3.56</u>	<u>3.09</u>		<u>3.35</u>	<u>3.3</u>	
2.5	2.52	**2.89**	**2.62**	2.56	**2.71**	
1.25	x	x	x	**2.63**	2.38	2.32

X – Not tested, CN – Copy Number, Lower percentages of tumour content < 7.5% were tested in duplicate or triplicate.

I could not establish a clinical cut point for HER2 status in this study as I detected only one *HER2* amplification in 55 ctDNA samples. However, Gevensleben et al. (2013), in their study, showed that samples with detected numbers of copies of more than 2.6 could be amplified. If I used this cut off here, some of the samples from low tumour DNA content could have been called positive. Three samples out of five levels 2.5% tumour content tests have crossed a threshold of 2.6 copies. The level of 1.25% tumour content was tested in triplicate, and only one sample has marginally crossed the cut point of 2.6 copies, therefore unable to call this amplification.

This shows how difficult it can be to detect amplification in the cfDNA samples with low tumour DNA content. Also, the very high copy number of the gene could be detected in a lower percentage of tumour content but also, a very low level of 3 or 4 copies might be difficult to detect in 10% of tumour DNA. The main issue is that we do not know how much tumour DNA is present in the cfDNA sample and the primary copy number in the tissue DNA when testing, which puts this testing at risk of detecting false negatives.

Detection of amplification in the sample with known tumour DNA content

The detection of gene amplification in ctDNA could be more confidently performed when tumour DNA content in cell-free DNA is known. The detection of somatic mutation in the same sample could help assess the content of tumour DNA. The allele of a mutation can estimate the percentage of ctDNA in the sample. For example, if *PIK3CA* mutation or any other variant was detected in the cell-free DNA sample at MAF of 10%, this can suggest that the sample contains at least 10% of tumour DNA. There is a possibility that this sample could contain more tumour DNA but probably not less. I have tested

five samples with the known allele frequency of *PIK3CA* mutation in ctDNA and presumed HER2 negative (based on IHC +/- FISH report of primary FFPE). I attempted to identify *HER2* amplification in these ctDNA samples.

Table 13 shows samples with an allele frequency of *PIK3CA* mutations and the detection of *HER2* amplification. This approach can potentially help determine whether the unamplified sample is truly unamplified as the sample contain enough tumour DNA where the amplification could be detected if it existed. Sample no 154 with known *PIK3CA* mutation at the allele frequency of 48.6%, suggesting a very high tumour DNA load in the sample, allowing for the detection of *HER2* amplification at 11.4 copies, Table 13. Sample no 150 and 175 were non-amplified samples as there was enough ctDNA to determine copy number variation. Sample no 001 has a likely negative result as the ctDNA content is borderline. However, sample no 144 has a very low ctDNA content of 2.5%. It can be challenging to assess amplification at this level, as this was established in the previous section; therefore, the result is inconclusive.

Table 13. *HER2* amplification detection in samples with *PIK3CA* mutation a different MAF.

Sample ID	*PIK3CA* mutation MAF	*HER2* CN	Amplified
001	6.4%	1.85	Likely negative
150	25.5%	2.15	Negative
154	48.6%	**11.4**	**Positive**
175	16.8%	1.87	Negative
144	2.5%	2.3	Inconclusive

MAF – Mutant Allele Frequency, CN – Copy Number

Table 14 shows other patients with known multiple or single point mutations in ctDNA samples in which amplifications in *MYC* or *FGFR1* gene were tested. In patient no 42, despite *PIK3CA* mutation at 7.84%, the *MYC* amplification result was inconclusive as it failed to meet the control merits described above and would require further sampling and testing to verify the result. If known previous mutation, this can help estimate how much tumour DNA is in cfDNA and help us decide on testing for amplifications. Unfortunately, this is not always possible in a clinical setting and depend on detecting a somatic mutation in the ctDNA sample.

Table 14. *HER2*, *MYC*, *FGFR1* detection in samples with known SNV mutations.

Sample ID	Gene	MAF	HER2 amplification	MYC amplification	FGFR1 amplification
17	*ESR1*	6.3%	Non-amplified	**Amplified**	Non-amplified
	TP53	18.2%			
42	*ESR1*	1.3%	Non-amplified	Non-amplified	Inconclusive
	PIK3CA	7.8%			
104	*PIK3CA*	37.8%	Non-amplified	Inconclusive	Non-amplified
	TP53	17.6%			
108	*PIK3CA*	20.4%	Non-amplified	**Amplified**	**Amplified**
35	*ESR1*	18.4%	Non-amplified	**Amplified**	**Amplified**

MAF – Mutant Allele Frequency, SNV – Single Nucleotide Variation. The inconclusive result if the sample did not meet control measures.

3.6.2 *MYC* amplification

MYC amplification has been considered a bad prognostic factor for breast cancer patients and can play a role in endocrine resistance, as described in the introduction chapter. However, *MYC* is not routinely tested in clinical practice as currently, there is no targeted therapy. The ddPCR method will be evaluated in this section as an exploratory method on the 55 end of treatment ctDNA samples, therefore unable to establish sensitivity and specificity in this setting.

Identification of clinically meaningful cut off to detect gene amplification.

Identification of the clinically meaningful threshold of any test for patients is a frequent problem in medical research. The establishment of technical cut-off for increased copy number could have been not challenging if all samples could be called amplified when the sample has more than two copies of the gene present in the sample. However, it has not been evaluated whether having three copies or six copies of a specific gene will have the same clinical effect on a breast cancer patient. Therefore, it is essential to establish the clinical threshold, which would consider the number of copies and be clinically meaningful to the patient and clinician. Therefore, the maximally selected rank statistics (MAXSTAT) was used for this project. MAXSTAT was evaluated in other studies to determine the clinical threshold (Hothorn and Lausen 2003; Lausen B et al. 2004). R code was taken from http://www.sthda.com/english/wiki/survminer-0-2-4.

This approach provides a classification of observations into two groups by a continuous or ordinal predictor variable. For this calculation, the copy number ratio (CN ratio) was evaluated, which is a number of copies of the gene of interest divided by the reference gene (for example, HER CN/EIF2C CN). The normal CN ratio should be 1. The clinical threshold was calculated using the CN ratio of a specific gene and progression-free survival (PFS) of 55 patients to find the significant difference between the two groups of patients, divided by the CN threshold. The cut-point at 1.3 copy number ratio, p=0.0025, was found significant, Figure 28. For these calculations, I have only included samples that had enough DNA to call CN ratio confidently. This required minimum of 400 droplets of reference gene droplets, and the total number of droplets was >10000. 50 of the end of treatment ctDNA samples were qualified for this test.

Figure 28. Determination of *MYC* amplification cut point by MAXSTAT statistics.
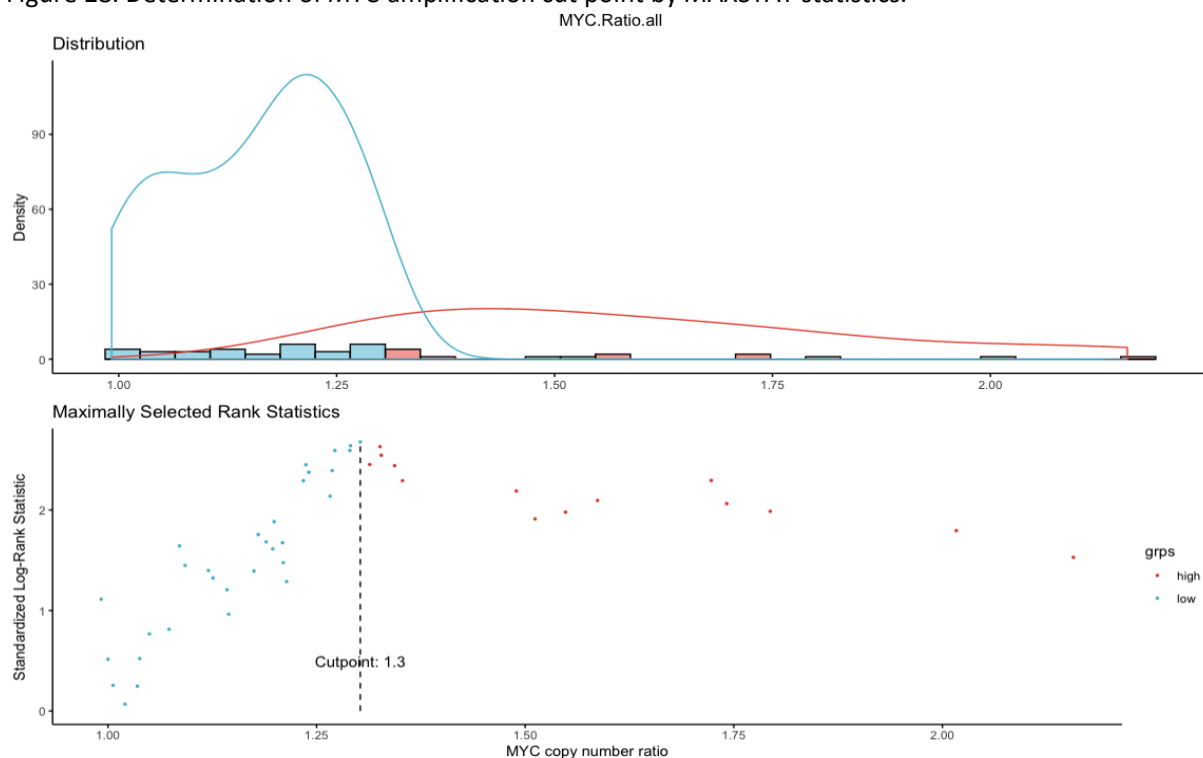
This figure illustrates the distribution of *MYC* copy number ratios and the determined cut-off, which has potential clinical relevance concerning PFS.

The PFS for two groups divided by a cut-point of 1.3 CN ratio was assessed by the Kaplan-Mayer curve in Figure 29. A statistically significant PFS difference of 3.5 months, p = 0.002, was identified. This difference of 3.5 months has a significant clinical difference in favour of the un-amplified group. This could suggest that a true small increase in the copy number of *MYC* gene in ctDNA could have a significant clinical impact on patients' PFS.

Figure 29. Kaplan-Meier Curves presenting PFS between MYC amplified and non-amplified groups.

Progression free survival by MYC amplification in FFPE/ctDNA

Number at risk

MYC	0	3	6	9	12	15	18	21	24
MYC non−amplified	33	24	12	10	6	4	3	1	1
MYC amplified	17	9	2	0	0	0	0	0	0
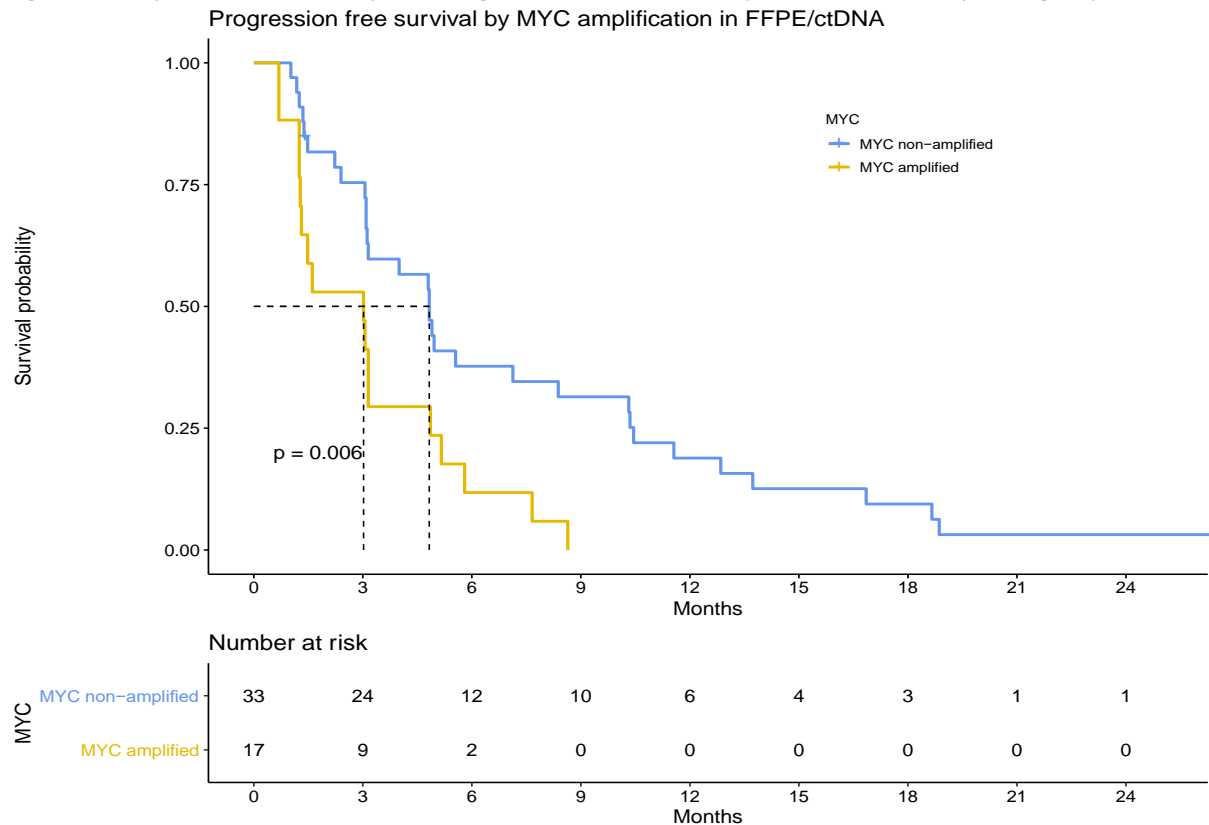
Kaplan-Meier Curves demonstrated 3.5 months difference in PFS between patients with *MYC* amplification and non-amplified *MYC*.

3.6.3 *FGFR1* Amplification

A similar analysis for the *FGFR1* gene was performed. The same ddPCR method but with *FGFR1* CNV assay with the same reference gene EIF2C was investigated and validated. The maximally selected rank statistics (MAXTAT) was applied to establish a provisional clinical threshold. From 55 of the end of treatment cfDNA samples, 52 samples yield results. We found the *FGFR1* copy number ratio threshold at 1.76, p = 0.002, Figure 30.

The progression-free survival for two groups divided by a cut-point of 1.76 CN ratio was assessed by the Kaplan-Mayer curve in Figure 31. A statistically significant PFS difference of 3.1 months, p = 0.0004, was identified. This difference of 3.1 months has a significant clinical difference in favour of the un-amplified group. This could suggest that a higher increase in the copy number of the *FGFR1* gene could have a significant clinical impact on patients' PFS.

Figure 30. Determination of *FGFR1* amplification cut-point by MAXSTAT statistics.
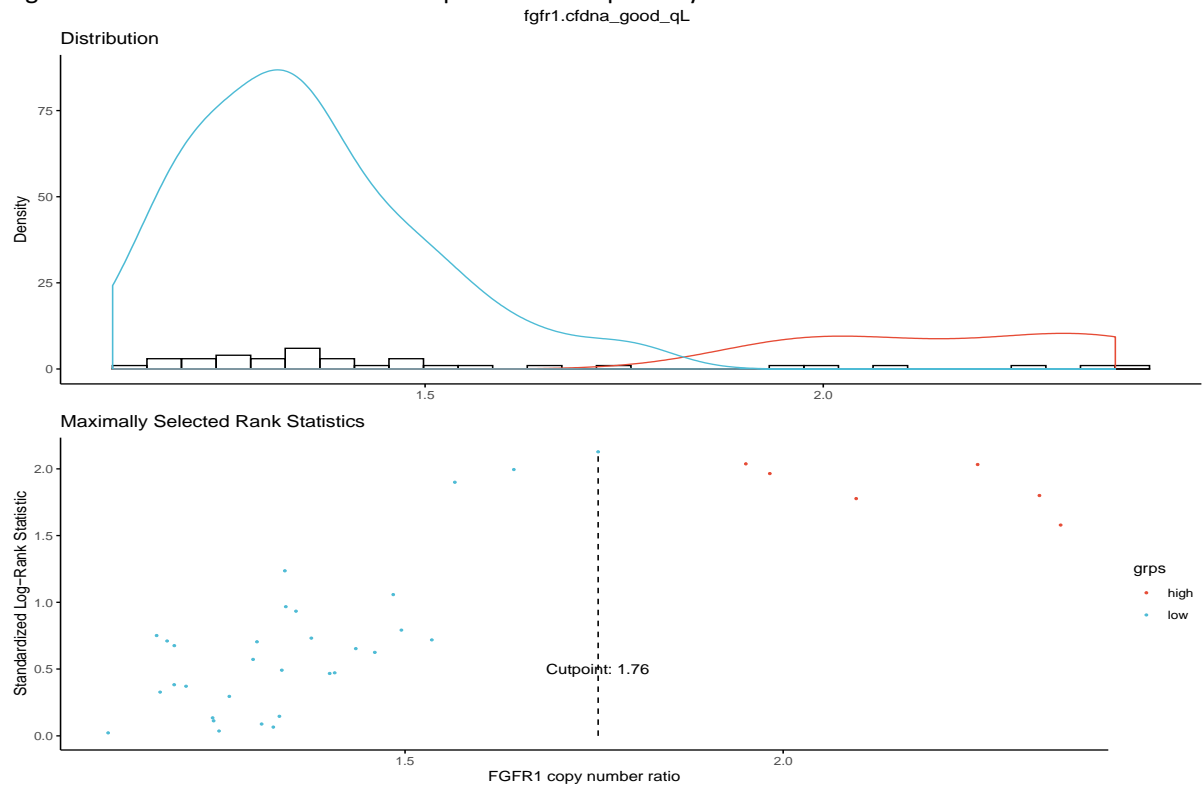
Figure 31. Kaplan-Meier Curves presenting PFS when *FGFR1* amplification
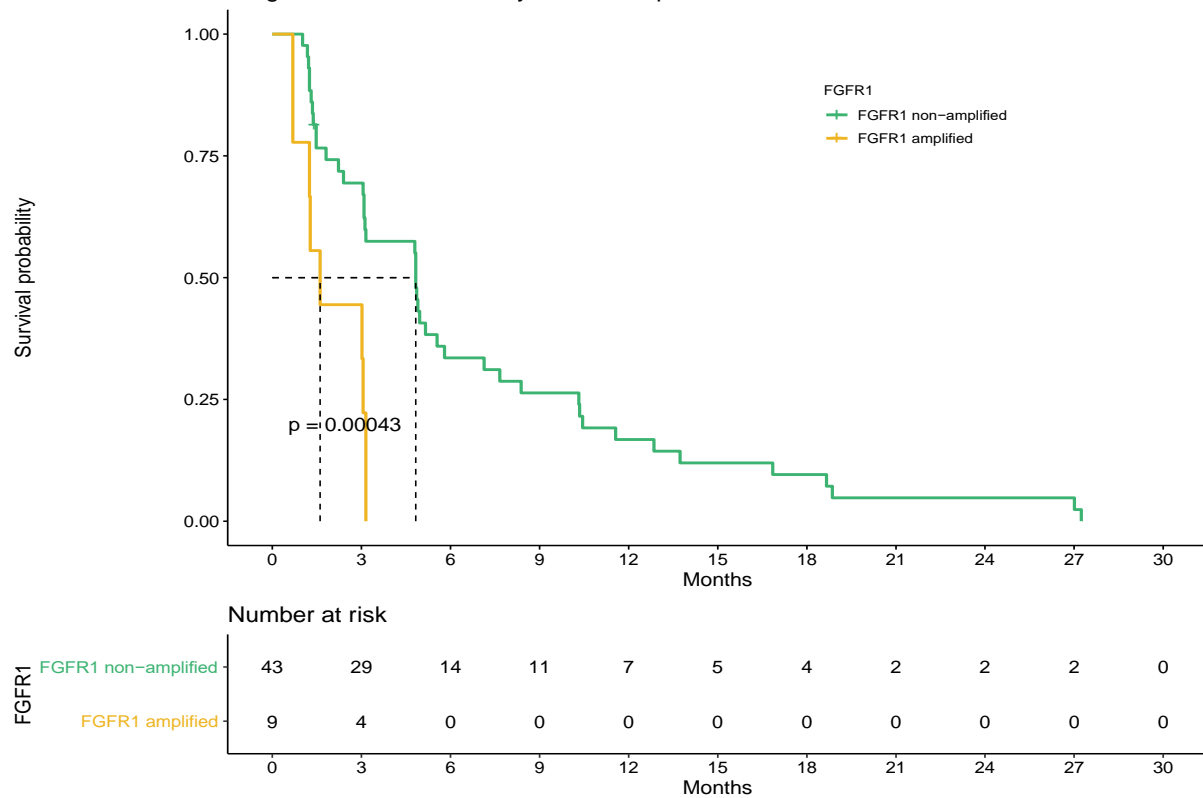
3.6.4 Summary of CNV Detection

Copy number variations can be challenging to detect in ctDNA. This can depend on ctDNA content in cfDNA and the primary number of copies of a specific gene. The higher content of ctDNA and the high level of gene copies in the sample would increase amplification detection. The ctDNA content in cfDNA could be identified before testing for gene amplification by detecting common somatic mutations. The number of gene copies could be assessed in tissue DNA, but new biopsies are not always possible.

The increased number of copies of the gene could have a different clinical effect, depending on the gene's functional role. It seems that a small increase in *MYC* copies can play a significant clinical role. However, for amplified *FGFR1* to have a clinical effect, it requires a higher number of gene copies. It is vital to detect gene amplification in samples tissue or ctDNA. However, it is also essential to identify the clinical limit of detection for each gene to ensure this genetic change can be used as a biomarker in future clinical trials and clinical practice. This would require further validation in future studies where gene amplification detection is correlated with clinical information.

4. Molecular Assessment of Baseline ctDNA and FFPE DNA to Identify SNVs Associated with Resistance to Endocrine Therapy Received Prior Trial Treatment.

4.1 Introduction

In this chapter, I intended to detect biomarkers associated with resistance to endocrine therapy in baseline FFPE DNA and ctDNA samples. This chapter investigates the utility of baseline ctDNA matched to FFPE DNA in 34 patients with metastatic endocrine-resistant breast cancer treated with endocrine therapy before FAKTION trial enrolment. In this chapter, I explore mutation detection using Next Generation Sequencing (NGS) panel and droplet digital PCR (ddPCR) and assess concordance between tissue and plasma samples, identify reasons for discordance and correlate with clinicopathological features.

4.2 Hypothesis, Aims and Objectives

4.2.1 Hypothesis and Aims

This chapter aims to test the hypothesis that multiple mutations in *PIK3CA*, *AKT1*, *PTEN*, *ESR1* and *TP53* genes can be detected in baseline FFPE DNA and matched ctDNA. Furthermore, I aimed to identify potential reasons for discordance between matched samples.

4.2.2 Objectives

This project aimed to determine the ability and limitations of the NGS panel and ddPCR in detecting low-frequency mutations in ctDNA. In this chapter, the objectives are:

- To explore the ability to detect mutations in *PIK3CA*, *AKT1*, *PTEN*, *ESR1*, *TP53* in baseline ctDNA and FFPE DNA using 44-gene NGS panel and ddPCR.
- To assess detected mutations' concordance between ctDNA matched to FFPE DNA samples.
- To identify potential reasons for discordance between samples.
- To identify the correlation between mutation detection and clinicopathological features of patients with endocrine-resistant breast cancer.

4.3 Single Nucleotide Variation Detection in Baseline Samples in Patients with Endocrine-Resistant Breast Cancer.

Objectives: Can 44-gene NGS panel and digital droplet PCR detect mutations in PIK3CA, AKT1, PTEN, ESR1, TP53 in baseline ctDNA and FFPE DNA, and if so, what is the concordance between FFPE DNA and ctDNA samples? What are the potential reasons for discordances?

34 Patients for this chapter were randomly selected from 140 FAKTION trial patients with the complete set of baseline tissue and blood samples available at the time of experiments. These baseline samples were collected prior to randomisation in the FAKTION trial. The concordance assessment between 34 FFPE samples and 34 matched plasma samples (total 68 samples) was performed, Figure 32. All patients had histologically confirmed invasive breast cancer, which was ER-positive and HER2-negative at diagnosis. Patient clinicopathological characteristics of this cohort of patients compared to the patients in the FAKTION trial are presented in Table 15.

Figure 32. Diagram illustrating patient selection for Chapter 4.
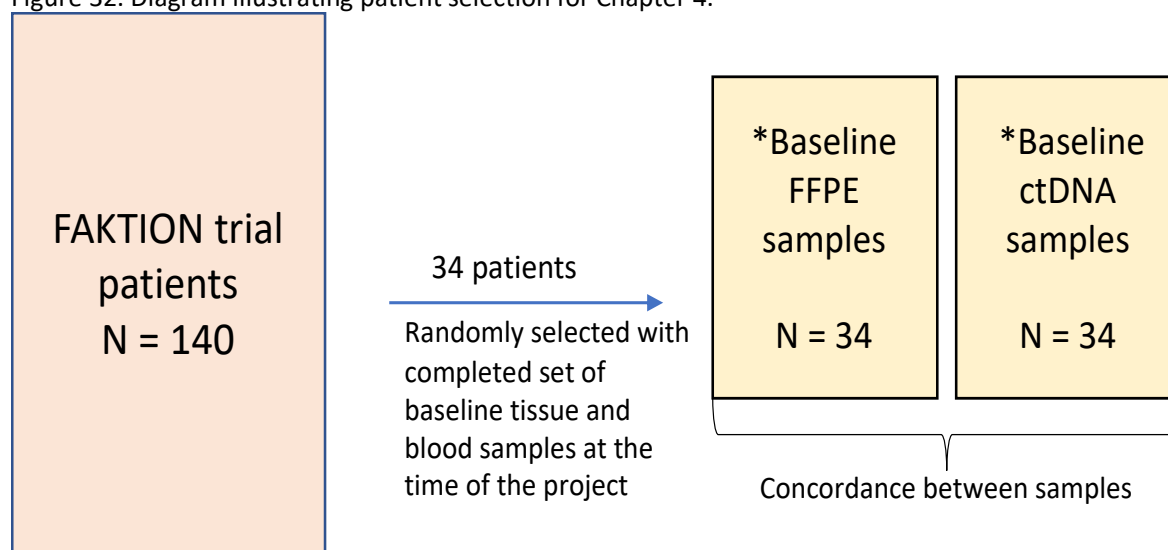
*Baseline samples collected prior treatment received in FAKTION trial

Table 15. Clinicopathological characteristics of 34 patients in comparison to FAKTION patient population.

	n=34*	Ful + Capi (n=69)	Ful only (n=71)
Median Age	63(43-81)	62 (42-81)	61 (40-82)
Histopathological subtype			
IDC	27 (79%)	57 (83%)	58 (82%)
ILC	2 (6%)	4 (6%)	12 (17%)
mixed IDC/ILC	2 (6%)	5 (7%)	0
Other	1 (3%)	3 (4%)	1 (1%)
NA	2 (6%)	0	0
Number of disease sites			
1mt site	14 (41%)	15 (22%)	19 (27%)
>2 met site	18 (53%)	54 (78%)	52 (73%)
NA	2 (6%)	0	0
Metastatic sites			
Brain	0 (0%)	1 (1%)	1 (1%)
Liver	10 (29%)	32 (46%)	29 (41%)
Lung	8 (24%)	30 (43%)	28 (39%)
Bone	28 (82%)	58 (84%)	55 (77%)
Lymph nodes	10 (29%)	28 (41%)	30 (42%)
Pericardial or pleural	2 (6%)	5 (7%)	3 (4%)
Chest wall or skin	1 (3%)	1 (1%)	3 (4%)
Other visceral	2 (6%)	2 (3%)	1 (1%)
Previous adjuvant endocrine therapy			
yes	23 (68%)	60 (87%)	65 (92%)
no	10 (29%)	9 (13%)	6 (8%)
NA	1 (3%)	0	0
Previous endocrine treatment (metastatic or locally advanced setting)			
0 lines	6 (18%)	9 (13%)	6 (8%)
1 line	23 (68%)	39 (57%)	45 (63%)
≥2 lines	4 (12%)	20 (29%	20 (28%)
NA	1(3%)	1(1%)	0

*n=34 patients evaluated in this project from 140 FAKTION patients, Ful – fulvestrant, Capi – capivasertib, n – number of patients, NA - Not Available, IDC - Invasive ductal carcinoma, ILC - invasive lobular cancer

Overview of detected mutations in the PIK3CA, AKT, PTEN, ESR1 and TP53 genes in ctDNA and FFPE DNA are presented in Table 16. Most relevant genes to the PI3K/AKT pathway will be evaluated in the first instance, followed by *ESR1* mutations associated with endocrine resistance. In addition, *TP53* mutations were assessed as essential factors, although not directly related to resistance.

Table 16. Mutation detection in PIK3CA, AKT1, PTEN, ESR1, TP53 gene in ctDNA and FFPE DNA.

Pt ID	PIK3CA FFPE	PIK3CA ctDNA	AKT1 FFPE	AKT1 ctDNA	PTEN FFPE	PTEN ctDNA	ESR1 FFPE	ESR1 ctDNA	TP53 FFPE	TP53 ctDNA
79	●	●								
123	●	●			●	●				
4	●	●								
71	●	●						●		
129	●	●						●		
110	●	●			●					
122	●	●	NA		NA		NA	●	NA	
34	●	●								
104	●	●							●	●
84	●	●								
44	*	*						●		
42	●									
57	●						●		●	
80	●		●							
99	●									
145	●									
94	●								●	●
36	●									
138	●								●	
108		●							●	
35								●		
21										
106										
23										
65										
38										
45								●		
17								●	●	●
77								●		
111					●				●	
115									●	●
51								●	●	
132			●	●						
131			●	●						
Concor.	71%		97%		94%		73%		88%	

* Two different PIK3CA mutations detected in ctDNA and FFPE DNA. Dark colours - represent mutation detection in the specific gene. Light colours – represents – wild type. NA – Sample not available for NGS analysis, Concor. – Concordance between FFPE DNA and ctDNA.

4.3.1 *PIK3CA* Mutation

Objectives: Can 44-gene NGS panel and ddPCR detect mutations in PIK3CA gene in baseline ctDNA and FFPE DNA? What is the concordance between these samples?

4.3.1.1 *PIK3CA* mutation status and concordance between FFPE DNA and ctDNA

24 (71%) of 34 patients had concordant PIK3CA status between ctDNA and matched FFPE DNA samples, which included 10 patients with PIK3CA mutation and 14 patients with wild-type PIK3CA in both samples, Table 16.

10 (29%) of 34 patients had discordant PIK3CA status, including nine patients with *PIK3CA* mutation detected in FFPE DNA only and two patients with PIK3CA present in ctDNA. **Patient 44** had two different PIK3CA mutations detected in ctDNA and FFPE DNA and therefore was included in the discordant group, Table 16

A total of 23 PIK3CA mutations were found in 20 (58.8%) patients (exon 20 – p.H1047R (8), p.H1047L (2), p.H1043I (1), exon 9 (p.E545K, p.E542K) (5), p.E726K (3), p.E970K (1), p.N345K (1), p.E110Del (1), p.C378W (1)). Three patients had two PIK3CA mutations detected, Figure 33 and Table 17.

All mutations in this study were detected by a 44-gene targeted NGS panel, except for *PIK3CA* exon 9 mutations (p.E545K, p.E542K) which were not covered by the panel. The multiplex ddPCR PIK3CA exon 9 assay was used to detect one of two *PIK3CA* p.E545K or p.E542K mutations. The positive results of this test can be read as 'positive mutation in exon 9 (p.E545K, p.E542K)' but cannot be characterised as described in chapter 3 (section 3.4.2). Mutations in exon 20 (p.H1047R and p.H1047L) were confirmed using multiplex ddPCR PIK3CA exon 20 assay.

Figure 33. *PIK3CA* mutations' positions in *PIK3CA* functional domains and the frequency of mutations detected in FFPE and ctDNA in this project.
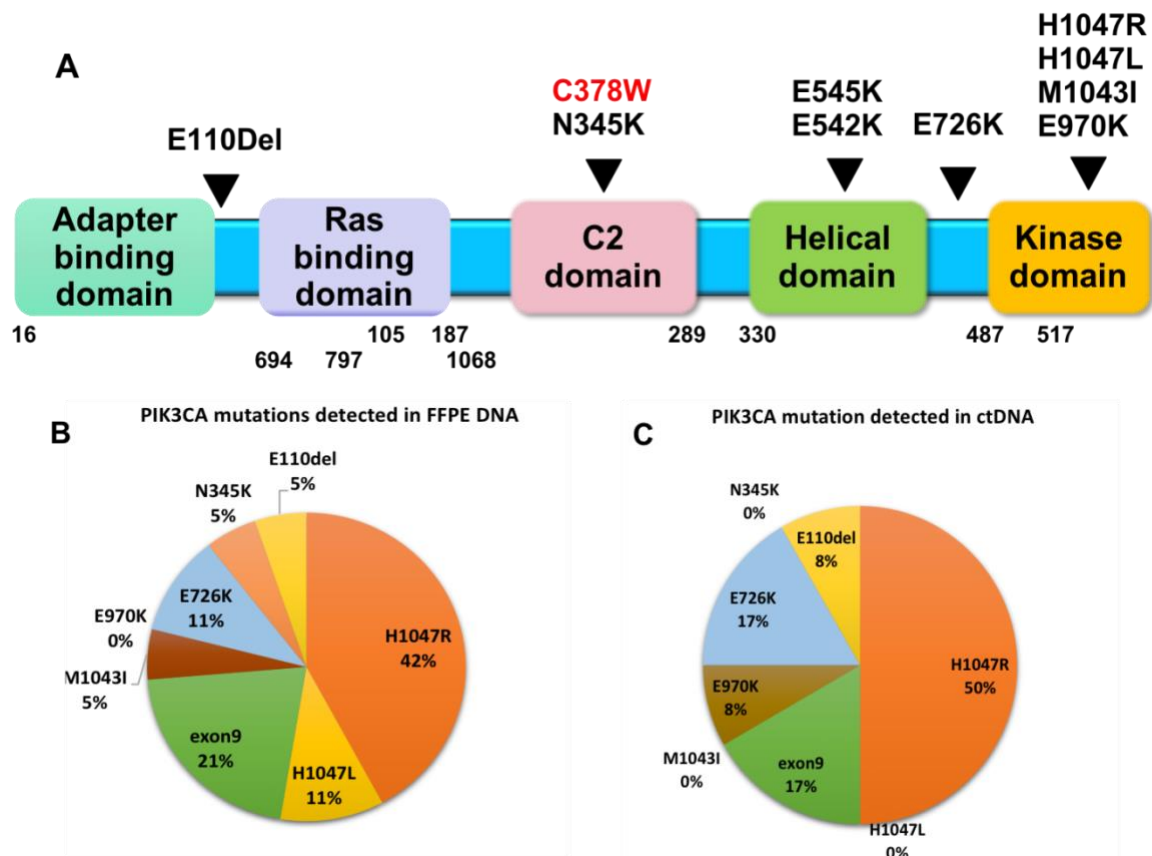
A *PIK3CA* functional domains represent mutations found in this study **B** Frequency of mutations in FFPE DNA and ctDNA **C**.

The mutation in ctDNA might be challenging to detect for various reasons. The use of ctDNA has its limitations. The detection could be affected by: inadequate sample handling, the presence of a very low amount of ctDNA related to the burden and cell turnover of the tumour, the discrimination of ctDNA from cfDNA, and the accurate quantification of the number of mutant DNA fragments in the sample using diagnostic tests (Diaz and Bardelli 2014). Test sensitivity could be affected by a low cfDNA yield or insufficient sensitivity of methods to detect very low-frequency mutations. FFPE samples contain more tumour DNA as has been taken directly from cancer cells. Although there would be normal cells in the sample, the proportion of tumour DNA to normal tissue DNA is much higher and can be estimated by the pathologist. However, formalin fixation of the sample can damage DNA strands that create false positives results. The biopsy is also taken from a tiny part of the tumour, and cells with the mutation can be missed due to intratumour heterogeneity.

4.3.1.2 Evaluation of PIK3CA discordance

Objectives: What are the potential reasons for PIK3CA discordances between FFPE DNA and ctDNA?

PIK3CA detection in ctDNA versus sampling

Technical factors, such as adequate sample handling and transport to the central laboratory, storage, the time between collection and analysis, can play a significant role in mutation detection in ctDNA. In the FAKTION trial, sample collection had its protocol and was performed by trained staff. Blood sample collection in Streck tubes and time between collection and analysis was strictly supervised. If the sample arrived at the laboratory after 94 hours, then another sample request was issued. Despite all these strict protocols, technical errors can still happen.

Influence of endocrine therapy on the mutation detection in ctDNA

Despite clinical disease progression, endocrine therapy could continue to slow cancer growth or decrease cell turnover and release less DNA to the bloodstream. The lower amount of DNA could affect mutation detection in ctDNA. 'Washout period' of a few days or weeks when the patient is not on anticancer treatment could increase ctDNA release as the cancer growth or cell turnover increases.

In 12 patients with *PIK3CA* variant detected in ctDNA, 7 (58.3%) had samples collected whilst on the endocrine treatment, and 5 (41.6%) were not on treatment. In 8 patients which no *PIK3CA* mutation detected in ctDNA but had mutation present in FFPE DNA, 5 (62.5%) patients were actively taking endocrine therapy, and 2 (25%) were not on treatment, 1 had no date of last treatment (Fisher test, p=0.0656, two-tailed). **The analysis suggested that endocrine therapy did not significantly influence the *PIK3CA* mutation detection in the ctDNA.**

ctDNA concentration and methodological issues

Table 17 shows DNA concentrations of the samples with the final library concertation and sequencing depth. I assessed ctDNA concentration extracted from the plasma of patients to assess whether patients with PIK3CA detected had higher levels of ctDNA. Interestingly, the average concertation of cfDNA samples with wild type *PIK3CA* was slightly higher than the concentration of samples with

positive *PIK3CA* mutation, 18.6ng/ml of plasma and 16.9ng/ml of plasma, respectively. However, **no significant difference in DNA concertation means between the two groups was found** (Mann-Whitney, p=0.664)**.** The total minimum requirement of cfDNA concentration for ddPCR was 2ng, and for the 44-gene targeted panel was 5-10ng.

In patients with discordant results, I reviewed the NGS performance to evaluate if the discordant result could be due to technical issues in library preparation or sequencing performance. Low concertation of DNA in the final stage of library preparation could suggest a failure of the process. Only if more DNA material was available, the library preparation was repeated prior to sequencing. Insufficient sequencing coverage could also explain why mutations were not detected. For example, the main reason for the discordance in patient 94 was a low sequencing depth of the ctDNA sample (p.N345K – 116X). In Patient 44 insufficient coverage of FFPE DNA (p.E970K - 18X) could also be the main reason for discordance, Table 17.

Table 17. PIK3CA concordance and discordance between FFPE and ctDNA.

| Pt ID | PIK3CA | | Variant | FFPE | | | | | | ctDNA | | | | |
	FFPE	ctDNA		Tumour %	FFPE DNA con (ng/ul)	Final Lib (ng/ul)	Seq Depth	PIK3CA NGS AF(%)	ddPCR AF(%)	ctDNA con (ng/ml)	Final Lib (ng/ul)	Seq Depth	PIK3CA NGS AF(%)	ddPCR AF(%)
79			*exon 9	80	35.4	18.8	NT	NT	6	33.20	8.7	NT	NT	2.00
123			E110del	NA	5.6	13.8	2411	29.1	NT	21.80	12.2	2195	38	NT
4			H1047R	70	0.6	16.3	12067	21.5	NT	5.5	12.8	6000	9.7	7.2
71			H1047R	40	0.9	17.8	3274	30.3	34.6	8.9	16.0	7467	2.8	2.2
129			E726K	NA	39.9	5.2	1057	6.1	NT	4.42	9.1	3541	10.0	NT
110			H1047R	80	3.4	15.8	16310	33.8	30.0	11.4	13.9	7625	3.1	2.5
			C378W				9663	30.8	NT			4729	3.3	NT
122			H1047R	NA	4.0	NT	NT	NT	32.1	7.18	21.0	9432	15.3	17.1
34			H1047R	90	39.1	16.8	12926	35.0	32	13.20	14.7	9530	2.2*	NT
104			H1047R	80	2.9	12.5	5713	70.2	70.7	7.7	13.9	9367	8.7	11.1
84			E726K	80	7.0	11.6	1887	21.0	NT	18.9	9.7	3153	3.5	NT
44	*	*	M1043I	40	0.1	3.5	13990	42.5	NT	43.4	11.6	14677	0	NT
			E970K				18	0	NT			12371	7.4	NT
42			H1047R	45	20.0	15.7	4542	36.9	36.6	8.8	6.9	6378	0	0
			E726K				1503	9.1	NT			2098	0	NT
57			H1047R	25	0.4	5.2	4527	39.8	39.5	49.6	4.9	4037	0	0
80			H1047L	NA	18.8	12.9	5363	12.6	11.6	7.56	14.3	7062	0	0
99			H1047L	90	46.2	18.6	12271	56	NT	12.22	13.0	11758	0	fail
145			*exon9	70	4.7	15.8	NT	NT	32.8	17.32	11.6	NT	NT	0
94			N345K	NA	20.3	17.6	1790	33.5	NT	13.12	17.0	116	0	NT
36			*exon 9	90	26.0	15.4	NT	NT	13	6.9	16.0	NT	NT	0
138			*exon9	NA	7.7	9.1	NT	NT	33.4	16.92	20.2	NT	NT	0
108			*exon 9	80	32.0	6.0	NT	NT	0	26.8	14.6	NT	NT	18.7

*Exon 9 – (p.E542K, p.E545K), NT - Not tested, AF –Allele Frequency, * AF detected under the limit of detection, Final Lib – Final Library DNA concentration, Tumour % - estimated tumour cell content (%), DNA con – DNA concentration, Seq depth – sequencing depth.

***PIK3CA* concordance and time interval between FFPE and blood sample**

Patients in this study had biopsy or resection performed at primary diagnosis, recurrence of the disease or disease progression. Plasma samples were taken before the FAKTION trial randomisation; therefore, there was a significant time interval between tissue and blood samples in most patients.

In 10 (50%) patients with a concordant *PIK3CA* mutation in FFPE DNA and ctDNA, the median time gap was 4.2 years (range of 1.9 – 17.1 years, log-rank test, p=0.52), Table 18. In 10 (50%) patients with discordant *PIK3CA* status, the median time between samples was 9 years (range 0.1 – 16.7, log-rank test, p=0.52), which was more than twice longer than the concordant group and almost three times longer than patients with wild-type *PIK3CA,* the median gap time of 2.6 years (range 0.02 – 14.3 years). The time intervals between samples for each patient are presented in Table 19.

Table 18. Median time intervals between FFPE and plasma for patients with *PIK3CA* (years).

Concordance between FFPE and ctDNA		PIK3CA wild-type
Yes	**No**	
Number of pt	10	10	14
Median time between samples(years)	4.2	9	2.6
Range (years)	1.9 - 17.1	0.1 - 16.7	0.02-14.3
p value	0.52		

The time difference between the samples collection of two matched samples (FFPE and plasma) can influence the discordance data and reflect cancer biology. The longer gap between samples could allow for biology cancer to change. This could account for difficulty detecting mutation in ctDNA and discordance between FFPE DNA and ctDNA samples.

Table 19. Clinicopathological features of patients in this project.

Pt ID	PIK3CA		Age	Histology	Time between FFPE and plasma (years)	Biopsy site	Metastatic sites
	FFPE	ctDNA					
79	■	■	54	IDC	**12.5**	primary	Bone + lung
123	■	■	70	IDC	5.4	primary	Bone + liver
4	■	■	76	IDC	4.1	primary	LN
71	■	■	76	IDC	1.9	**metastases**	Bone + LN
129	■	■	63	IDC	**17.1**	primary	Bone
110	■	■	71	IDC	2.1	primary	Bone + liver + lung + LN
122	■	■	71	**ILC**	**7.9**	primary	Bone + liver
34	■	■	57	IDC	4.3	**metastases**	Bone
104	■	■	52	IDC	2.7	primary	Bone + lung + LN
84	■	■	74	IDC	2.2	**metastases**	Bone + liver
44	*	*	66	IDC	9.2	**metastases**	Bone
42	■		57	IDC	**14.9**	primary	Bone + liver + pleural + LN
57	■		56	IDC	0.9	primary in met set	Bone
80	■		54	IDC	2.9	primary	Bone
99	■		68	IDC	**8.5**	primary	Bone + lung
145	■		59	mixed	**12.6**	primary	Bone
94	■		53	NA	NA	**metastases**	NA
36	■		58	IDC	**16.7**	primary	Bone
138	■		72	IDC	16	primary	Bone + lung + adrenal
108		■	57	IDC	**8.9**	primary	Bone + liver
35			43	IDC	**7.9**	primary	Bone + liver + pleural + LN
21			61	mixed	**8.2**	primary	Liver
106			76	IDC	3.8	Primary in met set	Bone
23			66	**ILC**	2.0	primary	Bone
65			55	IDC	1.2	primary	Bone + lung + LN
38			66	IDC	1.6	primary	Bone + LN
45			81	IDC	NA	primary	Chest wall
17			59	IDC	3.9	primary	Bone + LN
77			70	other	2.5	primary	Bone
111			49	IDC	**14.3**	primary	Bone + Liver
115			70	IDC	NA	**metastases**	Bone + Liver + Lung + LN
51			67	IDC	1.5	primary	LN
132			64	IDC	NA	primary	Bone + lung
131			55	NA	2.7	**metastases**	NA

IDC - Invasive Ductal Carcinoma, ILC - Invasive Lobular Carcinoma, mixed – mixed IDC and ILC, "primary in met set" – biopsy taken from primary breast tumour in the metastatic setting.

PIK3CA status versus clinicopathological features

Objective: Is It possible to find a correlation between mutation detection and clinicopathological features of patients with endocrine-resistant breast cancer?

A variety of clinicopathological features were collected, such as age, histology, the burden of disease in stage IV breast cancer, to explore correlation with the concordance and discordance of *PIK3CA*, Table 20.

Table 20. Clinicopathological characteristics of patients.

	Total n	FFPE			ctDNA			Total n	Concordant PIK3CA		
		PIK3CA MT	PIK3CA WT	p	PIK3CA MT	PIK3CA WT	p		yes	no	p
Age											
>63	17	9	8	0.73	7	10	0.47	9	6	3	0.37
<=63	17	10	7		5	12		11	4	7	
Histology											
Ductal	27	16	11		11	16		17	9	8	
Lobular	2	1	1	0.94	1	1	1.00	1	1	0	0.36
Mixed	2	1	1		0	2		1	0	1	
Metstatic site											
liver	10	5	5	0.63	5	5	0.32	6	4	2	0.63
lung	8	5	3	1.00	3	5	1.00	5	3	2	1.00
bone	28	**17**	11	0.29	**11**	17	1.00	18	**9**	**9**	1.00
LN	10	5	5	0.63	4	6	1.00	5	4	1	0.30
other	5	2	3	0.63	0	5	0.13	2	0	2	0.21
Number of metastatic sites											
1 met	14	8	6	0.928	**4**	10	0.471	8	**3**	5	0.37
>1met	18	10	8		**8**	10		11	**7**	4	

At randomisation, the median age of the 34 patients was 63 years and was used as a cut off between younger and older patients. No statistical difference was found between age groups (chi-square, p=0.37), Table 20. The most common histological subtype for breast cancer is invasive ductal carcinoma (IDC), and in this study, the majority (79%) of patients had IDC histology. Therefore, it was difficult to find an association with the cancer subtype.

PIK3CA mutation vs burden of the disease

All patients in this study had stage IV of breast cancer, which means that their breast cancer had invaded one or more other organs like bone, liver, lung, lymph nodes, or others. Stage IV definition covers a broad range of metastatic diseases. The metastatic disease of a patient with a small metastatic bony lesion will be defined as stage IV and the patient with extensive disease involving bone, liver, lung, and brain. A single metastatic site can also have different degrees of extensiveness. For example, one single lesion in bone versus disease spread throughout the skeleton. Staging does not inform us about the severity of the metastatic disease. Moreover, the survival of this patient with or without treatment will be different. Patients with single bone metastasis can survive years, but the survival of a patient with multiple extensive metastases can be counted in weeks or months.

Patients with different sites involvement can represent different molecular profiles which can complicate any analysis. Patients in this study had multiple organs involved, apart from the brain, as those patients were excluded from the trial. Table 20 shows the distribution of metastatic sites involved in the entire cohort of patients with distinction for *PIK3CA* status. Other studies suggested that *PIK3CA* mutations can be associated with liver and bone metastasis (Daneshmand et al. 2012; Ruiz et al. 2019).

In this study, there were 14 (41%) of 34 patients with one metastatic site, 11 (32%) of 34 patients with two metastatic sites, 3 (8.8%) patients with three metastatic sites, 4 (11.8%) patients with four metastatic sites, and two patients with no data available. The majority of patients (82.3%) in this project had bone metastases. Interestingly, patients with more than one metastatic site had more *PIK3CA* mutations detected in ctDNA (67% vs 33%) and much higher positive concordance between FFPE DNA and ctDNA samples (70% vs 30%), Table 20 and Figure 35.

10 of 14 patients with the single metastatic site had bone metastases, and 2 of 14 patients had lymphadenopathy, one patient was with chest wall metastasis, and one was with liver metastases. Only 3 of 10 patients with bone disease and 1 of 2 with lymphadenopathy had *PIK3CA* detected in ctDNA.

Figure 34. *PIK3CA* status in FFPE DNA, ctDNA, *PIK3CA* concordance vs Metastatic sites.

Pt ID	PIK3CA FFPE	PIK3CA ctDNA	Liver	Lung	Bone	Lymph	Other
79							
123							
4							
71							
129							
110							
122							
34							
104							
84							
44	*	*					
42							
57							
80							
99							
145							
94			NA	NA	NA	NA	NA
36							
138							
108							
35							
21							
106							
23							
65							
38							
45							
17							
77							
111							
115							
51							
132							
131			NA	NA	NA	NA	NA

* Two different PIK3CA mutations detected in ctDNA and FFPE DNA. Dark colours - represent the presence of a mutation in the column for PIK3CA detection or the presence of metastasis in the specific site. Light colours – represent – wild type in the PIK3CA column or no metastasis present in the specific site. NA – data not available.

Figure 35. *PIK3CA* status in FFPE DNA and ctDNA versus the number of metastatic sites.

PIK3CA detection in ctDNA and concordance versus number of metastatic sites
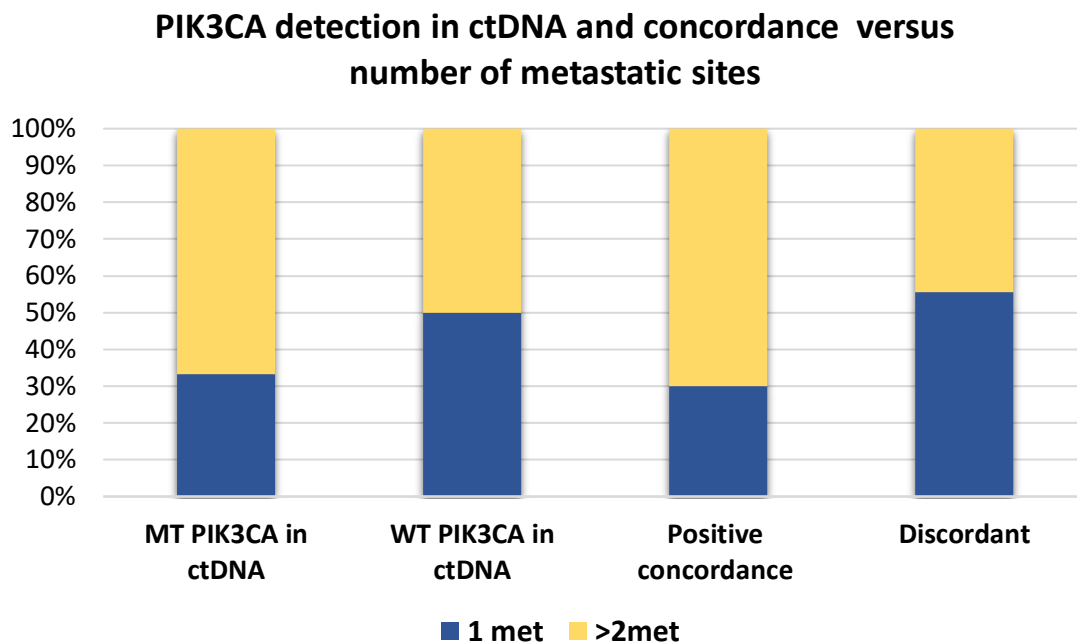
MT *PIK3CA – PIK3CA* mutation, WT- Wild type *PIK3CA*

The findings could suggest that a more advanced disease with multiple metastatic sites sheds more DNA into the bloodstream, and therefore, there is a higher chance of detecting a mutation in ctDNA. However, in patients with a single, non-visceral metastatic site, detecting mutation in ctDNA could be more challenging and be a reason for discordance between FFPE DNA and ctDNA. There is a possibility that the nonvascular metastatic site could shed less or no DNA to circulation or have a different genetic profile.

PIK3CA detection in FFPE and treatment exposure.

27 (79.4%) of 34 patients had tissue taken from the primary tumour, and 7 (20.6%) of 34 patients had a biopsy taken from the metastatic lesion.

14 (73.7%) of 19 patients with *PIK3CA* mutation detected in FFPE DNA had the biopsy or resection of their primary tumour performed before commencing systemic therapy (treatment-naïve). 7 (50%) of the 14 patients had *PIK3CA* mutation concordant between FFPE DNA and matched ctDNA sample. Other 50% of patients had *PIK3CA* mutation discordant with *PIK3CA* present only in FFPE DNA.

5 of 19 (26.3%) patients had *PIK3CA* mutation detected in metastatic FFPE DNA. 3 (60%) of 5 patients also had *PIK3CA* mutation concordant between FFPE and ctDNA samples. **Patient 44** had two different PIK3CA mutations detected in matched samples. These patients had many years free of disease before relapse, and the tissue was taken from the metastatic lesion at the time of disease relapse, Table 21.

Table 21. Treatment exposure in patients who had tissue assessed from the metastatic lesion.

patient ID	Primary Surgery	Adj endocirne therapy (years)	Primary metastatic	Time between primary Dx and relapse (years)	PIK3CA mutation	FFPE DNA MAF(%)	ctDNA MAF(%)**	Time between blood and tissue (years)	Number of endocrine Tx	Total time on endocrine Tx (years)
94	.	.	.	.	N345K	33.50%	0	NA	NA	NA
44	Yes	5.1	.	14.3	M1043I/E970K	42.5%	7.4%	9.2	3	8.6
71	Yes	5.1	.	22.0	H1047R	30.3%	2.2%	1.9	2	1.9
115	Yes	5.1	.	11.3	.	.	.	NA	2	1.3
34	Yes	2.7	.	4.2	H1047R	35.0%	2.2%	4.3	1***	2.7 ***
131	.	.	yes	.	.	.	.	2.7	1	2.1
84	Yes	.	yes	.	E726K	21.0%	3.5%	2.2	1	2.3

* M1043I detected in FFPE DNA, E970K detected in ctDNA. ** PIK3CA mutation in baseline ctDNA at the recruitment to FAKTION trial, after endocrine resistance to endocrine therapy in the metastatic setting. *** This patient had a disease relapse while receiving adjuvant endocrine therapy. ND – Not detected.

This shows that *PIK3CA* concordance is more likely to be found between FFPE from metastatic lesions and ctDNA samples taken in the metastatic setting. Therefore, assessing concordance between FFPE DNA from the primary tumour and ctDNA sample taken in metastatic could be a potential reason for discordance.

PIK3CA detection vs endocrine therapy

All patients in this study were treated with at least one line of endocrine therapy, which had to include AIs before entering the FAKTION trial. In this project, 14 (41.2%) patients had one endocrine treatment, 10 (29.4%) had two endocrine therapies, 9 (26.5%) had three treatments, and one (2.9%) had no data available. In addition, 17 (50%) patients received only AIs, and 17 (50%) received a combination of AIs with tamoxifen in the adjuvant or metastatic setting. The median duration of endocrine therapy for these patients was six years. I have assessed three factors that could influence *PIK3CA* concordance and detection of *PIK3CA* mutation in ctDNA, using chi-square test: 1 - the number of endocrine treatments (1 or > 1), 2 - tamoxifen with AI versus AI only, 3 - duration of endocrine therapy, Table 22.

Table 22. Endocrine treatment versus *PIK3CA* mutation detection.

	Total n	FFPE			ctDNA			Total n	Concordant PIK3CA		
		PIK3CA MT	PIK3CA WT	p	PIK3CA MT	PIK3CA WT	p		yes	no	p
Number of endocirne therapies											
1 treatment	14	**6**	8	0.247	**3**	11	0.16	6	**3**	3	1
>=2 treatments	19	**12**	7		**9**	10		13	**7**	6	
Endocrine thrapy type											
Tamoxifen and AI	17	**10**	7	0.611	**7**	10	0.554	11	5	6	0.65
AI only	17	**8**	8		5	11		8	5	3	
Duration of endocrine therpay											
> = 6 years	17	**11**	6	0.3	**7**	10	0.473	12	5	7	0.65
<6 yras	17	8	9		5	12		8	5	3	

AI-Aromatase Inhibitors, MT mutation, WT- wild-type

Figure 36. *PIK3CA* status versus the number of endocrine therapies received by patients.

PIK3CA status in ctDNA and concordance vesus number of endocrine therpies
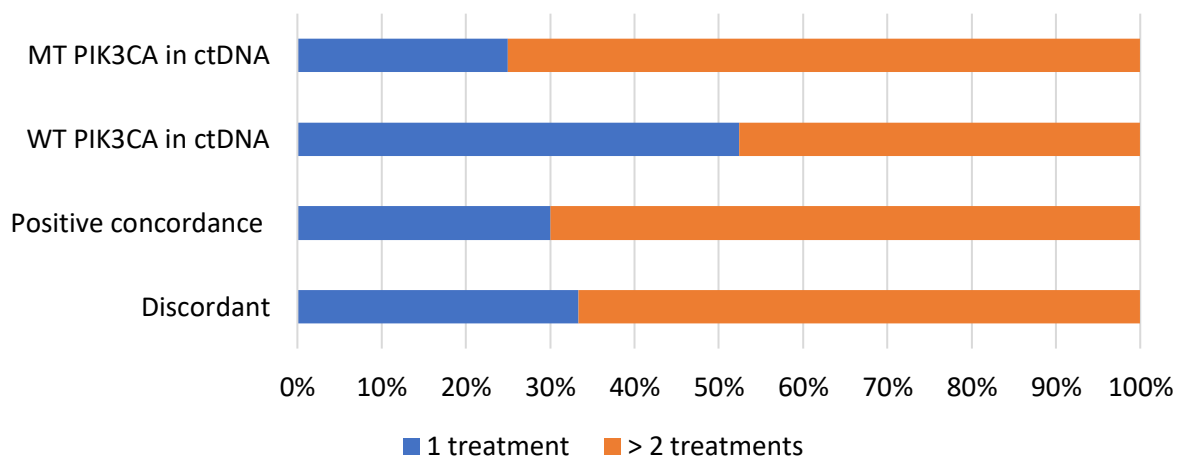
Concordant/Discordant PIK3CA mutation between FFPE DNA and ctDNA, MT – Mutated PIK3CA, WT – wild-type PIK3CA.

No statistical difference was found between groups of patients in the three assessments above. However, patients treated with more than one endocrine treatment are more likely to have *PIK3CA* mutation detected in ctDNA, Figure 36.

4.3.2 *AKT1* Mutations

Objectives: Can 44-gene NGS panel and ddPCR detect mutations in AKT1 in baseline ctDNA and FFPE DNA? What is the concordance between these samples? What are the reasons for discordances?

AKT1 gene is a vital gene included in the *PIK3CA*/AKT pathway, activated by p.E17K mutation. I found 3 of 34 (8.8%) patients with *AKT1* p.E17K mutation in this study. *AKT1* p.E17K All mutations were found using the NGS panel and validated by ddPCR. 2 of 3 patients had concordant results between FFPE DNA and matched ctDNA. However, 1 of 3 had a discordant result with missing AKT mutation in the ctDNA, Table 23.

Looking at the results in Table 23 and Table 24, I could identify potential reasons for discordance in **patient 80**. No technical issues related to the library preparation and sequencing performance were found. However, looking at clinical aspects, **patient 80** had had a single nonvascular metastatic site (bone) which could have a different genetic profile or shed less ctDNA to the bloodstream, and therefore, no AKT and PIK3CA mutations were detected in ctDNA.

Table 23. *AKT1* mutations found in FFPE DNA and ctDNA

Pt ID	Gene	Mutation	FFPE						ctDNA				
			% Tumour	DNA con (ng/ul)	Final Lib (ng/ul)	Seq Depth	NGS MAF (%)	ddPCR MAF (%)	DNA con (ng/ml)	Final Lib (ng/ul)	Seq Depth	NGS MAF (%)	ddPCR MAF (%)
80	AKT1	E17K	NA	18.8	12.9	2268	5.7	9.8	7.6	14.3	4679	0	0
	PIK3CA	H1047L				5363	12.6	11.6			7062	0	0
131	AKT1	E17K	NA	31.3	14.3	3680	42.3	38.5	14.2	9.7	5600	0.5*	0.7
132	AKT1	E17K	NA	4.6	17.7	3760	38.8	32.6	5.2	8.9	5962	3.6	2.9

NA – data not available, MAF - Mutant Allele Frequency, NT - Not tested, * AF detected under the limit of detection, DNA con – DNA concentration, Seq depth – sequencing depth, Final Lib – Final Library DNA concentration, Tumour % - estimated tumour cell content (%).

Table 24. Age, Histology and Metastatic sites for *AKT1* positive patients.

Pt ID	Age	Histology	Time between FFPE and ctDNA (years)	Biopsy site	Metastatic sites
80	54	IDC	2.9	Primary	Bone
131	55	NA	2.7	Metastases	NA
132	64	IDC	NA	Primary	Bone + lung

IDC – Invasive Ductal Carcinoma, NA – data not available.

AKT1 p.E17K mutation can be detected in the FFPE DNA and ctDNA samples using the 44-gene NGS panel. The single non-visceral metastasis could potentially be a reason for discordance.

4.3.3 *PTEN* Mutations

Objectives: Can the 44-gene NGS panel detect mutations in PTEN in baseline ctDNA and FFPE DNA? What is the concordance between these samples? What are the reasons for discordances?

PTEN gene is a tumour suppressor gene that plays an essential role in regulating the PI3K/AKT pathway. Loss of *PTEN* function or mutation that causes loss of function can activate this pathway. I found 3 (8.8%) of 34 patients with *PTEN* mutations using only the 44-gene NGS panel. One patient had concordant PTEN mutations between FFPE DNA and ctDNA matched samples. 2 of 3 patients had discordant results with undetected PTEN mutations in ctDNA, Table 25.

Two *PTEN* mutations (p.C136R and p.R130Q) detected could have caused *PTEN* loss of expression, confirmed by IHC. Pathogenic *PTEN* p.D92V mutation did not cause a loss of *PTEN* expression but could contribute to the loss of *PTEN* function.

Table 25. *PTEN* mutation detected in FFPE DNA and ctDNA, *PTEN* expression in FFPE by IHC.

Pt ID	Gene	Mutation	FFPE					ctDNA			
			% Tumour	DNA con (ng/ul)	Final Lib (ng/ul)	Seq Depth	NGS MAF (%)	DNA con (ng/ml)	Final Lib (ng/ul)	Seq Depth	NGS MAF (%)
123	**PTEN**	**C136R**	NA	5.6	13.8	3678	**34.3**	21.8	12.2	4286	**27.1**
	PIK3CA	E110del				2411	29.1			2195	38
111	**PTEN**	**R130Q**	70	18.1	5.3	1005	**6.4**	14.7	9.0	4181	**0**
	TP53	D281Rfs				8740	26.4			16678	0
110	**PTEN**	**D92V**	80	3.4	15.8	3208	**33.2**	11.4	13.9	1276	**0**
	PIK3CA	H1047R				16310	33.8			7625	3.1
	PIK3CA	C378W				9663	30.8			4729	3.3

IHC – Immunohistochemistry - 0 – Loss of *PTEN* expression, 3 – normal *PTEN* expression, Pt no – Patient number. MAF - Mutant Allele Frequency, Final Lib – Final Library DNA concentration, Tumour % - estimated tumour cell content (%), Seq depth – sequencing depth.

Table 26. Clinicopathological features of patients with *PTEN* mutation.

Pt ID	Age	Histology	Time between FFPE and ctDNA (years)	Biopsy site	IHC PTEN result	Metastatic sites
123	70	IDC	5.4	Primary	0	Bone + Liver
111	49	IDC	**14.3**	Primary	0	Bone + Liver
110	71	IDC	2.1	Primary	3	Bone + Liver + Lung + LN

Pt no – Patient number. IDC – Invasive Ductal Carcinoma, LN – Lymph nodes

Potential reasons for discordance in these patients could be technical or biological. For example, in **patient 110**, insufficient sequencing depth could be the main reason for not detecting *PTEN* mutation in ctDNA. However, in **patient 111** could be a long time interval between FFPE and plasma of 14.3 years. The molecular biology of cancer could have changed over time and under multiple treatments exposures like chemotherapy, radiotherapy and endocrine therapy.

NGS can detect *PTEN* mutations in primary tumour FFPE DNA and ctDNA. The reasons for *PTEN* discordance between these samples could be biological or technical.

4.3.4 *ESR1* Mutations

Objectives: Can 44-gene NGS panel and ddPCR detect mutations in ESR1 in baseline ctDNA and FFPE DNA? What is the concordance between these samples? What are the reasons for discordances?

10 (29.4%) of 34 patients were found *ESR1* mutations, and all mutations were found to be discordant between FFPE DNA and ctDNA. 9 of 10 patients had *ESR1* mutation detected in ctDNA only, using NGS and ddPCR. 1 of 10 patients had ESR1 mutation detected in FFPE DNA from the primary tumour in a metastatic setting, but no prior endocrine therapy was received.

In this section, ESR1 mutation discordance between FFPE DNA from the primary tumour or metastatic lesion with no prior treatment exposure and ctDNA was expected. However, ESR1 concordance was expected between FFPE DNA from metastatic lesions and ctDNA exposed to prior AI treatment. In this project, two patients (**44** and **71**) had metastatic lesions tested. However, the metastatic tumours were biopsied prior to commencing endocrine treatment; therefore, no *ESR1* mutations were expected in these lesions.

Other potential reasons for not detecting *ESR1* mutation in FFPE tissue could be low FFPE DNA yield and poor sequencing coverage. For example, in **patient 45**, the FFPE DNA was of poor quality and had very low DNA concertation and sequenced with a coverage of 66. Thus, the mutation would not be detected with this level of coverage even if it was present in the sample. Unfortunately, there was no further DNA material available to confirm with ddPCR.

The ESR1 discordance between primary FFPE and ctDNA samples was in keeping with current literature. ESR1 mutations were mainly detected in ctDNA samples in patients with acquired AIs resistance.

Table 27. ESR1 mutations detected in FFPE DNA and ctDNA.

| Pt ID | ESR1 | | Gene | Mutation | FFPE | | | | | | ctDNA | | | | |
	FFPE	ctDNA			Tumour %	DNA con (ng/ul)	Final Lib (ng/ul)	Seq Depth	NGS MAF (%)	ddPCR MAF (%)	DNA con (ng/ml)	Final Lib (ng/ul)	Seq Depth	NGS MAF (%)	ddPCR MAF (%)
57			ESR1	Y537S	25	0.4	5.2	3111	**12.5**	**13.5**	49.6	4.9	4156	**0**	0
			PIK3CA	H1047R				4527	39.8	39.5			4037	0	0
			TP53	P142S				1973	5.7	NT			2568	**0**	NT
17			ESR1	D538G	NA	1.3	13.1	3977	**0**	NT	30.2	17.1	4827	**2.0***	NT
			TP53	N131Y				4859	71.7	NT			6912	9.2	NT
44			ESR1	D538G	40	0.1	3.5	1588	**0**	NT	43.4	11.6	6929	**2.9**	NT
			PIK3CA	M1043I				13990	42.5	NT			14677	0	NT
			PIK3CA	E970K				18	0	NT			12371	7.4	NT
71			ESR1	E380Q	40	0.9	17.8	7351	**0**	NT	8.9	16.0	13568	**1.4***	NT
			PIK3CA	H1047R				3274	30.3	34.6			7467	2.8	2.2
77			ESR1	Y537S	60	0.3	15.5	10326	**0**	NT	42.0	16.7	6440	**5.0**	NT
129			ESR1	E380Q	NA	39.9	5.2	5253	**0**	NT	4.42	9.1	14760	**8.0**	NT
			PIK3CA	E726K				1057	6.1	NT			3541	10	NT
51			ESR1	Y537C	80	2.5	15.0	4122	**0**	0	6.8	11.5	5147	**9.2**	5.6
			TP53	G244V				2603	40.5	NT			4818	21.7	NT
122			ESR1	Y537C	NA	4.1	NT	NT	NT	**0**	7.18	21.0	6978	**1.4***	1.5
			PIK3CA	H1047R				NT	NT	32.1			9432	15.3	17.1
35			ESR1	D538G	NA	16.2	16.7	2861	**0**	NT	21.6	12.8	5569	**12.8**	NT
45			ESR1	D538G	80	0.8	4.4	**66**	**0**	**0**	25.8	17.6	6700	**0.8***	NA

Pt ID – Patient number, MAF – Mutation Allele Frequency, *Mutation detected under the limit of detection. NT – Not tested, NA – data not available, Final Lib – Final Library DNA concentration, Tumour % - estimated tumour cell content (%),, DNA con – DNA concentration, Seq depth – sequencing depth.

Table 28. Clinicopathological characteristics of patients with *ESR1* mutations

Pt ID	Age	Histology	Time between FFPE and ctDNA (years)	FFPE source	Metastatic sites
57	56	IDC	0.9	primary in met set	Bone
17	59	IDC	3.9	primary	Bone + Left SCF LN
44	66	IDC	9.2	**metastases**	Bone
71	76	IDC	1.9	**metastases**	Bone + LN
77	70	NA	2.5	primary	Bone
129	63	IDC	**17.1**	primary	Bone
51	67	IDC	1.5	primary	LN
122	71	**ILC**	7.9	primary	Bone + Liver
35	43	IDC	7.9	primary	Bone + Liver + LN + Pleural
45	81	IDC	NA	primary	Chest wall

Pt ID – Patient number, IDC – Invasive Ductal Carcinoma, ILC – Invasive Lobular Carcinoma. LN – Lymph node, SCF supraclavicular fossa metastasis.

4.3.5 *TP53* Mutations

Objectives: Can 44-gene NGS panel detect mutations in the TP53 gene in baseline ctDNA and FFPE DNA? What is the concordance between these samples? What are the reasons for discordances?

In this project, I found 9 (23.5%) of 34 patients with *TP53* mutations. 5 of 9 patients had *TP53* mutations concordant between FFPE DNA and ctDNA samples. 4 of 9 had discordant TP53 mutations between samples, Table 29. In this group of patients, it has become apparent that most TP53 mutations are co-existent with other mutations like *PIK3CA*, *ESR1*, *PTEN.* The most common co-existing mutations were in the *PIK3CA* gene (5 variants); others were in the *ESR1* gene (4 variants) and *PTEN* gene (1 variant), Table 29.

The potential reasons for discordance for patients 57 and 111 were discussed in previous sections. In **patients 108 and 138**, TP53 mutations were not detected in ctDNA potentially due to a long-time gap between samples (8.9 and 16 years) as no technical reasons were identified, Table 30.

Clinicopathological characteristics are presented in Table 30. The median age at randomisation of patients with mutated *TP53* was 56 (range 49 -72), and the even younger median age of 53 at biopsy or resection of the tumour when *TP53* mutation was first detected. This group of patients appeared to be younger than patients with wild-type *TP53* with a median age of 66 (43 – 81) and 61 at the time

of tissue sampling. These patients present with the extensive disease with at least two or more metastatic sites, suggesting more aggressive disease. Furthermore, the more aggressive disease is associated with high cancer cell turnover and could contribute to increased shedding of ctDNA, which enable mutations detection in ctDNA and better concordance between FFPE and ctDNA samples.

TP53 mutations appear to be more common in younger women with more aggressive disease, which could contribute to increased shedding of ctDNA and better concordance between FFPE and plasma samples. However, the reasons for discordance could be biological, with a long gap between samples. In addition, the *TP53* mutations commonly co-occur with other activating mutations, and their presence can potentially affect the treatment that involves endocrine therapy with inhibitors of the PI3K/AKT pathway.

Table 29. *TP53* mutations detected in FFPE and ctDNA.

Pt ID	TP53 FFPE	TP53 ctDNA	Gene	Mutation	FFPE Tumour %	FFPE DNA con (ng/ul)	FFPE Final Lib (ng/ul)	FFPE Seq Depth	FFPE NGS MAF (%)	ctDNA DNA con (ng/ml)	ctDNA Final Lib (ng/ul)	ctDNA Seq Depth	ctDNA NGS MAF (%)
115			TP53	N131del	NA	3.3	17.0	6005	**7.7**	4.7	13.0	4587	**10.9**
94			TP53	C277F	NA	20.3	17.6	13255	**65.5**	13.1	17.0	19653	**0.7***
94			PIK3CA	N345K				1790	33.5			116	0
17			TP53	N131Y	NA	1.3	13.1	4859	**71.7**	30.2	17.1	6912	**9.2**
17			ESR1	D538G				3977	0			4827	2.0*
51			TP53	G244V	80	2.5	15.0	2603	**40.5**	6.8	11.5	4818	**21.7**
51			ESR1	Y537C				4122	0			5147	9.2
104			TP53	C176R	80	2.9	12.5	3046	**49.2**	7.7	13.9	5129	**4.9**
104			PIK3CA	H1047R				5713	70.2			9367	8.7
108			TP53	R280K	80	32.0	6.0	3988	**27.2**	26.8	14.6	12277	**0**
108			PIK3CA	*exon 9				NT	NT			NT	NT
57			TP53	P142S	25	0.4	5.2	1973	**5.7**	49.6	4.9	2568	**0**
57			PIK3CA	H1047R				4527	39.8			4037	0
57			ESR1	Y537S				3111	12.5			4156	0
111			TP53	D281Rfs	70.0	18.1	5.3	8740	**26.4**	14.7	9.0	16678	**0**
111			PTEN	R130Q				1005	6.4			4181	0
138			TP53	R337L	NA	7.7	9.1	3424	**17.4**	16.9	20.2	8522	**0**
138			PIK3CA	*exon9				NT	NT			NT	NT

Pt ID – Patient number, MAF – Mutation Allele Frequency, NA – data not available, NT - Not tested, * AF detected under the limit of detection, Final Lib – Final Library DNA concentration, Tumour % - estimated tumour cell content (%), DNA con – DNA concentration, Seq depth – sequencing depth.

Table 30. Clinicopathological features for patients with *TP53* mutations.

Pt ID	Age	Histology	Time between FFPE and plasma (years)	Biopsy site	Metastatic sites
115	70	IDC	0	**metastases**	Bone + Liver + Lung + LN
94	53	NA	NA	**metastases**	NA
17	59	IDC	3.9	primary	Bone + Left SCF LN
51	67	IDC	2.5	primary	LN
104	52	IDC	2.7	primary	Bone + lung + LN
108	57	IDC	8.9	primary	Bone + liver
57	56	IDC	0.9	primary in met set	Bone
111	49	IDC	**14.3**	primary	Bone + Liver
138	72	IDC	**16**	primary	Bone + lung + adrenal

Pt – Patient number, NA – Data not available, IDC – invasive ductal carcinoma LN – Lymph node, SCF supraclavicular fossa metastasis, primary in met set – primary in the metastatic setting.

4.4. Discussion and Clinical Implications.

Data presented in this chapter demonstrated that it is possible to detect various mutations in multiple genes in ctDNA and FFPE DNA using a 44-gene targeted NGS panel and ddPCR. Furthermore, the concordance of mutation detection between FFPE DNA and matched baseline ctDNA varied between genes, and multiple causes for discordance were described.

The potential reasons for mutations discordance between FFPE and ctDNA in this project could be due to:

- Technical issues include sample collection, sample handling, transport and storage, low cfDNA yield, poor quality DNA extraction, library preparation failures, low sequencing depth, sensitivity or specificity of the method.

- Quality skills of the person performing testing could contribute to false negative results. The assessment of multiple mutations in various genes and using two methods can help us investigate whether the mutation of interest was truly negative or positive.

- The significant time gap between plasma and tissue samples during which patients have been exposed to multiple adjuvant treatments and multiple endocrine therapies in a metastatic setting could affect the disease's biology. Other studies suggested that the longer time between samples, the higher risk of discordant samples (Jahangiri and Hurst 2019). This could be due to a change in cancer biology and exposure to multiple treatments.

- Assessment of concordance in primary versus metastatic setting. Ideally, to assess true concordance between samples, the evaluation of matched samples should occur in the diagnostic setting of primary or metastatic disease. Most FFPE samples were from the primary diagnostic tumours in this project, and plasma samples were taken in the metastatic or relapse setting. I noticed a higher sample concordance between the metastatic lesion and ctDNA than between samples with primary cancer tissue and ctDNA. This is in keeping with other reports where the concordance of *PIK3CA* between metastatic lesions and ctDNA is much higher than between primary lesions and ctDNA (Kodahl et al. 2018).

- Cancer biology with vascular versus nonvascular metastasis. Patients with single nonvascular metastatic sites had less likely to have concordant samples due to undetectable ctDNA. Similar findings were reported by Kodahl et al. (2018), who found that patients with missing the *PIK3CA* mutation in matched ctDNA samples had a nonvascular metastatic disease like bone or lymphadenopathy. On the other hand, patients with extensive disease with visceral metastasis can shed more ctDNA to the bloodstream and increase the chance of mutation concordance. Thus, clinical information about the type and number of metastatic sites involved could help understand and distinguish between technical or biological problems.

- Biological reasons where discordance between the primary tissue sample and ctDNA is expected. As an example, acquired resistant ESR1 mutations occur due to prolonged exposure to endocrine therapy. In this study, 26.5% ESR1 mutations were detected in ctDNA of patients with metastatic breast cancers with previous AI exposure, consistent with the literature (Fribbens et al. 2016). Furthermore, ESR1 mutation was also detected in the FFPE DNA of one patient (2.9%), which also was consistent with literature as Baselga et al. (2012), reported 3% of *ESR1* mutations in pretreatment tumour biopsies from the BOLERO-2 trial.

Other mutations like *TP53*, not directly associated with endocrine resistance, can provide valuable prognostic information about cancer as TP53 is a bad prognostic factor for many cancers. Patients with TP53 mutations present at a younger age with more extensive metastatic disease. This finding was also reported by another study (Gasco et al. 2002). Thus, these *TP53* driven cancers could potentially shed more DNA into the bloodstream, and *TP53* mutations and other mutations can be more likely detected in ctDNA samples. This may influence clinical management, and follow-up patients with a bad prognostic factor may require closer monitoring for disease progression signs or early switch to a different therapy.

Furthermore, *TP53* mutations often can co-exist with other mutations like *PIK3CA*, *ESR1*, *PTEN* genes. Other studies discovered the co-occurrence of *TP53-PIK3CA* at frequency 5.3 – 12.8% (Network 2012; Fountzilas et al. 2016; Li et al. 2018b). Previous in vitro study showed cooperativity of *TP53-PIK3CA* in breast carcinogenesis and demonstrated that this cooperation could increase genomic instability with subsequent more significant tumour heterogeneity (Croessmann et al. 2017). Also, in vivo studies have confirmed that *TP53* and *PIK3CA* mutations show cooperation in mice's breast tumour formation (Adams et al. 2011). The interesting question here is whether the co-occurrence of *PIK3CA* and *TP53* can affect response to capivasertib and fulvestrant, and it could be evaluated in the next larger phase III trial.

Understanding biological and technical reasons for possible discordance can help plan the detection of biomarkers in trials. This chapter suggests that it is possible to detect mutations within ctDNA. However, clinicians need to consider the technical aspect of genomic testing, biological evolution of cancer and clinicopathological information when assessing concordance between matched samples. Also, the results should be put in the context of individual patients medical history.

CtDNA testing has important implications in the diagnostic setting, detecting disease relapse, and monitoring disease during therapy. A blood test for ctDNA analysis is an attractive way to detect the presence of multiple mutations and could complement the analysis on a patient's original tumour biopsy or be a valid test when a biopsy of the primary tissue is impossible. However, there is a risk of a false negative result due to the reasons explained above. However, assessing several commonly mutated genes and repeat blood samples could help solve this problem. Furthermore, testing ctDNA could be a first test that is less invasive for the patient, and if no mutation is detected, tissue biopsy could be considered. This could help reduce the number of biopsies.

This chapter's results give bases for the next chapter where PIK3CA, AKT1, PTEN, ESR1, and TP53 mutations detected in baseline samples can be monitored in longitudinal samples whilst patients undergo experimental treatment - fulvestrant and capivasertib in FAKTION trial. The quantitative changes in allele frequency will be correlated with response to therapy.
.

5. Molecular Assessment of Response to Treatment in Longitudinal Plasma Samples in Patients Treated with Fulvestrant and *AKT1* Inhibitor.

5.1 Introduction

Chapter 3 focused on mutation detection in baseline tissue and ctDNA samples, using a 44-gene NGS panel and ddPCR. In this chapter, I have aimed to examine whether mutations detected in baseline samples can be tracked in the longitudinal ctDNA samples in response to the combination treatment of fulvestrant and capivasertib, using ddPCR and 44-gene NGS panel.

5.2 Hypothesis, Aims and Objectives

5.2.1 Hypothesis and Aims

This chapter aims to test the hypothesis that multiple single point mutations detected by NGS targeted panel in baseline ctDNA and FFPE DNA can be tracked in sequential ctDNA samples and correlated with the clinical response to the combination of fulvestrant and capivasertib.

5.2.2 Objectives

Using pre-treatment FFPE DNA and ctDNA samples, on day 1 of cycle 3 of treatment ctDNA samples and at the disease progression ctDNA samples, I aimed to track mutations and correlate with clinical response. In this chapter, the objectives are:

1. To explore the ability to detect mutations in longitudinal samples using ddPCR and 44-targeted NGS panel.
2. To assess the ability to correlate changes in mutation allele frequency of detected mutations in sequential samples with clinical response to the combination of fulvestrant and capivasertib.
3. To assess the role of concurrent mutations in the *TP53* gene on clinical response to trial treatment.

5.3 Translational Aspect of FAKTION Trial

The FAKTION trial was designed to investigate the efficacy of fulvestrant and capivasertib in patients with hormone-resistant metastatic breast cancer. Enrolled patients were randomly assigned to receive fulvestrant with either capivasertib or matching placebo until disease progression, unacceptable toxicity, or withdrawal of consent. As part of the trial, translational blood samples were collected at baseline, eight weeks of treatment, and the disease progression, Figure 37. In this chapter, I aimed to focus on response to fulvestrant and capivasertib. During the ongoing trial, the evaluation of both groups could put trial integrity at risk as it could potentially unblind treatment; therefore, I evaluated samples from patients of the experimental arm only.

Figure 37. CtDNA sample collection time points in the FAKTION trial.

CtDNA sample collection timepoints in the FAKTION trial
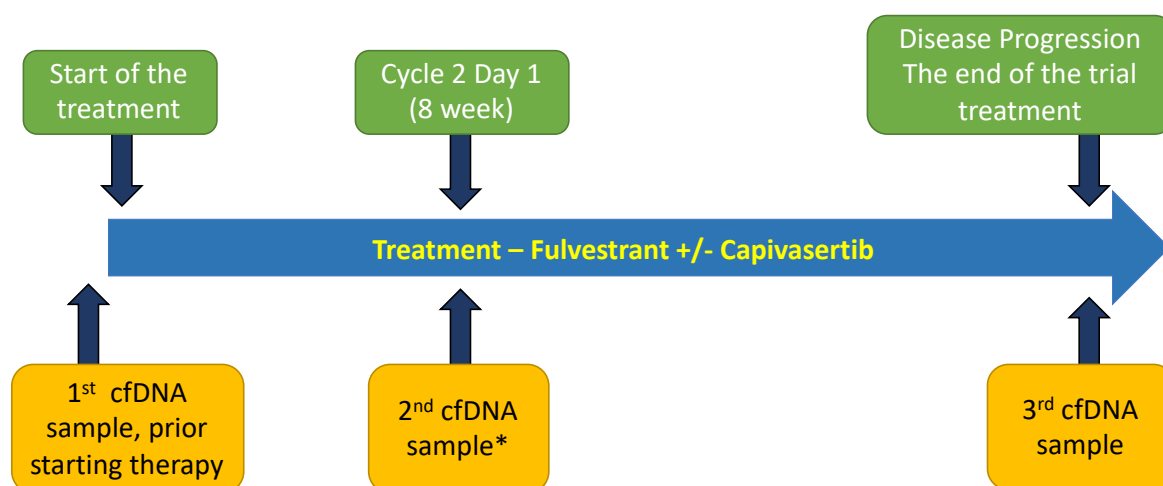
*Patient who experienced disease progression at 2 or 3 months would have had two samples and the 2nd sample will be the end of treatment sample

19 patients from 34 patients from chapter 4 were selected based on having the complete blood samples sets from all time points in the experimental arm. I analysed ctDNA at each time point from 19 patients treated with fulvestrant and capivasertib. However, 3 of 19 patients withdrew from the FAKTION trial due to intolerance of combination of treatment; therefore, these were excluded from analysis as unable to correlate mutations changes to the treatment response. In addition, 1 of 19

patients had no clinical data available at the time of the study. Therefore, I assessed genomic and clinical data for 15 patients in this chapter, Figure 38.

Figure 38. Overview of patients and sample flow in chapter 3 and 4.
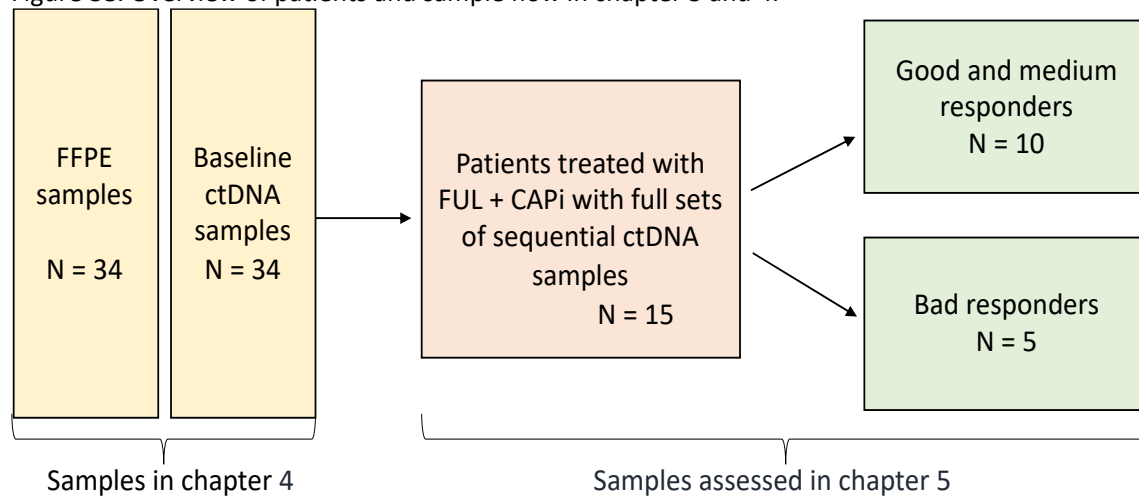
FUL – Fulvestrant, CAPi – Capivasertib

Clinicopathological features of the selected 15 patients evaluated in this chapter compared to the patient population in the FAKTION trial are presented in Table 31. In general, patients evaluated in this project had similar characteristics to patients in the FAKTION trial. However, the median PFS for the selected 15 patients was 4.8 months compared to 10.3 months for the entire patients' group treated with combination therapy. Interestingly, these patients had less lung metastasis (7%) compared to all patients in the FAKTION trial (39-43%) but more lymph nodes involved (60%, compared to 41- 42%), Table 31.

Table 31. Clinicopathological features for patients in FAKTION trial.

	Ful +Capi (n=15*)	Ful + Capi (n=69)	Ful only (n=71)
Median Age	59 (43-76)	62 (42-81)	61 (40-82)
Median PFS	**4.8**	10.3	4.8
Histopathological subtype			
IDC	13 (87%)	57 (83%)	58 (82%)
ILC	1 (7%)	4 (6%)	12 (17%)
mixed IDC/ILC	1 (7%)	5 (7%)	0
Other	0	3 (4%)	1 (1%)
Number of disease sites			
1 met site	5 (33%)	15 (22%)	19 (27%)
>2 met site	10 (67%)	54 (78%)	52 (73%)
Metastatic sites			
Brain	0	1 (1%)	1 (1%)
Liver	6 (40%)	32 (46%)	29 (41%)
Lung	**1 (7%)**	30 (43%)	28 (39%)
Bone	12 (80%)	58 (84%)	55 (77%)
Lymph nodes	**9 (60%)**	28 (41%)	30 (42%)
Pericardial or pleural	2 (13%)	5 (7%)	3 (4%)
Chest wall or skin	0	1 (1%)	3 (4%)
other visceral	0	2 (3%)	1 (1%)

*n=15 patient from 69 of Ful + Capi group evaluated in this project, IDC- Invasive ductal carcinoma, ILC - invasive lobular cancer

The 44-gene NGS panel was applied to baseline and end of treatment ctDNA samples. Mutations detected by the NGS method in PIK3CA, ESR1, AKT genes were tracked in sequential ctDNA samples using ddPCR. I aimed to correlate allele frequency changes of detected mutations with a radiological response and progression-free survival (PFS) and overall survival (OS). However, clinical data was not available until all genetic testing was completed.

In the first instance, I describe ten patients with three longitudinal ctDNA samples available. These patients have continued treatment after the first radiological response evaluation with computer tomography (CT). Patients whose CT scan reported by RECIST1.1 criteria stable disease, partial response, or complete response would have continued treatment beyond the first radiological assessment. These patients would have a blood sample collected at baseline, eight weeks of treatment and the third sample at the time of disease progression. Finally, five patients whose CT scan reported progressive disease at the first radiological assessment would have blood taken at the baseline and the disease progression. These patients would not have 8-week samples taken as this would be the same time as the disease progression. These samples were called the end of treatment samples. At this point, patients would discontinue treatment in the trial.

RECIST 1.1 criteria were used to determine objective tumour response for target lesions (Eisenhauer et al. 2009):

- Complete Response (CR) was defined as the disappearance of all target lesions, any pathological lymph nodes (target or non-target) reduced in the short axis to <10 mm.
- Partial Response (PR) was determined at least a 30% decrease in the sum of diameters of target lesions, taking as reference the baseline sum diameters.
- Progressive Disease (PD) was defined as a 20% increase in the sum of diameters of target lesions, taking as reference the smallest sum on study. In addition to the relative increase of 20%, the sum must also demonstrate an absolute increase of at least 5 mm. Also, the appearance of one or more new lesions was considered progression.
- Stable Disease (SD) was described as insufficient shrinkage to qualify for PR or insufficient increase to qualify for PD, taking as reference the smallest sum diameters while on the study. (Eisenhauer et al. 2009)

This cohort of 15 patients was divided into three groups based on time in which the treatment was initiated until disease progression (time to progression as Progression-Free Survival (PFS), Figure 39:

1. Good responders with PFS over 9 months – 5 patients.
2. Medium responders with PFS between 3 – 9 months – 5 patients.
3. Bad responders with PFS of less than 3 months – 5 patients.

Figure 39. Swimmer Plot presenting time to progression for each patient.
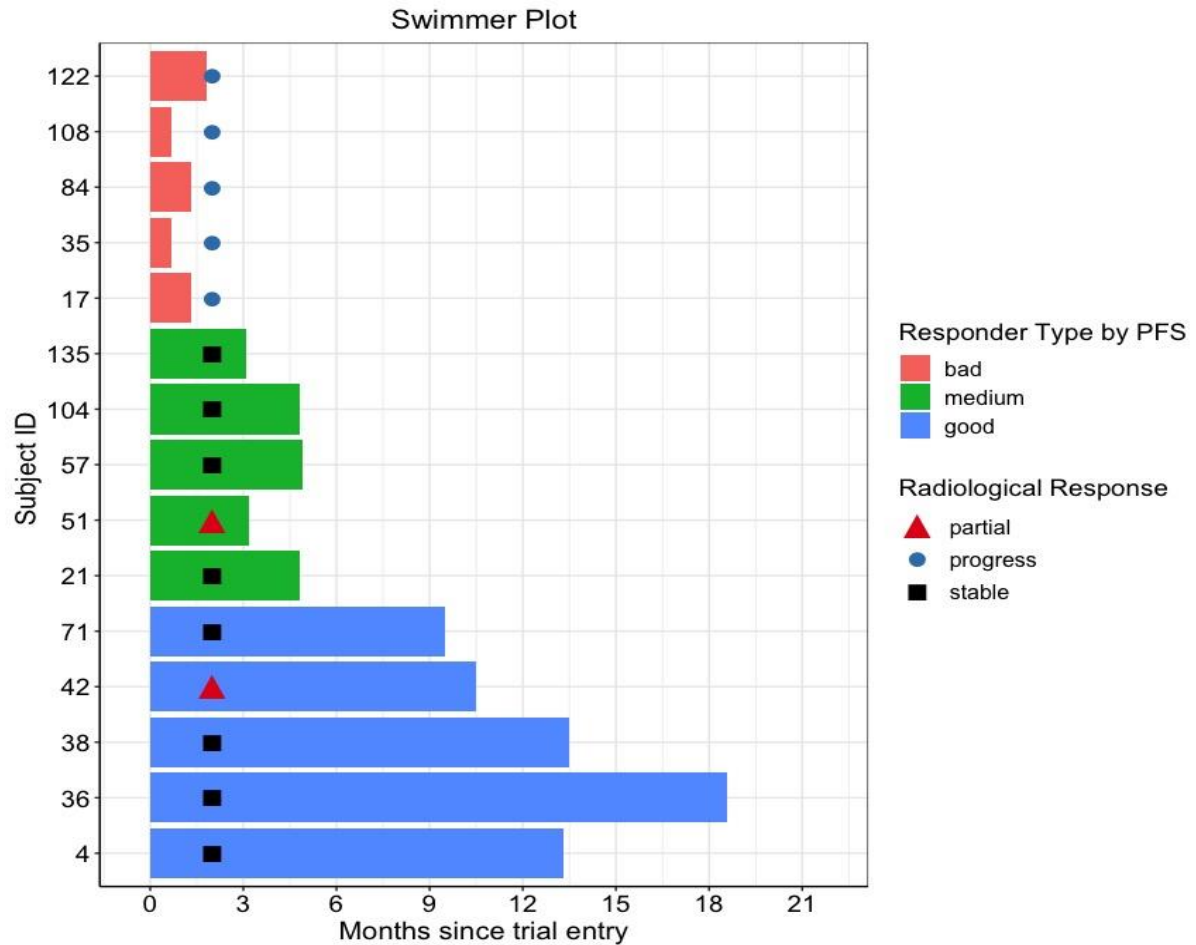
This figure shows three groups of patients based on Progression-Free Survival (PFS) in months. Patients with bad responses had progressive disease on CT scans. Patients with medium and good responses had a mixture of stable and partial radiological responses on CT scans.

5.4 Tracking Mutations in Patients with Response to Treatment

Objective: Can longitudinal ctDNA samples be used to monitor clinical outcomes in response to combination therapy of fulvestrant and capivasertib in patients from the FAKTION trial?

5.4.1 Good Responders

Objective: Can longitudinal ctDNA samples be used to identify disease response to combination therapy of fulvestrant and capivasertib?

5 out of 15 patients had a median PFS of 13.3 months (PFS range 9.5 – 18.5). Clinicopathological characteristics with the radiological response and PFS is presented in Table 32.

4 out of 5 patients had *PIK3CA* detected at baseline either in FFPE DNA or ctDNA. *PIK3CA* mutations were then tracked with ddPCR in ctDNA longitudinal samples at baseline, eight weeks and disease progression. Table 33 demonstrates mutation detection for each patient.

Table 32. Clinicopathological features of good responders.

Pt ID	Age	Histology	Metastatic sites	CT response	PFS (months)
4	76	IDC	LN	stable	13.3
71	76	IDC	bone + LN	stable	9.5
36	58	IDC	bone	stable	18.8
42	57	IDC	bone + LN + liver + pleural	partial	10.5
38	66	IDC	bone + LN	stable	13.5

Pt ID – Patient number, IDC – Invasive Ductal Carcinoma, LN – Lymph node, CT – Computer Tomography, PFS – Progression-Free Survival

Table 33. Mutation detection in longitudinal ctDNA samples in 5 good responders.

PT ID	Gene	Mutation	Baseline ctDNA				8 - week ctDNA		End of Treatment ctDNA			
			DNA con (ng/ml)	Seq Depth	NGS AF (%)	ddPCR AF (%)	DNA con (ng/ml)	ddPCR AF (%)	DNA con (ng/ml)	Seq Depth	NGS AF (%)	ddPCR AF (%)
4	PIK3CA	H1047R	5.5	6000	9.7	7.2	17.3	0	22.0	12603	7.3	8.6
	GATA3	M357TyrfsTer15		5726	7.0	NT		NT		5974	3.2	NT
71	PIK3CA	H1047R	8.9	7467	2.8	2.2	17.1	0	12.8	8552	1.2*	0.9
	ESR1	E380Q		13568	1.4*	NT		NT		6082	0	NT
36	PIK3CA	exon 9**	6.9	NT	NT	0	16.8	0	10.9	NT	NT	2.8
	ESR1	D538G		4195	0	0		0		7043	2.2*	1.4
	GATA3	D336GfsTer17		10255	0	NT		NT		8070	0.6*	NT
42	PIK3CA	H1047R	8.8	6378	0	0	18.3	0.6	11.6	9437	6.7	7.8
	ESR1	Y537S		3878	0	0		0		8032	3.5	1.3
38	BRCA2	W2788Ter	4.5	3376	5.8	NT	NT	NT	17.4	3150	0	NT

**Exon 9 – (either of p.E542K, p.E542K), NT – Not Tested, AF – Allele Frequency, * Detected under the limit of detection, DNA con – DNA concentration (ng per 1ml of plasma), Seq depth – sequencing depth, Allele frequency.

Figure 40. Mutation detection in longitudinal ctDNA samples in 5 good responders.
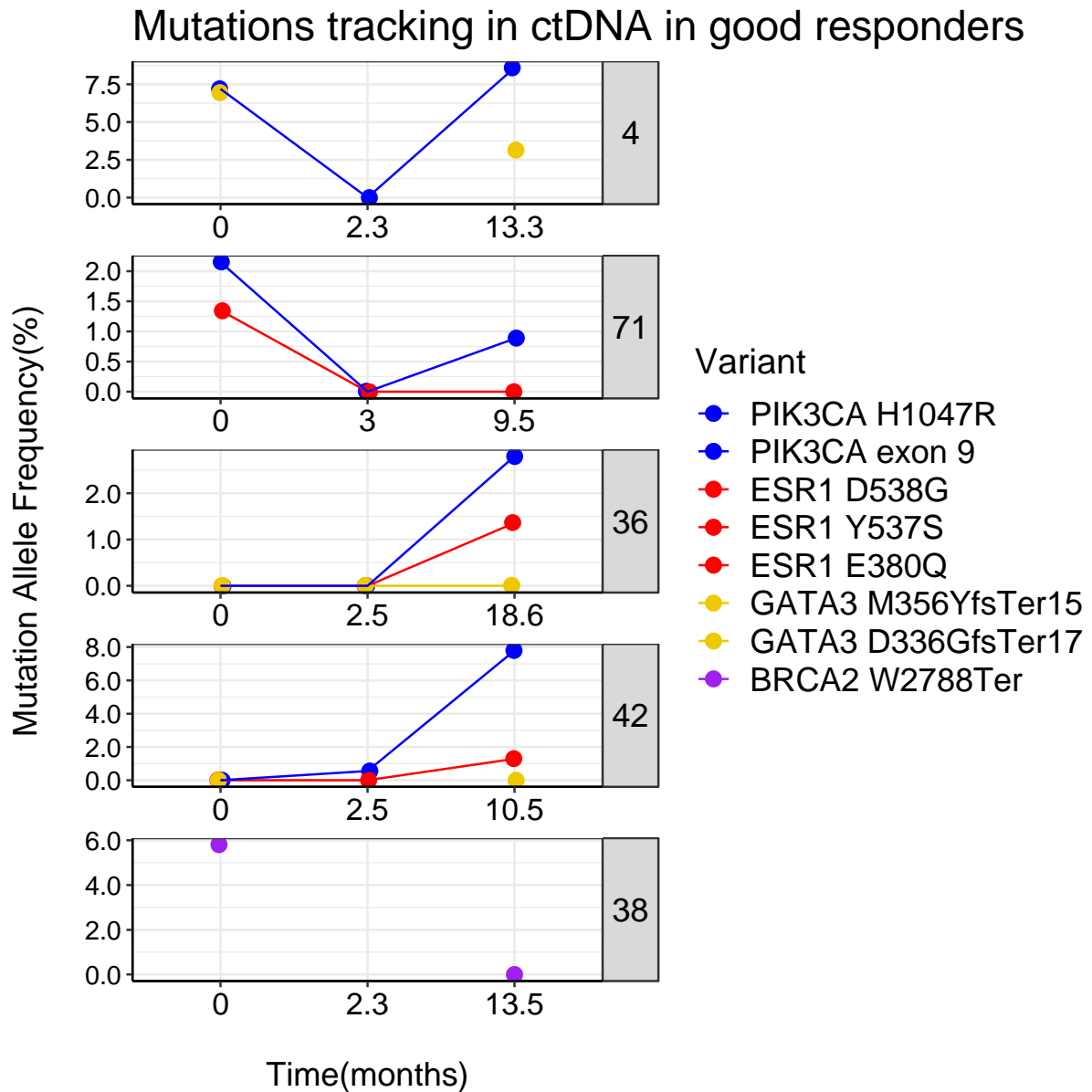
This figure shows changes in allele frequency of mutations in *PIK3CA, ESR1, GATA3* and *BRCA2* genes in five patients. The numbers (on the right) represent a unique patient number.

In good responders, the expected trend of mutant allele frequency (MAF) change would be that the mutations detected in baseline tissue and ctDNA samples have disappeared whilst responding to treatment but have reappeared when the disease progresses. This pattern was followed by only two patients (**4 and 71)**, Figure 40 and Table 33. The second trend recognised in this cohort of patients was that mutation was detected in a tissue but not in baseline ctDNA. However, mutation started to appear and become detectable at progression to experimental therapy (**patients 36 and 42)**, Figure 40 and Table 33.

Patients 4 and 71 have represented a similar molecular tracking pattern. In both patients, *PIK3CA* p.H1047R was detected in FFPE DNA and baseline ctDNA samples. These mutations had become undetectable in ctDNA after 2 – 3 months of being on treatment with the combination of fulvestrant and capivasertib, suggesting that the tumour has responded molecularly to the treatment. However, CT scans of the chest, abdomen and pelvis for both patients showed stable disease by RECIST1.1 criteria. I could not confirm whether the target lesion has shrunk on the CT scan as this data was not available. If the lesions were reduced up to 30% or increased up to 20%, the disease would be called stable disease, and the patient would be allowed to continue treatment. Also, visible lesions on a CT scan might not represent a viable tumour but may represent dying cells. This cannot be distinguished on the CT scan. The radiological response may require more time to show on the CT scan. However, these patients have responded at the molecular level as the mutation reduced to an undetectable level at 2-3 months. In both patients, *PIK3CA* p.H1047R became detectable again when the disease became radiologically progressive. In **patient 4**, the disease progression occurred after 13.3 months and in **patient 71**, after 19.5 months. The reappearance of *PIK3CA* mutations was correlated with the radiological progression of the disease. This shows that the burden of disease can be tracked not only radiologically but also molecularly. These are excellent examples of mutation disappearance whilst responding to treatment and reappearing while the disease progresses again. The fact that the mutation disappears to an undetectable level could potentially predict a good response to treatment.

Also, **patient 4** had *GATA3* p.M356YfsTer15 frameshift insertion detected in the FFPE DNA at the level of 13% AF, in baseline ctDNA at 6.95% and in progression sample at 3.15%. The 8-week sample was not assessed for this gene. The relevance of *GATA3* mutations is currently unclear. *GATA3* is a transcription factor that is frequently mutated in breast cancer. Mostly frameshifts are seen in 15% of ER-positive breast cancers. High *GATA3* expression is correlated with the luminal subtype of breast cancer and is associated with a better prognosis. The same study showed that *GATA3* did not affect

sensitivity to hormonal therapies (Gustin et al. 2017). Another study also confirmed that patients with *GATA3* mutations live longer than patients with wild-type *GATA3*. However, *GATA3* mutations found in zinc-finger 2 (ZnFn2) lead to distinct features: common detection in luminal B breast cancers and worse prognosis (Takaku et al. 2018). Splice site and truncation mutations found in exons 5–6 are frequently detected in luminal A breast cancers with better prognosis (Takaku et al. 2018).

P**atient 36 and 42,** *PIK3CA* mutations were detected in FFPE DNA but were not found in baseline ctDNA despite testing with two methods, NGS and ddPCR**.** The *PIK3CA* mutation has appeared in the ctDNA sample at the disease progression in both patients**. Patient 42,** *PIK3CA* mutation started to appear at a low level at 2.5 months of experimental treatment and had become detectable at disease progression. The two baseline ctDNA samples for both patients were also tested by AWMG laboratory staff with validated ddPCR assay used in the FAKTION trial and found negative for *PIK3CA* mutations. There are several reasons that none of the three mutations was detected in the baseline ctDNA samples: poor sample handling, low DNA concertation, technical issues or allele frequency of mutations were below the limit of detection of the method used in this project. At 2.5 months, **patient 36** had stable disease on the CT scan, and **patient 42** had a partial response. The interesting fact here is that **patient 42,** whose breast cancer has shrunk over 30% on the CT scan, but low allele frequency *PIK3CA* p.H1047R mutation was found in ctDNA. This could suggest that patient has had *PIK3CA* mutation in baseline at a higher level, but NGS and ddPCR failed to detect or the sample was compromised. In both patients, both mutations were detectable in ctDNA at disease progression. It is very unlikely this has appeared as a resistant mutation as was already present in primary tissue in both patients. The treatment with a combination of fulvestrant and capivasertib effectively kept the disease under control for both patients, **patient 36** over 18.8 months and **patient 42** for 10.5 months. Cancer has overcome this pathway's blockage and continued to grow, which was confirmed radiologically on the CT scans and was associated with the reappearance of *PIK3CA* mutations.

Also, in both **patients 36 and 42**, *ESR1* mutations were found in the end of treatment ctDNA samples. Both mutations were not detected in tumour tissue nor baseline and 8-week ctDNA samples, using both NGS and ddPCR methods. This suggests that these mutations appeared as part of acquired resistance to fulvestrant. The other possibility is that these mutations were present in baseline ctDNA samples, but the methods were not sensitive enough, or low DNA concentration or low-quality sample. The *ESR1* p.D538G mutation developed after 20.3 months in **patients 36,** and the *ESR1* p.Y537S mutation developed over 11.9 months in **patient 42**. There is a significant time gap between

baseline and the end of treatment samples, and therefore, more likely that the *ESR1* mutations have appeared over time.

Patient 38 had pathogenic mutation p.W2788Ter in *BRCA2* gene detected by 44-gene NGS panel at 93% AF in FFPE DNA and found in baseline ctDNA at 5.8% AF but was not detected in the end of treatment sample after 15.4 months. This could represent the evolution of cancer and heterogeneity or technical issues but would not be related to endocrine resistance or response to treatment. This patient had stable disease on CT scan after 2.3 months of treatment and PFS of 13.5 months. The patient remained alive at last follow up.

5.4.2 Medium Responders

Five patients with a median PFS of 4.8 months (range 3.1 – 4.9) were included in the medium responders' group. Clinicopathological features for medium responders are presented in Table 34. Three patients had combinations of mutations in *PIK3CA*, *ESR1*, *TP53* and *KMT2C* genes, one patient with a single mutation detected in the *HER2* genes, Table 35 and Figure 41. **Patient 21** had no detectable mutations in ctDNA.

Table 34. Clinicopathological features for medium responders.

Pt ID	Age	Histology	Metastatic sites	CT response	PFS (months)
104	52	IDC	bone + lung + LN	stable	4.8
57	56	IDC	bone	stable	4.9
51	67	IDC	LN	partial	3.2
135	53	IDC	bone + LN	stable	3.1
21	61	mix duct-lob	liver	stable	4.8

Pt ID – Patient number, IDC – Invasive Ductal Carcinoma, LN – Lymph node, CT – Computer Tomography, PFS – Progression-Free Survival

Table 35. Mutation detection in longitudinal ctDNA samples in 5 medium responders.

| Pt ID | Gene | Mutation | Baseline ctDNA | | | | 8 - week ctDNA | | End of Treatment ctDNA | | | |
			DNA con (ng/ml)	Seq Depth	NGS AF (%)	ddPCR AF (%)	DNA con (ng/ml)	ddPCR AF (%)	DNA con (ng/ml)	Seq Depth	NGS AF (%)	ddPCR AF (%)
104	PIK3CA	H1047R	7.7	9367	8.7	11.1	13.5	8.5	24.4	11072	35.2	37.8
	TP53	C176R		5129	4.9	NT		NT		4901	17.6	NT
57	PIK3CA	H1047R	49.6	4037	0	0	14.0	0	17.7	11588	2.3*	2.7
	ESR1	Y537S		4156	0	0		0		8525	1.2*	1.1
	KMT2C	D352Y		1455	2.8	NT		NT		4408	4.4	NT
51	ESR1	Y537C	6.8	5147	9.2	5.6	19.6	0	11.5	6496	0	0
	TP53	G244V		4818	21.7	NT		NT		6457	3.8	NT
135	HER2	A1216D	10.2	7218	42	NT	NT	NT	13.5	7231	38	NT

NT – Not Tested, AF – Allele Frequency, * Detected under the limit of detection, DNA con – DNA concentration (ng per 1ml of plasma), Seq depth – sequencing depth.

Figure 41. Mutation detection and longitudinal ctDNA samples in 5 medium responders

Mutations tracking in ctDNA in medium responders
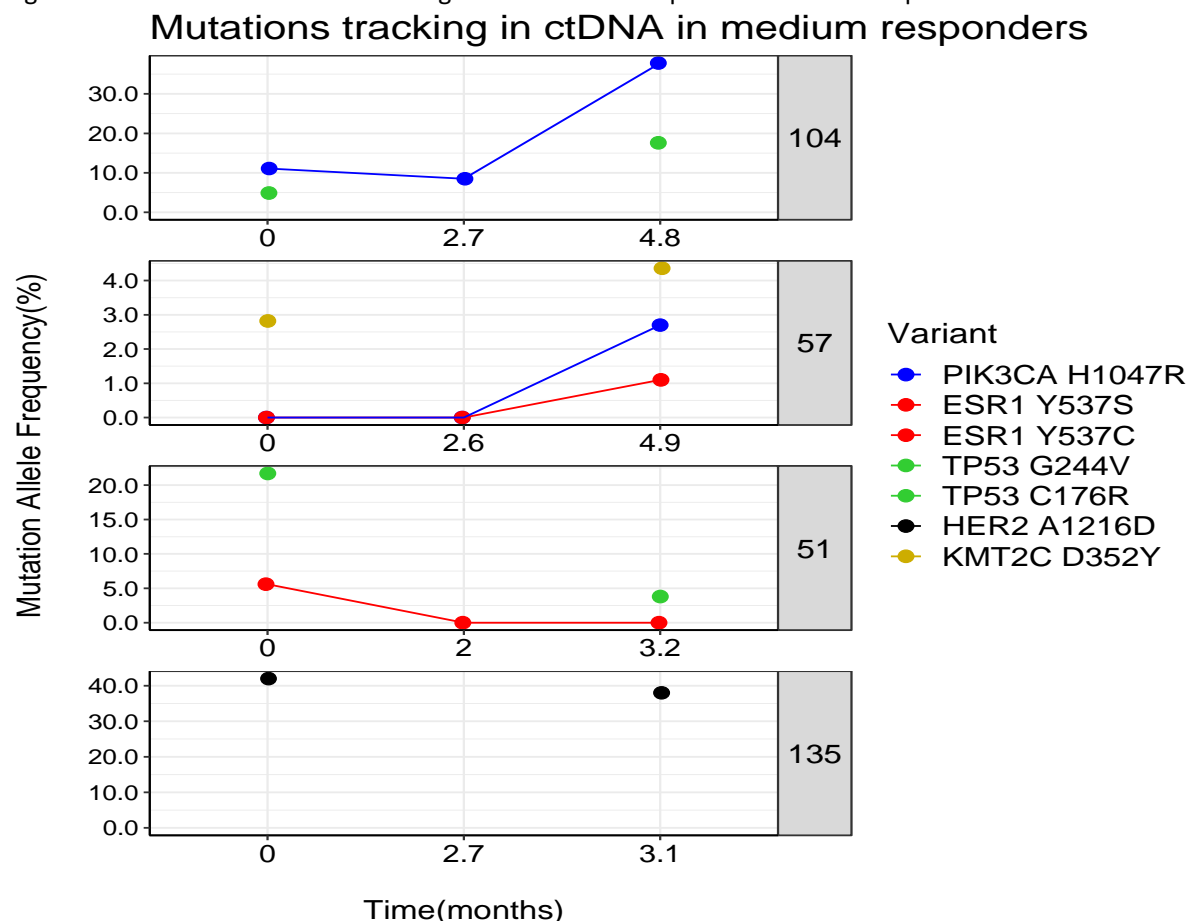
This figure shows changes in allele frequency of mutations in *PIK3CA*, *ESR1*, *TP53*, *MAP3K1*, *HER2* and *KMT2C* genes in five patients. The numbers(on the right) represent a unique patient number.

The expected trend in medium responders would be similar to good responders with the disappearance or reduction of MAF whilst the patient responds to treatment and the reappearance of the mutation during disease progression but over a shorter period of time. Unfortunately, only **patient 104** has fitted in this trend, Table 35 and Figure 41. The second trend was recognised in the previous cohort of patients where the mutation was detected in a tissue but not in baseline ctDNA. However, the mutation had become detectable at progression to experimental therapy (**patient 57),** Table 35 and Figure 41.

P**atient 104**, *PIK3CA* p.H1047R mutation was found in combination with *TP53* p.C176R mutation in FFPE DNA and detected in longitudinal ctDNA samples. These findings showed no significant drop in allele frequency of *PIK3CA* p.H1047R after 2.7 months, suggesting molecularly stable disease or possible resistance to treatment. The CT scan at 2.7 months showed stable disease. The fact that mutation has persisted could also suggest that the response to therapy was limited. This patient achieved a PFS of 4.8 months and overall survival of 7.4 months. The *TP53* p.C176R could contribute to the limited response to therapy as it was present in the baseline sample, and the allele frequency has tripled in the end of treatment ctDNA sample. The combination of fulvestrant and capivasertib would affect the cancer cell clones with activated PI3K/AKT pathway but would not influence *TP53* mutated cells or had a moderate effect on cells with both mutations. When analysing mutations in ctDNA, it is not possible to assess the mutational status of each cancer cell, which may have single or multiple mutational alterations. This patient could have experienced a minor response to treatment from inhibiting PI3K/AKT pathway, but the *TP53* clone could start rapidly growing. Therefore patient had experienced only a short period of stable disease. Both mutations had increased the AF in the end of treatment sample, Table 35. This could also suggest a cross-talk between the *TP53* and PI3K/AKT pathways or one pathway being an escape pathway. In patients with the combination of mutations, it could be more critical to eliminate more aggressive cell clones using other treatments such as chemotherapy or immunotherapy. If *PIK3CA* activated clone persisted, the patient could start a combination of fulvestrant and capivasertib after chemo- or immunotherapy.

Patient 57 was found to have *PIK3CA* p.H1047R mutation in the tissue DNA. This variant was not found in baseline and the 8-week ctDNA sample using both techniques, NGS and ddPCR. CT scan at these eight weeks showed stable disease. This trend is similar to one of the patterns in the good responders' group. This mutation appeared in the progression ctDNA sample at 6.3 months. A similar situation was with *ESR1* p.Y537S mutation, which was also detected in the primary FFPE sample and was

undetectable in the baseline and 8-week samples. However, it has appeared in the ctDNA sample at disease progression. *ESR1* and *PIK3CA* mutation in primary tissue could suggest primary endocrine resistance. Clinical data revealed that the patient has progressed within six months of endocrine therapy in the metastatic setting prior to the FAKTION trial. Mutations were not detected in the baseline sample, possibly due to poor sample handling. High DNA concertation could suggest the release of wild-type DNA from white cells and diluting low-frequency mutations.

The clinical relevance of *KMT2C* p.D352Y mutations is unclear, which may become more apparent when more genetic and clinical data available in the future. This mutation was found in the tissue DNA of **patient 57** at a very low level of 3% below the limit of detection (with tumour cellular content of 25%). Also, it was detected in baseline and the end of treatment ctDNA samples, Table 35. The pathogenic *TP53* p.P142S mutation was detected in primary FFPE at a low level of 5.7% AF but not detected in any ctDNA sample, suggesting a passenger mutation that could have been eliminated by previous treatments (chemotherapy or radiotherapy) or persisted at the undetectable allele frequency. This patient achieved a PFS of 4.9 months and an OS of 17.6 months in the FAKTION trial.

Patient 51 was found to have pathogenic *TP53* p.G244V (likely oncogenic - although was not clinically or functionally validated) mutation in tissue DNA at 40.5%. This variant was also detected in the baseline ctDNA sample at a level of 21.7% AF and also at a reduced level of 3.8% AF in the progression ctDNA sample at 3.2 months. Also, *ESR1* p.Y537C mutation was detected in the baseline ctDNA sample. *ESR1* variant was not detected at eight weeks when the patient's CT scan showed a partial response to treatment, which correlated with radiological response. However, *ESR1* mutation continued to be undetectable by both techniques in the progression ctDNA sample at 3.2 months of treatment. This could suggest that experimental treatment could have eliminated the *ESR1* mutation. However, the *TP53* mutation persisted, and the disease, despite partial radiological response on the first CT scan, has progressed just after 3.2 months on trial treatment. The patient survived for 18.9 months from entry to the trial.

These two sections showed that it is possible to track mutations in longitudinal samples. However, the correlation with clinical response to treatment was found in only 3 (33.3%) of 9 patients. This could be due to sample handling (collection, transport, storage), DNA extractions, the sensitivity of methods, and the competency of the person performing the test. Therefore, it is essential to

understand all the limitations (clinical and technical) of ctDNA testing and continue to improve the ctDNA evaluation process before it can be introduced to clinical practice.

5.4.3 Bad Responders

Objective: Can longitudinal ctDNA samples be used to identify disease resistance to combination therapy of fulvestrant and capivasertib?

Five patients were classified as bad responders due to disease progression at the first radiological assessment with PFS of less than three months. Clinicopathological features of all bad responders are presented in Table 36. Interestingly, 4 of 5 patients had two metastatic sites, and one patient had four metastatic sites. The most common metastatic sites were bone and liver.

The expected trend of molecular change would be that the allele frequency (AF) of mutations detected in baseline samples would be higher in the progression samples. Three patients **(17, 35, 108)** demonstrated this pattern, which was consistent with radiological progression. Two patients **(84 and 122)** demonstrated the opposite effect. Figure 42 and Table 37 show AF changes in the baseline and longitudinal samples.

Table 36. Clinicopathological features of bad responders.

| Pt ID	Age	Histology	Metastatic sites	CT response	PFS (months)
17	59	IDC	bone + LN	Progress	1.3
108	57	IDC	bone + liver	Progress	0.7
35	43	IDC	bone + liver + LN + pleural	Progress	0.7
84	74	IDC	bone + liver	Progress	1.3
122	71	ILC	bone + liver	Progress	1.2

Pt ID – Patient number, IDC – Invasive Ductal Carcinoma, LN – Lymph node, CT – Computer Tomography, PFS – Progression-Free Survival

Table 37. Mutation detection in longitudinal ctDNA samples in 5 bad responders.

Pt ID	Gene	Mutation	DNA con (ng/ml)	Baseline ctDNA			DNA con (ng/ml)	End of Treatment ctDNA		
				Seq Depth	NGS AF (%)	ddPCR AF (%)		Seq Depth	NGS AF (%)	ddPCR AF (%)
17	ESR1	D538G	30.2	4827	2.0*	NT	12.32	6600	6.3	NT
	TP53	N131Y		6912	9.2	NT		11185	18.2	NT
	KMT2C	R526P		8560	0	NT		10156	11.0	NT
	KMT2C	I323V		27485	0	NT		20441	1.5*	NT
	BRCA2	I1364L		3022	0	NT		4828	9.9	NT
108	PIK3CA	exon 9**	26.8	NT	NT	18.7	48.6	NT	NT	20.4
35	ESR1	D538G	21.6	5569	12.8	NT	30.6	8619	18.4	NT
84	PIK3CA	E726K	18.9	3153	3.5	NT	25.6	3635	1.0*	NT
	MAP2K4	Y318Ter		6146	6.1	NT		10464	1.5*	NT
	KMT2C	I373K		2590	3.2	NT		3274	2.3*	NT
122	PIK3CA	H1047R	7.18	9432	15.3	17.1	15.16	9771	0	0
	ESR1	Y537C		6978	1.4*	1.5		6303	0	0
	CDH1	Y797IfsTer19		8416	19.8	NT		1086	0	NT

**Exon 9 – (either of p.E542K, p.E542K),, NT – Not Tested, AF – Allele Frequency, *Detected under the limit of detection.

Figure 42. Mutation detection in longitudinal ctDNA samples in 5 bad responders.
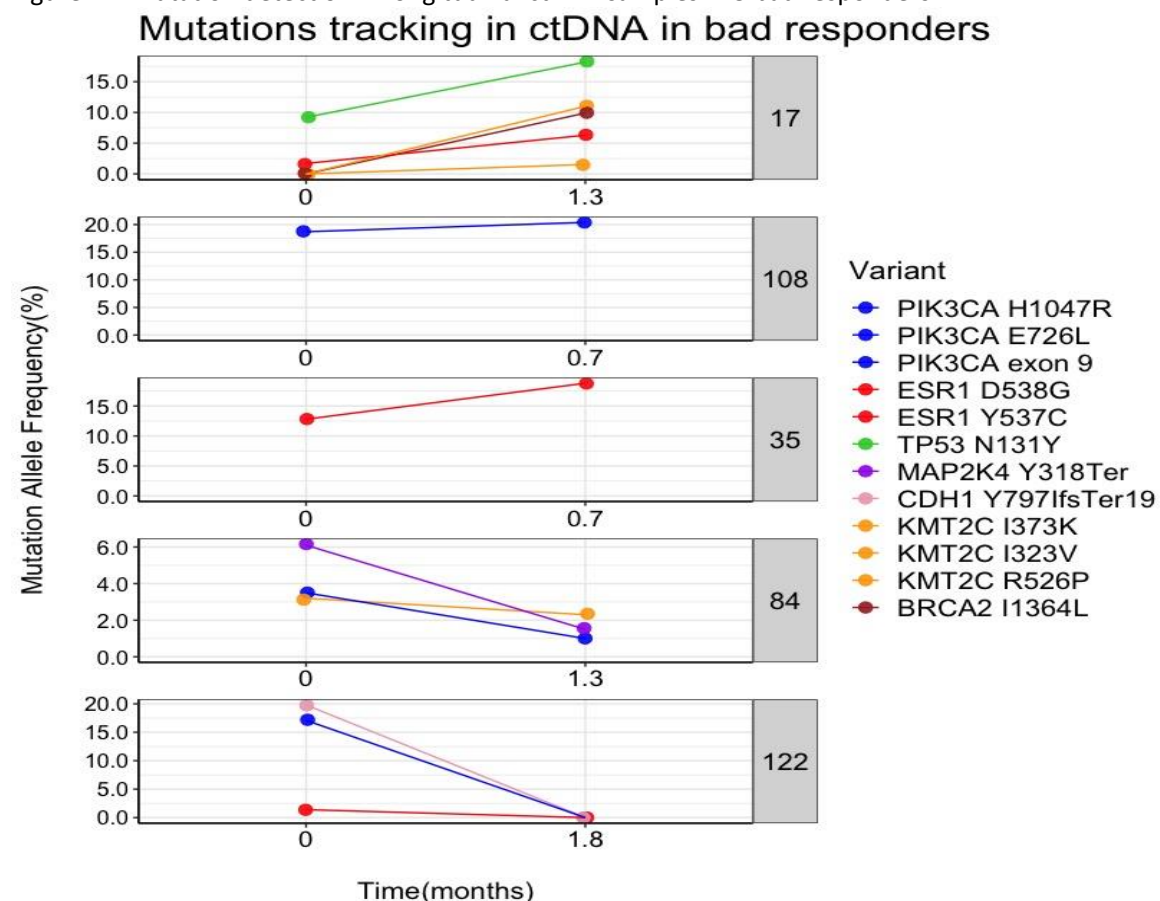
This figure shows changes in allele frequency of mutations in *PIK3CA*, *ESR1*, *TP53*, *MAP3K1*, CDH1, BRCA2 and *KMT2C* genes in five patients. The numbers (on the right) represent a unique patient number.

In **patient 17,** the AF of two mutations, *ESR1* p.D538G and *TP53* p.N131Y detected in the baseline ctDNA sample, had increased in the progression ctDNA sample at 2.3 months. *ESR1* p.D538G mutation was not present in the tissue DNA, suggesting that it has appeared after endocrine therapy previously received. The combination therapy of fulvestrant and capivasertib did not reverse this resistance as the AF of p.D538G has risen in the progression sample. *TP53* p.N131Y mutation was present in primary tissue biopsy at 71.7% AF. Primary tissue was taken 4.5 years before the trial entry. *TP53* mutation could be driving cancer growth. This *TP53* mutated clone was insensitive to the combination of fulvestrant and capivasertib and possibly be responsible for disease progression.

Multiple variants at different allele frequencies appeared in the progression ctDNA sample: *BRCA2* p.I1364L, *KMT2C* p.R526P, and *KMT2C* p.I323V, Table 37. These mutations may not be driving cancer mutations. However, the fact that mutations number increased in the end of treatment ctDNA samples could suggest that the tumour has increased its tumour mutational burden or genetic instability. This could increase the heterogeneity of breast cancer and contribute to disease progression. CT scan showed disease progression, and the patient had to discontinue trial treatment. The patient has progressed very rapidly on trial treatment with PFS of 1.3 months, but the patient remained alive for 13.4 months.

Similarly, in **patient 35,** the AF of *ESR1* p.D538G mutation was raised in longitudinal ctDNA samples, correlated with radiological disease progression on a CT scan, Table 36. This patient had a very short PFS of 0.7 months and survived for only 6.1 months. The trial combination therapy has not worked for this patient for an unclear reason. There could be other mutations or other types of mutations like amplification, deletions or translocations involved in cancer growth, but the 44-gene NGS panel could not detect them. Therefore, the next step would be to test for other types of mutations and look at expression analysis to identify the main drivers or resistance mutations for this cancer.

Also, in **patient 108,** the AF of *PIK3CA* exon 9 mutation allele frequency increased in the progression ctDNA sample. However, *TP53* p.R280K mutation detected in tissue DNA was not detected in any ctDNA samples, which could be due to technical or biological reasons. This patient had not responded to combination therapy of fulvestrant and capivasertib despite the activated PI3K/AKT pathway. This molecular disease progression was confirmed by radiological progression on a CT scan, Table 36. This raised the question of whether co-existent *TP53* mutation contributed to inadequate response to combination therapy.

Patients 84 and 122 demonstrate an opposite pattern to those patients above:

In **patient 122,** mutations detected in FFPE and the baseline ctDNA samples were not found in the progression ctDNA sample. The CT scan showed progressive disease, and the patient had a PFS of 1.2 months. The expectation here would be that mutations detected in baseline samples should have been detected in the samples at the time of disease progression at similar or higher AF. There could be several reasons for not detecting the mutations: 1 - compromised sample, 2 - two methods failed detection due to insufficient sensitivity, 3 - true molecular response but not visualised on CT scan as more time needed, 4 - true molecular response of targeted clone with the escalation of growth of other clones not tested by NGS panel, 5 - biological reason, with reduced ctDNA shedding into the bloodstream. The first reason seems most likely.

In **patient 84,** all mutations detected in baseline samples were also present in the end of treatment ctDNA sample but at a lower AF. This could be caused by a reduction in shedding of ctDNA into the bloodstream, and therefore it would suggest a molecular improvement or stability of the disease. However, radiologically breast cancer had progressed. This picture can be confusing for the clinician. It could be interpreted that the patient achieved a molecular response, or the presence of mutations in the progression sample can suggest that the disease is resistant to treatment. Other potential reasons are explained above for patient 122 that could also be valid here.

Longitudinal ctDNA samples tested in this patient group identified disease progression in 3 of 5 (60%) patients. This represents a better correlation rate of molecular changes with a clinical response for bad responders (60%) compared to the good and medium responders group (30%). This could be associated with a higher tumour burden that sheds more ctDNA into the bloodstream, increasing the chances of mutation detection.

5.5 Role of Other Mutations in Treatment Response

Objective: Can other detected mutations affect response to combination therapy of fulvestrant and capivasertib?

In this section, I looked at all mutations found in patients with different clinical responses. Figure 43 represents all mutations found in ctDNA at all time points. This chart shows a very interesting trend that mutations found in ctDNA in good responders are usually at lower allele frequencies than medium

or bad responders groups. Also, almost all mutations found in the good responders group were in *PIK3CA*, *ESR1* and *GATA3* genes. This group had a single driving activated PI3K/AKT pathway, which was effetely blocked by fulvestrant and capivasertib, and therefore these patients had significantly longer clinical responses.

Furthermore, Figure 43 demonstrates multiple mutations in various genes detected at higher AF in ctDNA in medium and bad responders groups, suggesting that these cancers might have had more than one pathway activated and were more heterogeneous. Interestingly, *TP53* mutations were mainly present in medium or bad responders groups but not in good responders. These patients had a very limited response to fulvestrant and capivasertib. This could suggest that stratification based on one gene like *PIK3CA* or *AKT1* might not be sufficient to define which patient will respond to treatment. It is essential to consider other biomarkers that dominate or drive cancer growth. Although there is no multitargeted therapy for very heterogeneous cancers available and there is no therapy for *TP53* driven cancers, these patients may respond to standard chemotherapy. Chemotherpay generally works on dividing cells by interfering with the cell cycle. This can help stratify patients in future trials and create an arm for concurrent or sequential chemotherapy and hormonal therapy with targeted therapy like *AKT1* inhibitor.

Figure 43. Patients with all mutations in all samples divided by PFS.
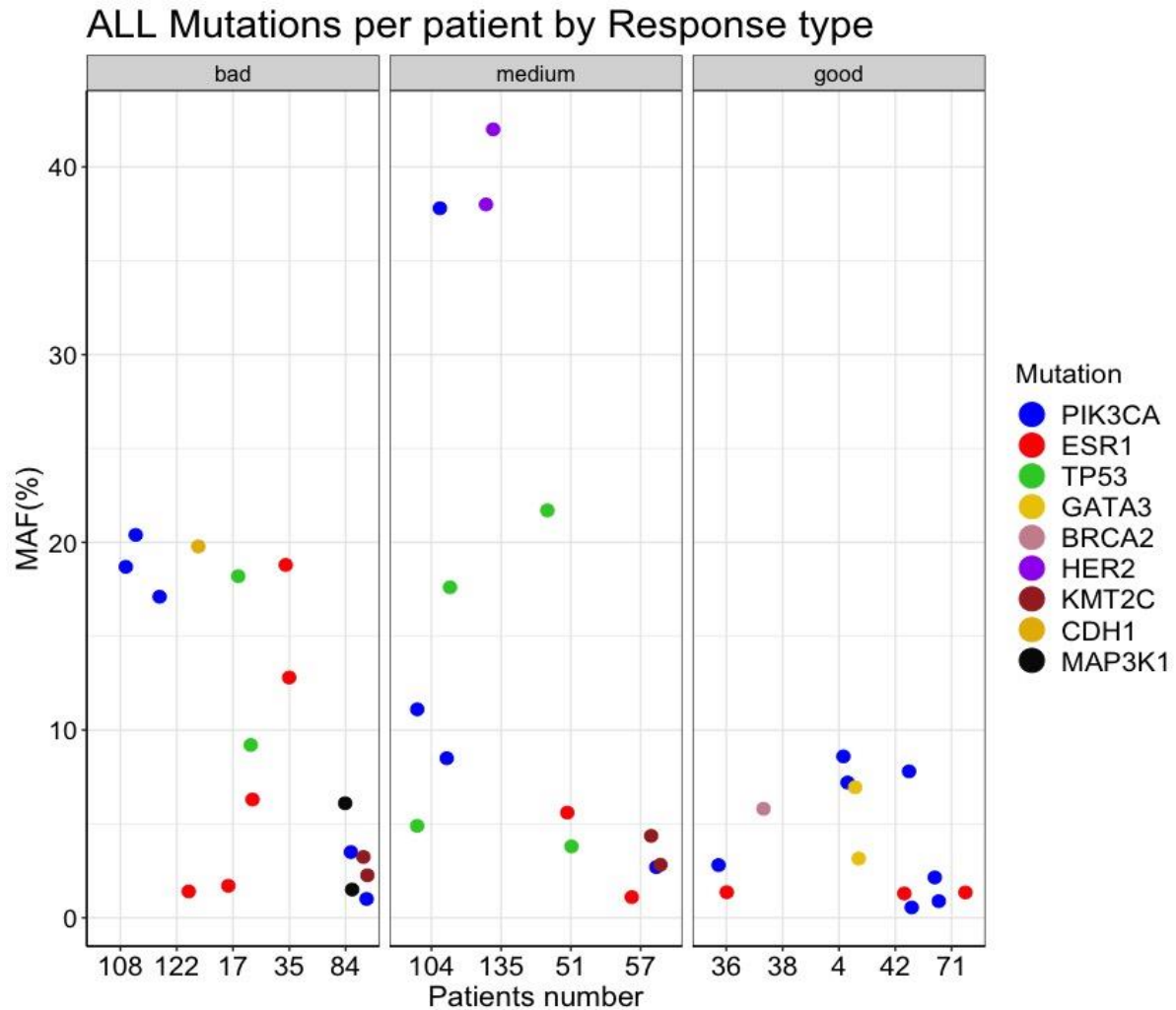
Mutation presence and mutant allele frequency MAF versus Progression-Free Survival (PFS) in all ctDNA samples (Baseline, 8-week, End of treatment samples). PFS: good (>9 months – good responder), medium (3-9 months – medium responder) and bad (<3 months – bad responder).

Co-existing mutations with activating PI3K/AKT pathway mutations could potentially affect response to combination therapy of fulvestrant and capivasertib. The future trial could consider testing a more comprehensive range of biomarkers to better identify patients for novel treatments. Patients with the activated one pathway can have an excellent durable response to treatment. However, patients with co-existent bad prognostic factors might need a different therapeutic approach, where a new treatment is tested against standard treatment in the prospective translational clinical trial.

5.6 Summary and Discussion

In this chapter, I have looked at detecting mutations in baseline and longitudinal ctDNA samples using ddPCR and the 44-gene NGS panel in patients treated with fulvestrant and capivasertib in the FAKTION trial. This study aimed to see if detected mutations at baseline samples can be tracked in longitudinal samples. I have shown they can be detected in baseline samples and tracked only in some patients but not all. Furthermore, the change in mutant allele frequency corresponded to clinical response only in 43% of patients. Therefore, ctDNA might not be the best circulating biomarker to monitor the disease in clinical practice yet. However, testing and detecting multiple mutations in related genes and using two methods may help identify some undetected mutations. For example, if three mutations were detected in FFPE or ctDNA sample, but none of them has been detected in the longitudinal sample could suggest a compromised sample. However, if one of the three mutations detected in ctDNA could suggest a biological reason. It is vital to identify potential technical issues, including issues with sample collection, transport, and storage, with methods such as assay failure, method error, low sequencing coverage, sensitivity, specificity and human error. Trained technician perform specific techniques daily would be more competent than the researcher who performs these techniques only several times. Understanding cancer biology and the technical limitations could improve mutation detection in ctDNA in future studies and enable introduction to clinical practice with confidence.

The FAKTION trial focused on testing specific mutations in the *PIK3CA* gene, and this was the basis to randomise patients into two treatments arms. I showed that mutation detection in other genes, such as pathogenic mutations in the *TP53* gene, could play a role in resistance to combination therapy. As mentioned previously, *TP53-PIK3CA* mutations occur in breast cancers in 5.3 – 12.8% (TCGA 2012; Fountzilas et al. 2016; Li et al. 2018b). *TP53-PIK3CA* co-mutation is associated with worse overall survival in colorectal cancer (Li et al. 2018a). In this study, patients with breast cancer that harbour *PIK3CA* and *TP53* co-mutation had no response or short response to combination fulvestrant and capivasertib. The overall survival and further evaluation of the clinical effect of dual mutations in breast cancer should be explored in larger clinical trials.

Heterogeneous cancers with multiple mutations could be more aggressive and difficult to treat. It could be challenging to achieve long-term responses to targeted therapy by inhibiting the growth of the one cell clone as other cell clones will continue to grow. Figure 43 shows that the long-term

responders to combination therapy of fulvestrant and capivasertib were those who had *PIK3CA*, *ESR1*, *GATA3* mutations detected. Patients with multiple mutations, including *TP53*, had a short duration of response even if they had initially stable disease or partial response on CT scan. Medium responders had a similar genetic profile to bad responders, and their response did not last long as the longest PFS in this group was six months. This hypothesis can be explored in the next larger phase III trials. In the future, most cancers will have whole genome or extensive panel sequencing, which will help us identify multiple frequently mutated genes in specific cancers. However, doctors will need to understand what information these mutations carry regarding prognostic or predictive value to make an informed decision about treating patients with the best treatment.

It is also essential to explore other types of mutations that could explain trial treatment resistance or response. In the next chapter, I will be discussing gene amplification in breast cancer that can play a role in endocrine resistance and potentially affect response to the combination treatment of fulvestrant and capivasertib.

6. Copy Number Variation (CNV) Detection in Circulating Tumour DNA Samples and Its Influence on Treatment Response and Clinical Outcome of Patients Treated Within FAKTION Trial

6.1 Introduction

In two previous chapters, I focused on single point mutation detection related to endocrine resistance in FFPE and ctDNA samples. In this chapter, I investigate the detection of other molecular changes like gene amplification associated with endocrine resistance in ctDNA using ddPCR. The analysis was performed on the end of treatment ctDNA samples of 55 patients with metastatic endocrine-resistant breast cancer treated within the FAKTION trial, including 20 patients treated with combination therapy of fulvestrant with capivasertib and 35 patients treated with fulvestrant only. As there is no known time of gene amplification development as a result of endocrine resistance. It can be assumed that patients with the longest time on endocrine therapy, including fulvestrant in the FAKTION trial, would have had the highest chance for gene amplification to develop. Therefore, the end of treatment cfDNA samples were the most appropriate sample to test as these patients had exhausted all possible endocrine therapies. In addition, cfDNA samples collected at the time of cancer progression would potentially contain a higher ctDNA fraction and further increase the chance of detecting amplifications.

6.2 Hypothesis, Aims and Objectives

6.2.1 Hypothesis and Aims

This chapter aimed to test the hypothesis that multiple gene amplification (*HER2*, *MYC*, *FGFR1*) can be detected in ctDNA in patients with breast cancer as a result of endocrine resistance. In addition, *HER2*, *MYC*, *FGFR1* amplifications detected in ctDNA have utility in predicting clinical outcome and influence response to treatment received in the FAKTION trial.

6.2.2 Objectives

Using 55 the end of treatment ctDNA samples, I aimed to expand molecular biomarker detection of CNVs in ctDNA samples. In this chapter, the objectives are:

1. To explore the ability to detect *HER2*, *MYC* and *FGFR1* amplification using ddPCR in the end of treatment ctDNA samples collected in the FAKTION trial.
2. To assess the concordance of detected CNVs between FFPE DNA and ctDNA using ddPCR to identify possible conversion.
3. To correlate detected CNVs with clinical outcomes in the FAKTION trial
4. To determine the utility of CNVs in ctDNA to improve the patients' selection for therapy in future trials.

6.3 Copy Number Variation Detection

The most common amplified and best-described gene in breast cancer is the *HER2* gene, located at the 17q21-24 chromosome. *HER2* is amplified in 25-30% of breast cancers (Hudis 2007). Other frequently amplified genes in breast cancer are c-*MYC* and *FGFR1*. *MYC* encodes a transcription factor, a key regulator of cell growth, metabolism, proliferation, differentiation, and apoptosis. *MYC* is amplified in about 15% of breast cancers and is associated with a high risk of relapse and death (Green et al. 2016). *FGFR1* encodes the tyrosine kinase receptor, which belongs to the fibroblast growth factor receptor family and is amplified in 9 - 15% of breast cancers (Turner et al. 2010). *FGFR1* amplification has been linked with poor prognosis in breast cancer (Jang et al. 2012). In addition, all three amplifications have been associated with endocrine resistance, as described in the introduction chapter. In addition, *MYC* amplification can be associated with resistance to the PI3K/AKT pathway inhibitors (Jang et al. 2012).

In the FAKTION trial, all breast cancers were *HER2* negative based on the primary tumour's pathological report. The rate of molecular conversion from a primary HER2-negative tumour to HER2-positive metastatic breast cancer is 9.7% (Lower et al. 2009). This suggested that the molecular conversion of primary breast cancer occurs during disease progression. Retesting metastatic lesions could allow the patients with acquired *HER2* amplification to receive HER2-targeted therapy, leading to better survival outcomes (Tchou et al. 2015; Kim et al. 2018). Therefore, this group of patients was an ideal group to re-evaluate *HER2* status. However, in the FAKTION trial, a re-biopsy of tumour or metastatic lesion was not indicated before commencing fulvestrant +/- capivasertib. However, all patients had ctDNA samples collected before and after treatment. The end of treatment ctDNA samples were used for CNV testing as they were collected after patients exhausted all endocrine therapies, including fulvestrant, and some received capivasertib. Therefore, these samples had the

highest chance to detect the actual conversion of HER2 and other amplifications as they were collected from patients that had the longest time on endocrine therapy (before and during the FAKTION trial), Figure 44.

Figure 44. Overview of patient selection for this project.
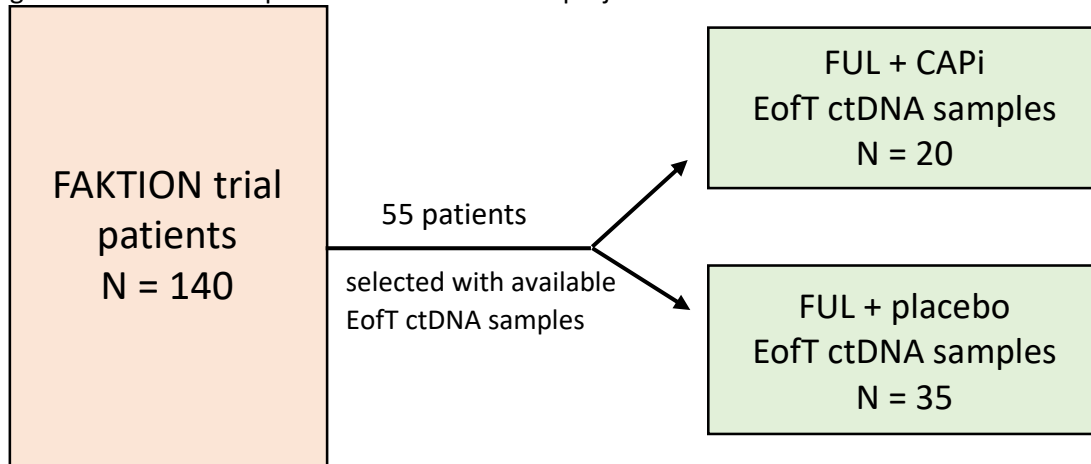
EofT – End of treatment ctDNA samples collected at time of cancer progression in FAKTION trial, N = number of patients, FUL – fulvestrant, CAPi - capivasertib

In this chapter, I present the detection of the three amplifications *HER2*, *MYC* and *FGFR1* in ctDNA samples and FFPE DNA in 55 patients from the FAKTION trial, using ddPCR, Table 38. Furthermore, I will evaluate whether these amplifications can affect clinical outcomes to fulvestrant with and without capivasertib.

Table 38. *HER2*, *MYC*, *FGFR1* amplification detection in FFPE DNA and ctDNA by ddPCR in 55 patients from FAKTION trial.

ID	FFPE			ctDNA			PFS	Response	Treatment arm
	HER2	MYC	FGFR1	HER2	MYC	FGFR1			
16		NT					1.41	Bad	F+ A
17							1.31	Bad	F+ A
35							0.69	Bad	F+ A
108							0.69	Bad	F+ A
148		NT	NT				1.48	Bad	F+ A
156		NT					1.18	Bad	F+ A
57		NT	NT				4.90	Medium	F+ A
104		NT	NT		UN		4.83	Medium	F+ A
135		NT	NT				3.12	Medium	F+ A
143		NT					4.96	Medium	F+ A
144		NT	NT				3.15	Medium	F+ A
150		NT	NT				4.83	Medium	F+ A
151					UN		3.15	Medium	F+ A
166			NT				6.60	Medium	F+ A
2		NT	NT				10.32	Good	F+ A
9		UN					27.24	Good	F+ A
10		NT	UN				27.01	Good	F+ A
42					UN	UN	10.48	Good	F+ A
86		NT					12.85	Good	F+ A
97		NT	NT				13.73	Good	F+ A
11		UN	UN				1.61	Bad	F
31		NT					2.40	Bad	F
53							1.28	Bad	F
60		UN	UN				1.81	Bad	F
66		NT	NT				2.23	Bad	F
73							1.25	Bad	F
85							1.35	Bad	F
121		UN	UN				1.22	Bad	F
125		NT					1.02	Bad	F
134		NT	NT				1.25	Bad	F
141		NT	NT				1.38	Bad	F
147							1.25	Bad	F
154							1.48	Bad	F
18					UN		4.86	Medium	F
26		NT					4.83	Medium	F
33		UN					3.15	Medium	F
39			NT				7.66	Medium	F
52		NT	NT				3.09	Medium	F
67		NT	NT				5.55	Medium	F
82					UN		5.16	Medium	F
92		NT	NT				7.13	Medium	F
103		NT	NT				3.09	Medium	F
109			UN				3.02	Medium	F
118						UN	8.64	Medium	F
127		NT					3.06	Medium	F
139		NT					4.80	Medium	F
142							8.38	Medium	F
175							3.06	Medium	F
119		NT	NT			UN	4.4	Medium	F
1		NT	UN				10.45	Good	F
13		NT	NT				18.86	Good	F
41		NT	NT				18.66	Good	F
78		NT					10.35	Good	F
116		NT					11.56	Good	F
6		NT	NT				16.85	Good	F
Methods	IHC +/-FISH, ddPCR	ddPCR	ddPCR	ddPCR	ddPCR	ddPCR	X	X	X

Dark colours – Amplified, Light colour – Non-amplified. UN – Unknown –tested but inconclusive result. CN – Copy number, NT – Not Tested, ID - Patient ID, PFS – Progression-Free Survival, F - Fulvestrant, F + A – Fulvestrant + Capivasertib.

6.3.1 *HER2* Amplification

Objective: Can HER2 amplification be detected in the end of treatment ctDNA samples of patients in the FAKTION trial? Could the detected HER2 amplification be an effect of biomarker transition?

In this study, I tested 55 of the end of treatment ctDNA samples from 55 patients in the FAKTION trial, using ddPCR for *HER2* amplification (as described in chapter 3, section 3.6.1) to find the true transition of *HER2* non-amplified to amplified. The end of treatment ctDNA samples were collected at the progression to trial treatment (fulvestrant +/- capivasertib). Patients recruited to the trial were previously reported to be ER-positive and HER2-negative in primary tissue. These patients have become resistant to oral endocrine therapy and to fulvestrant +/- capivasertib, which gives the highest chance of detecting genuine *HER2* transition if it existed.

1 (1.8%) patient out of 55 was found to have *HER2* amplification at the level of 7.9 copies in the end of treatment sample. The baseline ctDNA sample collected prior to trial treatment had *HER2* amplification at 11.7 copies. The ddPCR method identified 16.2 copies in the FFPE DNA, which was normal on the pathological report. IHC was performed at the diagnosis and reported as *HER2* non-amplified (1+), Table 39. Due to a discrepancy in the results, the trial repeated IHC and performed FISH. Both tests resulted in high amplification of the *HER2* gene; IHC was reported as amplified (3+), and FISH reported 15.8 copies, Table 39. This has helped validate the ddPCR method used to test ctDNA and the FFPE DNA. Results from tissue using FISH were similar to results from ddPCR. Therefore, this patient was eligible for treatment with Herceptin. The *HER2* status was detected first from a non-invasive blood test. Although I have not proven the conversion of *HER2* status in this cohort of patients, I have shown that this test can detect *HER2* amplification from the blood test. The new HER2 amplification detection in primary tissue was reported to the Centre for Trials Research at Cardiff University.

Table 39. Methods used to test *HER2* amplification in FFPE DNA and ctDNA in one patient.

Method	Primary FFPE	FFPE repeat	ctDNA BL	ctDNA EoT
IHC	1+	3+	NT	NT
FISH	NT	15.8 CN	NT	NT
ddPCR	x	16.2 CN	11.7 CN	7.9 CN

NT not tested as the test cannot be performed on ctDNA samples. BL – Baseline sample, EoT – end of treatment sample, CN – Copy number.

HER2 amplification was detected in ctDNA and primary tissue FFPE DNA of one patient out of 55 patients from the FAKTION trial. However, *HER2* amplification was not acquired as it was detected in primary tissue and baseline ctDNA sample. Therefore, no actual HER2 transition was detected. This highlights how important it is to establish a *HER2* status correctly and re-evaluate for the trials.

6.3.2 *MYC* Amplification

Objective: Can MYC amplification be detected in the end of treatment ctDNA samples, and how the presence of MYC amplification in samples can affect PFS and OS in patients treated in the FAKTION trial?

This section presents *MYC* amplification detection results in the end of treatment ctDNA samples from 55 FAKTION trial patients, as described in chapter 3, section 3.6.2. The 2.6 copy number cut-off was used to assign ctDNA samples as amplified. The threshold was determined using maximally selected rank statistics. These 55 ctDNA samples were from patients that have had developed resistance to fulvestrant +/- capivasertib. I attempted to correlate *MYC* amplification with clinical outcomes using PFS and OS. This aimed to examine whether *MYC* amplification can be treated as a predictive marker for resistance to fulvestrant alone and in combination with capivasertib. *MYC* amplification can play a role in resistance to PI3K inhibitors, as described in the introduction chapter, section 1.3.2. Pre-clinical cell line studies suggested that MYC amplification could create a potential escape pathway for capivasertib, but this has not been evaluated in clinical settings.

12 (21.8%) of 55 samples were found to have *MYC* amplification, 38 (69.1%) of 55 samples were *MYC* non-amplified, 5 (9%) samples were assigned as inconclusive. *MYC* amplification was correlated with PFS and OS in 55 patients, Table 40. The Kaplan-Meier curves and the cox-regression were used to analyse the survival difference between the *MYC* amplified and non-amplified groups. 5 patients with inconclusive results were excluded from the analysis. A difference of 3.5 months in PFS (p=0.002) and 5.2 months in OS (p=0.014) between two groups favoured *MYC* non-amplified group, Table 40 and Figure 45. The difference between the groups in PFS and OS were found to be clinically and statistically significant. The high Hazard Ratio suggested that patients with *MYC* amplification had a higher risk of disease progression events and death risk, Table 40. This may suggest that *MYC* amplification is a bad prognostic factor, and the prognosis would be worse in MYC-amplified patients regardless of the treatment received.

Table 40. Summary of PFS, OS of patients with *MYC* status detected in ctDNA.

ctDNA	Total number	PFS					OS				
		median PFS	HR	95% CI lower	95% CI upper	p value	median OS	HR	95% CI lower	95% CI upper	p value
MYC amp	12	1.3	2.83	1.41	5.68	0.002	13.4	3.22	1.20	8.62	0.014
MYC non-amp	38	4.8					18.7				

PFS -Progression-free survival, OS – Overall Survival, HR – Hazard Ratio, CI – Confidence Interval, *MYC* amp – amplification, *MYC* non- amp - non-amplified

Figure 45. Kaplan-Meier Curves presenting PFS and OS by *MYC* status in ctDNA.

Progression free survival by MYC amplification detected in ctDNA

Number at risk

MYC	0	3	6	9	12	15	18	21	24	27	30
MYC non-amplified	38	27	13	11	7	5	4	2	2	2	0
MYC amplified	12	4	2	0	0	0	0	0	0	0	0

Overall survival by MYC amplification in ctDNA

Number at risk

MYC	0	3	6	9	12	15	18	21	24	27	30	33	36	39
MYC non-amplified	37	31	22	18	16	11	7	4	3	3	2	1	0	0
MYC amplified	12	9	8	7	5	3	2	1	0	0	0	0	0	0
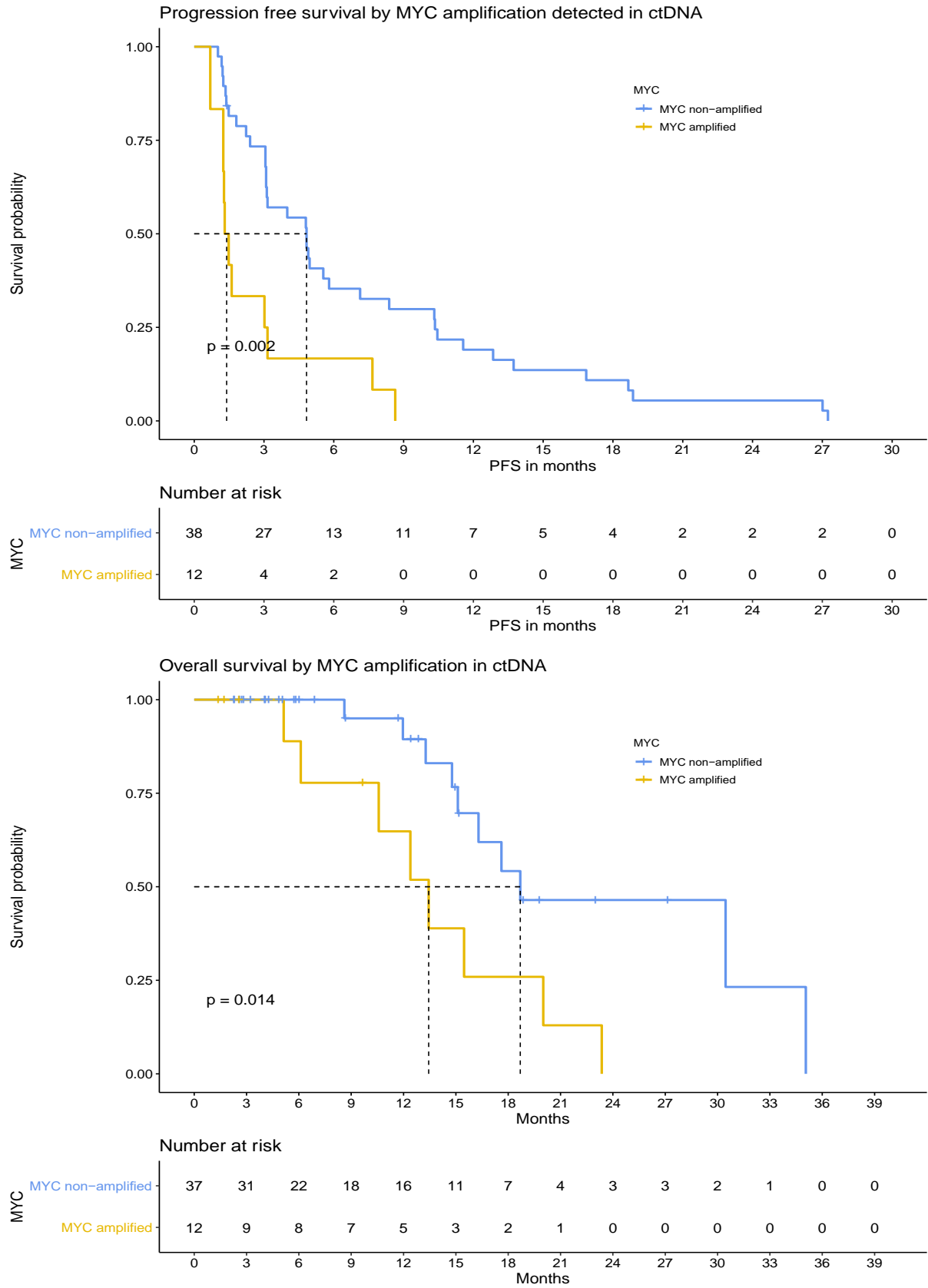
6.3.2.1 *MYC* status in ctDNA and matched FFPE DNA

Objective: Can MYC amplification be detected in the FFPE DNA and matched ctDNA? If so, what is the concordance?

23 FFPE samples with matched ctDNA samples were tested for *MYC* amplification. 14 (61%) of 23 of FFPE samples were found *MYC* amplified, 4 of 23 (17%) non-amplified, 5 of 23 (22%) inconclusive. Samples with inconclusive results were excluded from further analysis, leaving 14 evaluable patients. 11 (78.6%) of 14 patients had MYC status concordant FFPE DNA and ctDNA, including 9 patients with MYC amplified and 2 patients with MYC non-amplified in both samples. Conversely, 3 (21.4%) of 14 patients were discordant, including 2 patients with detected MYC amplification only in FFPE DNA and one patient with acquired MYC amplification in the end of treatment ctDNA sample, Table 41.

Table 41. *MYC* concordance between FFPE and ctDNA.

ID	FFPE		ctDNA		PFS	Response	Treatment arm
	MYC	CN	*MYC*	CN			
11	UN	4.30	[dark red]	4.04	1.6	Bad	F
53	[dark red]	4.94	[dark red]	5.24	1.3	Bad	F
60	UN	8.90	[light red]	2.56	1.8	Bad	F
73	[dark red]	9.34	[dark red]	4.32	1.2	Bad	F
85	[light red]	3.74	[light red]	2.54	1.3	Bad	F
121	UN	3.36	[light red]	2.52	1.2	Bad	F
147	[light red]	2.90	[dark red]	4.74	1.2	Bad	F
154	[dark red]	18.76	[dark red]	9.52	1.5	Bad	F
18	[dark red]	5.32	UN	2.60	4.9	Medium	F
33	UN	7.56	[dark red]	3.58	3.2	Medium	F
39	[dark red]	4.56	[dark red]	6.24	7.7	Medium	F
82	[dark red]	10.84	UN	3.10	5.2	Medium	F
109	[dark red]	5.42	[dark red]	4.76	3	Medium	F
118	[dark red]	5.42	[dark red]	3.44	8.6	Medium	F
142	[light red]	2.30	[dark red]	2.56	8.4	Medium	F
175	[dark red]	5.74	[dark red]	2.60	3.1	Medium	F
17	[dark red]	10.50	[dark red]	3.48	1.3	Bad	F + A
35	[dark red]	5.84	[dark red]	5.42	0.7	Bad	F + A
108	[dark red]	8.14	[dark red]	3.02	0.7	Bad	F + A
151	[dark red]	10.34	UN	2.98	3.2	Medium	F + A
166	[dark red]	4.86	[light red]	2.58	6.6	Medium	F + A
9	UN	5.14	[light red]	2.46	27.2	Good	F + A
42	[light red]	2.22	UN	2.54	10.5	Good	F + A

Dark red colours – *MYC* amplified samples. Light red colour – *MYC* non-amplified sample. UN – Unknown – inconclusive result. NA – FFPE not available for testing, CN – Copy number, ID - Patient ID, PFS – Progression-Free Survival, F - Fulvestrant, F + A – Fulvestrant + Capivasertib.

In two patients (**166 and 175**), *MYC* amplification was detected in FFPE DNA (in patient **166** from the metastatic lesion and in **175** from primary tissue) but not in the ctDNA sample. Patient 166 had *MYC* amplification in the FFPE sample only a few months before blood was taken. Therefore, it would be expected to detect *MYC* amplification in ctDNA. For **patient 175**, the time between both samples was not available. The reasons for discordance could be; 1 - compromised ctDNA samples, 2 - failure to detect by ddPCR as low number of amplified copies, 3 - biology of cancer – very low amount of ctDNA in the bloodstream for amplification to be detected.

Patient 147 with *MYC* amplification detected only in the ctDNA sample had two years between FFPE and ctDNA samples. This could suggest that patient had acquired the *MYC* amplification over time in

response to multiple treatments. However, there was a possibility that *MYC* amplification was not detected in FFPE DNA due to inadequate sample quality or method error.

This section showed that *MYC* copy number variations could be detected in ctDNA and the FFPE DNA, using ddPCR with the concordance of 78.6%.

6.3.2.2 *MYC* amplification in FFPE DNA/ctDNA versus PFS and OS

Objective: How does MYC amplification in these samples affect PFS and OS in 55 patients treated in the FAKTION trial?

In this section, I present a survival analysis with new *MYC* status, based on *MYC* amplification detection in one of the samples, FFPE or ctDNA, Table 42.

17 patients were found to have *MYC* amplification in either FFPE DNA or ctDNA samples. 5 patients had inconclusive results and were excluded from the analysis. I was interested in how the new *MYC* status would affect PFS and OS. The p values remained low, and the difference in PFS remained statistically significant but not clinically as only 1.8 months difference in PFS was found. The main reason for this could be that *MYC* present in ctDNA suggests a high amplification level in the tumour in metastatic settings, which could be more relevant than detecting *MYC* amplification in the primary tissue performed many years ago. Possibly more up to date results are more valid than testing old tissue samples. Also, a lower PFS difference could be due to a small number of patients. However, the OS of the 5.2 months difference remained statistically and clinically significant (p=0.0044), and hazard ratios did not change significantly, Table 42 and Figure 46.

Table 42. Summary of PFS, OS of patients with *MYC* status detected in FFPE/ctDNA.

ctDNA/ FFPE DNA	Total number	PFS					OS				
		median PFS	HR	95% CI lower	95% CI upper	p value	median OS	HR	95% CI lower	95% CI upper	p value
MYC amp	17	3.02	2.83	1.41	5.68	0.006	13.44	3.96	1.43	10.98	0.004
MYC non-amp	33	4.83					18.69				

PFS -Progression-free survival, OS – Overall Survival, HR – Hazard Ratio, CI – Confidence Interval, *MYC* amp – amplification, *MYC* non- amp - non-amplified

Figure 46. Kaplan-Meier Curves presenting PFS and OS by *MYC* status in ctDNA and/or FFPE DNA.

Progression free survival by MYC amplification in FFPE/ctDNA

Overall survival by MYC amplification in FFPE or ctDNA
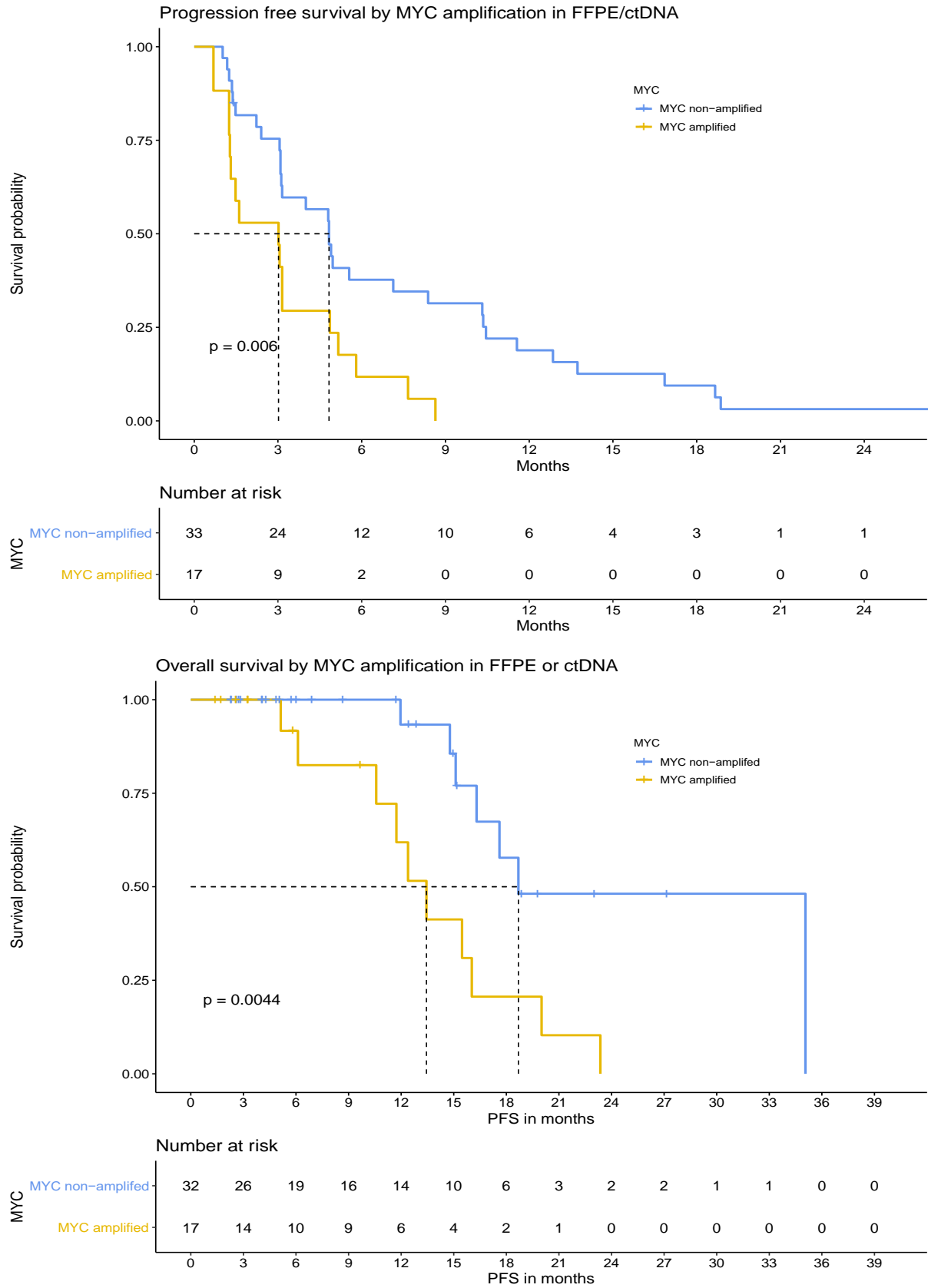
Regardless of treatment received, patients had shorter PFS and OS compared to patients with no *MYC* **amplification. I could not show that** *MYC* **amplification can be acquired resistant mutation to endocrine treatment and capivasertib. However, I have shown that ctDNA samples can be used to assess** *MYC* **status.** *MYC* **amplifications in ctDNA carry vital prognostic information, and they should be explored further in larger studies.**

6.3.3 *FGFR1* Amplification

Objective: Can FGFR1 amplification be detected in the end of treatment ctDNA samples, and how the FGFR1 amplification found in ctDNA affect PFS and OS in a patient treated in the FAKTION trial?

This section shows *FGFR1* amplification detection results using ddPCR and correlation with clinical outcomes. This aimed to examine whether *FGFR1* amplification can be treated as a bad prognostic factor or a predictive marker for resistance to fulvestrant +/- capivasertib. Capivasertib would not directly affect the *FGFR1* pathway, but *FGFR1* amplification was found to play a role in resistance to CDK4/6 inhibitors and PI3K inhibitors in other studies (Drago et al. 2019). However, it has not been established if this stands for AKT1 inhibitors. Therefore, I attempted to assess whether *FGFR1* amplification as a single marker or in combination with other markers can contribute to resistance to fulvestrant and capivasertib.

55 end of treatment ctDNA samples were tested for *FGFR1* amplification using ddPCR, described in chapter 3, section 3.6.3. The 3.4 copy number cut-off was used to assign ctDNA samples as amplified. The threshold was determined using maximally selected rank statistics. *FGFR1* amplification was found in 9 (13.4%) ctDNA samples, 43 (78.2%) samples were assigned as *FGFR1* non-amplified, and 3 (5.4%) unassigned with inconclusive results, Table 38. Survival analysis was performed for this group of patients based on *FGFR1* status in ctDNA samples, Table 43.

Patients with *FGFR1* amplification detected in ctDNA samples were found to have a shorter median PFS of 1.6 months (0.69 -3.15), and patients with no amplification detected had 4.8 months (1.02 – 27.24), p - 0.0004. The high Hazard Ratio suggests that patients with *FGFR1* amplification progress faster than patients with normal *FGFR1* copies, Table 43 and Figure 47. However, the overall survival difference of 3.9 months (p=0.073) favouring the *FGFR1* non-amplified group was not statistically

significant due to small numbers of patients who reached the survival event at the time of data analysis, Table 43 and Figure 47.

Table 43. Summary of PFS, OS of patients with *FGFR1* status detected in ctDNA.

FGFR1 ctDNA	Total number	PFS					OS				
		median PFS	HR	95% CI lower	95% CI upper	p value	median OS	HR	95% CI lower	95% CI upper	p value
Amp	9	1.6	3.81	1.7	8.56	0.0004	12.4	2.49	0.89	6.97	0.073
Non-amp	43	4.8					16.3				

PFS -Progression-free survival, OS – Overall Survival, HR – Hazard Ratio, CI – Confidence Interval, *FGFR1* amp – amplification, *FGFR1* non- amp - non-amplified

Figure 47. Kaplan-Meier Curves presenting PFS and OS by *FGFR1* status in ctDNA.

Progression free survival by FGFR1 amplification in ctDNA

Overall Survival by FGFR1 amplification in ctDNA
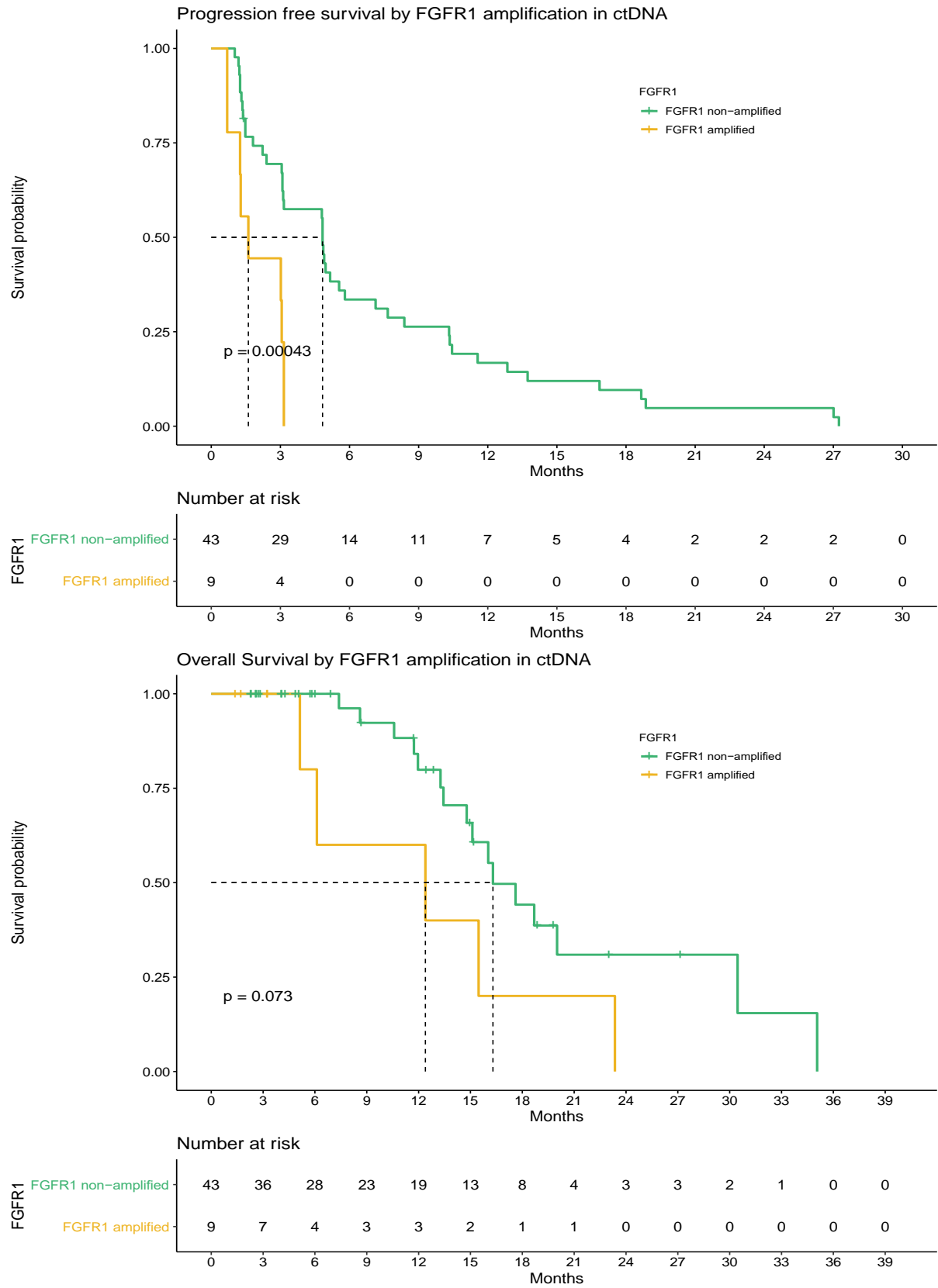
6.3.3.1 *FGFR1* **Amplification in FFPE and ctDNA**

Objective: Can FGFR1 amplification be detected in the FFPE DNA and matched ctDNA samples? If so, what is the concordance?

FFPE DNA with matched ctDNA from 34 patients were tested for *FGFR1* amplification with ddPCR, as described in chapter 3, section 3.6.3.

9 (26%) of 34 FFPE samples were found to have *FGFR1* gene amplified, 18 (53%) of 34 were *FGFR1* non-amplified, 7 (21%) inconclusive. 9 patients with inconclusive results in either FFPE DNA or ctDNA were excluded from concordance analysis.

20 (80%) of 25 evaluable patients had FGFR1 status concordant between FFPE DNA and ctDNA, including 5 patients with FGFR1 amplification and 15 patients with non-amplified FGFR1 in both matched samples, Table 44.

5 (20%) of 25 patients had discordant FGFR1 status, including 3 patients with FGFR1 amplification detected only in FFPE DNA and 2 patients with FGFR1 amplification in ctDNA only, Table 44.

Table 44. *FGFR1* concordance between FFPE and ctDNA

ID	FFPE		ctDNA		PFS	Response	Treatment arm
	FGFR1	CN	*FGFR1*	CN			
11	UN	4.84		**4.19**	1.6	Bad	F
31		2.76		2.59	2.4	Bad	F
53		**4.04**		**5.24**	1.3	Bad	F
60	UN	2.86		2.57	1.8	Bad	F
73		2.32		2.69	1.2	Bad	F
85		3.11		2.68	1.3	Bad	F
121	UN	2.82		2.99	1.2	Bad	F
125		3.34		2.75	1	Bad	F
147		2.37		**4.73**	1.2	Bad	F
154		2.07		2.54	1.5	Bad	F
18		**4.93**		2.71	4.9	Medium	F
26		1.83		2.81	4.8	Medium	F
33		**4.01**		**3.96**	3.2	Medium	F
82		3.25		2.65	5.2	Medium	F
109	UN	3.07		**5.18**	3	Medium	F
118		**6.13**	UN	4.51	8.6	Medium	F
127		**5.76**		3.07	3.1	Medium	F
139		2.57		2.71	4.8	Medium	F
142		2.44		2.87	8.4	Medium	F
175		**7.96**		**6.85**	3.1	Medium	F
1	UN	2.23		2.67	10.4	Good	F
116		**9.56**		2.67	11.6	Good	F
16		3.57		2.61	1.4	Bad	F+ A
17		3.73		2.8	1.3	Bad	F+ A
35		**5.81**		**4.68**	0.7	Bad	F+ A
108		2.05		**5.12**	0.7	Bad	F+ A
156		2.22		2.6	1.2	Bad	F+ A
143		2.39		2.92	5	Medium	F+ A
151		**16.28**		**4.78**	3.2	Medium	F+ A
166	UN	4.15		3.29	6.6	Medium	F+ A
9		3.07		3.13	27.2	Good	F+ A
10	UN	4.4		2.68	27	Good	F+ A
42		1.73	UN	3.16	10.5	Good	F+ A
86		2.31		3.07	12.8	Good	F+ A

Dark green colours –FGFR1 amplified samples. Light green colour –FGFR1 non-amplified sample. UN – Unknown –inconclusive result. CN – Copy number, NT not tested, ID - Patient ID, PFS – Progression-Free Survival, F - Fulvestrant, F + A – Fulvestrant + Capivasertib.

Two patients (**108** and **147**) with *FGFR1* amplification detected in ctDNA but not in FFPE DNA had time intervals between samples nine and two years, respectively, Table 44. These patients were previously

exposed to multiple treatments before recruitment to the FAKTION trial. Therefore, they could acquire *FGFR1* amplification, or false negatives were detected in FFPE DNA due to potential technical issues.

Three patients (**18, 116, 127**) had *FGFR1* amplification detected in primary tumours only. The possible reasons for not detecting *FGFR1* amplification in ctDNA could be: 1 - poor blood sample handling, 2 - method error or insufficient sensitivity, 3 - biological reason: surgical treatment eliminated the primary disease, but the relapsed metastatic disease has a different genetic profile, 4 - the shedding of DNA to bloodstream could have been affected by multiple treatments stabilising disease.

This section showed that *FGFR1* amplification could be detected in FFPE DNA and ctDNA using ddPCR, with the concordance of 80% between both samples.

6.3.3.2 *FGFR1* amplification in FFPE DNA/ctDNA versus PFS and OS

Objective: How does FGFR1 amplification in the FFPE DNA/ctDNA affect PFS and OS in 55 patients treated in the FAKTION trial?

I have performed survival analysis on this group of patients, using Kaplan-Meier curves and Cox regression, based on the detection of *FGFR1* amplification in either FFPE DNA or ctDNA samples. However, the median PFS and OS differences were not clinically or statically significant, Table 45 and Figure 48.

In contrast to *MYC* analysis, FGFR1 survival analysis did not reveal significant differences in PFS and OS. Thus, *FGFR1* status might not play a role as a prognostic biomarker, or it may affect survival when FGFR1 is very highly amplified or present with other mutations or amplifications.

Table 45. Summary of PFS, OS of patients with *FGFR1* status detected in FFPE/ctDNA.

FGFR1 ctDNA/FFPE	Total number	PFS					OS				
		median PFS	HR	95% CI lower	95% CI upper	p value	median OS	HR	95% CI lower	95% CI upper	p value
Amp	13	3.0	1.89	0.97	3.66	0.055	15.5	2.12	0.76	5.91	0.14
Non-amp	35	4.8					17.6				

PFS -Progression-free survival, OS – Overall Survival, HR – Hazard Ratio, CI – Confidence Interval, *FGFR1* amp – amplification, *FGFR1* non- amp - non-amplified

Figure 48. Kaplan-Meier Curves presenting PFS and OS by *FGFR1* status in ctDNA and/or FFPE DNA.

Progression free survival by FGFR1 status in FFPE/ctDNA

Overall survival by FGFR1 ststus in FFPE/ctDNA
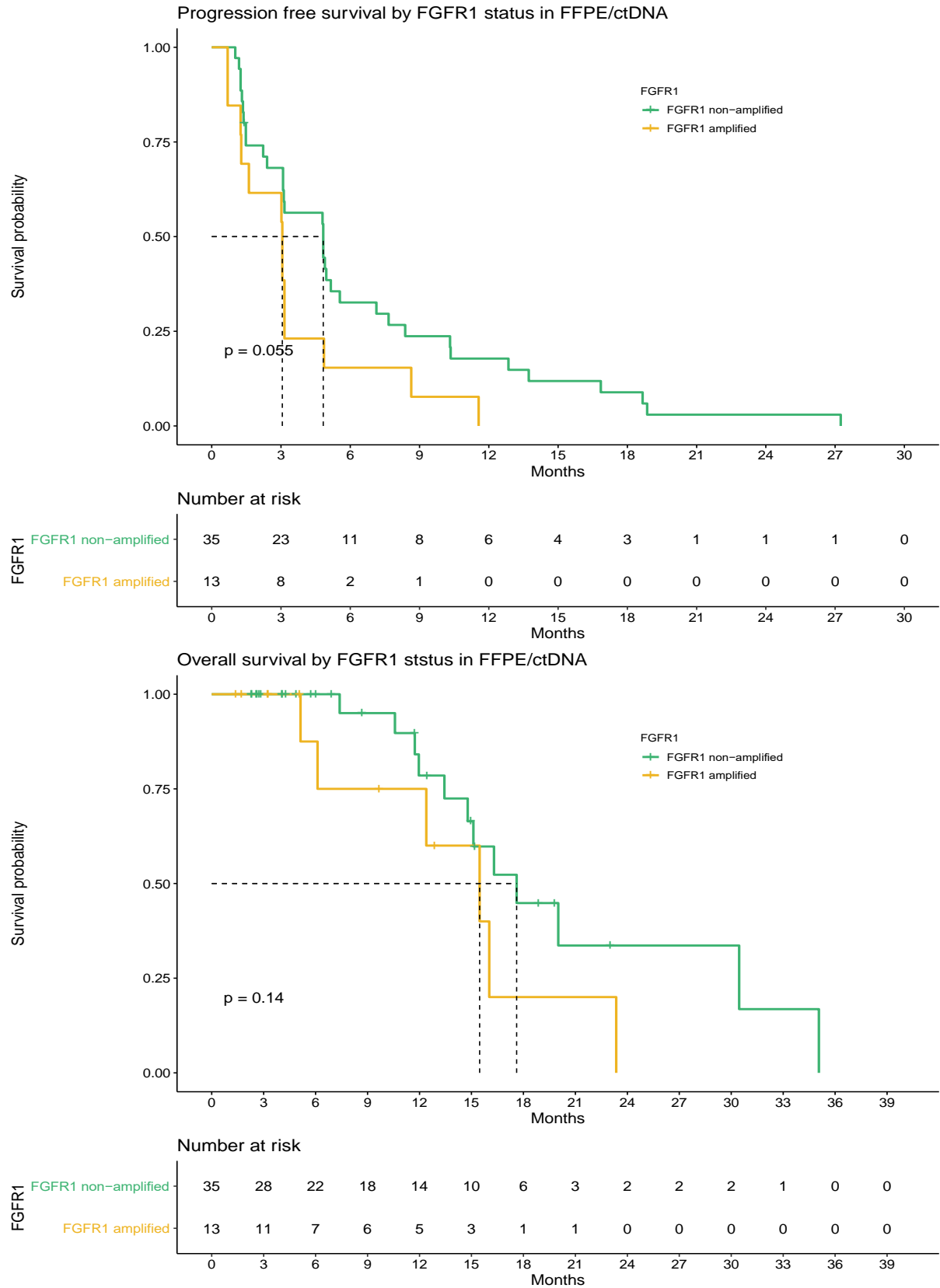
6.4. MYC and FGFR1 Status Versus Treatment Arms

Objective: Can MYC and FGFR1 amplification influence treatment response to fulvestrant and the combination of fulvestrant and capivasertib? Which amplification is more critical in response to treatment?

In this cohort of 55 patients, 20 patients received combination therapy of fulvestrant and capivasertib, and 35 have received fulvestrant only. *MYC* and *FGFR1* status were defined as detection of amplification in ctDNA or FFPE DNA samples. PFS in each treatment group, according to *MYC* and *FGFR1* status, is presented in Table 46.

Table 46. Median PFS for both treatments in the FAKTION trial as per *MYC* and *FGFR1* status (FFPE/ctDNA).

Treatment	Amp status ctDNA/FFPE	Patients	PFS					
MYC			median PFS	Range PFS	HR	95% CI lower	95% CI upper	p value
FUL + CAPi	Amp	5	1.31	0.7 -5.8	2.94	0.92	9.38	0.053
	Non-amp	12	4.83	1.2 -27.0				
FUL	Amp	12	3.04	1.3 -7.6	2.04	0.94	4.41	0.061
	Non-amp	21	4.8	1.0 - 8.9				
FGFR1								
FUL + CAPi	Amp	3	0.7	0.7 - 3.1	5.13	1.20	22.28	0.01
	Non-amp	14	4.8	1.2 - 27.2				
FUL	Amp	10	3.1	1.3 - 11.6	1.41	0.645	3.07	0.38
	Non-amp	21	4.8	1.0 - 18.9				

FUL – fulvestrant, CAPi – Capivasertib (AKT inhibitor), Amp – Amplification, No – number, HR Hazard Ratio, PFS – Progression-Free Survival.

6.4.1 Patients Treated with Fulvestrant and Capivasertib

Objective: Can MYC and FGFR1 amplification influence treatment response to the combination of fulvestrant and capivasertib?

In the group of 20 patients who received the combination of fulvestrant and capivasertib. 5 patients were found to have *MYC* amplification, including 3 patients with concordant MYC amplification and 2 patients with MYC amplification only detected in ctDNA. In addition, 3 of these 5 patients also had *FGFR1* amplification, Table 47. 3 patients had inconclusive results and were excluded from the analysis.

Table 47. HER2, *MYC*, *FGFR1* amplification detection in FFPE DNA and cfDNA in patients treated with fulvestrant + capivasertib.

ID	FFPE			ctDNA			PFS	Response
	HER2	MYC	FGFR1	HER2	MYC	FGFR1		
16		NT					1.4	Bad
17							1.3	Bad
35							0.7	Bad
108							0.7	Bad
148		NT	NT				1.5	Bad
156		NT					1.2	Bad
57		NT	NT				4.9	Medium
104		NT	NT	UN			4.8	Medium
135		NT	NT				3.1	Medium
143		NT					5.0	Medium
144		NT	NT				3.2	Medium
150		NT	NT				4.8	Medium
151					UN		3.2	Medium
166			NT				6.6	Medium
2		NT	NT				10.3	Good
9		UN					27.2	Good
10		NT	UN				27.0	Good
42					UN	UN	10.5	Good
86		NT					12.8	Good
97		NT	NT				13.7	Good

Dark colours – Amplified, Light colour – Non-amplified. UN – Unknown –inconclusive result. CN – Copy number, NT – Not Tested, ID - Patient ID, PFS – Progression-Free Survival (months), F - Fulvestrant, F + A – Fulvestrant + Capivasertib.

In the bad responders' group, whose PFS was below 3 months, 3 (50%) of 6 patients had concordant *MYC* amplification confirmed in ctDNA and FFPE DNA, Table 47. In addition, **patient 35** had concordant *FGFR1* amplification, and **patient 108** had FGFR1 amplification detected in ctDNA only. These three patients had a poor median PFS of 0.7 months (range 0.7-1.3).

In the medium responders' group, whose PFS ranged between 3 – 9 months: 2 of 8 (25%) patients were found to have *MYC* amplification in FFPE DNA only. One of these patients also had concordant *FGFR1* amplification in both FFPE DNA and ctDNA samples.

Interestingly, in the good responders' group, whose PFS was over 9 months, there were no patients with *MYC* or *FGFR1* amplification detected in ctDNA, and all of them had good PFS of 13.3 months (range 10.3-27.2), Table 47.

The median PFS for 5 *MYC* amplified patients was 1.3 month (0.7 – 6.6) and for 3 *FGFR1* amplified patients was 0.7 months (0.7-3.2) compared to PFS of 4.9 months (1.2-27.0) in the non-amplified group, HR =2.939 (95% CI 0.92 – 9.38), p=0.053. There was 3.6 months difference in PFS (p=0.053) for patients with *MYC* amplification and a bigger PFS difference of 4.2 months(p=0.012) for patients with *FGFR1* amplification, considered separately. However, it is difficult to identify which of the two amplifications contribute to worse PFS in patients with co-existing amplifications.

MYC and FGFR1 amplification were mainly found in bad and medium responders to combination therapy, which could negatively influence treatment response.

6.4.2 Patients Treated with Fulvestrant

Objective: Can MYC and FGFR1 amplification influence treatment response to fulvestrant?

In the 35 patients treated with fulvestrant only, 12 patients had *MYC* amplification detected, and 10 patients had *FGFR1* amplification, Table 48. 6 patients with inconclusive results either in *MYC* or *FGFR1* group were excluded from the analysis.

Table 48. HER2, *MYC*, *FGFR1* amplification detection in FFPE DNA and cfDNA in patients treated with fulvestrant.

ID	FFPE			ctDNA			PFS	Response
	HER2	*MYC*	*FGFR1*	HER2	*MYC*	*FGFR1*		
11		UN	UN				1.6	Bad
31		NT					2.4	Bad
53							1.3	Bad
60		UN	UN				1.8	Bad
66		NT	NT				2.2	Bad
73							1.2	Bad
85							1.3	Bad
121		UN	UN				1.2	Bad
125		NT					1.0	Bad
134		NT	NT				1.2	Bad
141		NT	NT				1.4	Bad
147							1.2	Bad
154							1.5	Bad
18					UN		4.9	Medium
26		NT					4.8	Medium
33		UN					3.2	Medium
39			NT				7.7	Medium
52		NT	NT				3.1	Medium
67		NT	NT				5.6	Medium
82					UN		5.2	Medium
92		NT	NT				7.1	Medium
103		NT	NT				3.1	Medium
109			UN				3.0	Medium
118						UN	8.6	Medium
127		NT					3.1	Medium
139		NT					4.8	Medium
142							8.4	Medium
175							3.1	Medium
119		NT	NT			UN	4.4	Medium
1		NT	UN				10.4	Good
13		NT	NT				18.9	Good
41		NT	NT				18.7	Good
78		NT	NT				10.3	Good
116		NT					11.6	Good
6		NT	NT				16.9	Good

Dark colours – Amplified, Light colour – Non-amplified. UN – Unknown –inconclusive result. CN – Copy number, NT – Not Tested, ID - Patient ID, PFS – Progression-Free Survival, F - fulvestrant, F + A – fulvestrant + capivasertib.

In the bad responders' group, 5 (38.5%) of 13patients had *MYC* amplification detected in either of

FFPE DNA or ctDNA samples, Table 48. 4 of 5 patients had co-existing amplifications: 3 patients with

FGFR1 amplification in ctDNA and one patient with *HER2* amplification in both ctDNA and FFPE DNA. The median PFS of these 5 patients was very poor of 1.3 months.

In medium responders, 7 of 16 (44.8%) patients had *MYC* amplification, and 6 (37.5%) of 16 patients had *FGFR1* amplification, Table 48. 5 patients had *FGFR1* amplification co-existed with *MYC* amplification. The median PFS for these patients in this group was 4.0 months.

In the good responders' group, we can note that there were no patients with *MYC* amplification, and only one patient had *FGFR1* amplification detected in a tissue but not in the end of treatment ctDNA sample and therefore difficult to predict how significant *FGFR1* amplification was in tissue in the primary tumour. It might not have been relevant in the metastatic setting. Patients in this group had an excellent response to fulvestrant with a median PFS of 14.2 months (range 10.4-18.9).

A similar pattern to the previous group can be noticed in the patient group that *MYC* and *FGFR1* amplifications were mainly present in bad and medium responders. It was challenging to establish which amplification plays the most crucial role in the poor response group. However, *MYC* and *FGFR1* amplifications seem to co-exist in both groups.

6.4.3 Discussion

This section shows that the detection of *MYC* and *FGFR1* amplification can influence both treatments' responses: fulvestrant and fulvestrant with capivasertib. *FGFR1* amplification seems to co-exist with *MYC* amplification. In this study, it is difficult to identify which one is more important or whether the presence of both can cause a worse clinical outcome than one amplification. However, this study shows that fulvestrant on its own and with capivasertib cannot effectively overcome endocrine resistance and inhibit PI3K/AKT1 pathway in patients with *MYC* or/and *FGFR1* amplification.

This raises the question of whether patients with *MYC* amplification with or without *FGFR1* amplification should receive endocrine treatment with fulvestrant or in combination with capivasertib. The trial needs to identify patients who will benefit from new therapy and identify patients who might not respond. There have been suggestions that targeting *MYC*-regulated pathways combined with inhibitors of other oncogenic pathways, such as ER/PR, HER2 and PI3K/AKT1 pathways, could provide a promising therapeutic strategy for breast cancer (Xu et al. 2010).

This shows how important is the identification of multiple mutations and their clinical importance. Analysing of series of relevant biomarkers could help create a better selection system for patients for future trials and treatments. Previous trials with *FGFR1* targeted therapy failed to identify a biomarker that will select patients. The reason for this could have been that the main focus was on the detection of *FGFR1* amplification, but *MYC* or other genes were not assessed. This will need to be addressed in future trials with targeted therapy.

6.5. Combined Data of CNVs and SNVs of 55 Patients.

6.5.1 Patient with Detected CNVs and SNVs

Objective: How can the detection of CNVs and SNVs in ctDNA and FFPE DNA influence response to treatments in the FAKTION trial?

In the previous section of this chapter, I presented copy number variation of HER2, *MYC*, *FGFR1* genes data for 55 patients found in the end of treatment ctDNA samples and part of the matched baseline FFPE samples using ddPCR. In this section, I added *PIK3CA* data collected as part of the FAKTION trial. All the 55 patients had *PIK3CA* tested for mutations in exon 9 (p.E542K, p.E542K) and exon 20 (p.E542K, p.H1047L) in baseline FFPE and ctDNA samples. In addition, there was also available data from baseline (FFPE and ctDNA) and longitudinal samples (ctDNA) for 8 patients from chapter 4.

Table 49 shows a summary of mutations detection in 6 genes (CNV - *MYC*, *FGFR1*, HER2, SNV- *PIK3CA*, *ESR1*, *TP53*) in ctDNA at any time and in FFPE DNA for each patient. The data is not complete, as not all the patients were tested for TP53 and ESR1 mutations. These have been marked in the table as not tested. Despite incomplete data, we can see an exploratory pattern that could be evaluated in future projects.

Table 49. Combined data for 55 patients divided by treatment and response type.

ID	FFPE						ctDNA						PFS	Response	Treatment arm
	HER2	MYC	FGFR1	PIK3CA	TP53	ESR1	HER2	MYC	FGFR1	PIK3CA	TP53	ESR1			
16		NT			NT	NT					NT	NT	1.4	Bad	F+ A
17													1.3	Bad	F+ A
35													0.7	Bad	F+ A
108													0.7	Bad	F+ A
148		NT	NT		NT	NT					NT	NT	1.5	Bad	F+ A
156		NT			NT	NT				UN	NT	NT	1.2	Bad	F+ A
57		NT	NT										4.9	Medium	F+ A
104		NT	NT					UN					4.8	Medium	F+ A
135		NT	NT										3.1	Medium	F+ A
143		NT			NT	NT					NT	NT	5.0	Medium	F+ A
144		NT	NT		NT	NT					NT	NT	3.2	Medium	F+ A
150		NT	NT	NA	NT	NT					NT	NT	4.8	Medium	F+ A
151					NT	NT		UN			NT		3.2	Medium	F+ A
166			NT		NT	NT					NT		6.6	Medium	F+ A
2		NT	NT		NT	NT					NT	NT	10.3	Good	F+ A
9	UN				NT	NT					NT		27.2	Good	F+ A
10		NT	UN		NT	NT					NT	NT	27.0	Good	F+ A
42							UN	UN					10.5	Good	F+ A
86		NT			NT	NT					NT	NT	12.8	Good	F+ A
97		NT	NT	NA	NT	NT					NT	NT	13.7	Good	F+ A
11		UN	UN		NT	NT					NT		1.6	Bad	F
31		NT			NT	NT					NT	NT	2.4	Bad	F
53					NT	NT					NT		1.3	Bad	F
60		UN	UN		NT	NT					NT		1.8	Bad	F
66		NT	NT		NT	NT					NT	NT	2.2	Bad	F
73					NT	NT					NT		1.2	Bad	F
85					NT	NT					NT		1.3	Bad	F
121		UN	UN		NT	NT					NT		1.2	Bad	F
125		NT			NT	NT					NT	NT	1.0	Bad	F
134		NT	NT	NA	NT	NT					NT	NT	1.2	Bad	F
141		NT	NT		NT	NT					NT	NT	1.4	Bad	F
147					NT	NT					NT		1.2	Bad	F
154					NT	NT					NT		1.5	Bad	F
18					NT	NT		UN			NT		4.9	Medium	F
26		NT		UN	NT	NT					NT	NT	4.8	Medium	F
33	UN				NT	NT					NT		3.2	Medium	F
39			NT		NT	NT					NT		7.7	Medium	F
52		NT	NT	NA	NT	NT					NT	NT	3.1	Medium	F
67		NT	NT		NT	NT					NT	NT	5.6	Medium	F
82					NT	NT		UN			NT		5.2	Medium	F
92		NT	NT		NT	NT					NT	NT	7.1	Medium	F
103		NT	NT		NT	NT					NT	NT	3.1	Medium	F
109			UN		NT	NT					NT		3.0	Medium	F
118					NT	NT				UN	NT		8.6	Medium	F
127		NT			NT	NT					NT	NT	3.1	Medium	F
139		NT			NT	NT					NT	NT	4.8	Medium	F
142					NT	NT					NT		8.4	Medium	F
175					NT	NT					NT		3.1	Medium	F
119		NT	NT	NA	NT	NT				UN	NT		4.4	Medium	F
1		NT	UN		NT	NT					NT	NT	10.4	Good	F
13		NT	NT		NT	NT					NT	NT	18.9	Good	F
41		NT	NT		NT	NT					NT	NT	18.7	Good	F
78		NT	NT		NT	NT					NT	NT	10.3	Good	F
116		NT			NT	NT					NT	NT	11.6	Good	F
6		NT	NT		NT	NT					NT	NT	16.9	Good	F
Method	IHC +/- FISH, ddPCR	ddPCR	ddPCR	ddPCR, NGS	NGS	ddPCR, NGS	ddPCR	ddPCR	ddPCR	ddPCR, NGS	NGS	ddPCR, NGS	X	X	X

The dark colours of each column demonstrate positive mutations. Lighter colours represent negative mutations. ID – Patient ID, NT – not tested, UN - unknown despite testing, NA - sample not available, F – Fulvestrant, F+A – Fulvestrant and AKT1 inhibitor, NGS – Next Generation Sequencing, ddPCR- digital droplet PCR.

Figure 49. All available mutations data in patients by response type.
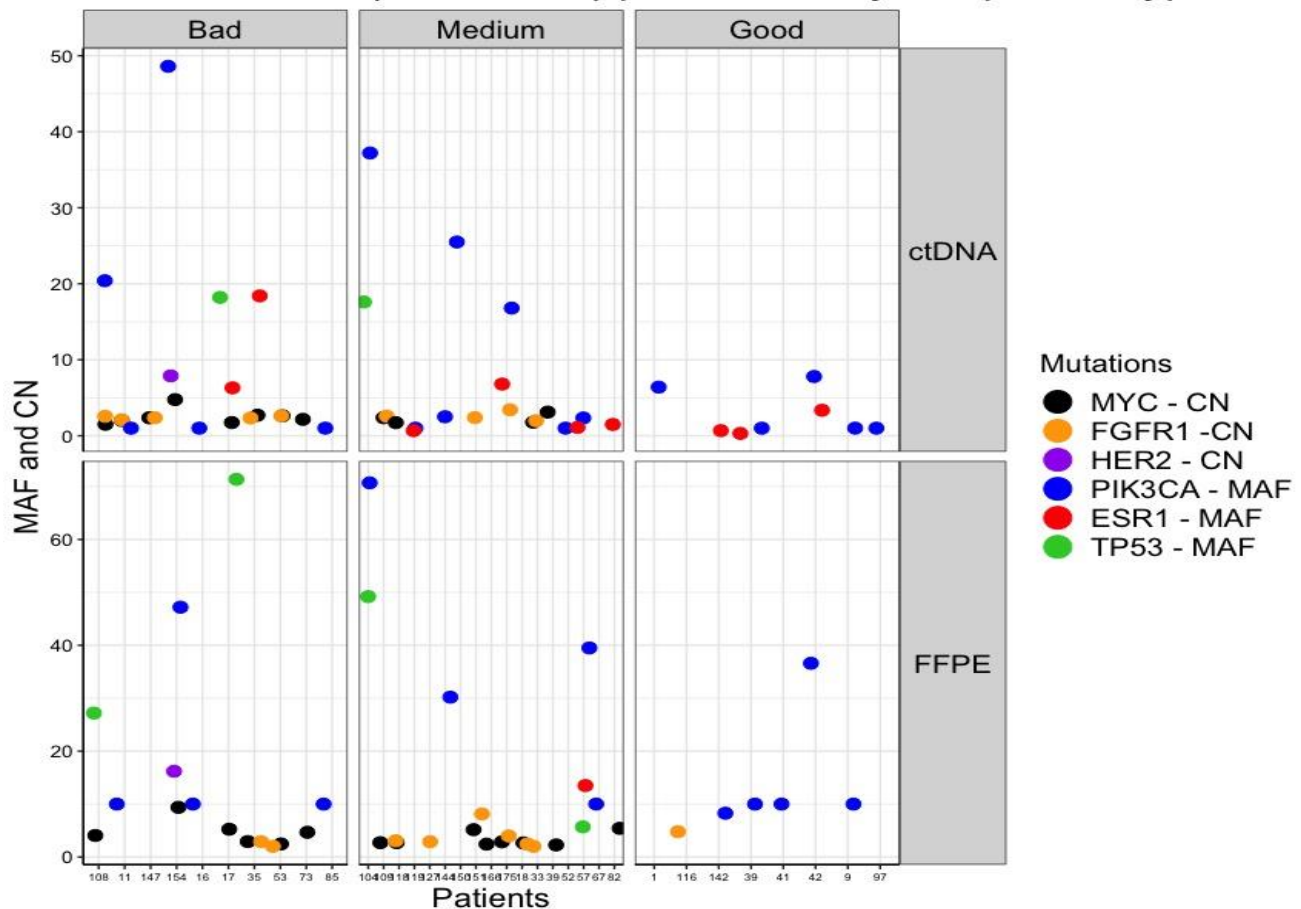
MAF – Mutant Allele frequency (%), CN - Copy Number. Response by PFS – good (>9 months), medium (3-9 months), bad (<3 months).

In Table 49 and Figure 49, I aimed to show the magnitude of all mutations, SNVs are presented by mutant allele frequency (MAF), and CNVs are presented by a number of copies (CN). A similar pattern as in chapter 4 can be noticed. In good responders, there were fewer mutations than in medium and poor responders. *TP53* mutations, *MYC* and *FGFR1* amplifications were present mainly in the bad and medium responders. In the good responders' group, mostly *PIK3CA* and *ESR1* mutations were detected, and the MAF in ctDNA were lower than medium and bad responders. This could suggest that cancers with multiple genetic modifications could be resistant to both treatments, or the response to treatment could be short-lived as medium responders in this project achieved a median PFS of 4.8 months (with the longest 8.4 months) in both treatments' arms. The presence of *MYC* amplification can predict resistance to PI3K inhibitors (Dey et al. 2015), and this could apply to AKT inhibitors but needs more evidence. *MYC*, *FGFR1* and *TP53* alterations could contribute to the limited response to treatment.

Patient 154, with *HER2* amplification detected in tissue and ctDNA, was also found to have *MYC* amplification and *PIK3CA* mutation in both samples, Table 49. Detection of multiple mutations, *HER2* and *MYC* amplification and *PIK3CA* mutation could suggest heterogeneous disease with multiple cancer pathways activated and, therefore, potentially more aggressive disease. This could potentially explain why the patient did not respond to the fulvestrant, Table 49.

This section showed that point mutations in the *TP53* gene and amplification of HER2, *MYC* and *FGFR1* genes were mainly present in bad and medium responders in both treatment groups in the FAKTION trial. However, point mutations mainly in *PIK3CA* and *ESR1* genes were detected in the good responders' group with no additional mutations. In addition, the MAF of these mutations in ctDNA appeared to be lower compared to the medium and bad responders group.

6.5.2 Patients with No Mutations Detected

Objective: What were the clinical outcomes for patients with no mutations detected in this project? Did the number of mutations influence PFS?

In Figure 49, I showed mutational data for patients with at least one detected mutation in both treatment groups. However, 21 (38%) of 55 patients had no mutations detected. In Table 50, I present patients with no mutations and with at least one mutation and their clinical responses to both treatments based on PFS.

Table 50. Patients with no mutations versus patients with at least one mutation found, divided by treatment group and response type.

Mutation presence in any sample	Treatment	total number of patients	Response		
			bad	medium	good
No mutation	F+A	7(13%)	2	2	3
	F	14(25%)	7	4	3
	Total	21(38%)	9(43%)	6(28.5%)	6(28.5%)
>=1 mutation	F+A	13(24%)	4	6	3
	F	21(38%)	6	12	3
	Total	34(62%)	10(29%)	18(53%)	6(18%)

F – Fulvestrant, F+A – Fulvestrant and Capivasertib, Response by PFS – good(> 9 months), medium(3-9 months), bad(< 3 months).

Median PFS for patients with no mutations was 3.1 months and 3.8 months for patients with at least one mutation present in any sample. No statistical difference in PFS (p=0.89) was found when comparing two groups, Figure 50. This statement is limited by small numbers of patients and incomplete data as not all mutations were tested for all participants. Nevertheless, investigating this group of patients is essential as potential other molecular pathways involved were not explored in this project.

This section showed that 57% of patients with no detected mutations responded to both treatments, and 43% failed to respond. Therefore, it is important to characterise this patient group molecularly and explain why some patients responded and others did not.

Figure 50. PFS assessment between two patients groups with Kaplan-Meier Survival Curves.

Kaplan−Meier Survival Curves by Number of mutations detected in both samples(FFPE and ctDNA)
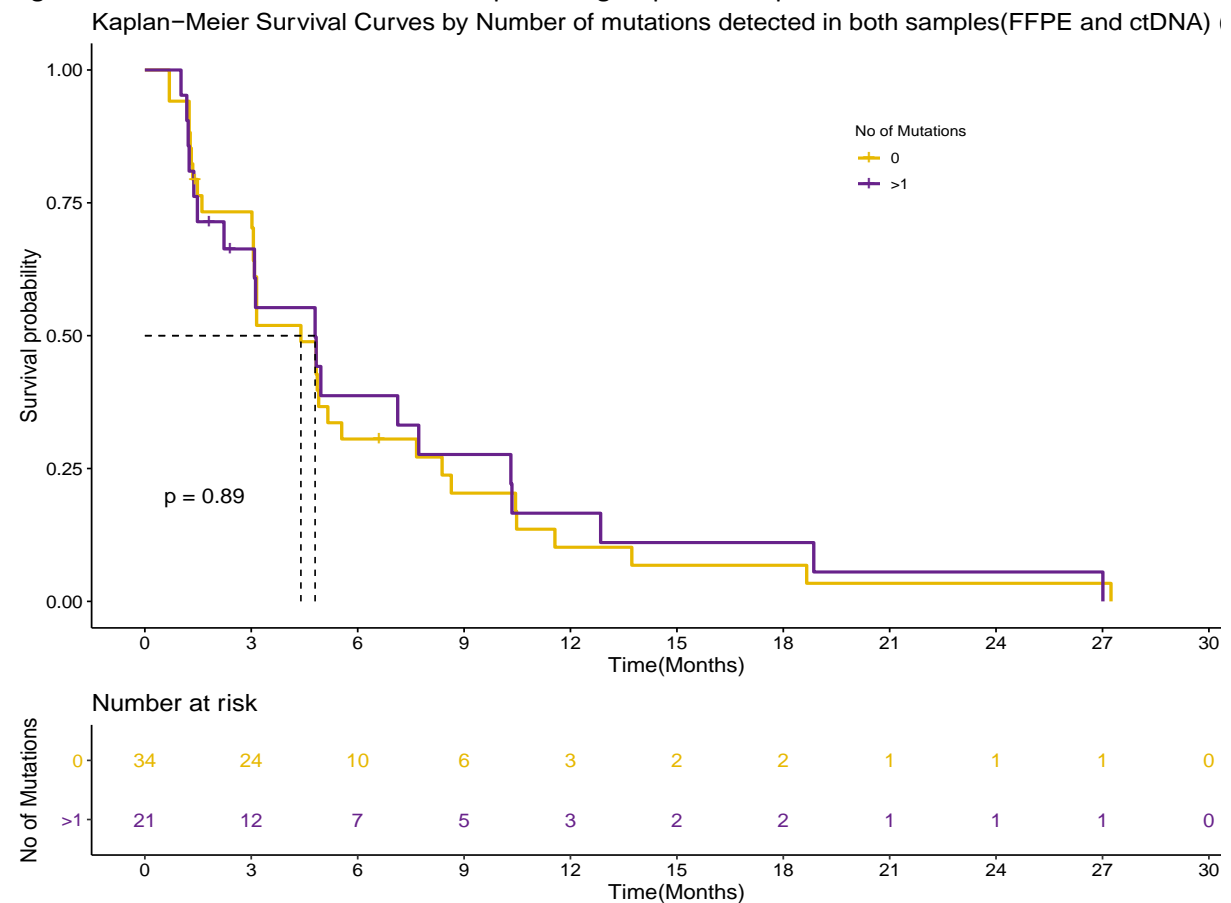
6.5.3 Discussion

In this section, I showed that combined data of SNVs and CNVs offers valuable information about the genetic profile of endocrine-resistant breast cancer. In the FAKTION trial, investigators assessed *PIK3CA* mutations and correlated with response to capivasertib, but unfortunately, no association was found (Jones et al. 2020). Assessment of one biomarker in the trial setting might be misleading. The co-existing biomarkers could influence the trial results. Multiple genetic alterations carry prognostic and predictive information. The additional information about mutations in *TP53*, *MYC*, HER2, *FGFR1* gene presence could explain why some patients had not responded or had a minimal benefit from therapy. The information about multiple mutations can be essential information for clinicians. The patient could be monitored closely as the response to treatment might be short-lived.

In the FAKTION trial, combination therapy aimed to block the oestrogen receptor and PI3K/AKT pathway. This can be a very effective treatment for ER-positive tumours with an activated PI3K/AKT pathway. However, how effective can this treatment be if not only the PI3K/AKT pathway is active? Can the presence of other mutations influence response to treatment and survival? If so, should standard treatment like chemotherapy be considered rather than targeted therapy until better therapy is available? There is currently no tool available to tell clinicians which patient will respond to treatment and what would be the duration of response. The most relevant biomarkers could be examined to predict treatment response in future studies to enable select patients with better precision for clinical trials and future clinical practice.

Patients with no mutations detected require further investigations for other biomarkers, which could help us identify these patients and offer them more effective treatment. In the next step, it would be essential to perform comprehensive genetic profiling of these tumours. There could be other molecular mechanisms involved in treatment resistance; for example non – coding RNAs (ncRNAs) had been described as an important regulator of the PI3K/AKT pathway (Dong et al. 2014; Benetatos et al. 2017). The ncRNAs could directly or indirectly target multiple pathway components (PI3K, AKT, PTEN, mTOR). The endocrine resistance is multifactorial and complex. There are more resistance mechanisms than has been described so far in the literature and therefore need to be discovered. Future studies would need to improve the characterisation of resistant breast cancer and optimise samples collections and methods. Testing other circulating or tissue biomarkers could help us identify

other resistance mechanisms. New biomarkers would need to be further evaluated in phase II and III trials.

7 General Discussion: The Translational Use of Circulating Tumour DNA

Endocrine-resistant breast cancer has been the focus of this thesis. Despite the improvement in breast cancer treatments, many patients still experience resistance to therapy and die of metastatic breast cancer. There is an urgent need for developing biomarkers for breast cancer, for use in clinical trials and clinical practice. These biomarkers would help patient stratification to different anti-cancer therapies, detection of early response or resistance to treatment and response monitoring.

Circulating tumour DNA has been extensively studied in multiple clinical trials across multiple tumour sites to detect specific biomarkers and monitor patient response to therapy. Over the last decade, there has been a significant improvement in testing DNA with new genetic technologies, such as next-generation sequencing and droplet digital PCR. This thesis applied these methods to tumour tissue samples and ctDNA samples from patients with endocrine-resistant breast cancer from the FAKTION trial.

7.1 Summary of Key Findings

In chapter 4, the 44-gene breast cancer NGS panel successfully identified mutations in baseline breast cancer tissue DNA and ctDNA. Mutations found in *PIK3CA*, AKT and *PTEN* genes were mainly detected in primary tumours. In contrast, *ESR1* mutations were found mainly in ctDNA, which suggests acquired endocrine resistance, consistent with the literature. Interestingly, *ESR1* mutations could appear and persist through treatment with aromatase inhibitors, tamoxifen and fulvestrant.

Mutations found in the *TP53* gene, although not directly associated with endocrine resistance, were evaluated in this project from the prognostic point of view. Most patients with *TP53* mutation also had concomitant *ESR1*, *PIK3CA* or *PTEN* mutations. Only one patient had a single *TP53* mutation detected. The *TP53* mutation concordance between tissue DNA and ctDNA samples was high compared to other mutations. *TP53* mutations are most frequent in breast cancer (15–71%) (Pharoah et al. 1999; Hill and Sommer 2002), with aggressive phenotypes (high histological grade, large size, lymph node metastasis and low hormone receptor expression) and in patients <60 years old (Olivier et al. 2006). In this project, patients with *TP53* mutations were younger patients, compared to the rest

of the patients (median age 56 versus 65 years) and had noticeably more aggressive disease with multiple metastatic sites. Although *TP53* is more common in triple-negative breast cancers, it can still be present in oestrogen-positive breast cancer, as described in this study. The high burden tumours would shed more ctDNA into the bloodstream, and mutations more likely to be detected in ctDNA samples. Also, tracking mutations in longitudinal samples could potentially be more successful.

In this chapter, I have also attempted to explain the reasons for discordant *PIK3CA* mutation detection. The discordance could be influenced by biological reason of tumour evolution, clinical reasons such as multiple endocrine treatments received over a long period, the disease's burden, and technical reasons like inadequate sample collection, failure of the method and data analysis.

In chapter 5, I detected mutations in baseline FFPE and ctDNA samples. I monitored them in sequential ctDNA samples in patients with breast cancer who received fulvestrant and capivasertib. Patients were divided into three groups (bad, medium, good responders) based on PFS as a response to combination therapy. Most mutations were trackable in ctDNA and followed the expected pattern of response. However, in some patients, the detected baseline mutations could not be monitored. There could be many possible reasons, including technical issues with sample handling or method errors.

Also, in the good responders' group, mutations found in *PIK3CA*, *AKT1*, *PTEN* or *ESR1* genes were at lower frequencies than bad and medium responders. Furthermore, GATA3 mutations were only found in the good responders' group and not in other groups. In contrast, *TP53* mutations were mainly detected in bad and medium responders. Noticeably, patients with *TP53* detected in baseline ctDNA could be easily tracked in sequential samples. These patients had no response or a very short response to the combination of fulvestrant and capivasertib.

In chapter 6, I have demonstrated that HER2, *FGFR1*, *MYC* amplification, which plays a role in endocrine resistance in breast cancer patients (Rani et al. 2019), can be detected in ctDNA. *HER2* amplification was found in ctDNA and primary FFPE DNA of one patient in the FAKTION trial who was expected to be *HER2* negative from the initial IHC report. Although the transition from non-amplified *HER2* to amplified *HER2* can occur in 6-9% (Regitnig et al. 2004; Lower et al. 2009), it was not demonstrated in the study. *MYC* and *FGFR1* amplification were mainly found in the ctDNA samples in the bad and medium responders groups, regardless of the trial's treatment. In addition, *FGFR1* amplification was commonly present with *MYC* amplification. This project showed that patients with

these amplifications might not respond or have a short response to fulvestrant with or without capivasertib. This raises the question of whether broader detection of prognostic biomarkers prior to commencing treatment could improve patient selection for trials and treatment in the future.

7.2 Implementation of Genetic Testing in Clinical Trials and Clinical Practice

7.2.1 Benefits and Limitations of Sequential ctDNA Samples Testing

This thesis has shown that multiple mutations can be detected in tissue DNA and ctDNA using NGS and ddPCR techniques. Sequential ctDNA samples can be taken in 'real-time' as the patients undergo anti-cancer therapy, which allows tracking of the mutations detected in baseline samples. Mutant allele frequency of the mutations can change over time, depending on the treatment response. In patients with good response to therapy, decreased MAF or undetectable mutation would be expected in longitudinal samples compared to baseline samples. In patients with poor response, stable or increase in MAF would be anticipated. This would allow detecting early response to treatment, reassuring clinicians and patients that the treatment is working and worth continuing. The detection of early progression would allow for early discontinuation of ineffective treatment and prevent patients from toxicities. There is a strong clinical need to have early response biomarkers, which would help inform clinicians of early response before the radiological or clinical response.

In addition, after initial response to treatment, sequential sampling can help detect disease progression of the disease when MAF of tracked mutations is starting to rise or by detecting new resistant mutations. This could allow clinicians to decide about changing the treatment early before clinical progression. Also, testing samples at clinical progression allows detecting known resistant mutations and discovering new resistant mutations. New resistant mutations can be further studied and help the pharmaceutical industry work on new, more effective drugs. This has been a successful strategy for EGFR inhibitors in EGFR positive lung cancers. A newer generation of anti-EGFR therapy has improved and has become more effective in patients with acquired resistant T790M EGFR mutations.

However, even though ctDNA can be a promising biomarker and could offer better disease monitoring than radiological or clinical monitoring, it has not been widely used in current clinical practice for disease monitoring. I have demonstrated in chapter 5 that the molecular patterns were not always

followed as expected in the three response groups presented. Lack of consistency creates uncertainty and could be the main barrier that ctDNA as a response biomarker has not been introduced to clinical practice. In this project, I could not identify the specific reasons why the expected pattern was not followed. However, multiple gene testing and using more than one method could help identify potential technical reasons. For example, patient 122 in chapter 5, who had three mutations (*PIK3CA*, *ESR1* and *CDH1*) detected in baseline samples, had no mutations detected in the end of treatment sample collected at the time of disease progression. These samples were tested with two techniques, NGS and ddPCR. The expectation was to detect at least one of the mutations with one of the methods in the end of treatment ctDNA sample. This could suggest that the sample's quality was low due to inadequate sample handling or issues with the testing assay. Handling, processing samples and validation and Quality Control/Quality Assurance of assays, can be a real issue, and mistakes can be repeated and not be identified if only one method used and only one mutation is tested. The results could be wrongly interpreted as a good molecular response to treatment as tracking mutation become undetectable. Testing sequential samples with gene panels and possibly using two mutation detection techniques and close correlation with the clinical response could help resolve technical issues and be validated in future clinical trials. Once the process is optimised and standardised, it could be used with confidence in clinical practice.

7.2.2 Role of ctDNA in the Detection of Copy Number Variations

CtDNA samples can be a useful biomarker in detecting single point mutations and other mutations such as copy number variation. *HER2* amplification in breast cancer has not only revolutionised the treatment for breast cancer but has added important information about the prognosis of breast cancers compared to *HER2* non-amplified breast cancers. Also, recent studies have shown that *HER2* can play a role in endocrine resistance (Shou et al. 2004). *HER2* amplification is identified in current practice, mainly in tissue. Despite multiple studies, including this one, have shown that it is possible to detect *HER2* amplification in ctDNA, this test has not been used in clinical practice. With more validation and standardisation of the *HER2* testing in ctDNA, this could find utility in diagnostics where patients who are too unwell for biopsy or any other reason cannot undergo tissue biopsy. *HER2* amplification identified in ctDNA could offer a patient an opportunity to receive anti-*HER2* therapy, which would otherwise not be possible without testing.

In addition, I have also demonstrated in Chapter 6 that other amplifications can be detected in ctDNA, such as *MYC* and *FGFR1* amplifications. These amplifications can have a significant impact on prognosis and response to new endocrine treatment with targeted therapy. It has been shown in previous studies that amplification can appear over time as an effect of resistance to chemotherapy (Thomas C. King 2007). MET amplification was also found to play a role in resistance to EGFR therapy in EGFR-mutated lung cancer (Turke et al. 2010) and *MYC* amplifications in ALK-translocated lung cancer (Rihawi et al. 2019). Therefore, it would be valid to monitor amplifications that play a prognostic and predictive role in the new treatments in breast cancer.

CtDNA could be used for the detection of multiple amplifications and their monitoring. Also, ctDNA could help to detect new resistant amplifications. Multiple gene amplification testing could be added to biomarker testing, allowing patients selection for new treatments with higher precision in clinical trials. However, this would require further investigations, validation and standardisation within clinical trials to become a valid test in clinical practice in the future.

7.2.3 Challenges of Using ctDNA in Clinical Trials and Practise

CtDNA can be a valuable source of genetic information and can help in molecular profiling of the tumour at multiple cancer progression stages. ctDNA is more likely to represent the entire tumour's genetic profile as it is shed to the bloodstream from multiple cancer metastatic lesions, compared to tissue biopsy, which is from the small part of the primary or metastatic lesion. Also, a small biopsy is a snapshot of the tumour but does not necessarily represent the entire metastatic disease's genetic profile. CtDNA seems a very promising biomarker to support personalised cancer therapy. However, there are limitations in analytical sensitivity due to low concentrations of ctDNA in plasma samples, technical aspects, and clinical factors. The validation of ctDNA in clinical trials can be challenging due to clinical and technical reasons.

Before clinical trial treatment, many cancer patients undergo multiple treatments such as surgery, radiotherapy, chemotherapy, and hormonal therapy. Multiple treatments, particularly previous chemotherapy, can affect patients' veins. In phase I and II clinical trials, patients have more often blood tests than in standard practice, which is necessary to ensure the new drugs' safety. Therefore, a translational research blood test might not be a priority for the clinical staff. Also, clinical staff might find difficulty obtaining a blood sample when taken so often, and patients could have damaged veins.

Some patients might have refused a blood test. All trials will have protocols provided to all participating centres to inform medical and nursing staff how the ctDNA samples should be taken and processed. However, samples still can be missed or taken incorrectly. Repeating sampling could be challenging within a trial. Highly specialised trial centres can be localised far from patients' houses, and therefore repeating the research sample might not be possible.

The handling of the sample may affect the quality of the DNA. The specific tubes (Streck tubes) were provided for ctDNA collection in the FAKTION trial. For example, specific instructions were given on how many times the tube needs to be rotated before sending to the laboratory. This procedure could potentially be missed as this is not a routine procedure with other blood tests. Many minor mistakes can happen on the way between sample collection before arriving at the laboratory. Wrongly handled samples could affect detecting ctDNA as this carries the risk of wild type DNA being realised from white cells. Testing a low-quality sample can confuse the result and interpretation with clinical findings.

Collection of blood in Streck tubes allowed 96 hours for the samples to reach the laboratory. Unfortunately, some samples arrived after that time. These samples needed repeating, but this required arranging for the patient another appointment, and sometimes this could occur during the following visit for the next cycle of treatment. This blood sample would be taken at a different time of ongoing treatment. In the FAKTION trial, 8-week samples, which should have been taken on day 1 of cycle 3 of treatment, arrived at different times, at 2- or 4-months. CT scans assessing clinical response were performed between 2-3 months. In this situation, the correlation of detecting early response before a clinical response can be impossible. In phase III trials, the challenges can be even more prominent, and they must be considered and addressed to find a way of improving sample collections in clinical trials.

Despite the best efforts in sample collection, there is still the risk of errors during sample processing in the laboratory. Trials use the central laboratory for testing and storage, using validated and standardised protocols for separating plasma from blood, storage, and ctDNA extraction. In FAKTION, dedicated technicians in AWMG Laboratory performed the plasma separation and ctDNA extraction from blood samples. However, human error can still happen in processing and storage.

I found that the concentration of total extracted baseline cfDNA in FAKTION samples was low. When this trial was conducted, there were only a few platforms available for cfDNA extraction. Newer platforms facilitate obtaining higher yields of cfDNA from patients' samples, which will need to be evaluated in future research and trials.

NGS platforms valuable method offers an opportunity to screen multiple genes in one run. However, NGS can be prone to generating multiple artefacts, especially with low DNA input. Several NGS techniques and bioinformatic pipelines have been used by different research groups to eradicate artefacts and increase true variant calling. Despite ongoing improvements in NGS technology and bioinformatic analysis, there is no consensus regarding the NGS technique and bioinformatics protocols. Recently in the USA, Food and Drug Administration (FDA) has approved Foundation Medicine genetic profiling of tissue and ctDNA as the first diagnostic genetic testing platform. However, these tests still require a good quality sample with sufficient cfDNA to process the sample.

Droplet digital PCR is a method that allows detecting low allele frequency variants in ctDNA. However, the sensitivity of variant detection by ddPCR seemed to be dependent on the amount of input DNA, where more DNA allows increased sensitivity for variant detection. This is an essential aspect of the ctDNA analysis, given that total cfDNA concertation can be as low as 1ng. In the literature, there are variable cut-offs used for mutation detection. This method requires further standardisation not only in the research field but also in clinical practice. As the sensitivity depends on DNA input, several thresholds might need to be developed to detect mutations. Also, ddPCR used for amplification detection will require further technical and clinical validations in prospective large clinical trials to ensure the results are accurate and sensitive enough to be applied in clinical settings.

This study showed a good concordance between the NGS and ddPCR methods (R^2 = 0.990). NGS platform allows high-throughput sequencing of multiple genes, whilst ddPCR enabled very sensitive and specific gene mutations detection in low-concertation cfDNA samples. Newer NGS panels can achieve the limit of detection of allele frequency below 1%. However, mutations detected below 1% can also result from sequencing artefact; therefore, confirmation with a second reliable and more sensitive (0.01%) method like ddPCR would be indicated. Using both methods for mutation detection could potentially increase confidence in results when used as a diagnostic tool in clinical practice.

Despite the limitations of current technology and ctDNA analysis, it can still be a valuable sample as it is a minimally invasive blood test. It can be taken several times and analysed as patients undergo multiple systemic therapies. There are ongoing trials in breast cancer, such as PLASMAMATCH (ICR-2018) and c-TRAK TN (CRUK-2018), which will validate the clinical utility of ctDNA in breast cancer. The treatment decisions are based on results from ctDNA to confirm that ctDNA can be an accurate biomarker and that acting on changes in ctDNA levels by commencing additional therapies will improve survival.

7.3 Future Directions

At present, there are no validated biomarkers used in the clinical setting to predict response and the length of response to a combination of endocrine therapy with targeted therapy in patients with breast cancer. In the USA, recently FDA approved Alpelisib for patients with *PIK3CA*-mutated breast cancer based on phase III SOLAR-1 trial. The *PIK3CA* mutations can be detected in tissue DNA or ctDNA. However, the detection of *PIK3CA* can only predict potential response to treatment but cannot predict response duration. Patients in this trial were not stratified based on other molecular prognostic markers. In the FAKTION trial, patients were stratified based on primary versus secondary endocrine resistance, measurable versus non-measurable disease and based on *PIK3CA*/*PTEN* status.

In chapter 5 and 6, I have shown the importance of concomitant prognostic factors like *TP53* mutations or *MYC* amplification. Patient with these mutations had no response to treatment, or the response was limited despite having targeted therapy for the activated PI3K/AKT pathway. It has been reported that TP53 somatic mutations are important as prognostic and predictive factors (Huszno and Grzybowska 2018). As mentioned previously, breast cancer with *TP53* mutations is more likely to be aggressive and resistant to multiple therapies (Huszno and Grzybowska 2018). The importance of *TP53* mutations was recently recognised in ALK-translocated lung cancers (Alidousty et al. 2018; Ross Camidge D et al. 2020). *TP53* mutations negatively affected crizotinib response and were correlated with shorter PFS in ALK-positive lung cancer patients (Song et al. 2019). Andersson et al. showed worse survival for *TP53*-mutated breast cancer patients receiving adjuvant chemotherapy (Andersson et al. 2005). The inclusion of *TP53* mutation in testing should be considered in patients' stratification in future large breast cancer clinical trials. Prospective analysis of a large number of patients data verified by stage, number of metastatic sites and AKT1 inhibitor will clarify the actual clinical value of TP53 mutations in response to treatment and prognostication. The molecular biomarkers might be as

important as clinical factors for patient stratification. For example, having concomitant *TP53* mutations with *PIK3CA* or *AKT1* could affect the PFS and OS to AKT inhibitor. It would be beneficial for the clinician to understand prognostic molecular markers in clinical settings as this will allow making an informed decision with the patient about the treatment.

Furthermore, it is essential to consider all the molecular changes that are detected in breast cancer. In chapter 6, section 6.5, I demonstrated that patients could have multiple SNVs and CNVs. However, I could not show whether the number of mutations is important or whether some mutations are more important than the other. This will need to be evaluated in future research. There are currently online tools like Adjuvant online or PREDICT and genetically driven methods like Oncotype DX, which help clinicians decide whether adjuvant chemotherapy would benefit a patient. Currently, there is no such tool in metastatic settings. Creating a tool for metastatic breast cancer that will consider clinical information and include molecular genetic profiling will provide clinicians with valuable information about the most successful treatment for individual patients and help predict the approximate duration of response.

The new prospective phase III trial after FAKTION should consider testing genes correlated with the PI3K/AKT pathway and adding relevant genes. Patients with single detected mutation or multiple but within one pathway PI3K/AKT, with no other mutations detected, would be stratified into two groups: fulvestrant and placebo versus fulvestrant and capivasertib. This patient selection would be more appropriate as a patient will be chosen with the affected pathway and excluding other pathways being involved. This could show the actual activity of the new drug in selected patients. Patients whom we have detected mutations in PI3K/AKT pathway and the concomitant mutations such as *TP53* mutation, *MYC* amplification could be randomised to two or three groups: fulvestrant with capivasertib versus standard chemotherapy versus fulvestrant with placebo. This part of the study could identify the best treatment for these patients until new therapy is discovered.

8. Appendices

8.1 ESR1 Mutations Positive Controls from gblock

ESR1 mutated gblocks were used in the verification of ESR1 mutations assays due to the lack of genomic mutation-positive DNA available for testing. Gblocks are synthetically made DNA fragments, and 1ng gblock DNA is not equivalent to 1ng of genomic DNA. In 1ng genomic DNA (3.3^9bp) is ~300 copies of the target gene in the background of other gens. In contrast, 1ng of gblock DNA has ~2 billion copies of pure synthetic DNA (500bp) of only target (e.g. ESR1) gene with no background of genomic DNA; therefore, this required serial dilutions to the operating range of the Bio-Rad ddPCR system (~9000 copies per ul). Double-stranded DNA, 500 bp, was made on request by Integrated DNA Technologies for each ESR1 mutation and wild-type ESR1. These samples were required to be diluted by more than a factor of 1,000,000 for useable levels for a ddPCR system of ~9000 copies per ul. The formula for determining how many DNA fragments were contained in 1ng of gblock is presented in Figure 51 (Prediger 2013). Diluted mutated gblock DNA fragments were mixed with wild-type gblock DNA fragments to achieve 5% of mutant allele frequency (MAF). This sample was used as a positive control for ESR1 ddPCR runs and further diluted for limit detection assessment.

The Droplet Generator produces approximately 20.000 droplets per sample, with the expectation of one DNA copy per droplet; therefore, overloading the droplet generator with over 20.000 copies per reaction can reduce sensitivity.

Figure 51. The formula for converting from nanograms to copy number(Prediger 2013).

$$\text{number of copies (molecules)} = \frac{X \text{ ng} * 6.0221 \text{ x } 10^{23} \text{ molecules/mole}}{(N * 660 \text{ g/mole})^{\dagger} * 1 \text{ x } 10^{9} \text{ ng/g}}$$

X = amount of amplicon (ng), N = length of dsDNA amplicon, 660 g/mole = average mass of 1 bp dsDNA, 6.0221 x 10^{23} - Avogadro's number

8.2 Comparison and Validation of Reference Genes

Three reference genes were evaluated to establish, which would be most appropriate for CNV testing. AP3B1 and EIF2C were recommended and already validated by Bio-Rad company. EIF2C validated with HER2, MYC, FGFR1. EFTUD2 was used as the reference gene for the HER2 copy number assay. EFTUD2 gene was identified by Gevensleben et al. (2013) group as a stable gene that is not amplified with HER2 in HER2-amplified cancers. Also, in non-amplified tumours, the EFTUD2 locus has a highly stable

171

copy number ratio with HER2 locus, compared to other reference gene UBBP4 (Gevensleben et al. 2013). The sequence of the EFTUD2 probes and primes was sent to Bio-rad for manufacturing a reference gene assay which was then tested with Bio-Rad HER2 CNV assay.

Gradient temperature was performed for the EFTUD2 gene, and 60°C was found to be the optimal temperature for the HER2 CNV PCR assay. AP3B1 and EIF2C were 'off the shelf' reference genes with validation gradient temperature recommendation of 60°C. Bio-Rad validated EIF2C with HER2, MYC, FGFR1 CNV assays.

The results showed that the HER2:EFTUD2 assay has a constantly reduced ratio in amplified and non-amplified FFPE DNA and cfDNA, Table 51 and Figure 52. In ctDNA, when the minimal increase in copy number can suggest amplification, testing with this reference gene would lower the CN ratios falsely, leading to an increased risk of false negatives.

Table 51. HER2:EFTUD2 versus HER2:EIF2C assay tested with multiple samples.

ID no	Sample type	HER2:EIFT2C			HER2:EFTUD2		
		Ratio	95% CI high	95% CI low	Ratio	95% CI high	95% CI low
1	FFPE-Amp	4.49	4.91	4.06	4.44	4.79	4.09
2	FFPE-Amp	4.21	4.61	3.81	4.03	4.4	3.66
3	FFPE-Non-Amp	1.01	1.07	0.95	0.94	0.99	0.89
4	FFPE-Non-Amp	1.09	1.15	1.03	0.91	0.96	0.86
5	FFPE-Non-Amp	1.05	1.11	1	0.91	0.96	0.86
6	ctDNA-Non-Amp	1.12	1.24	0.99	1	1.1	0.89
7	ctDNA-Non-Amp	1.11	1.23	0.99	0.92	1.02	0.83

Figure 52. Comparison of EFTUD2 vs EIF2C for HER2 CNV assay.
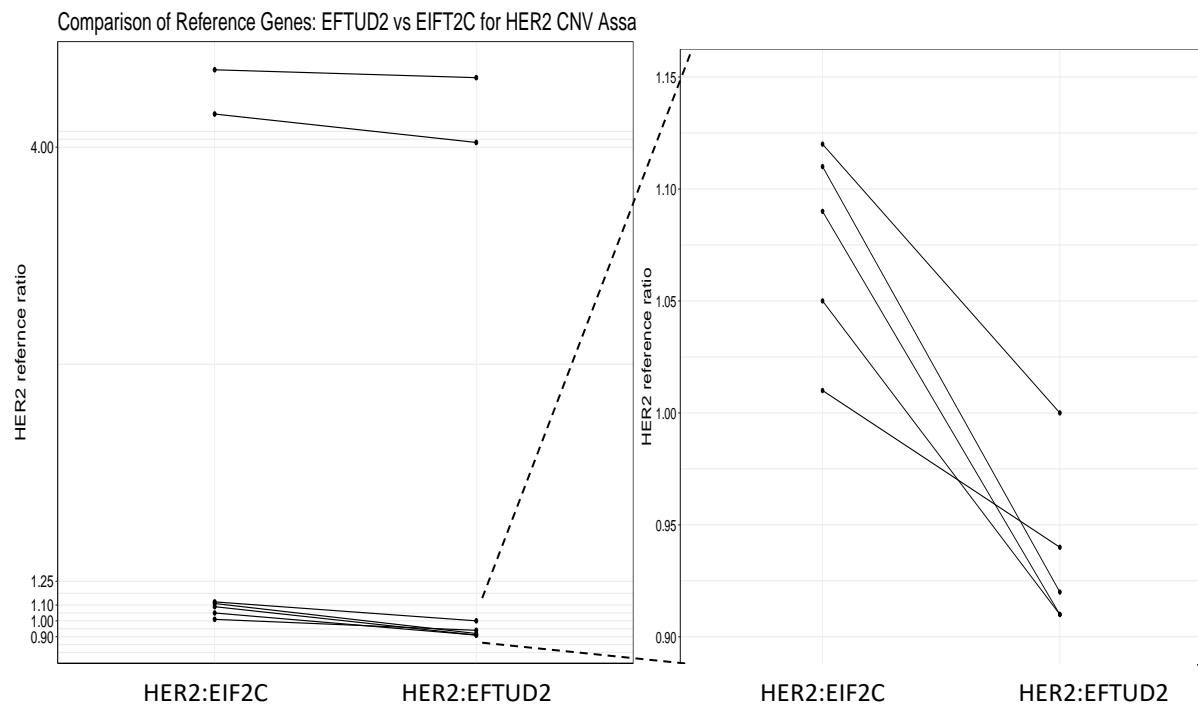
Figure 52 illustrates the difference in testing the same sample with the same HER2 copy number assay but different reference genes – EFTUD2 and EIF2C. The graph on the right is a magnified part of a lower segment of the left graph.

Figure 53 demonstrates the difference in testing the same sample with three different reference genes. In samples with high tumour DNA content, all three reference genes can be used as all will be able to detect amplification, although the CNV ratio may differ. However, using the EFTUD2 reference gene in samples with 5% tumour content could risk not detecting amplification. The AP3B1 reference gene is inconsistent in detecting amplifications in very low tumour DNA content 2.5% and 1.25%, Figure 53. For this project, EIF2C was chosen to be used as a reference gene as the most consistent gene and would not lower the results artificially and detect amplification in cfDNA with 5% of ctDNA.

Figure 53. Determination of HER2 Copy Number by ddPCR using three reference genes in samples with different tumour DNA content.

Determination of copy number via ddPCR using 3 refernce genes
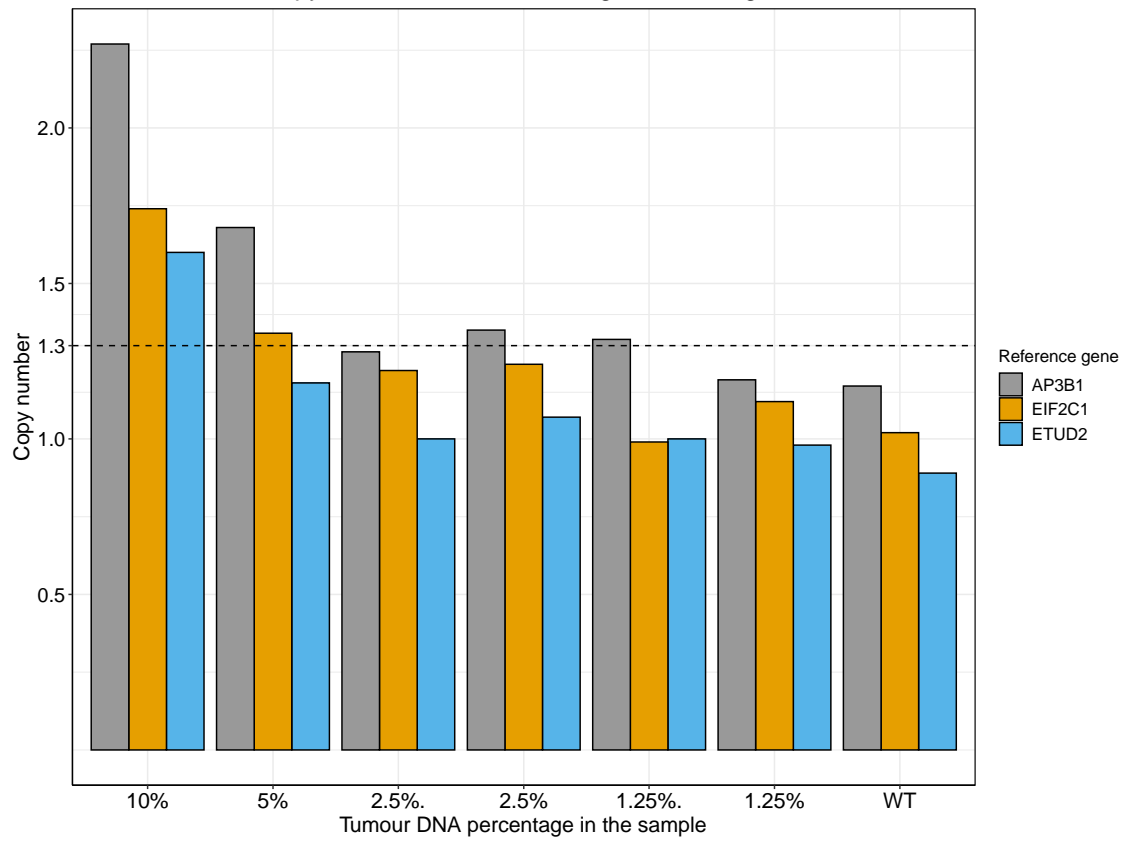
8.3 DNA extraction results with NGS library concentrations

Table 52. FFPE DNA and cfDNA extraction results and final library concentrations for chapter 4 and 5.

Pt ID	FFPE			CfDNA		
	Tumour %	DNA con. (ng/ul)	Final Lib ng/ul	cfDNA con in plasma (ng per 1 ml of plasma)	cfDNA con. in elusion volume (ng/ul)	Final Lib con (ng/ul)
4	70	0.6	16.3	5.5	0.3	12.8
17	NA	1.3	13.1	30.2	1.5	17.1
21	NA	44.8	16.6	64.4	3.2	19.2
23	NA	13.5	11.4	5	0.3	6.6
34	90	39.1	16.8	13.2	0.3	14.7
35	NA	16.2	16.7	21.6	1.1	12.8
36	90	26	15.4	6.9	0.6	16
38	NA	1	12	9	0.2	13.2
42	45	20	15.7	8.8	1	6.9
44	40	0.1	3.5	43.4	2.2	11.6
45	80	0.8	4.4	25.8	1.3	17.6
51	80	2.5	15	6.8	0.3	11.5
57	25	0.4	5.2	49.6	2.5	4.9
65	75	12	14.5	20.8	1	11.7
71	40	0.9	17.8	8.9	0.4	16
77	60	0.3	15.5	42	2.1	16.7
79	80	35.4	18.8	33.2	0.3	8.7
80	NA	18.8	12.9	7.6	0.4	14.3
84	80	7	11.6	18.9	0.9	9.7
94	NA	20.3	17.6	13.1	0.7	17
99	90	46.2	18.6	12.2	0.6	13
104	80	2.9	12.5	7.7	0.4	13.9
106	60	0.1	4	12	0.6	13
108	80	32	6	26.8	1.3	14.6
110	80	3.4	15.8	11.4	0.6	13.9
111	70	18.1	5.3	14.7	0.7	9
115	NA	3.3	17	4.7	0.2	13
122	NA	NT	NT	7.2	0.4	21
123	NA	5.6	13.8	21.8	1.1	12.2
129	NA	39.9	5.2	4.4	0.2	9.1
131	NA	31.3	14.3	14.2	0.7	9.7
132	NA	4.6	17.7	5.2	0.3	8.9
138	NA	7.7	9.1	16.9	0.8	20.2
145	70	4.7	15.8	17.3	0.9	11.6

Pt ID – Patient number, DNA con – DNA concentration, Final Library DNA concentration for NGS, NA – data not available, Tumour % - estimated tumour cell content

Table 53. End of treatment cfDNA extractions and final library concentrations for 15 patients in chapter 5.

Pt ID	cfDNA con in plasma (ng per 1 ml of plasma)	cfDNA con. in elusion volume (ng/ul)	Final Lib con (ng/ul)
End of Treatment cfDNA extractions and final library concentrations			
4	22.0	1.1	16.6
17	12.3	0.616	12.2
21	11.7	0.585	8.7
35	30.6	1.53	7.4
36	10.1	0.505	12.8
38	17.4	0.871	19.4
42	9.2	0.46	12
51	11.5	0.573	15.3
57	14.3	0.713	15.5
71	12.8	0.64	18.5
84	25.6	1.28	14.6
104	17.8	0.89	13.9
108	48.6	2.43	15.4
122	15.2	0.758	13.6
135	13.5	0.675	17.9

Pt ID – Patient number, DNA con – DNA concentration, Final Library DNA concentration for NGS,

Table 54. End of treatment cfDNA extractions for chapter 6.

Pt ID	cfDNA con in plasma - ng per 1 ml of plasma	cfDNA con. in elusion volume (ng/ul)
	End of Treamtnet cfDNA extractions	
1	67.0	3.4
2	12.6	0.6
6	13.5	0.7
9	44.8	2.2
10	22.8	1.1
11	32.6	1.6
13	21.4	1.1
16	58.2	2.9
17	12.9	0.6
18	7.7	0.4
26	24.4	1.2
31	11.9	0.6
33	138.0	6.9
35	40.4	2.0
39	87.6	4.4
41	10.1	0.5
42	3.2	0.2
52	984.0	49.2
53	28.2	1.4
57	3.0	0.2
60	10.2	0.5
66	12.9	0.6
67	14.3	0.7
73	13.3	0.7
78	13.2	0.7
82	23.6	1.2
85	12.3	0.6
86	10.8	0.5
92	84.0	4.2
97	24.6	1.2
103	13.0	0.7
104	11.5	0.6
108	41.0	2.1
109	25.0	1.3
116	16.9	0.8
118	13.8	0.7
119	127.8	6.4
121	12.8	0.6
125	70.2	3.5
127	129.0	6.5
134	19.0	0.9
135	16.2	0.8
139	10.4	0.5
141	14.3	0.7
142	30.0	1.5
143	16.0	0.8
144	17.1	0.9
147	56.0	2.8
148	21.8	1.1
150	17.5	0.9
151	17.6	0.9
154	224.0	11.2
156	61.0	3.1
166	14.9	0.7
175	10.1	0.5

9. References

Abbosh, C. et al. 2017. Phylogenetic ctDNA analysis depicts early-stage lung cancer evolution. *Nature* 545(7655), pp. 446-451. doi: 10.1038/nature22364

Abel, H. J. and Duncavage, E. J. 2013. Detection of structural DNA variation from next generation sequencing data: a review of informatic approaches. *Cancer Genet* 206(12), pp. 432-440. doi: 10.1016/j.cancergen.2013.11.002

Adams, J. R. et al. 2011. Cooperation between Pik3ca and p53 mutations in mouse mammary tumor formation. *Cancer Res* 71(7), pp. 2706-2717. doi: 10.1158/0008-5472.CAN-10-0738

Addie, M. et al. 2013. Discovery of 4-amino-N-[(1S)-1-(4-chlorophenyl)-3-hydroxypropyl]-1-(7H-pyrrolo[2,3-d]pyrimidin-4-yl)piperidine-4-carboxamide (AZD5363), an orally bioavailable, potent inhibitor of Akt kinases. *J Med Chem* 56(5), pp. 2059-2073. doi: 10.1021/jm301762v

Ali, S. et al. 1993. Modulation of transcriptional activation by ligand-dependent phosphorylation of the human oestrogen receptor A/B region. *EMBO J* 12(3), pp. 1153-1160.

Alidousty, C. et al. 2018. Genetic instability and recurrent MYC amplification in ALK-translocated NSCLC: a central role of TP53 mutations. *J Pathol* 246(1), pp. 67-76. doi: 10.1002/path.5110

Allott, E. H. et al. 2016. Intratumoral heterogeneity as a source of discordance in breast cancer biomarker classification. *Breast Cancer Res* 18(1), p. 68. doi: 10.1186/s13058-016-0725-1

Andersson, J. et al. 2005. Worse survival for TP53 (p53)-mutated breast cancer patients receiving adjuvant CMF. *Ann Oncol* 16(5), pp. 743-748. doi: 10.1093/annonc/mdi150

André, F. et al. 2019. Alpelisib for PIK3CA -Mutated, Hormone Receptor–Positive Advanced Breast Cancer. *N Engl J Med* 380(20), pp. 1929-1940. doi: 10.1056/NEJMoa1813904

Angus, L. et al. 2017. ESR1 mutations: Moving towards guiding treatment decision-making in metastatic breast cancer patients. *Cancer Treatment Reviews* 52, pp. 33-40. doi: http://dx.doi.org/10.1016/j.ctrv.2016.11.001

Aparicio, S. and Caldas, C. 2013. The implications of clonal genome evolution for cancer medicine. *N Engl J Med* 368(9), pp. 842-851. doi: 10.1056/NEJMra1204892

Aravanis, A. M. et al. 2017. Next-Generation Sequencing of Circulating Tumor DNA for Early Cancer Detection. *Cell* 168(4), pp. 571-574. doi: 10.1016/j.cell.2017.01.030

Arteaga, C. L. et al. 2011. Treatment of HER2-positive breast cancer: current status and future perspectives. *Nat Rev Clin Oncol* 9(1), pp. 16-32. doi: 10.1038/nrclinonc.2011.177

Arthur, L. M. et al. 2014. Changes in PIK3CA mutation status are not associated with recurrence, metastatic disease or progression in endocrine-treated breast cancer. *Breast Cancer Res Treat* 147(1), pp. 211-219. doi: 10.1007/s10549-014-3080-x

Aspinall, S. R. et al. 2004. The proliferative effects of 5-androstene-3 beta,17 beta-diol and 5 alpha-dihydrotestosterone on cell cycle analysis and cell proliferation in MCF7, T47D and MDAMB231 breast cancer cell lines. *J Steroid Biochem Mol Biol* 88(1), pp. 37-51. doi: 10.1016/j.jsbmb.2003.10.011

Assou, S. et al. 2014. Non-invasive pre-implantation genetic diagnosis of X-linked disorders. *Med Hypotheses* 83(4), pp. 506-508. doi: 10.1016/j.mehy.2014.08.019

Babina, I. S. and Turner, N. C. 2017. Advances and challenges in targeting FGFR signalling in cancer. *Nat Rev Cancer* 17(5), pp. 318-332. doi: 10.1038/nrc.2017.8

Bachelot, T. et al. 2012. Randomized phase II trial of everolimus in combination with tamoxifen in patients with hormone receptor-positive, human epidermal growth factor receptor 2-negative metastatic breast cancer with prior exposure to aromatase inhibitors: a GINECO study. *J Clin Oncol* 30(22), pp. 2718-2724. doi: 10.1200/jco.2011.39.0708

Bachman, K. E. et al. 2004. The PIK3CA gene is mutated with high frequency in human breast cancers. *Cancer Biol Ther* 3(8), pp. 772-775. doi: 10.4161/cbt.3.8.994

Bahassi, e. M. and Stambrook, P. J. 2014. Next-generation sequencing technologies: breaking the sound barrier of human genetics. *Mutagenesis* 29(5), pp. 303-310. doi: 10.1093/mutage/geu031

Barbany, G. et al. 2019. Cell-free tumour DNA testing for early detection of cancer - a potential future tool. *J Intern Med* 286(2), pp. 118-136. doi: 10.1111/joim.12897

Baselga, J. et al. 2012. Everolimus in Postmenopausal Hormone-Receptor–Positive Advanced Breast Cancer. *N Engl J Med.* 366(6), pp. 520-529. Epub 2011 Dec 2017 doi:2010.1056/NEJMoa1109653.

Bauer, T. M. et al. 2015. Targeting PI3 kinase in cancer. *Pharmacol Ther* 146, pp. 53-60. doi: 10.1016/j.pharmthera.2014.09.006

Bellacosa, A. et al. 2005. Activation of AKT kinases in cancer: implications for therapeutic targeting. *Adv Cancer Res* 94, pp. 29-86. doi: 10.1016/S0065-230X(05)94002-5

Bender, L. M. and Nahta, R. 2008. Her2 cross talk and therapeutic resistance in breast cancer. *Front Biosci* 13, pp. 3906-3912. doi: 10.2741/2978

Benetatos, L. et al. 2017. The crosstalk between long non-coding RNAs and PI3K in cancer. *Med Oncol* 34(3), p. 39. doi: 10.1007/s12032-017-0897-2

Beresford, M. et al. 2011. A qualitative systematic review of the evidence base for non-cross-resistance between steroidal and non-steroidal aromatase inhibitors in metastatic breast cancer. *Clin Oncol (R Coll Radiol)* 23(3), pp. 209-215. doi: 10.1016/j.clon.2010.11.005

Bettegowda, C. et al. 2014. Detection of circulating tumor DNA in early- and late-stage human malignancies. *Sci Transl Med* 6(224), p. 224ra224. doi: 10.1126/scitranslmed.3007094

Bio-Rad. Limit of Detection and the Rule of Three.*Rare Mutation Detection,   Best Practices Guidelines*. https://www.bio-rad.com/webroot/web/pdf/lsr/literature/Bulletin_6628.pdf, p. 9.

Bioinformatics, B. 2016. *Soft-clipping of reads may add potentially unwanted alignments to repetitive regions*. Available at: https://sequencing.qcfail.com/articles/soft-clipping-of-reads-may-add-potentially-unwanted-alignments-to-repetitive-regions/ [Accessed.

Biosearch, L. 2016. *Application note: Improved Function with Double-Quenched BHQ® Probes for qPCR*. Available at: https://biosearchassets.blob.core.windows.net/assets/app-note-improved-function-double-quenched-probes.pdf [Accessed.

Bosetti, C. et al. 2012. The decline in breast cancer mortality in Europe: an update (to 2009). *Breast* 21(1), pp. 77-82. doi: 10.1016/j.breast.2011.08.001

Brufsky, A. M. and Dickler, M. N. 2018. Estrogen Receptor-Positive Breast Cancer: Exploiting Signaling Pathways Implicated in Endocrine Resistance. *Oncologist*, doi: 10.1634/theoncologist.2017-0423

Butler, T. M. et al. 2015. Exome Sequencing of Cell-Free DNA from Metastatic Cancer Patients Identifies Clinically Actionable Mutations Distinct from Primary Disease. *PLoS One* 10(8), p. e0136407. doi: 10.1371/journal.pone.0136407

Campbell, I. G. et al. 2004. Mutation of the PIK3CA gene in ovarian and breast cancer. *Cancer Res* 64(21), pp. 7678-7681. doi: 10.1158/0008-5472.CAN-04-2933

Campone, M. et al. 2018. Buparlisib plus fulvestrant versus placebo plus fulvestrant for postmenopausal, hormone receptor-positive, human epidermal growth factor receptor 2-negative, advanced breast cancer: Overall survival results from BELLE-2. *Eur J Cancer* 103, pp. 147-154. doi: 10.1016/j.ejca.2018.08.002

Cardoso, F. et al. 2014. ESO-ESMO 2nd international consensus guidelines for advanced breast cancer (ABC2). *Breast* 23(5), pp. 489-502. doi: 10.1016/j.breast.2014.08.009

Cerami, E. et al. 2012. The cBio cancer genomics portal: an open platform for exploring multidimensional cancer genomics data. *Cancer Discov* 2(5), pp. 401-404. doi: 10.1158/2159-8290.cd-12-0095

Chan, A. et al. 2020. Final Efficacy Results of Neratinib in HER2-positive Hormone Receptor-positive Early-stage Breast Cancer From the Phase III ExteNET Trial. *Clin Breast Cancer*, doi: 10.1016/j.clbc.2020.09.014

Chan, K. C. et al. 2013. Cancer genome scanning in plasma: detection of tumor-associated copy number aberrations, single-nucleotide variants, and tumoral heterogeneity by massively parallel sequencing. *Clin Chem* 59(1), pp. 211-224. doi: 10.1373/clinchem.2012.196014

Chan, S. et al. 2005. Phase II study of temsirolimus (CCI-779), a novel inhibitor of mTOR, in heavily pretreated patients with locally advanced or metastatic breast cancer. *J Clin Oncol* 23(23), pp. 5314-5322. doi: 10.1200/jco.2005.66.130

Chen, Z. et al. 2015. Cross-talk between ER and HER2 regulates c-MYC-mediated glutamine metabolism in aromatase inhibitor resistant breast cancer cells. *J Steroid Biochem Mol Biol* 149, pp. 118-127. doi: 10.1016/j.jsbmb.2015.02.004

Clark, A. S. et al. 2002. Constitutive and inducible Akt activity promotes resistance to chemotherapy, trastuzumab, or tamoxifen in breast cancer cells. *Mol Cancer Ther* 1(9), pp. 707-717.

Cohen, J. D. et al. 2018. Detection and localization of surgically resectable cancers with a multi-analyte blood test. *Science* 359(6378), pp. 926-930. doi: 10.1126/science.aar3247

Creighton, C. J. et al. 2008. Development of resistance to targeted therapies transforms the clinically associated molecular profile subtype of breast tumor xenografts. *Cancer Res* 68(18), pp. 7493-7501.

Croessmann, S. et al. 2019. Combined Blockade of Activating ERBB2 Mutations and ER Results in Synthetic Lethality of ER+/HER2 Mutant Breast Cancer. *Clin Cancer Res* 25(1), pp. 277-289.

Croessmann, S. et al. 2018. C2 Domain Deletions Hyperactivate Phosphoinositide 3-kinase (PI3K), Generate Oncogene Dependence, and Are Exquisitely Sensitive to PI3K. *Clin Cancer Res* 24(6), pp. 1426-1435. doi: 10.1158/1078-0432.CCR-17-2141

Croessmann, S. et al. 2017. PIK3CA mutations and TP53 alterations cooperate to increase cancerous phenotypes and tumor heterogeneity. *Breast Cancer Res Treat* 162(3), pp. 451-464. doi: 10.1007/s10549-017-4147-2

CRUK. 2017. Breast cancer statistics. http://www.cancerresearchuk.org: Cancer Research UK.

Curtit, E. et al. 2013. Discordances in estrogen receptor status, progesterone receptor status, and HER2 status between primary breast cancer and metastasis. *Oncologist* 18(6), pp. 667-674. doi: 10.1634/theoncologist.2012-0350

Daneshmand, M. et al. 2012. Detection of PIK3CA Mutations in Breast Cancer Bone Metastases. *ISRN Oncol* 2012, p. 492578. doi: 10.5402/2012/492578

Davies, B. R. et al. 2012. Preclinical pharmacology of AZD5363, an inhibitor of AKT: pharmacodynamics, antitumor activity, and correlation of monotherapy activity with genetic background. *Mol Cancer Ther* 11(4), pp. 873-887. doi: 10.1158/1535-7163.mct-11-0824-t

Davies, C. et al. 2011. Relevance of breast cancer hormone receptors and other factors to the efficacy of adjuvant tamoxifen: patient-level meta-analysis of randomised trials. *Lancet* 378(9793), pp. 771-784. doi: 10.1016/s0140-6736(11)60993-8

Dawson, S. J. et al. 2013. Analysis of circulating tumor DNA to monitor metastatic breast cancer. *N Engl J Med* 368(13), pp. 1199-1209. doi: 10.1056/NEJMoa1213261

Dbouk, H. A. et al. 2013. Characterization of a tumor-associated activating mutation of the p110β PI 3-kinase. *PLoS One* 8(5), p. e63833.

Deeks, E. D. 2017. Neratinib: First Global Approval.*Drugs*. Vol. 77. New Zealand, pp. 1695-1704.

DeFeo-Jones, D. et al. 2005. Tumor cell sensitization to apoptotic stimuli by selective inhibition of specific Akt/PKB family members. *Mol Cancer Ther* 4(2), pp. 271-279.

Delaloge, S. et al. 2019. Effects of neratinib on health-related quality of life in women with HER2-positive early-stage breast cancer: longitudinal analyses from the randomized phase III ExteNET trial.*Ann Oncol*. Vol. 30. England: © The Author(s) 2019. Published by Oxford University Press on behalf of the European Society for Medical Oncology For permissions, please email: journals.permissions@oup.com., pp. 567-574.

Dey, N. et al. 2015. MYC-xing it up with PIK3CA mutation and resistance to PI3K inhibitors: summit of two giants in breast cancers. *Am J Cancer Res* 5(1), pp. 1-19.

Diaz, L. A. and Bardelli, A. 2014. Liquid biopsies: genotyping circulating tumor DNA. *J Clin Oncol* 32(6), pp. 579-586. doi: 10.1200/JCO.2012.45.2011

Diehl, F. et al. 2008. Circulating mutant DNA to assess tumor dynamics. *Nat Med* 14(9), pp. 985-990. doi: 10.1038/nm.1789

Donahue, T. R. et al. 2012. Integrative survival-based molecular profiling of human pancreatic cancer. *Clin Cancer Res* 18(5), pp. 1352-1363. doi: 10.1158/1078-0432.CCR-11-1539

Dong, P. et al. 2014. The impact of microRNA-mediated PI3K/AKT signaling on epithelial-mesenchymal transition and cancer stemness in endometrial cancer. *J Transl Med* 12, p. 231. doi: 10.1186/s12967-014-0231-0

Douillard, J. Y. et al. 2014. First-line gefitinib in Caucasian EGFR mutation-positive NSCLC patients: a phase-IV, open-label, single-arm study. *Br J Cancer* 110(1), pp. 55-62. doi: 10.1038/bjc.2013.721

Drago, J. N., A. Spring, L. Moy B. Juric, D. Isakoff, SJ. Iafrate, A. J. Ellisen, LW. Bardia, A. 2017. FGFR gene amplification and response to endocrine therapy in metastatic hormone receptor positive (HR+) breast cancer. *Journal of Clinical Oncology* 35, doi: 10.1200/JCO.2017.35.15_suppl.1013

Drago, J. Z. et al. 2019. FGFR1 Amplification Mediates Endocrine Resistance but Retains TORC Sensitivity in Metastatic Hormone Receptor-Positive (HR(+)) Breast Cancer. *Clin Cancer Res* 25(21), pp. 6443-6451. doi: 10.1158/1078-0432.ccr-19-0138

Dupont Jensen, J. et al. 2011. PIK3CA mutations may be discordant between primary and corresponding metastatic disease in breast cancer. *Clin Cancer Res* 17(4), pp. 667-677. doi: 10.1158/1078-0432.CCR-10-1133

Eisenhauer, E. A. et al. 2009. New response evaluation criteria in solid tumours: revised RECIST guideline (version 1.1). *Eur J Cancer* 45(2), pp. 228-247. doi: 10.1016/j.ejca.2008.10.026

Elbauomy Elsheikh, S. et al. 2007. FGFR1 amplification in breast carcinomas: a chromogenic in situ hybridisation analysis. *Breast Cancer Res* 9(2), p. R23. doi: 10.1186/bcr1665

Ellis, J. M. et al. 2015. Fulvestrant 500 mg Versus Anastrozole 1 mg for the First-Line Treatment of Advanced Breast Cancer: Overall Survival Analysis From the Phase II FIRST Study. *Journal of Clinical Oncology* 33 pp. 3781-3787 doi: 10.1200/jco.2015.61.5831

Ellis, M. J. et al. 2012. Whole-genome analysis informs breast cancer response to aromatase inhibition. *Nature* 486(7403), pp. 353-360. doi: 10.1038/nature11143

Ellis, M. J. et al. 2008. Outcome Prediction for Estrogen Receptor–Positive Breast Cancer Based on Postneoadjuvant Endocrine Therapy Tumor Characteristics *Journal of the National Cancer Institute* 100, pp. 1380 − 1388.

Ellis, M. J. et al. 2006. Estrogen-independent proliferation is present in estrogen-receptor HER2-positive primary breast cancer after neoadjuvant letrozole. *J Clin Oncol* 24(19), pp. 3019-3025. doi: 10.1200/JCO.2005.04.3034

Engelman, J. A. et al. 2006. The evolution of phosphatidylinositol 3-kinases as regulators of growth and metabolism. *Nat Rev Genet* 7(8), pp. 606-619. doi: 10.1038/nrg1879

Fanning, S. W. et al. 2016. Estrogen receptor alpha somatic mutations Y537S and D538G confer breast cancer endocrine resistance by stabilizing the activating function-2 binding conformation. *Elife* 5, doi: 10.7554/eLife.12792

Feng, J. et al. 2004. Identification of a PKB/Akt hydrophobic motif Ser-473 kinase as DNA-dependent protein kinase. *J Biol Chem* 279(39), pp. 41189-41196. doi: 10.1074/jbc.M406731200

Fernandez-Cuesta, L. et al. 2016. Identification of Circulating Tumor DNA for the Early Detection of Small-cell Lung Cancer. *EBioMedicine* 10, pp. 117-123. doi: 10.1016/j.ebiom.2016.06.032

Fiala, C. and Diamandis, E. P. 2018. Utility of circulating tumor DNA in cancer diagnostics with emphasis on early detection. *BMC Med* 16(1), p. 166. doi: 10.1186/s12916-018-1157-9

Finn, R. S. et al. 2017. Overall survival results from the randomized phase II study of palbociclib (P) in combination with letrozole (L) vs letrozole alone for frontline treatment of ER+/HER2− advanced breast cancer (PALOMA-1; TRIO-18). doi: 10.1200/JCO.2017.35.15_suppl.1001

Finn, R. S. et al. 2015. The cyclin-dependent kinase 4/6 inhibitor palbociclib in combination with letrozole versus letrozole alone as first-line treatment of oestrogen receptor-positive, HER2-negative, advanced breast cancer (PALOMA-1/TRIO-18): a randomised phase 2 study. *Lancet Oncol* 16(1), pp. 25-35. doi: 10.1016/S1470-2045(14)71159-3

Finn, R. S. et al. 2009. PD 0332991, a selective cyclin D kinase 4/6 inhibitor, preferentially inhibits proliferation of luminal estrogen receptor-positive human breast cancer cell lines in vitro. *Breast Cancer Res* 11(5), p. R77. doi: 10.1186/bcr2419

Formisano, L. et al. 2017. Gain-of-function kinase library screen identifies FGFR1 amplification as a mechanism of resistance to antiestrogens and CDK4/6 inhibitors in ERþ breast cancer. *In: Proceedings: AACR 108th annual meeting* (Apr 1-5, 2017; Washington, DC. Abstract 1008 .), doi: 10.1158/1538-7445.am2017-1008

Fountzilas, G. et al. 2016. TP53 mutations and protein immunopositivity may predict for poor outcome but also for trastuzumab benefit in patients with early breast cancer treated in the adjuvant setting. *Oncotarget* 7(22), pp. 32731-32753. doi: 10.18632/oncotarget.9022

Fox, E. M. et al. 2011. A kinome-wide screen identifies the insulin/IGF-I receptor pathway as a mechanism of escape from hormone dependence in breast cancer. *Cancer Res* 71(21), pp. 6773-6784. doi: 10.1158/0008-5472.CAN-11-1295

Frenel, J. S. et al. 2015. Serial Next-Generation Sequencing of Circulating Cell-Free DNA Evaluating Tumor Clone Response To Molecularly Targeted Drug Administration. *Clin Cancer Res* 21(20), pp. 4586-4596. doi: 10.1158/1078-0432.ccr-15-0584

Fribbens, C. et al. 2016. Plasma ESR1 Mutations and the Treatment of Estrogen Receptor-Positive Advanced Breast Cancer. *J Clin Oncol* 34(25), pp. 2961-2968. doi: 10.1200/JCO.2016.67.3061

Frogne, T. et al. 2009. Activation of ErbB3, EGFR and Erk is essential for growth of human breast cancer cell lines with acquired resistance to fulvestrant. *Breast Cancer Res Treat* 114(2), pp. 263-275. doi: 10.1007/s10549-008-0011-8

Fu, X. et al. 2013. Biology and therapeutic potential of PI3K signaling in ER+/HER2-negative breast cancer. *Breast* 22 Suppl 2, pp. S12-18. doi: 10.1016/j.breast.2013.08.001

Fung-Leung, W. P. 2011. Phosphoinositide 3-kinase delta (PI3Kδ) in leukocyte signaling and function.*Cell Signal*. Vol. 23. England: © 2010 Elsevier Inc, pp. 603-608.

Gale, D. et al. 2018. Development of a highly sensitive liquid biopsy platform to detect clinically-relevant cancer mutations at low allele fractions in cell-free DNA. *PLoS One* 13(3), p. e0194630. doi: 10.1371/journal.pone.0194630

Gao, J. et al. 2013. Integrative analysis of complex cancer genomics and clinical profiles using the cBioPortal. *Sci Signal* 6(269), p. pl1. doi: 10.1126/scisignal.2004088

Garcia-Murillas, I. et al. 2015. Mutation tracking in circulating tumor DNA predicts relapse in early breast cancer. *Sci Transl Med* 7(302), p. 302ra133. doi: 10.1126/scitranslmed.aab0021

Gasco, M. et al. 2002. The p53 pathway in breast cancer. *Breast Cancer Res* 4(2), pp. 70-76. doi: 10.1186/bcr426

Geisler, J. and Lønning, P. E. 2001. Resistance to endocrine therapy of breast cancer: recent advances and tomorrow's challenges. *Clin Breast Cancer* 1(4), pp. 297-308; discussion 309. doi: 10.3816/CBC.2001.n.004

Gevensleben, H. et al. 2013. Noninvasive detection of HER2 amplification with plasma DNA digital PCR. *Clin Cancer Res* 19(12), pp. 3276-3284. doi: 10.1158/1078-0432.ccr-12-3768

Goetz, M. P. et al. 2017. MONARCH 3: Abemaciclib As Initial Therapy for Advanced Breast Cancer. *J Clin Oncol* 35(32), pp. 3638-3646. doi: 10.1200/JCO.2017.75.6155

Gonzalez-Angulo, A. M. et al. 2013. Abstract 2531: Safety, pharmacokinetics, and preliminary activity of the α-specific PI3K inhibitor BYL719: Results from the first-in-human study. *Journal of Clinical Oncology 31, no. 15_suppl*, pp. 2531-2531. doi: DOI: 10.1200/jco.2013.31.15_suppl.2531

Grandori, C. et al. 2000. The Myc/Max/Mad network and the transcriptional control of cell behavior. *Annu Rev Cell Dev Biol* 16, pp. 653-699. doi: 10.1146/annurev.cellbio.16.1.653

Green, A. R. et al. 2016. MYC functions are specific in biological subtypes of breast cancer and confers resistance to endocrine therapy in luminal tumours. *Br J Cancer* 114(8), pp. 917-928. doi: 10.1038/bjc.2016.46

Guo, H. et al. 2015. The PI3K/AKT Pathway and Renal Cell Carcinoma. *J Genet Genomics* 42(7), pp. 343-353. doi: 10.1016/j.jgg.2015.03.003

Gupta, S. et al. 2007. Binding of ras to phosphoinositide 3-kinase p110alpha is required for ras-driven tumorigenesis in mice. *Cell* 129(5), pp. 957-968. doi: 10.1016/j.cell.2007.03.051

Gustin, J. P. et al. 2017. frameshift mutation promotes tumor growth in human luminal breast cancer cells and induces transcriptional changes seen in primary. *Oncotarget* 8(61), pp. 103415-103427. doi: 10.18632/oncotarget.21910

Gut, M. et al. 1999. One-tube fluorogenic reverse transcription-polymerase chain reaction for the quantitation of feline coronaviruses. *J Virol Methods* 77(1), pp. 37-46. doi: 10.1016/s0166-0934(98)00129-3

Gutierrez, M. C. et al. 2005. Molecular changes in tamoxifen-resistant breast cancer: relationship between estrogen receptor, HER-2, and p38 mitogen-activated protein kinase.*J Clin Oncol*. Vol. 23. United States, pp. 2469-2476.

Ha, J. H. et al. 2014. Serial Serum HER2 Measurements for the Detection of Breast Cancer Recurrence in HER2-Positive Patients. *J Breast Cancer* 17(1), pp. 33-39. doi: 10.4048/jbc.2014.17.1.33

Haddadi, N. et al. 2018. PTEN/PTENP1: 'Regulating the regulator of RTK-dependent PI3K/Akt signalling', new targets for cancer therapy. *Mol Cancer* 17(1), p. 37. doi: 10.1186/s12943-018-0803-3

Hanahan, D. and Weinberg, R. A. 2011. Hallmarks of cancer: the next generation. *Cell* 144(5), pp. 646-674. doi: 10.1016/j.cell.2011.02.013

Hanamura, T. and Hayashi, S. I. 2017. Overcoming aromatase inhibitor resistance in breast cancer: possible mechanisms and clinical applications. *Breast Cancer*, doi: 10.1007/s12282-017-0772-1

Head, S. R. et al. 2014. Library construction for next-generation sequencing: overviews and challenges. *Biotechniques* 56(2), pp. 61-64, 66, 68, passim. doi: 10.2144/000114133

Hehir-Kwa, J. Y. et al. 2015. Exome sequencing and whole genome sequencing for the detection of copy number variation. *Expert Rev Mol Diagn* 15(8), pp. 1023-1032. doi: 10.1586/14737159.2015.1053467

Helsten, T. et al. 2016. The FGFR Landscape in Cancer: Analysis of 4,853 Tumors by Next-Generation Sequencing. *Clin Cancer Res* 22(1), pp. 259-267. doi: 10.1158/1078-0432.CCR-14-3212

Hennessy, B. T. et al. 2005. Exploiting the PI3K/AKT pathway for cancer drug discovery. *Nat Rev Drug Discov* 4(12), pp. 988-1004. doi: 10.1038/nrd1902

Heredia, N. J. et al. 2013. Droplet Digital™ PCR quantitation of HER2 expression in FFPE breast cancer samples. *Methods* 59(1), pp. S20-S23. doi: http://dx.doi.org/10.1016/j.ymeth.2012.09.012

Hers, I. et al. 2011. Akt signalling in health and disease. *Cell Signal* 23(10), pp. 1515-1527. doi: 10.1016/j.cellsig.2011.05.004

Hill, K. A. and Sommer, S. S. 2002. p53 as a mutagen test in breast cancer. *Environ Mol Mutagen* 39(2-3), pp. 216-227. doi: 10.1002/em.10065

Hindson, B. J. et al. 2011. High-throughput droplet digital PCR system for absolute quantitation of DNA copy number. *Anal Chem* 83(22), pp. 8604-8610. doi: 10.1021/ac202028g

Hinz, N. and Jücker, M. 2019. Distinct functions of AKT isoforms in breast cancer: a comprehensive review. *Cell Commun Signal* 17(1), p. 154. doi: 10.1186/s12964-019-0450-3

Honma, N. et al. 2011. Sex steroid hormones in pairs of tumor and serum from breast cancer patients and pathobiological role of androstene-3β, 17β-diol. *Cancer Sci* 102(10), pp. 1848-1854. doi: 10.1111/j.1349-7006.2011.02018.x

Hortobagyi, G. N. et al. 2016. Correlative Analysis of Genetic Alterations and Everolimus Benefit in Hormone Receptor-Positive, Human Epidermal Growth Factor Receptor 2-Negative Advanced Breast Cancer: Results From BOLERO-2. *J Clin Oncol* 34(5), pp. 419-426. doi: 10.1200/jco.2014.60.1971

Hortobagyi, G. N. et al. 2019. Updated results from MONALEESA-2, a phase III trial of first-line ribociclib plus letrozole versus placebo plus letrozole in hormone receptor-positive, HER2-negative advanced breast cancer. *Ann Oncol* 30(11), p. 1842. doi: 10.1093/annonc/mdz215

Hothorn, T. and Lausen, B. 2003. On the Exact Distribution of Maximally Selected Rank Statistics. *Computational Statistics & Data Analysis* 43, pp. 121–137

Howell, J. A. and Sharma, R. 2016. The clinical role of 'liquid biopsy' in hepatocellular carcinoma. *Hepat Oncol* 3(1), pp. 45-55. doi: 10.2217/hep.15.38

Hrebien, S. et al. 2019. Early ctDNA dynamics as a surrogate for progression-free survival in advanced breast cancer in the BEECH trial. *Ann Oncol* 30(6), pp. 945-952. doi: 10.1093/annonc/mdz085

Hrebien, S. et al. 2016. Reproducibility of Digital PCR Assays for Circulating Tumor DNA Analysis in Advanced Breast Cancer. *PLoS One* 11(10), p. e0165023. doi: 10.1371/journal.pone.0165023

Huang, A. et al. 2016. Detecting Circulating Tumor DNA in Hepatocellular Carcinoma Patients Using Droplet Digital PCR Is Feasible and Reflects Intratumoral Heterogeneity. *J Cancer* 7(13), pp. 1907-1914. doi: 10.7150/jca.15823

Hudis, C. A. 2007. Trastuzumab--mechanism of action and use in clinical practice. *N Engl J Med* 357(1), pp. 39-51. doi: 10.1056/NEJMra043186

Huggett, J. F. and Whale, A. 2013. Digital PCR as a novel technology and its potential implications for molecular diagnostics. *Clin Chem* 59(12), pp. 1691-1693. doi: 10.1373/clinchem.2013.214742

Huszno, J. and Grzybowska, E. 2018. TP53 mutations and SNPs as prognostic and predictive factors in patients with breast cancer. *Oncol Lett* 16(1), pp. 34-40. doi: 10.3892/ol.2018.8627

Hyman, D. M. et al. 2017. AKT Inhibition in Solid Tumors With AKT1 Mutations. *J Clin Oncol* 35(20), pp. 2251-2259. doi: 10.1200/jco.2017.73.0143

Ikenoue, T. et al. 2005. Functional analysis of PIK3CA gene mutations in human colorectal cancer. *Cancer Res* 65(11), pp. 4562-4567. doi: 10.1158/0008-5472.CAN-04-4114

Illumina. 2010. *Illumina Sequencing Technology*. Available at: https://www.illumina.com/documents/products/techspotlights/techspotlight_sequencing.pdf [Accessed.

Illumina. 2020. *Differences Between NGS and Sanger Sequencing*. Available at: https://www.illumina.com/science/technology/next-generation-sequencing/ngs-vs-sanger-sequencing.html [Accessed.

Im, S. A. et al. 2019. Overall Survival with Ribociclib plus Endocrine Therapy in Breast Cancer. *N Engl J Med* 381(4), pp. 307-316. doi: 10.1056/NEJMoa1903765

Jahangiri, L. and Hurst, T. 2019. Assessing the Concordance of Genomic Alterations between Circulating-Free DNA and Tumour Tissue in Cancer Patients. *Cancers (Basel)* 11(12), doi: 10.3390/cancers11121938

Jahr, S. et al. 2001. DNA fragments in the blood plasma of cancer patients: quantitations and evidence for their origin from apoptotic and necrotic cells. *Cancer Res* 61(4), pp. 1659-1665.

Jang, M. et al. 2012. FGFR1 is amplified during the progression of in situ to invasive breast carcinoma. *Breast Cancer Res* 14(4), p. R115. doi: 10.1186/bcr3239

Jerusalem, G. et al. 2018. Everolimus Plus Exemestane vs Everolimus or Capecitabine Monotherapy for Estrogen Receptor-Positive, HER2-Negative Advanced Breast Cancer: The BOLERO-6 Randomized Clinical Trial. *JAMA Oncol* 4(10), pp. 1367-1374. doi: 10.1001/jamaoncol.2018.2262

Jeselsohn, R. et al. 2014. Emergence of constitutively active estrogen receptor-α mutations in pretreated advanced estrogen receptor-positive breast cancer. *Clin Cancer Res* 20(7), pp. 1757-1767. doi: 10.1158/1078-0432.CCR-13-2332

Jhaveri, K. and Modi, S. 2015. Ganetespib: research and clinical development. *Onco Targets Ther* 8, pp. 1849-1858.

Jiang, P. et al. 2015. Lengthening and shortening of plasma DNA in hepatocellular carcinoma patients. *Proc Natl Acad Sci U S A* 112(11), pp. E1317-1325. doi: 10.1073/pnas.1500076112

Jiang, W. et al. 2018. The PIK3CA E542K and E545K mutations promote glycolysis and proliferation via induction of the β-catenin/SIRT3 signaling pathway in cervical cancer. *J Hematol Oncol* 11(1), p. 139. doi: 10.1186/s13045-018-0674-5

Johnston, S. 2004. Fulvestrant and the sequential endocrine cascade for advanced breast cancer. *Br J Cancer* 90 Suppl 1, pp. S15-18. doi: 10.1038/sj.bjc.6601632

Johnston, S. et al. 2009. Lapatinib combined with letrozole versus letrozole and placebo as first-line therapy for postmenopausal hormone receptor-positive metastatic breast cancer.*J Clin Oncol*. Vol. 27. United States, pp. 5538-5546.

Johnston, S. R. 2010. New strategies in estrogen receptor-positive breast cancer. *Clin Cancer Res* 16(7), pp. 1979-1987. doi: 10.1158/1078-0432.ccr-09-1823

Jones, R. H. et al. 2020. Fulvestrant plus capivasertib versus placebo after relapse or progression on an aromatase inhibitor in metastatic, oestrogen receptor-positive breast cancer (FAKTION): a multicentre, randomised, controlled, phase 2 trial. *Lancet Oncology*, doi: 10.1016/S1470-2045(19)30817-4

Jung, K. et al. 2010. Cell-free DNA in the blood as a solid tumor biomarker--a critical appraisal of the literature. *Clin Chim Acta* 411(21-22), pp. 1611-1624. doi: 10.1016/j.cca.2010.07.032

K, P. et al. 2016. Next Generation Sequencing of Circulating Cell-Free DNA for Evaluating Mutations and Gene Amplification in Metastatic Breast Cancer. *Clin Chem* 9, p. 261834.

Kaneda, M. M. et al. 2016. PI3Kγ is a molecular switch that controls immune suppression. *Nature* 539(7629), pp. 437-442.

Katso, R. et al. 2001. Cellular function of phosphoinositide 3-kinases: implications for development, homeostasis, and cancer. *Annu Rev Cell Dev Biol* 17, pp. 615-675. doi: 10.1146/annurev.cellbio.17.1.615

Kaufman, B. et al. 2009. Trastuzumab plus anastrozole versus anastrozole alone for the treatment of postmenopausal women with human epidermal growth factor receptor 2-positive, hormone receptor-positive metastatic breast cancer: results from the randomized phase III TAnDEM study.*J Clin Oncol*. Vol. 27. United States, pp. 5529-5537.

Kim, Y. G. et al. 2018. Breast cancer stem cells in HER2-negative breast cancer cells contribute to HER2-mediated radioresistance and molecular subtype conversion: clinical implications for serum HER2 in recurrent HER2-negative breast cancer. *Oncotarget* 9(5), pp. 5811-5822. doi: 10.18632/oncotarget.23528

Kinugasa, H. et al. 2015. Droplet digital PCR measurement of HER2 in patients with gastric cancer. *Br J Cancer* 112(10), pp. 1652-1655. doi: 10.1038/bjc.2015.129

Kirkegaard, T. et al. 2005. AKT activation predicts outcome in breast cancer patients treated with tamoxifen. *J Pathol* 207(2), pp. 139-146. doi: 10.1002/path.1829

Kivioja, T. et al. 2011. Counting absolute numbers of molecules using unique molecular identifiers. *Nat Methods* 9(1), pp. 72-74. doi: 10.1038/nmeth.1778

Kodahl, A. R. et al. 2018. Correlation between circulating cell-free PIK3CA tumor DNA levels and treatment response in patients with PIK3CA-mutated metastatic breast cancer. *Mol Oncol* 12(6), pp. 925-935. doi: 10.1002/1878-0261.12305

Kreutz, J. E. et al. 2011. Theoretical design and analysis of multivolume digital assays with wide dynamic range validated experimentally with microfluidic digital PCR. *Anal Chem* 83(21), pp. 8158-8168. doi: 10.1021/ac201658s

Krop, I. E. et al. 2016. Pictilisib for oestrogen receptor-positive, aromatase inhibitor-resistant, advanced or metastatic breast cancer (FERGI): a randomised, double-blind, placebo-controlled, phase 2 trial. *Lancet Oncol* 17(6), pp. 811-821. doi: 10.1016/s1470-2045(16)00106-6

Lai, Y. L. et al. 2008. PIK3CA exon 20 mutation is independently associated with a poor prognosis in breast cancer patients. *Ann Surg Oncol* 15(4), pp. 1064-1069. doi: 10.1245/s10434-007-9751-7

Lanman, R. B. et al. 2015. Analytical and Clinical Validation of a Digital Sequencing Panel for Quantitative, Highly Accurate Evaluation of Cell-Free Circulating Tumor DNA. *PLoS One* 10(10), p. e0140712. doi: 10.1371/journal.pone.0140712

Lannigan, D. A. 2003. Estrogen receptor phosphorylation. *Steroids* 68(1), pp. 1-9.

Lauring, J. et al. 2013. The phosphoinositide-3-kinase-Akt-mTOR pathway as a therapeutic target in breast cancer. *J Natl Compr Canc Netw* 11(6), pp. 670-678.

Lausen B et al. 2004. Assessment of Optimally Selected Prognostic Factors. *Biometrical Journal* 46(3), pp. 364-374. doi: DOI: 10.1002/bimj.200310030

Lee, H. R. et al. 2012. Functions and physiological roles of two types of estrogen receptors, ERα and ERβ, identified by estrogen receptor knockout mouse. *Lab Anim Res* 28(2), pp. 71-76. doi: 10.5625/lar.2012.28.2.71

Levine, D. A. et al. 2005. Frequent mutation of the PIK3CA gene in ovarian and breast cancers. *Clin Cancer Res* 11(8), pp. 2875-2878. doi: 10.1158/1078-0432.CCR-04-2142

Li, A. J. et al. 2018a. PIK3CA and TP53 mutations predict overall survival of stage II/III colorectal cancer patients. *World J Gastroenterol* 24(5), pp. 631-640. doi: 10.3748/wjg.v24.i5.631

Li, G. et al. 2018b. Prevalence and spectrum of AKT1, PIK3CA, PTEN and TP53 somatic mutations in Chinese breast cancer patients. *PLoS One* 13(9), p. e0203495. doi: 10.1371/journal.pone.0203495

Li, S. Y. et al. 2006. PIK3CA mutations in breast cancer are associated with poor outcome. *Breast Cancer Res Treat* 96(1), pp. 91-95. doi: 10.1007/s10549-005-9048-0

Li, W. et al. 2018c. Akt1 inhibition promotes breast cancer metastasis through EGFR-mediated β-catenin nuclear accumulation. *Cell Commun Signal* 16(1), p. 82. doi: 10.1186/s12964-018-0295-1

Li, X. et al. 2014. LIF promotes tumorigenesis and metastasis of breast cancer through the AKT-mTOR pathway. *Oncotarget* 5(3), pp. 788-801. doi: 10.18632/oncotarget.1772

Li, Z. et al. 2018d. Upregulation of IRS1 Enhances IGF1 Response in Y537S and D538G ESR1 Mutant Breast Cancer Cells. *Endocrinology* 159(1), pp. 285-296. doi: 10.1210/en.2017-00693

Liu, P. et al. 2011. Oncogenic PIK3CA-driven mammary tumors frequently recur via PI3K pathway-dependent and PI3K pathway-independent mechanisms. *Nat Med* 17(9), pp. 1116-1120. doi: 10.1038/nm.2402

LoRusso, P. M. 2016. Inhibition of the PI3K/AKT/mTOR Pathway in Solid Tumors. *J Clin Oncol* 34(31), pp. 3803-3815. doi: 10.1200/jco.2014.59.0018

Lower, E. E. et al. 2009. HER-2/neu expression in primary and metastatic breast cancer. *Breast Cancer Res Treat* 113(2), pp. 301-306. doi: 10.1007/s10549-008-9931-6

Lønning, P. E. 2009. Lack of complete cross-resistance between different aromatase inhibitors; a real finding in search for an explanation? *Eur J Cancer* 45(4), pp. 527-535. doi: 10.1016/j.ejca.2008.10.019

Mandel, P. and Metais, P. 1948. Les acides nucléiques du plasma sanguin chez l'homme. *C R Seances Soc Biol Fil* 142(3-4), pp. 241-243.

Manning, B. D. and Cantley, L. C. 2007. AKT/PKB signaling: navigating downstream. *Cell* 129(7), pp. 1261-1274. doi: 10.1016/j.cell.2007.06.009

Marcom, P. K. et al. 2007. The combination of letrozole and trastuzumab as first or second-line biological therapy produces durable responses in a subset of HER2 positive and ER positive advanced breast cancers. *Breast Cancer Res Treat* 102(1), pp. 43-49. doi: 10.1007/s10549-006-9307-8

Marczynski, G. T. et al. 2020. Circulating tumor DNA (ctDNA) detection is associated with shorter progression-free survival in advanced melanoma patients. *Sci Rep* 10(1), p. 18682. doi: 10.1038/s41598-020-75792-1

Mayer, I. A. et al. 2017. A Phase Ib Study of Alpelisib (BYL719), a PI3Kα-Specific Inhibitor, with Letrozole in ER+/HER2- Metastatic Breast Cancer. *Clin Cancer Res* 23(1), pp. 26-34. doi: 10.1158/1078-0432.ccr-16-0134

McDonald, B. R. et al. 2019. Personalized circulating tumor DNA analysis to detect residual disease after neoadjuvant therapy in breast cancer. *Sci Transl Med* 11(504), doi: 10.1126/scitranslmed.aax7392

McDonough, S. J. et al. 2019. Use of FFPE-derived DNA in next generation sequencing: DNA extraction methods. *PLoS One* 14(4), p. e0211400. doi: 10.1371/journal.pone.0211400

Meric-Bernstam, F. et al. 2014. Concordance of genomic alterations between primary and recurrent breast cancer. *Mol Cancer Ther* 13(5), pp. 1382-1389. doi: 10.1158/1535-7163.MCT-13-0482

Miller, T. W. et al. 2011a. Phosphatidylinositol 3-kinase and antiestrogen resistance in breast cancer. *J Clin Oncol* 29(33), pp. 4452-4461. doi: 10.1200/JCO.2010.34.4879

Miller, T. W. et al. 2011b. A gene expression signature from human breast cancer cells with acquired hormone independence identifies MYC as a mediator of antiestrogen resistance. *Clin Cancer Res* 17(7), pp. 2024-2034. doi: 10.1158/1078-0432.CCR-10-2567

Miller, W. R. and Larionov, A. A. 2012. Understanding the mechanisms of aromatase inhibitor resistance. *Breast Cancer Res* 14(1), p. 201. doi: 10.1186/bcr2931

Morgan, D. O. 1997. Cyclin-dependent kinases: engines, clocks, and microprocessors. *Annu Rev Cell Dev Biol* 13, pp. 261-291. doi: 10.1146/annurev.cellbio.13.1.261

Mosele, F. et al. 2020. Outcome and molecular landscape of patients with PIK3CA-mutated metastatic breast cancer. *Ann Oncol* 31(3), pp. 377-386. doi: 10.1016/j.annonc.2019.11.006

Murphy, C. G. and Dickler, M. N. 2015. The Role of CDK4/6 Inhibition in Breast Cancer. *Oncologist* 20(5), pp. 483-490. doi: 10.1634/theoncologist.2014-0443

Murphy, C. G. and Dickler, M. N. 2016. Endocrine resistance in hormone-responsive breast cancer: mechanisms and therapeutic strategies. *Endocr Relat Cancer* 23(8), pp. R337-352. doi: 10.1530/ERC-16-0121

Nagata, S. 2000. Apoptotic DNA fragmentation. *Exp Cell Res* 256(1), pp. 12-18. doi: 10.1006/excr.2000.4834

Nayar, U. et al. 2019. Acquired HER2 mutations in ER(+) metastatic breast cancer confer resistance to estrogen receptor-directed therapies.*Nat Genet*. Vol. 51. United States, pp. 207-216.

Network, C. G. A. 2012. Comprehensive molecular portraits of human breast tumours. *Nature* 490(7418), pp. 61-70. doi: 10.1038/nature11412

Nik-Zainal, S. et al. 2012. The life history of 21 breast cancers. *Cell* 149(5), pp. 994-1007. doi: 10.1016/j.cell.2012.04.023

Nitulescu, G. M. et al. 2018. The Akt pathway in oncology therapy and beyond (Review). *Int J Oncol* 53(6), pp. 2319-2331. doi: 10.3892/ijo.2018.4597

Novartis, P. 2020. Study of Safety and Efficacy of Alpelisib With Everolimus or Alpelisib With Everolimus and Exemestane in Advanced Breast Cancer Patients, Renal Cell Cancer and Pancreatic Tumors. https://clinicaltrials.gov/: ClinicalTrials.gov Identifier: NCT02077933.

O'Leary, B. et al. 2018. Early circulating tumor DNA dynamics and clonal selection with palbociclib and fulvestrant for breast cancer. *Nat Commun* 9(1), p. 896. doi: 10.1038/s41467-018-03215-x

Oesterreich, S. and Davidson, N. E. 2013. The search for ESR1 mutations in breast cancer. *Nat Genet* 45(12), pp. 1415-1416. doi: 10.1038/ng.2831

Olivier, M. et al. 2006. The clinical value of somatic TP53 gene mutations in 1,794 patients with breast cancer. *Clin Cancer Res* 12(4), pp. 1157-1167. doi: 10.1158/1078-0432.CCR-05-1029

Page, K. et al. 2013. Influence of plasma processing on recovery and analysis of circulating nucleic acids. *PLoS One* 8(10), p. e77963. doi: 10.1371/journal.pone.0077963

Page, K. et al. 2006. The importance of careful blood processing in isolation of cell-free DNA. *Ann N Y Acad Sci* 1075, pp. 313-317. doi: 10.1196/annals.1368.042

Pao, W. et al. 2005. Acquired resistance of lung adenocarcinomas to gefitinib or erlotinib is associated with a second mutation in the EGFR kinase domain. *PLoS Med* 2(3), p. e73. doi: 10.1371/journal.pmed.0020073

Papa, A. et al. 2014. Cancer-associated PTEN mutants act in a dominant-negative manner to suppress PTEN protein function. *Cell* 157(3), pp. 595-610. doi: 10.1016/j.cell.2014.03.027

Pardee, A. B. 1989. G1 events and regulation of cell proliferation. *Science* 246(4930), pp. 603-608.

Parkinson, C. A. et al. 2016. Exploratory Analysis of TP53 Mutations in Circulating Tumour DNA as Biomarkers of Treatment Response for Patients with Relapsed High-Grade Serous Ovarian Carcinoma: A Retrospective Study. *PLoS Med* 13(12), p. e1002198. doi: 10.1371/journal.pmed.1002198

Parla, J. S. et al. 2011. A comparative analysis of exome capture. *Genome Biol* 12(9), p. R97. doi: 10.1186/gb-2011-12-9-r97

Perey, L. et al. 2007. Clinical benefit of fulvestrant in postmenopausal women with advanced breast cancer and primary or acquired resistance to aromatase inhibitors: final results of phase II Swiss Group for Clinical Cancer Research Trial (SAKK 21/00). *Annals of Oncology* 18(1), pp. 64–69.

Perez-Garcia, J. et al. 2018. Targeting FGFR pathway in breast cancer. *Breast* 37, pp. 126-133. doi: 10.1016/j.breast.2017.10.014

Pharoah, P. D. et al. 1999. Somatic mutations in the p53 gene and prognosis in breast cancer: a meta-analysis. *Br J Cancer* 80(12), pp. 1968-1973. doi: 10.1038/sj.bjc.6690628

Piccart, M. et al. 2014. Everolimus plus exemestane for hormone-receptor-positive, human epidermal growth factor receptor-2-negative advanced breast cancer: overall survival results from BOLERO-2†. *Ann Oncol* 25(12), pp. 2357-2362. doi: 10.1093/annonc/mdu456

Practices, G. B. 2016. *Perform local realignment around indels*. Available at: https://gatkforums.broadinstitute.org/gatk/discussion/7156/howto-perform-local-realignment-around-indels [Accessed.

Prediger, E. 2013. *Calculations: Converting from nanograms to copy number*. Integrated DNA Technologies. Available at: https://www.idtdna.com/pages/education/decoded/article/calculations-converting-from-nanograms-to-copy-number [Accessed.

Pérez-Tenorio, G. et al. 2014. Clinical value of isoform-specific detection and targeting of AKT1, AKT2 and AKT3 in breast cancer. *Breast cancer Man* 3(5), pp. 409–421. doi: https://doi.org/10.2217/bmt.14.35

Pérez-Tenorio, G. and Stål, O. 2002. Activation of AKT/PKB in breast cancer predicts a worse outcome among endocrine treated patients. *Br J Cancer* 86(4), pp. 540-545. doi: 10.1038/sj.bjc.6600126

Qiagen. 2015. *GeneRead DNAseq Targeted Panels V2 Handbook*. Available at: https://www.qiagen.com/af/resources/resourcedetail?id=0c3d3eb1-ff6b-43f2-8eb6-810f2449051f(=en [Accessed: June 2015].

Qureshi, A. and Pervez, S. 2010. Allred scoring for ER reporting and it's impact in clearly distinguishing ER negative from ER positive breast cancers. *J Pak Med Assoc* 60(5), pp. 350-353.

Racca, F. E. et al. 2016. Prognostic and therapeutic implications of fibroblast growth factor receptors (FGFRs) 1 and 2 gene amplifications in patients (pts) with advanced breast cancer (ABC). *Journal of Clinical Oncology* 34(Suppl; abstr 537), p. Suppl; abstr 537. doi: 10.1200/JCO.2016.34.15_suppl.537

Rani, A. et al. 2019. Endocrine Resistance in Hormone Receptor Positive Breast Cancer–From Mechanism to Therapy. *Frontiers in Endocrinology*, doi: 10.3389/fendo.2019.00245

Raynaud, F. I. et al. 2009. Biological properties of potent inhibitors of class I phosphatidylinositide 3-kinases: from PI-103 through PI-540, PI-620 to the oral agent GDC-0941. *Mol Cancer Ther* 8(7), pp. 1725-1738. doi: 10.1158/1535-7163.MCT-08-1200

Razavi, P. et al. 2018. The Genomic Landscape of Endocrine-Resistant Advanced Breast Cancers. *Cancer Cell* 34(3), pp. 427-438.e426. doi: 10.1016/j.ccell.2018.08.008

Regitnig, P. et al. 2004. Change of HER-2/neu status in a subset of distant metastases from breast carcinomas. *J Pathol* 203(4), pp. 918-926. doi: 10.1002/path.1592

Reis-Filho, J. S. et al. 2006. FGFR1 emerges as a potential therapeutic target for lobular breast carcinomas. *Clin Cancer Res* 12(22), pp. 6652-6662. doi: 10.1158/1078-0432.CCR-06-1164

Renner, O. et al. 2008. Activation of phosphatidylinositol 3-kinase by membrane localization of p110alpha predisposes mammary glands to neoplastic transformation. *Cancer Res* 68(23), pp. 9643-9653. doi: 10.1158/0008-5472.can-08-1539

Ribas, R. et al. 2015. AKT Antagonist AZD5363 Influences Estrogen Receptor Function in Endocrine-Resistant Breast Cancer and Synergizes with Fulvestrant (ICI182780) In Vivo. *Mol Cancer Ther* 14(9), pp. 2035-2048. doi: 10.1158/1535-7163.MCT-15-0143

Rihawi, K. et al. 2019. MYC Amplification as a Potential Mechanism of Primary Resistance to Crizotinib in ALK-Rearranged Non-Small Cell Lung Cancer: A Brief Report. *Transl Oncol* 12(1), pp. 116-121. doi: 10.1016/j.tranon.2018.09.013

Riva, F. et al. 2017. Patient-Specific Circulating Tumor DNA Detection during Neoadjuvant Chemotherapy in Triple-Negative Breast Cancer. *Clin Chem* 63(3), pp. 691-699. doi: 10.1373/clinchem.2016.262337

Robinson, D. R. et al. 2013. Activating ESR1 mutations in hormone-resistant metastatic breast cancer. *Nature genetics* 45(12), pp. 1446-1451. doi: 10.1038/ng.2823

Rodon, J. et al. 2014. Phase I dose-escalation and -expansion study of buparlisib (BKM120), an oral pan-Class I PI3K inhibitor, in patients with advanced solid tumors. *Invest New Drugs* 32(4), pp. 670-681. doi: 10.1007/s10637-014-0082-9

Ross Camidge D et al. eds.*Oncology, A.S.o.C.* 2020. *Abstract 9517: Correlation of baseline molecular and clinical variables with ALK inhibitor efficacy in ALTA-1L. J Clin Oncol 38: 2020 (suppl; abstr 9517).* Virtual, American Society of Clinical Oncology - Annual meeting.

Ross, J. S. and Cronin, M. 2011. Whole cancer genome sequencing by next-generation methods. *Am J Clin Pathol* 136(4), pp. 527-539. doi: 10.1309/ajcpr1svt1vhugxw

RS, F. et al. 2016. Palbociclib and Letrozole in Advanced Breast Cancer. *N Engl J Med* 375(20), pp. 1925-1936. doi: 1910.1056/NEJMoa1607303.

Rugo, H. S. et al. 2016. Improving Response to Hormone Therapy in Breast Cancer: New Targets, New Therapeutic Options. *Am Soc Clin Oncol Educ Book* 35, pp. e40-54. doi: 10.1200/edbk_159198

Ruiz, A. et al. 2019. Chronological occurrence of PI3KCA mutations in breast cancer liver metastases after repeat partial liver resection. *BMC Cancer* 19(1), p. 169. doi: 10.1186/s12885-019-5365-2

Saal, L. H. et al. 2005. PIK3CA mutations correlate with hormone receptors, node metastasis, and ERBB2, and are mutually exclusive with PTEN loss in human breast carcinoma. *Cancer Res* 65(7), pp. 2554-2559. doi: 10.1158/0008-5472-CAN-04-3913

Sakai, H. et al. 2018. HER2 genomic amplification in circulating tumor DNA and estrogen receptor positivity predict primary resistance to trastuzumab emtansine (T-DM1) in patients with HER2-positive metastatic breast cancer. *Breast Cancer*, doi: 10.1007/s12282-018-0861-9

Salimi, M. and Sedaghati Burkhani, S. 2019. Integrity and Quantity Evaluation of Plasma Cell-Free DNA in Triple Negative Breast Cancer. *Avicenna J Med Biotechnol* 11(4), pp. 334-338.

Samorodnitsky, E. et al. 2015. Evaluation of Hybridization Capture Versus Amplicon-Based Methods for Whole-Exome Sequencing. *Hum Mutat* 36(9), pp. 903-914. doi: 10.1002/humu.22825

Samuels, Y. and Waldman, T. 2010. Oncogenic mutations of PIK3CA in human cancers. *Curr Top Microbiol Immunol* 347, pp. 21-41. doi: 10.1007/82_2010_68

Sarker, D. et al. 2015. First-in-human phase I study of pictilisib (GDC-0941), a potent pan-class I phosphatidylinositol-3-kinase (PI3K) inhibitor, in patients with advanced solid tumors. *Clin Cancer Res* 21(1), pp. 77-86. doi: 10.1158/1078-0432.ccr-14-0947

Sasano, H. et al. 2009. In situ estrogen production and its regulation in human breast carcinoma: from endocrinology to intracrinology. *Pathol Int* 59(11), pp. 777-789. doi: 10.1111/j.1440-1827.2009.02444.x

Sawyer, C. et al. 2003. Regulation of breast cancer cell chemotaxis by the phosphoinositide 3-kinase p110delta. *Cancer Res* 63(7), pp. 1667-1675.

Scheid, M. P. and Woodgett, J. R. 2001. PKB/AKT: functional insights from genetic models. *Nat Rev Mol Cell Biol* 2(10), pp. 760-768. doi: 10.1038/35096067

Schettini, F. et al. 2016. Hormone Receptor/Human Epidermal Growth Factor Receptor 2-positive breast cancer: Where we are now and where we are going. *Cancer Treat Rev* 46, pp. 20-26. doi: 10.1016/j.ctrv.2016.03.012

Schiavon, G. et al. 2015. Analysis of ESR1 mutation in circulating tumor DNA demonstrates evolution during therapy for metastatic breast cancer. *Science Translational Medicine* 7(313), pp. 313ra182-313ra182. doi: 10.1126/scitranslmed.aac7551

Schmid, P. et al. 2020. Capivasertib Plus Paclitaxel Versus Placebo Plus Paclitaxel As First-Line Therapy for Metastatic Triple-Negative Breast Cancer: The PAKT Trial. *J Clin Oncol* 38(5), pp. 423-433. doi: 10.1200/jco.19.00368

Schmid, P. et al. 2019. Fulvestrant Plus Vistusertib vs Fulvestrant Plus Everolimus vs Fulvestrant Alone for Women With Hormone Receptor-Positive Metastatic Breast Cancer: The MANTA Phase 2 Randomized Clinical Trial. *JAMA Oncol* 5(11), pp. 1556-1563. doi: 10.1001/jamaoncol.2019.2526

Schmitz, K. J. et al. 2004. Prognostic relevance of activated Akt kinase in node-negative breast cancer: a clinicopathological study of 99 cases. *Mod Pathol* 17(1), pp. 15-21. doi: 10.1038/modpathol.3800002

Schwartzberg, L. S. et al. 2010. Lapatinib plus letrozole as first-line therapy for HER-2+ hormone receptor-positive metastatic breast cancer. *Oncologist* 15(2), pp. 122-129.

Shah, O. J. et al. 2004. Inappropriate activation of the TSC/Rheb/mTOR/S6K cassette induces IRS1/2 depletion, insulin resistance, and cell survival deficiencies. *Curr Biol* 14(18), pp. 1650-1656. doi: 10.1016/j.cub.2004.08.026

Shajahan-Haq, A. N. et al. 2014. MYC regulates the unfolded protein response and glucose and glutamine uptake in endocrine resistant breast cancer. *Mol Cancer* 13, p. 239. doi: 10.1186/1476-4598-13-239

Shang, Y. et al. 2000. Cofactor dynamics and sufficiency in estrogen receptor-regulated transcription. *Cell* 103(6), pp. 843-852.

Shapiro, G. I. 2006. Cyclin-dependent kinase pathways as targets for cancer treatment. *J Clin Oncol* 24(11), pp. 1770-1783. doi: 10.1200/JCO.2005.03.7689

Shapiro, G. I. et al. 2014. Phase I safety, pharmacokinetic, and pharmacodynamic study of SAR245408 (XL147), an oral pan-class I PI3K inhibitor, in patients with advanced solid tumors. *Clin Cancer Res* 20(1), pp. 233-245. doi: 10.1158/1078-0432.ccr-13-1777

Shariati, M. and Meric-Bernstam, F. 2019. Targeting AKT for cancer therapy. *Expert Opin Investig Drugs* 28(11), pp. 977-988. doi: 10.1080/13543784.2019.1676726

Shaw, J. A. and Stebbing, J. 2014. Circulating free DNA in the management of breast cancer. *Ann Transl Med* 2(1), p. 3. doi: 10.3978/j.issn.2305-5839.2013.06.06

Sherr, C. J. 1995. D-type cyclins. *Trends Biochem Sci* 20(5), pp. 187-190.

Shoda, K. et al. 2017. Monitoring the HER2 copy number status in circulating tumor DNA by droplet digital PCR in patients with gastric cancer. *Gastric Cancer* 20(1), pp. 126-135. doi: 10.1007/s10120-016-0599-z

Shoda, K. et al. 2015. HER2 amplification detected in the circulating DNA of patients with gastric cancer: a retrospective pilot study. *Gastric Cancer* 18(4), pp. 698-710. doi: 10.1007/s10120-014-0432-5

Shomali, M. et al. 2021. SAR439859, a Novel Selective Estrogen Receptor Degrader (SERD), Demonstrates Effective and Broad Antitumor Activity in Wild-Type and Mutant ER-Positive Breast Cancer Models. *Mol Cancer Ther* 20(2), pp. 250-262. doi: 10.1158/1535-7163.mct-20-0390

Shou, J. et al. 2004. Mechanisms of tamoxifen resistance: increased estrogen receptor-HER2/neu cross-talk in ER/HER2-positive breast cancer. *J Natl Cancer Inst* 96(12), pp. 926-935. doi: 10.1093/jnci/djh166

Sighoko, D. et al. 2014. Discordance in hormone receptor status among primary, metastatic, and second primary breast cancers: biological difference or misclassification? *Oncologist* 19(6), pp. 592-601. doi: 10.1634/theoncologist.2013-0427

Singh, H. et al. 2018. U.S. Food and Drug Administration Approval: Neratinib for the Extended Adjuvant Treatment of Early-Stage HER2-Positive Breast Cancer.*Clin Cancer Res*. Vol. 24. United States: ©2018 American Association for Cancer Research., pp. 3486-3491.

Skandalis, S. S. et al. 2014. Cross-talk between estradiol receptor and EGFR/IGF-IR signaling pathways in estrogen-responsive breast cancers: focus on the role and impact of proteoglycans. *Matrix Biol* 35, pp. 182-193. doi: 10.1016/j.matbio.2013.09.002

Sledge, G. W. et al. 2019. The Effect of Abemaciclib Plus Fulvestrant on Overall Survival in Hormone Receptor-Positive, ERBB2-Negative Breast Cancer That Progressed on Endocrine Therapy-MONARCH 2: A Randomized Clinical Trial. *JAMA Oncol*, doi: 10.1001/jamaoncol.2019.4782

Smyth, L. and Hudis, C. 2015. Adjuvant hormonal therapy in premenopausal women with breast cancer. *Indian J Med Paediatr Oncol* 36(4), pp. 195-200. doi: 10.4103/0971-5851.171530

Song, P. et al. 2019. Concomitant TP53 mutations with response to crizotinib treatment in patients with ALK-rearranged non-small-cell lung cancer. *Cancer Med* 8(4), pp. 1551-1557. doi: 10.1002/cam4.2043

Sparano, J. A. et al. 2019. Clinical and Genomic Risk to Guide the Use of Adjuvant Therapy for Breast Cancer. *N Engl J Med* 380(25), pp. 2395-2405. doi: 10.1056/NEJMoa1904819

Stasik, S. et al. 2018. An optimized targeted Next-Generation Sequencing approach for sensitive detection of single nucleotide variants. *Biomol Detect Quantif* 15, pp. 6-12. doi: 10.1016/j.bdq.2017.12.001

Steffensen, K. D. et al. 2014. Prognostic importance of cell-free DNA in chemotherapy resistant ovarian cancer treated with bevacizumab. *Eur J Cancer* 50(15), pp. 2611-2618. doi: 10.1016/j.ejca.2014.06.022

Stroun, M. et al. 2001. About the possible origin and mechanism of circulating DNA apoptosis and active DNA release. *Clin Chim Acta* 313(1-2), pp. 139-142. doi: 10.1016/s0009-8981(01)00665-9

Tabernero, J. et al. 2008. Dose- and schedule-dependent inhibition of the mammalian target of rapamycin pathway with everolimus: a phase I tumor pharmacodynamic study in patients with advanced solid tumors. *J Clin Oncol* 26(10), pp. 1603-1610. doi: 10.1200/jco.2007.14.5482

Takaku, M. et al. 2018. GATA3 zinc finger 2 mutations reprogram the breast cancer transcriptional network. *Nat Commun* 9(1), p. 1059. doi: 10.1038/s41467-018-03478-4

Tan, J. and Yu, Q. 2013. Molecular mechanisms of tumor resistance to PI3K-mTOR-targeted therapy. *Chin J Cancer* 32(7), pp. 376-379. doi: 10.5732/cjc.012.10287

TCGA. 2012. Comprehensive molecular portraits of human breast tumours. *Nature* 490(7418), pp. 61-70. doi: 10.1038/nature11412

Tchou, J. et al. 2015. Monitoring serum HER2 levels in breast cancer patients. *Springerplus* 4, p. 237. doi: 10.1186/s40064-015-1015-6

Thangavel, C. et al. 2011. Therapeutically activating RB: reestablishing cell cycle control in endocrine therapy-resistant breast cancer. *Endocr Relat Cancer* 18(3), pp. 333-345. doi: 10.1530/ERC-10-0262

Thierry, A. R. et al. 2016. Origins, structures, and functions of circulating DNA in oncology. *Cancer Metastasis Rev* 35(3), pp. 347-376. doi: 10.1007/s10555-016-9629-x

Thierry, A. R. et al. 2010. Origin and quantification of circulating DNA in mice with human colorectal cancer xenografts. *Nucleic Acids Res* 38(18), pp. 6159-6175. doi: 10.1093/nar/gkq421

Thoma, C. 2018. Prostate cancer: Pitfalls of liquid biopsy tests. *Nat Rev Urol* 15(2), p. 69. doi: 10.1038/nrurol.2017.222

Thomas C. King. 2007. Neoplasia. In: King, T.C. ed. *Elsevier's Integrated Pathology*. ScienceDirect, pp. 111-143.

Torga, G. and Pienta, K. J. 2018. Patient-Paired Sample Congruence Between 2 Commercial Liquid Biopsy Tests. *JAMA Oncol* 4(6), pp. 868-870. doi: 10.1001/jamaoncol.2017.4027

Toy, W. et al. 2013. ESR1 ligand-binding domain mutations in hormone-resistant breast cancer. *Nat Genet* 45(12), pp. 1439-1445. doi: 10.1038/ng.2822

Toy, W. et al. 2017. Activating *ESR1* Mutations Differentially Affect the Efficacy of ER Antagonists. *Cancer Discov* 7(3), pp. 277-287. doi: 10.1158/2159-8290.CD-15-1523

Treilleux, I. et al. 2013. Abstract 510: Predictive markers of everolimus efficacy in hormone receptor positive (HR+) metastatic breast cancer (MBC): Final results of the TAMRAD trial translational study. Journal of Clinical Oncology 31, no. 15_suppl.

Turke, A. B. et al. 2010. Preexistence and clonal selection of MET amplification in EGFR mutant NSCLC. *Cancer Cell* 17(1), pp. 77-88. doi: 10.1016/j.ccr.2009.11.022

Turner, N. and Grose, R. 2010. Fibroblast growth factor signalling: from development to cancer. *Nat Rev Cancer* 10(2), pp. 116-129. doi: 10.1038/nrc2780

Turner, N. et al. 2010. FGFR1 amplification drives endocrine therapy resistance and is a therapeutic target in breast cancer. *Cancer Res* 70(5), pp. 2085-2094. doi: 10.1158/0008-5472.CAN-09-3746

Turner, N. C. et al. 2019. BEECH: a dose-finding run-in followed by a randomised phase II study assessing the efficacy of AKT inhibitor capivasertib (AZD5363) combined with paclitaxel in patients with estrogen receptor-positive advanced or metastatic breast cancer, and in a PIK3CA mutant sub-population. *Ann Oncol* 30(5), pp. 774-780. doi: 10.1093/annonc/mdz086

Turner, N. C. et al. 2020. Circulating tumour DNA analysis to direct therapy in advanced breast cancer (plasmaMATCH): a multicentre, multicohort, phase 2a, platform trial. *Lancet Oncol* 21(10), pp. 1296-1308. doi: 10.1016/s1470-2045(20)30444-7

Turner, N. C. et al. 2018. Overall Survival with Palbociclib and Fulvestrant in Advanced Breast Cancer. *N Engl J Med* 379(20), pp. 1926-1936. doi: 10.1056/NEJMoa1810527

Vivanco, I. and Sawyers, C. L. 2002. The phosphatidylinositol 3-Kinase AKT pathway in human cancer. *Nat Rev Cancer* 2(7), pp. 489-501. doi: 10.1038/nrc839

Wang, C. et al. 2011. Estrogen induces c-myc gene expression via an upstream enhancer activated by the estrogen receptor and the AP-1 transcription factor. *Mol Endocrinol* 25(9), pp. 1527-1538. doi: 10.1210/me.2011-1037

Wang, P. et al. 2009. Characterization of the oestrogenic activity of non-aromatic steroids: are there male-specific endogenous oestrogen receptor modulators? *Br J Pharmacol* 158(7), pp. 1796-1807. doi: 10.1111/j.1476-5381.2009.00467.x

Wang, Q. et al. 2017a. Akt as a target for cancer therapy: more is not always better (lessons from studies in mice). *Br J Cancer* 117(2), pp. 159-163.

Wang, W. et al. 2017b. Characterization of the release and biological significance of cell-free DNA from breast cancer cell lines. *Oncotarget* 8(26), pp. 43180-43191. doi: 10.18632/oncotarget.17858

Watts, C. K. et al. 1995. Antiestrogen inhibition of cell cycle progression in breast cancer cells in associated with inhibition of cyclin-dependent kinase activity and decreased retinoblastoma protein phosphorylation. *Mol Endocrinol* 9(12), pp. 1804-1813. doi: 10.1210/mend.9.12.8614416

Weigelt, B. et al. 2005. Breast cancer metastasis: markers and models. *Nat Rev Cancer* 5(8), pp. 591-602. doi: 10.1038/nrc1670

Weinberg, R. A. 1995. The retinoblastoma protein and cell cycle control. *Cell.* 81(3), pp. 323-330.

Wiley, G. B. et al. 2014. Use of next-generation DNA sequencing to   analyze genetic variants in rheumatic disease. *Arthritis Res Ther* 16(6), p. 490. doi: 10.1186/s13075-014-0490-4

Williams, M. R. et al. 2000. The role of 3-phosphoinositide-dependent protein kinase 1 in activating AGC kinases defined in embryonic stem cells. *Curr Biol* 10(8), pp. 439-448. doi: 10.1016/s0960-9822(00)00441-3

Wolff, A. C. et al. 2013. Randomized phase III placebo-controlled trial of letrozole plus oral temsirolimus as first-line endocrine therapy in postmenopausal women with locally advanced or metastatic breast cancer. *J Clin Oncol* 31(2), pp. 195-202. doi: 10.1200/jco.2011.38.3331

Wu, H. et al. 2019. The distinct clinicopathological and prognostic implications of PIK3CA mutations in breast cancer patients from Central China. *Cancer Manag Res* 11, pp. 1473-1492. doi: 10.2147/CMAR.S195351

Xu, J. et al. 2010. MYC and Breast Cancer. *Genes Cancer* 1(6), pp. 629-640. doi: 10.1177/1947601910378691

Yamamoto-Ibusuki, M. et al. 2015. Targeted therapies for ER+/HER2- metastatic breast cancer. *BMC Med* 13, p. 137. doi: 10.1186/s12916-015-0369-5

Yang, J. et al. 2019. Targeting PI3K in cancer: mechanisms and advances in clinical trials. *Mol Cancer* 18(1), p. 26. doi: 10.1186/s12943-019-0954-x

Yardley, D. A. et al. 2013. Everolimus plus exemestane in postmenopausal patients with HR(+) breast cancer: BOLERO-2 final progression-free survival analysis. *Adv Ther* 30(10), pp. 870-884. doi: 10.1007/s12325-013-0060-1

Yi, K. H. and Lauring, J. 2016. Recurrent AKT mutations in human cancers: functional consequences and effects on drug sensitivity. *Oncotarget* 7(4), pp. 4241-4251. doi: 10.18632/oncotarget.6648

Zhang, J. et al. 2014. PEAR: a fast and accurate Illumina Paired-End reAd mergeR. *Bioinformatics* 30(5), pp. 614-620. doi: 10.1093/bioinformatics/btt593

Zhao, L. and Vogt, P. K. 2008. Helical domain and kinase domain mutations in p110alpha of phosphatidylinositol 3-kinase induce gain of function by different mechanisms. *Proc Natl Acad Sci U S A* 105(7), pp. 2652-2657. doi: 10.1073/pnas.0712169105